

NN08 201,1561

Elisabeth H.S. van Duin

## **Sediment transport, light and algal growth in the Markermeer**

A two-dimensional water quality model for a shallow lake

Proefschrift ter verkrijging van de graad van  
doctor in de landbouw- en milieuwetenschappen,  
op gezag van de rector magnificus,  
dr. H.C. van der Plas  
in het openbaar te verdedigen  
op vrijdag 20 november 1992  
des namiddags te vier uur in de aula  
van de Landbouwuniversiteit te Wageningen.

ISBN 557990

1

CENTRALE LANDBOUWCATALOGUS



0000 0491 4962

BIBLIOTHEEK  
LANDBOUWUNIVERSITEIT  
WAGENINGEN

Promotor: dr. L. Lijklema  
hoogleraar Waterkwaliteitsbeheer

## **Sediment transport, light and algal growth in the Markermeer**

**A two-dimensional water quality model for a shallow lake**

**E.H.S. van Duin**

De verdediging van het proefschrift en de daarbij behorende stellingen wordt gehouden op 20 november 1992, om 16.00 uur in de aula van de Landbouwniversiteit, Generaal Foulkesweg 3 te Wageningen.

Aansluitend op de promotie wordt een receptie gehouden.



## Stellingen

behorende bij het proefschrift van E.H.S. van Duin, 1992.  
Sediment transport, light and algal growth in the Markermeer.  
A two-dimensional water quality model for a shallow lake.

1. De voorlopige conclusie van de Commissie IJff, dat de kans op het optreden van tijdelijke bloei van blauwalgen, met name *Oscillatoria agardhii*, in de randmeren van een toekomstige Markerwaard zou toenemen in vergelijking met de huidige situatie in het Markermeer, wordt door de uitkomsten van modelberekeningen onderschreven. *(dit proefschrift)*
2. De indeling van gesuspendeerde stof in fracties op basis van valsnelheid is een goed concept, zowel voor het modelleren van resuspensie en sedimentatie, als voor de berekening van de bijdrage van sediment aan de uitdoving van licht in water. Daarnaast maakt het de koppeling van sedimenttransportmodellering en lichtmodellering een stuk eenvoudiger. *(dit proefschrift)*
3. - Het gedrag van gesuspendeerde stof en het lichtklimaat in ondiepe meren waarop de wind een grote invloed heeft, kunnen niet afdoende worden gemodelleerd met zogenaamde nul- of één-dimensionale modellen. Hiervoor zijn twee-dimensionale modellen noodzakelijk. *(dit proefschrift)*  
- Voor het modelleren van de groei van algen in ondiepe meren zijn zogenaamde nul- of één-dimensionale modellen evenmin toereikend. Helaas is de beschikbare kennis van de complexe processen die een rol spelen bij de groei van algen momenteel nog zo beperkt, dat de waarde van algengroeimodellen meer ligt in het vergroten van het inzicht in deze processen dan in de directe bruikbaarheid voor beheerstoepassingen.
4. In de onderzoekswereld wordt veel geld verspild doordat onderzoekers niet over niet geslaagde methoden publiceren.
5. De snelheid waarmee mode en trends elkaar afwisselen in hedendaags onderzoek op het gebied van integraal waterkwaliteitsbeheer, bijvoorbeeld van actief biologisch beheer naar ecologische oeverzones, leidt tot ad hoc en ongestructureerd onderzoek.
6. Met de term 'denk-model' kan het gebrek aan kwantitatieve kennis van relevante processen misschien worden versluierd, maar zeker niet worden gecompenseerd.
7. Het onderbrengen van meetactiviteiten en onderzoeksactiviteiten in aparte specialistische afdelingen, komt het overleg tussen onderzoeker en waarnemer en daarmee de kwaliteit van de meetresultaten niet ten goede.
8. Bij hiërarchische organisaties kunnen initiatieven het effectiefst worden gesmoord door toepassing van de derde wet van Parkinson: *'Delay is the deadliest form of denial'*.
9. Geuite kritiek van ouders, wier kinderen volledig thuis verzorgd worden, op kinderdagverblijven, lijkt veelal meer te zijn ingegeven door de wens tot een legitiematie van de eigen keuze dan door kennis van het functioneren van die kinderdagverblijven.

10. De koppeling van beschikbare middelen voor universitaire instellingen aan het aantal studenten en de snelheid waarmee deze studenten hun studie afronden, leidt automatisch tot een afname van de kwaliteit van de opleiding. Het is de vraag of de samenleving daar op lange termijn mee gediend is. *Vrij naar Cornelis Lely: Een volk dat leeft investeert in onderwijs.*
11. De dubbele betekenis van het woord monster in de Nederlandse taal kan niet op toeval berusten.



## Abstract

*E.H.S. van Duin:*

*Sediment transport, light and algal growth in the Markermeer.*

*A two-dimensional model for a shallow lake*

*PhD-thesis Agricultural University Wageningen,*

*Department of Nature Conservation, The Netherlands.*

*ISBN 90-369-1096-X*

This thesis reports on a study of the water quality in the Markermeer, focusing on the relationships between sediment transport, the light field and the growth of *Oscillatoria agardhii*. The study comprises two aspects: an extensive data collection program with the data analysis, and the development, calibration and application of a set of dynamic models, in order to assess the effect of management measures on these water quality aspects.

The data collection program contained weekly and hourly monitoring of water quality variables. Characteristics of the sediment and characteristics of the light field were measured in fall velocity experiments with various sediment samples. Experiments were conducted with light and dark bottles and with a large perspex cylinder filled with *Oscillatoria agardhii* and placed in the lake. These experiments produced information on the growth characteristics of *Oscillatoria agardhii* in the Markermeer and on different kinds of adaptation of growth parameters to the light conditions.

The model that has been developed to simulate the effect of management measures on the water quality of the Markermeer focusing on the effect of *Oscillatoria agardhii*, combines a sediment transport model (*STRESS-2d*), a light attenuation routine (*CLEAR*) and a growth model for *Oscillatoria agardhii* (*ALGA*). With the integrated model the effect of two management scenarios has been evaluated: the construction of the Markerwaard and increased flushing with water from the IJsselmeer.



## Voorwoord

Hoe klein leek de wereld toen in de zomer van 1986 professor Lijklema mijn interesse polste voor een baan bij de mij wel bekende Rijksdienst voor de IJsselmeerpolders (RIJP) in Lelystad: een dienst en een stad waarmee ik ben opgegroeid. Na overleg met de RIJP werd ik aangesteld als hoofd van de secties Waterkwaliteit en Afvoerhydrologie. Door een personeelsstop bij de RIJP werd ik ingehuurd via de Vakgroep Waterzuivering van de Landbouwniversiteit. Ik zou mij met name gaan bezighouden met het Waterkwaliteitsonderzoek Westelijke Randmeren (van de nog aan te leggen Markerwaard) en het Stedelijk Wateronderzoek Lelystad. Het eerste zou dan tot een promotie kunnen leiden.

Inmiddels is het zes jaar later en het bewuste onderzoek heeft inderdaad geleid tot een promotie, al is de naam van het onderzoek gaandeweg veranderd in het waterkwaliteitsonderzoek Markermeer. De weg daartoe werd met name gekenmerkt door reorganisaties, herindelingen, veranderingen in de personeelsbezetting en naamsveranderingen. Door de variërende personeelsbezetting werd de continuïteit van het onderzoek nogal eens bedreigd en heeft uiteindelijk een groot aantal verschillende mensen gedurende kortere of langere tijd aan het onderzoek meegewerkt. Alle personen die in die periode bij de sectie Waterkwaliteit werkzaam zijn geweest, hebben wel op enige wijze aan dit onderzoek bijgedragen. Zowel die personen die direct bij de RIJP werkzaam waren, alsmede studenten, dienstweigeraars en zij die ingehuurd werden via de Heidemij. Allen ben ik daarvoor zeer erkentelijk, waarbij ik toch speciaal wil noemen: de mannen van het eerste uur, Andries Oldenkamp, Jan van Tjonger en Martin Scholten; de Friezen van het laatste uur, Yde Bruinsma en Jaap Postma en, speciaal voor haar loyaliteit, Cornelië Peels. Zonder hun bijdrage was dit onderzoek nooit zover gekomen. Het model STRESS-2d zou zonder de bijdrage van Martin nooit geworden zijn wat het nu is en zou een niet te doorgronden programma zonder overzichtelijke uitvoer zijn gebleven. Ook buiten de sectie hebben velen in het Smedinghuis een bijdrage geleverd. Zonder volledig te kunnen zijn, wil ik toch Wil van de Geer en zijn medewerkers noemen, inclusief de altijd behulpzame bemanning van de vaartuigen. Van de dagen aan boord heb ik altijd erg genoten. Ook de medewerkers van de Technische Dienst, van het laboratorium en de bibliotheek ben ik zeer dankbaar voor hun inzet, die vaak hun verplichtingen te boven ging. Tevens wil ik noemen de medewerkers van de Wetenschappelijke Afdeling en speciaal de subafdeling Waterhuishouding. Van een aantal heb ik directe steun ontvangen bij het onderzoek en het schrijven van dit proefschrift: Henk Wolters, Herman Winkels, Steven Vermij, Menno-Bart van Eerden en Cees Berger. En dan Bart Schultz, zonder hem zou het mij nooit gelukt zijn alle voetangels en klemmen, die her en der werden opgeworpen, uit de weg te ruimen en het onderzoek af te ronden. Zoals hij mij begeleidde zonder bemoeizuchtig te worden, maakte het werken met hem tot een groot genoegen.

In de loop van het onderzoek werden de banden met Wageningen steeds nauwer. Het maandelijks overleg met Bert Lijklema heb ik altijd zeer prettig gevonden en verplichtte mij elke maand iets tastbaars te produceren. In alle jaren van onze samenwerking heeft Bert steeds een groot vertrouwen in mij getoond hetgeen mij bijzonder stimuleerde. Ook enkele van mijn Wageningse collega's hebben hun bijdragen aan het slagen van deze promotie geleverd: Hans Aalderink, Christiaan Toet, Rudi Roijackers en Rob Portielje.

Tijdens onze wekelijkse autotocht naar Lelystad ontdekten Gerard Blom en ik dat onze beider onderzoeken een grote overlap vertoonden en besloten wij tot samenwerking. Uit deze intensieve samenwerking is het model STRESS-2d voortgekomen. Ook hebben onze discussies hun invloed gehad op de formulering van het lichtmodel. Bovenal was onze samenwerking altijd bijzonder gezellig. Hoe hij en Kees van de Guchte, tot hun middel in een moerasachtig meertje in Zweden, onze kano probeerden te redden, heeft mijn kijk op slibrijke wateren voor altijd bepaald.

Aan het afronden en het drukklaar maken van dit proefschrift heeft een aantal personen een zeer kundige bijdrage geleverd, waar ik hen toch voor wil bedanken: Willem Visscher, Hanneke van de Velde, Piet van Reeuwijk en de Geogroep.

Een groot aantal mensen zijn ongenoemd gebleven. Mijn familie en vrienden ben ik veel verschuldigd voor het geduld dat zij, met name het laatste jaar, hebben opgebracht. Aan Suzan hoop ik de verloren tijd te kunnen goedmaken. Klaas heeft de laatste jaren de voorwaarden geschapen om dit proefschrift te kunnen afronden. Ik hoop voor hem dezelfde stimulerende factor te kunnen zijn die hij voor mij was en is.

Juni 1992  
Liz van Duin

## Curriculum vitae

Elisabeth H.S. van Duin werd geboren op 26 maart 1961 in Wageningen. In 1979 behaalde zij het Atheneum-B-diploma aan de Scholengemeenschap Lelystad. In dat jaar begon zij ook haar studie aan de toenmalige Landbouwhogeschool in Wageningen.

Zij begon haar studie in de richting Levensmiddelentechnologie, maar verruilde die na twee jaar voor de studierichting Milieuhygiëne, specialisatie Waterzuivering. Haar eerste doctoraalvak betrof een onderzoek naar de zuurstofhuishouding in het Wolderwijd. Dit onderzoek voerde zij grotendeels uit bij de sectie Waterkwaliteit van de Rijksdienst voor de IJsselmeerpolders in Lelystad. Tijdens dit onderzoek kwam zij voor het eerst in aanraking met de systeemanalytische benadering binnen het waterkwaliteitsonderzoek en de ontwikkeling van simulatiemodellen en besloot zij zich hierin te specialiseren. Na modelstudies aan de Johns Hopkins University in Baltimore, V.S., bij het Zuiveringschap Hollandse Eilanden en Waarden in Dordrecht en bij de vakgroep Waterzuivering van de Landbouwhogeschool behaalde Van Duin in 1986 haar doctoraal diploma aan de inmiddels herdoopte Landbouwuniversiteit.

In oktober 1986 trad Van Duin in dienst bij diezelfde vakgroep Waterzuivering van de Landbouwuniversiteit. Gestationeerd bij de Rijksdienst voor de IJsselmeerpolders in Lelystad was zij gelijktijdig hoofd van de sectie Waterkwaliteit en van de sectie Afvoerhydrologie. In die positie werkte zij als projectleider van het Modelonderzoek Markermeer en het Stedelijk Wateronderzoek Lelystad. Inmiddels leidde een reorganisatie van de vakgroep waterzuivering tot het ontstaan van de sectie Waterkwaliteitsbeheer die valt onder de vakgroep Natuurbeheer. Daar vond Van Duin haar huidige werkkring als universitair docent.

# Contents

|   |    |
|---|----|
| <b>Samenvatting</b>   | 13 |
| <b>Summary</b>  | 23 |
| <b>1 Introduction</b>   | 31 |
| 1.1 History   | 31 |
| 1.1.1 The Zuiderzee project   | 31 |
| 1.1.2 Water quality in the IJsselmeer area                            | 33 |
| 1.2 Study outline   | 34 |
| 1.2.1 Background  | 34 |
| 1.2.2 Approach  | 35 |
| <b>2 The Markermeer</b>   | 39 |
| 2.1 Morphometry and morphology  | 39 |
| 2.1.1 Topography  | 39 |
| 2.1.2 Sediment  | 39 |
| 2.2 Limnology   | 44 |
| 2.2.1 Water balance   | 44 |
| 2.2.2 Water quality characteristics                                   | 46 |
| 2.2.3 Ecological aspects  | 46 |
| <b>3 Measurement methods and data analysis</b>                        | 49 |
| 3.1 Sampling strategy   | 50 |
| 3.1.1 Sampling sites  | 50 |
| 3.1.2 Sampling frequencies  | 52 |
| 3.2 Regular water quality measurements                                | 53 |
| 3.2.1 On site measurements  | 55 |
| 3.2.2 Sample analysis   | 57 |
| 3.3 Automatic measurement of water quality variables                  | 63 |
| 3.3.1 Suspended solids  | 65 |
| 3.3.2 Wind speed and direction  | 66 |
| 3.3.3 Water level and wave characteristics                            | 68 |
| 3.3.4 Flow velocity and direction                                     | 69 |
| 3.3.5 Irradiance and irradiance attenuation                           | 70 |
| 3.3.6 Dissolved oxygen concentration                                  | 76 |
| 3.3.7 Temperature   | 77 |
| 3.4 Sediment characteristics and relationships with light attenuation | 78 |
| 3.4.1 Sampling of sediment layers                                     | 78 |
| 3.4.2 Sediment traps  | 80 |
| 3.4.3 Fall velocity distribution experiments                          | 83 |
| 3.4.4 Specific attenuation coefficient                                | 89 |
| 3.5 Primary production experiments                                    | 94 |
| 3.5.1 General lay-out of the experiments                              | 94 |
| 3.5.2 Light and dark bottle experiments                               | 95 |
| 3.5.3 Cylinder experiments  | 99 |

|   |     |
|---|-----|
| <b>4 Sediment transport, resuspension and sedimentation (STRESS-2d)</b>                       | 105 |
| 4.1 Gross sedimentation   | 106 |
| 4.1.1 Estimation of the fall velocity distribution  | 107 |
| 4.1.2 Description of the sedimentation flux   | 109 |
| 4.2 Resuspension  | 109 |
| 4.2.1 Comparison of the contribution of different driving forces                              | 110 |
| 4.2.2 Wave hindcasting  | 110 |
| 4.2.3 Relationships for wave induced resuspension   | 116 |
| 4.3 Modelling of the sediment layers  | 118 |
| 4.3.1 Different concepts for sediment modelling   | 118 |
| 4.3.2 Numerical implications  | 119 |
| 4.4 Sediment transport  | 122 |
| 4.4.1 Vertical transport  | 122 |
| 4.4.2 Horizontal transport (WAQUA)  | 123 |
| 4.5 Model outline and parameter optimization  | 125 |
| 4.5.1 Model outline   | 126 |
| 4.5.2 Calibration of the water movement model   | 127 |
| 4.5.3 Optimization of the parameters of the sedimentation/resuspension model                  | 128 |
| 4.5.4 Validation of the STRESS-2d model   | 132 |
| <b>5 Under water light field</b>  | 141 |
| 5.1 Inherent optical properties   | 141 |
| 5.1.1 Properties of the radiation field   | 141 |
| 5.1.2 Properties of the aquatic medium  | 144 |
| 5.2 Apparent optical properties   | 146 |
| 5.2.1 Contribution of individual components to the attenuation coefficient                    | 147 |
| 5.2.2 Depth dependency of the attenuation coefficient   | 150 |
| 5.3 Combined Light Energy Attenuation Routine (CLEAR)   | 152 |
| 5.3.1 Model outline   | 152 |
| 5.3.2 Link with the STRESS-2d model   | 152 |
| 5.3.3 Validation of the light energy model  | 153 |
| <b>6 Growth of <i>Oscillatoria agardhii</i></b>   | 155 |
| 6.1 Phytoplankton growth in the IJsselmeer area   | 156 |
| 6.1.1 Phytoplankton succession in the IJsselmeer area   | 156 |
| 6.1.2 Habitat and growth characteristics of <i>Oscillatoria agardhii</i>                      | 158 |
| 6.1.3 Characteristics of the Markermeer in relation to growth of <i>Oscillatoria agardhii</i> | 161 |
| 6.1.4 Field experiments   | 163 |
| 6.2 Modelling the growth of <i>Oscillatoria agardhii</i>                                      | 173 |
| 6.2.1 Model SIMPLE  | 175 |
| 6.2.2 Model ALGA  | 179 |
| 6.3 Simulation of <i>Oscillatoria agardhii</i> with the integrated model                      | 186 |
| 6.3.1 Incorporation of ALGA in STRESS-2d and CLEAR  | 186 |
| 6.3.2 Optimization of the parameters of the integrated model                                  | 186 |

|          |   |            |
|----------|---|------------|
| 6.3.3    | Validation of the model ALGA  | 188        |
| <b>7</b> | <b>Application of the integrated model</b>  | <b>189</b> |
| 7.1      | Simulation of the present conditions  | 190        |
| 7.1.1    | Characterization of the simulation period   | 190        |
| 7.1.2    | Sediment transport and the light field for the present conditions   | 193        |
| 7.1.3    | Simulation of the growth of <i>Oscillatoria agardhii</i> for the present conditions                         | 200        |
| 7.2      | Simulations of the conditions after the impoldering of the Markerwaard                                      | 209        |
| 7.2.1    | Incorporation of the polder Markerwaard in the model schematization   | 209        |
| 7.2.2    | Sediment transport and the light field for the Markerwaard conditions                                       | 211        |
| 7.2.3    | Simulation of the growth of <i>Oscillatoria agardhii</i> for the Markerwaard conditions                     | 213        |
| 7.3      | Simulation of the conditions during increased flushing  | 215        |
| 7.3.1    | Incorporation of increased flushing in the model  | 215        |
| 7.3.2    | Sediment transport and the light field during increased flushing  | 216        |
| 7.3.3    | Simulation of the growth of <i>Oscillatoria agardhii</i> during increased flushing                          | 217        |
| <b>8</b> | <b>Conclusions</b>  | <b>219</b> |
| 8.1      | Characterisation of the physical conditions   | 219        |
| 8.1.1    | Suspended solids  | 219        |
| 8.1.2    | Light field   | 220        |
| 8.2      | Relationships between sediment transport and the light field and the growth of <i>Oscillatoria agardhii</i> | 221        |
| 8.2.1    | Monitoring  | 221        |
| 8.2.2    | Light and dark bottle experiments   | 221        |
| 8.2.3    | Cylinder experiments  | 221        |
| 8.3      | Model development and reliability   | 222        |
| 8.3.1    | Sediment transport, resuspension and sedimentation  | 222        |
| 8.3.2    | Light field   | 223        |
| 8.3.3    | Phytoplankton growth  | 224        |
| 8.4      | Applications  | 225        |
| 8.4.1    | Markerwaard   | 225        |
| 8.4.2    | Increased flushing  | 225        |
|          | <b>References</b>   | <b>227</b> |

## **Appendices**

|    |  |     |
|----|--|-----|
| 1  | Symbols and abbreviations  | 235 |
| 2  | Water balance of the Markermeer area   | 239 |
| 3  | Equipment  | 241 |
| 4  | Summary of weekly measurement data   | 245 |
| 5  | Data of the high frequency sampling periods  | 246 |
| 6  | Examples of incident irradiance measurements at Y112                                 | 253 |
| 7  | Composition of the nutrient solution   | 254 |
| 8  | Gross primary production rates related to the under water irradiance in the cylinder | 255 |
| 9  | Behaviour of the different wave models   | 260 |
| 10 | Optimization of the parameters of the sedimentation/ resuspension model              | 261 |
| 11 | Simulation of the bottle experiments with the model SIMPLE                           | 263 |
| 12 | Simulation of the cylinder experiments with the model SIMPLE                         | 265 |
| 13 | Simulation of the bottle experiments with the model ALGA                             | 267 |
| 14 | Simulation of the cylinder experiments with the model ALGA                           | 269 |
| 15 | Optimization of the parameters of the integrated model                               | 271 |
| 16 | Modified water balance   | 274 |

## Samenvatting

In dit proefschrift zijn de resultaten beschreven van een studie naar de waterkwaliteit van het Markermeer, welke zich concentreerde op de relatie tussen het sedimenttransport en het lichtklimaat enerzijds en de groei van de blauwalg *Oscillatoria agardhii* anderzijds. De studie bestond uit twee delen. Ten eerste de opzet van een uitgebreid meetprogramma met inbegrip van de gegevensanalyse en ten tweede de ontwikkeling, kalibratie en validatie van een set dynamische modellen.

### Het Markermeer

Het Markermeer is een groot, ondiep en zoet water, dat door een dijk gescheiden is van het IJsselmeer. Het Markermeergebied beslaat met inbegrip van het IJmeer en de Gouwzee een oppervlakte van ongeveer 68 000 hectare. De gemiddelde diepte van het meer bedraagt 3,6 meter. De bodem is vlak en voor ruim 60 procent bedekt met een fijne sliblaag, de IJsselmeerafzetting genaamd. Het meer wordt niet gevoed door belangrijke rivieren. Het water heeft daardoor een relatief lange verblijftijd van ongeveer anderhalf jaar.

Het Markermeer is geclassificeerd als een matig eutroof water. De gemiddelde fosforconcentratie bedraagt  $0,11 \text{ g} \cdot \text{m}^{-3}$  en de gemiddelde concentratie Kjeldahl-stofstof  $1,4 \text{ g} \cdot \text{m}^{-3}$ . Het doorzicht van het water is laag, de gemiddelde Secchi-schijf diepte bedraagt ongeveer 45 centimeter. De uitdoving van licht, uitgedrukt in de extinctiecoëfficiënt bedraagt  $3,5 \text{ m}^{-1}$ , met extreme waarden tot boven  $10 \text{ m}^{-1}$ . Deze hoge troebelheid wordt veroorzaakt door het hoge gehalte aan gesuspenderde stof, dat gemiddeld rond de  $45 \text{ g} \cdot \text{m}^{-3}$  ligt met maximumwaarden boven de  $150 \text{ g} \cdot \text{m}^{-3}$ . Door de grote strijklengten (tot 30 kilometer), de beperkte diepte (minder dan 5 meter), de vlakke bodemligging, het slibrijke sediment en de hoge windsnelheden die in het gebied kunnen optreden, is de opwerveling van sediment (resuspensie) van grote invloed op de waterkwaliteit in het gebied. De optredende resuspensie en sedimentatie van sediment veroorzaken vaak hoge maar vooral fluctuerende gehalten aan gesuspenderde stof. De uitdoving van lichtenergie in water hangt samen met het gehalte aan gesuspenderde stof. Daardoor is de beschikbaarheid van licht in de waterkolom ook wisselend en vaak laag.

De algensamenstelling van het Markermeer wordt gedomineerd door groenalgen. Soms treedt een tijdelijk ongewenste dominantie van blauwalgen op (blauwalgenbloei). Met name bloei van *Aphanizomenon flos-aqua* komt voor. Groei van *Oscillatoria agardhii* treedt regelmatig op, maar van bloei is geen sprake. De groei van waterplanten blijft beperkt tot de oeverzones en de Gouwzee.



## Achtergrond en opzet van de studie

De afwezigheid van bloei van de blauwalg *Oscillatoria agardhii* is een belangrijk kenmerk van de waterkwaliteit in het Markermeer. In het IJsselmeer en in de randmeren van Flevoland komt groei van *Oscillatoria agardhii* veel en overmatig voor. Met name in de randmeren leidt bloei van *Oscillatoria agardhii* tot ongewenste effecten. De vaak hoge en wisselende concentratie gesuspendeerde stof en het daarmee samenhangende lichtklimaat, werden verantwoordelijk geacht voor de afwezigheid van *Oscillatoria agardhii*-bloei in het Markermeer. Deze veronderstelling was echter meer gebaseerd op kwalitatieve dan op kwantitatieve gegevens.

De Houtribdijk is gesloten in 1976 en scheidt het Markermeer van het IJsselmeer. Oorspronkelijk was deze dijk bedoeld als de eerste stap in de aanleg van de Markerwaard, maar de Nederlandse publieke opinie ten aanzien van de inpoldering van het Markermeer veranderde en aanvullend onderzoek was nodig naar de kosten en effecten van de inpoldering. Onder andere was meer inzicht nodig in het effect van de aanleg van de Markerwaard op de waterkwaliteit in het overblijvende water: de Westelijke Randmeren. Omdat een gedeeltelijke inpoldering het transport van sediment en daarmee het lichtklimaat in het overblijvende water zal beïnvloeden, kan dit leiden tot ongunstige groeiomstandigheden voor algen en een toenemende groei van *Oscillatoria agardhii*. Behalve inpoldering worden andere inrichtings- en beheersmaatregelen voor het Markermeer overwogen, zoals aanpassing van de waterstand en verandering in de verblijftijd van het water in het meer. Ten einde het effect van mogelijke inrichtings- en beheersmaatregelen op de waterkwaliteit in het Markermeer te kunnen inschatten, was meer kwantitatieve informatie nodig over de fysische kenmerken van het systeem en hun effect op de groei van *Oscillatoria agardhii*.

Ten einde de kwantitatieve kennis van de fysische kenmerken van het Markermeer en het inzicht in de relaties tussen deze kenmerken en de groei van *Oscillatoria agardhii* te vergroten, is een uitgebreide veldstudie uitgevoerd. Deze bevatte een meerjarige monitoring van de waterkwaliteit op verschillende locaties in het Markermeer en een aantal kort durende experimenten met *Oscillatoria agardhii* in het veld.

Er is een dynamisch simulatiemodel ontwikkeld, waarin een sedimenttransport model (*STRESS-2d*) en een lichtuitdovingsroutine (*CLEAR*) samengevoegd zijn. Daarna zijn deze modellen gecombineerd met een bestaand algengroeiemodel (*ALGA*). Met het gecombineerde model zijn scenariostudies uitgevoerd, waarin het effect van verschillende beheersmaatregelen op de groei van *Oscillatoria agardhii* in het Markermeer is gesimuleerd.

## Meetprogramma en data analyse

Van 1987 tot en met 1989 is een uitgebreid meetprogramma uitgevoerd in het zomerhalfjaar (april tot en met november). In 1990 is een aantal aanvullende experimenten uitgevoerd. Het programma bevatte vier onderdelen:

- a een meetprogramma dat wekelijks op twee lokaties in het meer is uitgevoerd, waarbij werden bepaald: temperatuur, zuurstofconcentratie, zuurgraad, Secchi-schijfdiepte, extinctiecoëfficiënt, nutriëntconcentraties, concentratie gesuspendeerde stof, chlorofyl-a-concentratie, algensamenstelling en -aantallen;
- b continue registratie van zuurstof, instraling op verschillende diepte, zuurstofconcentratie, windsnelheid en -richting, waterstand, golfhoogte en golfperiode. Twee tot drie maal per jaar zijn gedurende twee weken, zes tot twaalf watermonsters per dag genomen, die geanalyseerd zijn op het gehalte gesuspendeerde stof;
- c karakteristieken van sediment- en extinctie-eigenschappen zijn onderzocht. De valsnelheidsverdeling in watermonsters, sedimentvalmateriaal en materiaal van de sedimenttoplaag is bepaald. In diezelfde experimenten is de specifieke extinctiecoëfficiënt bepaald van materiaal, gekarakteriseerd door een zekere valsnelheid;
- d primaire produktie-experimenten zijn uitgevoerd met *Oscillatoria agardhii* in het veld, met de klassieke lichte en donkere flessen-methode en met een aangepaste versie hiervan, waarin flessen door het water omhoog en naar beneden werden bewogen. Tevens zijn groeiexperimenten uitgevoerd in een perspex cilinder, gevuld met een *Oscillatoria agardhii*-suspensie, die in 1989 en 1990 gedurende enkele weken in het Markermeer stond opgesteld.

Aan de uitvoering van het meetprogramma en de analyse van watermonsters is veel inspanning besteed. Tevens is veel energie gestoken in het verbeteren van de meetnauwkeurigheid en het optimaliseren van de metingen met wisselend succes.

Bij analyse van de meetgegevens werden grote variaties aangetroffen in het gehalte en de samenstelling van de gesuspendeerde stof in het Markermeer. Het gehalte aan totaal gesuspendeerde stof varieerde tussen 7 en  $180 \text{ g} \cdot \text{m}^{-3}$ , het percentage organische stof van het totaal aan gesuspendeerde stof varieerde tussen de 15 en de 75 procent. Dit percentage nam af bij toenemende concentraties gesuspendeerde stof, doordat bij resuspensie van sediment de concentratie gesuspendeerde stof toenam, maar de bijdrage van organische stof afnam. De gemeten sedimentatieflux nam eveneens toe bij toenemende concentraties gesuspendeerde stof en varieerde tussen de 1 en de  $200 \text{ g} \cdot \text{m}^{-2} \cdot \text{h}^{-1}$ . De interne sedimentvrucht is geschat op ongeveer een miljard ton per jaar. De valsnelheidsverdeling varieerde eveneens met de concentratie gesuspendeerde stof. Indien de concentratie gesuspendeerde stof toenam, nam de relatieve bijdrage van deeltjes met een hoge valsnelheid toe. De gemiddelde valsnelheid van de deeltjes varieerde tussen de  $10 \cdot 10^{-6}$  en  $100 \cdot 10^{-6} \text{ m} \cdot \text{s}^{-1}$ .

De uitdoving van lichtenergie in water, uitgedrukt in de extinctiecoëfficiënt, toonde een significante relatie met de concentratie gesuspenderde stof. De mate van uitdoving per hoeveelheid gesuspenderde stof uitgedrukt in de specifieke extinctiecoëfficiënt, is echter niet constant. Wanneer de concentratie gesuspenderde stof verandert, verandert ook de specifieke extinctiecoëfficiënt. Deeltjes met een lagere valsnelheid hebben een hogere specifieke extinctiecoëfficiënt dan deeltjes die sneller bezinken. Dit wordt toegerekend aan het feit dat zowel de valsnelheid van deeltjes als de mate van uitdoving van deeltjes gerelateerd is aan de grootte van de deeltjes. De gemiddelde bijdrage van chlorofyl-a, gesuspenderde stof en water met de daarin opgeloste stoffen is geschat op respectievelijk 25, 57 en 18 procent. De bijdrage van gesuspenderde stof wordt met name veroorzaakt door deeltjes met een lage valsnelheid, doordat zowel hun verblijftijd in de waterfase als hun uitdoving per eenheid van massa groter is. Een geringe afname van de extinctiecoëfficiënt met de diepte is waargenomen op dagen waarop het water vrij helder was.

Uit analyse van de wekelijkse metingen bleek dat de chlorofyl-a-concentratie toenam wanneer het gehalte aan gesuspenderde stof hoger werd. Dit betekent dat de algenconcentratie wordt beïnvloed door resuspensie en sedimentatie. Daar staat tegenover dat een grote toename in de verhouding chlorofyl-a en organische stof is waargenomen wanneer de concentratie gesuspenderde stof afnam, wat alleen aan een groei van algen in de waterfase kan worden toegerekend.

In de experimenten met lichte en donkere flessen zijn maximale bruto produktiesnelheden van  $14 \text{ gO}_2\cdot\text{gChlorofyl-a}^{-1}\cdot\text{h}^{-1}$  gemeten. Groei van *Oscillatoria agardhii* trad op tijdens alle experimenten. De kwantitatieve relatie tussen de produktie en de beschikbare lichtenergie varieerde echter voor elk experiment, waarmee het belang van aanpassing van de groeiparameters aan de lichtomstandigheden is bevestigd. Ten einde het effect van verticale menging op de groei mee te nemen tijdens de experimenten, is een deel van de lichte flessen tijdens de experimenten op en neer bewogen in de waterkolom. Hoewel er wel sprake leek van enig effect van verticale menging op de groei, is geen eenduidige trend in het effect ontdekt.

Gedurende enkele weken in 1989 en 1990 is een 2.8 meter hoge perspex cilinder in het Markermeer geplaatst, die was gevuld met een suspensie van *Oscillatoria agardhii*. Door middel van een systeem van slangen en pompen, is de suspensie in de cilinder gemengd. Om de dag zijn watermonsters uit de cilinder genomen en is in de cilinder het zuurstofgehalte continu gemeten. De maximale bruto produktiesnelheid die in de cilinder is gemeten was gelijk aan die in de flessenexperimenten gemeten is en lag tussen de 12 en  $14 \text{ gO}_2\cdot\text{gChlorofyl-a}^{-1}\cdot\text{h}^{-1}$ . De maximale respiratie bij een temperatuur van ongeveer  $20^\circ\text{C}$  bedroeg  $2,5 \text{ gO}_2\cdot\text{gChlorofyl-a}^{-1}\cdot\text{h}^{-1}$ . Uit de meetresultaten bleek duidelijk dat de efficiëntie waarmee lichtenergie voor groei wordt aangewend niet constant is, maar regelmatig, zo niet continu, onderhevig is aan aanpassingen. Twee soorten aanpassingen zijn onderscheiden:

#### *snelle aanpassing*

bij zonsopgang is de efficiëntie waarmee lichtenergie wordt gebruikt voor groei hoog, maar dit kan veranderen gedurende de dag. Op dagen met hoge instralingswaarden (maximale dieptegemiddelde instraling  $> 200 \mu\text{E}\cdot\text{m}^{-2}\cdot\text{s}^{-1}$ ), treedt meestal binnen enkele uren aanpassing van de groeiparameters van *Oscillatoria agardhii* op. Op dagen met lagere instralingswaarden is dit verschijnsel niet waargenomen;

#### *langzame aanpassing*

aanpassing van groeiparameters aan omstandigheden met weinig licht (maximale dieptegemiddelde instraling  $< 100 \mu\text{E}\cdot\text{m}^{-2}\cdot\text{s}^{-1}$ ) treedt op binnen enkele dagen.

Hoewel de experimenten waardevolle informatie opleverden wat betreft de groeikarakteristieken van *Oscillatoria agardhii* in het specifieke lichtklimaat van het Markermeer, gaven de meetresultaten geen uitsluiting of het lichtklimaat van het Markermeer de beperkende factor is voor groei van *Oscillatoria agardhii* op de lange termijn.

### **Modelontwikkeling**

De modelontwikkeling is uitgevoerd in drie stappen. Gestart is met de ontwikkeling van een model voor sedimenttransport, resuspensie en sedimentatie in ondiepe meren en de kalibratie van dit model op de gegevens verzameld voor het Markermeer (STRESS-2d). Vervolgens is een model ontwikkeld en gekalibreerd, waarmee de uitdoving van licht door gesuspendeerde stof en door *Oscillatoria agardhii* is beschreven (CLEAR). Als laatste is het *Oscillatoria agardhii*-groeimodel ALGA gecombineerd met de beide andere modellen.

#### *Sediment transport, resuspensie en sedimentatie (STRESS-2d)*

Het tweedimensionale model voor Sediment Transport, Resuspensie en Sedimentatie in ondiepe meren (Shallow lakes) is ontwikkeld door Blom en Van Duin voor meren in het IJsselmeergebied. Met het model kunnen concentraties gesuspendeerde stof in de waterfase worden gesimuleerd. Het model gebruikt het bestaande tweedimensionale horizontale hydrodynamische model WAQUA als basis. Bij gebruik van WAQUA wordt een studiegebied verdeeld in een groot aantal compartimenten. Voor elk van deze compartimenten wordt binnen WAQUA de advectie-diffusie vergelijking opgelost. In STRESS-2d is deze advectie-diffusie vergelijking uitgebreid met een extra bronterm (resuspensie) en een extra putterm (sedimentatie).

De sedimentatieflux is berekend met een lineaire relatie tussen de concentratie gesuspendeerde stof en de bezinksnelheid. Om variaties in de bezinksnelheid te verrekenen zijn verschillende sedimentfracties gebruikt, welke zijn onderscheiden naar valsnelheid. In de toepassing

van *STRESS-2d* op het Markermeer zijn vier verschillende fracties gebruikt, die elk een ander deel van de valsnelheidsverdeling representeren.

De resuspensieflux is gerelateerd aan de orbitaalsnelheid aan de bodem, die wordt veroorzaakt door wind geïnduceerde golven. De orbitaalsnelheden aan de bodem zijn berekend uit de significante golfhoogte en -periode, die op hun beurt zijn berekend met een semi-empirisch model gebaseerd op de Sverdrup, Munk en Bretschneider-relaties. In dit steady-state-model zijn de golfhoogte en -periode ofwel door de strijklengte ofwel door de diepte beperkt. De overeenkomst tussen de gesimuleerde en de gemeten golfkarakteristieken was groot. Voor de relatie tussen de maximale orbitaalsnelheid aan de bodem en de resuspensieflux is een aangepaste versie van de relatie van Lam en Jacquet gebruikt. Resuspensie treedt alleen dan op wanneer de maximale orbitaalsnelheid een bepaalde grenswaarde, de zogenaamde kritische orbitaalsnelheid, overschrijdt. Voor de berekening van de resuspensieflux in *STRESS-2d* zijn dezelfde fracties gebruikt als in de berekening van de sedimentatieflux. Aan elke fractie is een eigen kritische orbitaalsnelheid toegekend. De waarde van deze parameters is samen met een proportionaliteitsparameter verkregen door parameteroptimalisatie, waarbij de gemeten concentraties gesuspendeerde stof en de gemeten sedimentatiefluxen zijn gebruikt.

Het bodemsediment is gemodelleerd met twee lagen: een dunne niet-cohese waterige toplaag met een kritische dikte van enkele millimeters en een laag met variabele dikte, die de IJsselmeerafzetting representeert. Tijdens perioden waarin de sedimentatie groter is dan de resuspensie zal de dikte van de toplaag groter worden dan de kritische dikte en wordt sediment getransporteerd van de toplaag naar de onderlaag (consolidatie). Tijdens perioden waarin de resuspensie groter is dan de sedimentatie wordt sediment getransporteerd van de onderlaag naar de toplaag (erosie). Daarnaast is een continue uitwisseling van sediment tussen de beide lagen berekend (turbatie). De snelheid waarmee sediment wordt getransporteerd door consolidatie, erosie en turbatie is constant. Het effect van de grootte van deze constanten is in de verschillende optimalisatieberekeningen vergeleken.

De waarden van de resuspensieparameters en de kritische dikte van de sedimenttoplaag zijn vastgesteld met behulp van formele parameterschattingsmethoden. Hiervoor zijn de *STRESS-2d*-relaties gebruikt, maar is het horizontaal transport verwaarloosd. De beste parametersets zijn vergeleken in simulatieberekeningen met het complete *STRESS-2d*-model. Met de uiteindelijk verkregen parameterset is het gehalte gesuspendeerde stof in het water van het Markermeer vrij nauwkeurig gesimuleerd voor ten minste 85 procent van de weersomstandigheden. Bij extreme windsnelheden nam de modelnauwkeurigheid af en is het gesuspendeerde stofgehalte vaak onderschat. Omdat extreme windsnelheden meestal buiten het groeiseizoen optreden, zijn deze minder interessant voor de toepassingen in dit project.

## Lichtklimaat

Voor de berekening van de hoeveelheid licht onder water, die beschikbaar is voor de groei van algen, is een subroutine ontwikkeld (*CLEAR*, Combined Light Energy Attenuation Routine) die op eenvoudige wijze kan worden gecombineerd met *STRESS-2d*.

In deze subroutine worden tijdseries van instraling afkomstig van het KNMI omgezet in de hoeveelheid lichtenergie die onder water beschikbaar is voor fotosynthese (PAR). Vervolgens wordt een dieptegemiddelde waarde van de verticale neerwaartse extinctiecoëfficiënt berekend. Deze coëfficiënt geeft de uitdoving van lichtenergie met de diepte weer. Bij de berekening wordt de bijdrage van de diverse lichtabsorberende en verstrooiende componenten berekend uit een lineaire relatie tussen de concentratie van elke component en zijn specifieke extinctiecoëfficiënt. In *CLEAR* is de bijdrage van vijf verschillende componenten onderscheiden, namelijk vier gesuspendeerde stoffracties en de bijdrage van *Oscillatoria agardhii*. De gesuspendeerde stoffracties zijn dezelfde die in het *STRESS-2d* model zijn gebruikt. De specifieke extinctiecoëfficiënt van elke fractie is gemeten in de valsnelheidsverdelingsexperimenten. Hoewel de nauwkeurigheid in de metingen niet groot was, zijn de resultaten van deze coëfficiënten redelijk consistent. Simulatie van de extinctiecoëfficiënt met het model leverde acceptabele resultaten op.

Met een over de diepte geïntegreerde versie van de Lambert-Beer-vergelijking wordt de dieptegemiddelde instraling berekend uit de dieptegemiddelde extinctie coëfficiënt en de instraling onder het wateroppervlak.

## Groei van *Oscillatoria agardhii*

Bij de modellering van groei van *Oscillatoria agardhii* in het Markermeer is uitgegaan van niet-evenwichtconcepten. Daarmee is competitie tussen algensoorten onderling uitgesloten, maar zijn tijdschalen en fluctuaties in omgevingsvariabelen veel belangrijker dan wanneer wordt uitgegaan van een evenwichtssituatie. Met twee dynamische modellen is de in de experimenten gemeten produktie van *Oscillatoria agardhii* gesimuleerd. De afwijking tussen gemeten en gesimuleerde waarde was groot bij gebruik van het model *SIMPLE*. In het model *SIMPLE* is de produktie van *Oscillatoria agardhii* gerelateerd aan beschikbaar licht volgens een Steele-relatie. Het model is voor elk experiment afzonderlijk gecalibreerd, wat resulteerde in zeer verschillende parametersets per experiment. Daaruit is geconcludeerd dat aanpassing van groeiparameters aan de lichtomstandigheden optreedt en dat het van belang is deze aanpassing in een *Oscillatoria agardhii*-model op te nemen.

In het model *ALGA*, dat ontwikkeld is door Vermij, is een aanpassing van parameters aan de lichtcondities ingebouwd. In het model zijn een onder- en bovengrens gedefinieerd waartussen de maximale produktie

en de efficiëntie waarmee licht wordt aangewend voor groei kunnen variëren. Indien de beschikbare lichtenergie in het water boven een bepaalde grenswaarde komt (hoge instralingscondities), dan naderen deze parameters de ondergrens. Komt de beschikbare lichtenergie onder de grenswaarde (lage instralingscondities), dan naderen zij hun bovengrens. Met deze benadering is rekening gehouden met de snelle aanpassing die is gemeten in de veldexperimenten. Het model is gebruikt voor de simulatie van de in de veldexperimenten gemeten producties, waarbij de grenswaarde voor hoge en lage lichtcondities is geoptimaliseerd. De geoptimaliseerde waarde was zo laag, dat de groeiparameters vrijwel continue gelijk waren aan hun bovengrens. Hoewel het modelleren van aanpassing van groeiparameters een verbetering is vergeleken met modellen met vaste groeiparameters, was het niet mogelijk met het model een nauwkeurige simulatie van de gemeten producties te geven.

De snelle aanpassing van groeiparameters aan de lichtcondities is in het model ALGA opgenomen, de langzame aanpassing is dat echter niet. Simulatie van de groei van *Oscillatoria agardhii* voor perioden van enkele maanden in de diepe delen van het meer, leverde redelijke resultaten op. De langzamere groei van *Oscillatoria agardhii* in de ondiepe delen ten opzichte van de groei in de diepe delen is met het model echter niet goed te simuleren. De beperkte groei van *Oscillatoria agardhii* in de ondiepe delen van het Markermeer kan echter wel een sleutelrol spelen in de afwezigheid van overmatige groei van deze algensoort in het meer.

Simulatie van de groei van *Oscillatoria agardhii* met de gecombineerde modellen STRESS-2d, CLEAR en ALGA leidde niet tot de verwachte resultaten. Dit is met name toe te schrijven aan het beperkt functioneren van biologische deel van het model. Dit kan verschillende oorzaken hebben, zoals: de constante verliessnelheid, de afwezigheid van langzame aanpassing van groeiparameters en het uitsluiten van competitie met andere algensoorten.

### **Modeltoepassing**

Met het geïntegreerde model is de huidige situatie gesimuleerd met tijdseries van 1988 en 1989. In het model WAQUA is geen rekening gehouden met neerslag en verdamping. Om bij de lange termijn simulaties met sluitende waterbalansen te rekenen zijn de in- en uitgelaten hoeveelheden water en de bijbehorende algenconcentraties aangepast. Simulatie van de concentratie gesuspenderde stof leidde tot goede resultaten, enkele veranderingen in de lokatie van de IJsselmeerafzetting waren echter onrealistisch. De overeenkomst tussen gemeten en berekende *Oscillatoria agardhii*-aantallen was slecht.

Een vergelijking is uitgevoerd tussen de gesimuleerde waterkwaliteit in de resterende wateren na aanleg van de Markerwaard en die van de

huidige situatie. Uit de resultaten blijkt dat het effect van de gedeeltelijke inpoldering van het Markermeer op het gesimuleerde gesuspendeerde stofgehalte en de extinctiecoëfficiënt groot is. Over het geheel genomen zijn het gesimuleerde concentraties gesuspendeerde stof en de extinctiecoëfficiënt na inpoldering beduidend lager dan in de huidige situatie. Dit is voornamelijk toe te schrijven aan een reductie in de strijklengten en veranderingen in het stromingspatroon. In de Gouwzee, het IJmeer en het Gooimeer is nauwelijks effect merkbaar. Hoewel enige voorzichtigheid betracht moet worden bij de interpretatie van de resultaten van het *Oscillatoria agardhii*-model, kan worden geconcludeerd dat in vergelijking met de huidige situatie de groei van *Oscillatoria agardhii* waarschijnlijk zal toenemen in de overblijvende wateren na aanleg van de Markerwaard. Dit komt overeen met de conclusie van de commissie IJff dat de kans op tijdelijke bloei van *Oscillatoria agardhii* toeneemt.

In een derde scenariostudie zijn de effecten van een verhoogde doorspoeling met IJsselmeerwater nagegaan. In deze scenariostudie is de verblijftijd van het water vrijwel gehalveerd. Uit de simulatieresultaten bleek dat het effect op de concentratie gesuspendeerde stof en de extinctiecoëfficiënt nihil is. Wel is in de simulatieresultaten een kleine toename van de *Oscillatoria agardhii*-concentratie geconstateerd, doordat de concentratie in het IJsselmeer meestal hoger is dan in het Markermeer. Deze verhoging is het grootst vlakbij de sluizen waar het IJsselmeerwater wordt ingelaten, maar neemt snel af door menging met het open water.



## Summary

This thesis reports on a study of the water quality of the Markermeer, focusing on the relationships between sediment transport, the light field and the growth of *Oscillatoria agardhii*. The study comprises two aspects: an extensive data collection program accompanied with the data analysis, and the development, calibration and application of a set of dynamical models.

### The Markermeer

The Markermeer is a large shallow fresh water lake in the centre of the Netherlands. The surface area of the Markermeer, including the IJmeer and the Gouwzee, is estimated at 68,000 hectares. The average depth is 3.6 metres. The lake bottom is rather flat and for 60 % covered with a fine silty layer, the IJsselmeer deposit. No major rivers discharge into the lake, the residence time of the water is estimated at 1.5 year.

The lake is marked moderately eutrophic, with mean phosphate concentrations of around  $0.11 \text{ g} \cdot \text{m}^{-3}$  and Kjeldahl nitrogen concentrations of approximately  $1.4 \text{ g} \cdot \text{m}^{-3}$ . The optical depth of the lake is low, with average values of around 45 centimetres. The average attenuation coefficient for light energy is  $3.5 \text{ m}^{-1}$ , with extreme values of over  $10 \text{ m}^{-1}$ . This low transparency of the lake water is caused by the high suspended solids content of the water, with extreme values higher than  $150 \text{ g} \cdot \text{m}^{-3}$  and a average values of approximately  $45 \text{ g} \cdot \text{m}^{-3}$ . Due to the high fetch (up to 30 kilometres), the limited depth (less than 5 metres), the flat bottom, the silty sediments and the high wind speeds occurring in the area, resuspension and sedimentation of sediment are important processes. They induce often high and fluctuating suspended solids concentrations. Hence, the availability of light energy in the water column is also fluctuating too and often low.

The phytoplankton composition of the lake is dominated by green algae. Blooms of blue-green algae occur, mainly of *Aphanizomenon flos-aqua*. Growth of *Oscillatoria agardhii* is observed regularly, but abundant blooms do not occur. The growth of epiphytes and submersed macrophytes is limited to the near shore areas and the Gouwzee.

### Study background and approach

The absence of persistent blooms of the blue-green algae *Oscillatoria agardhii* is a remarkable feature of the Markermeer. In the IJsselmeer and in the smaller Randmeren in the area, growth of *Oscillatoria agardhii* is abundant. Especially in the Randmeren, phytoplankton composition is generally dominated by blooms of *Oscillatoria agardhii*. The often high and fluctuating suspended solids concentration and the related

characteristic light field of the Markermeer are held responsible for the absence of blooms of *Oscillatoria agardhii*. However, this hypothesis was based on qualitative knowledge only.

In 1976 the Houtribdijk, a dike that separates the Markermeer from the IJsselmeer, was closed. This dike was meant to be the first step towards the construction of the polder the Markerwaard but the Dutch opinion towards the reclamation of the Markermeer changed. One of the emerging questions was that more knowledge was needed on the impact of the impoldering of the Markermeer on the water quality in the remaining water areas. As the impoldering will influence the extent of sediment transport and therewith the underwater light field, it may lead to unfavourable phytoplankton conditions and an increasing occurrence of temporary blooms of *Oscillatoria agardhii*, as was observed in other lakes in the area. Other management measures have been considered, among which the alteration of the water level and the reduction of the residence time. To assess the effects of different potential development and management measures, more quantitative information was needed on the characteristic physical conditions of the Markermeer and their effects on the growth of *Oscillatoria agardhii*. The need for an operational tool increased. This tool had to be able to quantify the effect of management measures on the light field and the growth of *Oscillatoria agardhii* in the Markermeer. Therefore, in 1984 a study was started to assess the consequences of regional developments for the water quality aspects in the Markermeer area that are related to the growth of *Oscillatoria agardhii*.

To increase the quantitative knowledge on the characteristic physical conditions of the Markermeer and the insight in the relationship between the growth of *Oscillatoria agardhii* and these characteristic conditions, an extensive field program has been carried out. This program contained both the detailed monitoring of the water quality of the Markermeer at different sites and more specific term experiments with *Oscillatoria agardhii*.

A dynamic simulation model is developed, which describes the characteristic sediment transport and light field in the Markermeer by combining a sediment transport model (*STRESS-2d*) and a light attenuation routine (*CLEAR*). Afterwards, these models were linked with an existing *Oscillatoria agardhii* growth model (*ALGA*). With the integrated models, scenario studies have been performed of the effect of different development and management measures on the occurrence of *Oscillatoria agardhii* in the Markermeer.

#### **Data collection and analysis**

The field program comprised the following parts:

- a a monitoring program during 1987, 1988 and 1989, with weekly measurements at two sites in the lake. This included measurements of

temperature, dissolved oxygen, pH, Secchi-depth, attenuation coefficient, nutrient concentration, suspended solid concentration, chlorophyll-a concentrations and phytoplankton cell numbers and composition;

- b continuous registration of water quality variables, including temperature, irradiance at different depths, dissolved oxygen concentration, wind speed and direction, water levels, wave height and wave period. Two to three times each year for a period of two weeks, suspended solids concentration was analyzed in 6 to 12 samples per day;
- c sediment characteristics and light attenuation characteristics were measured, including the fall velocity distribution measured in water samples, samples from sediment traps and from the sediment top layer. For suspended solids characterised by a certain fall velocity range, the specific attenuation coefficient was measured too;
- d primary production experiments with *Oscillatoria agardhii* suspensions were carried out in the field with classical light and dark bottle experiments and with a modified version of these experiments in which bottles were moved up and down the water column. Furthermore, growth experiments with *Oscillatoria agardhii* have been performed in a perspex cylinder placed in the Markermeer for a couple of weeks in 1989 and 1990 at Y112.

The effort taken in the measurement program and sample analysis was extensive. Much effort was also devoted to improve the accuracy of the measurements, although not always with success.

Analysis of the data showed that the suspended solids concentration and suspended solids composition are very variable in the Markermeer. The suspended solids content varied between 7 and 180 g·m<sup>-3</sup>, the percentage of the organic matter to the suspended solids concentration between 15 and 75%. This ratio decreased when the suspended solids concentration increased, because resuspension of sediment increased the suspended solids concentration but decreased the relative contribution of organic matter. The measured sedimentation flux increased also when the suspended solids concentration increased and varied between 1 and 200 g·m<sup>-2</sup>·h<sup>-1</sup>. The internal load of the lake is estimated in the order of magnitude of one billion tons per year. The fall velocity distribution varies with the total suspended solids concentration. The relative contribution of the solids with a high fall velocity increases when the suspended solids concentration is high. The mean fall velocity of the solids ranges from 10·10<sup>-6</sup> to 110·10<sup>-6</sup> m·s<sup>-1</sup>.

The attenuation of light energy in water, expressed in the attenuation coefficient, shows a significant correlation with the suspended solids content. However, the extent of light attenuation per amount of suspended solids mass (the specific attenuation), is not constant. When the suspended solids concentration changes, so does the specific attenuation coefficient. The specific attenuation of solids within a certain range of fall velocity however, is approximately constant. Solids with a smaller fall velocity, thus settle more slowly, show a higher attenuation of light

energy per unit concentration than solids which settle faster. This is attributed to the fact that both the fall velocity and the attenuation of light are related to the size of the solids. The average contribution of chlorophyll-a, suspended solids and water with dissolved substances to the total attenuation of light energy is estimated at respectively 25, 57 and 18%. The contribution of suspended solids is mainly due to the solids with small fall velocities. At days when the water was relatively clear, a slight decrease of the attenuation coefficient with the depth was noticed.

Analysis of the weekly obtained data showed that the chlorophyll-a concentration of the water increased along with the suspended solids concentration. Hence, the phytoplankton concentration is affected by resuspension and sedimentation. On the other hand, an increase in the chlorophyll-a/organic matter ratio has been observed when the suspended solids concentration decreased. This can be attributed to the effect of growth in the water phase.

In the light and dark bottle experiments, a maximum gross production of  $14 \text{ gO}_2 \cdot \text{gChla}^{-1} \cdot \text{h}^{-1}$  was measured. Growth of *Oscillatoria agardhii* occurred in all the experiments. The quantitative relation between the gross production and the available light energy varied for each experiment, indicating the importance of adaptation of growth parameters to the light conditions. Part of the light bottles were moved up and down the water column during the experiments, to incorporate the effect of vertical mixing on the production of algae. Though some effect of vertical mixing on the growth of *Oscillatoria agardhii* was found, no conclusive increase or decrease was observed.

A 2.8 metres high cylinder was placed in the Markermeer at Y112 and filled with a suspension of *Oscillatoria agardhii*. By a system of pumps and tubes, the suspension in the cylinder was mixed and samples were taken every two days. Dissolved oxygen concentrations were registered continuously. The same maximum gross production rates as in the bottle experiments is obtained: a range of  $12 - 14 \text{ gO}_2 \cdot \text{gChla}^{-1} \cdot \text{h}^{-1}$ . Maximum respiration rates of  $2.5 \text{ gO}_2 \cdot \text{gChla}^{-1} \cdot \text{h}^{-1}$  were observed for temperatures of around  $20^\circ\text{C}$ . The experimental data showed clearly that maximum production and the light utilization efficiency were not constant, but were frequently or even continuously, subject to adaptation. Two kinds of adaptation were observed:

- fast adaptation* at sunrise, light utilization efficiency is high but this may change during the day. During days with high maximum mean under water irradiance values ( $> 200 \mu\text{E} \cdot \text{m}^{-2} \cdot \text{s}^{-1}$ ), growth parameters of *O. agardhii* usually adapt to high light conditions within a few hours. During days with lower maximum values, growth parameters tend to keep their high efficiency;
- slow adaptation* adaptation of growth parameters to low irradiance levels (mean under water irradiance  $< 100 \mu\text{E} \cdot \text{m}^{-2} \cdot \text{s}^{-1}$ ) occurs within a few days.

Though the experiments produced valuable information about the growth characteristics of *Oscillatoria agardhii* under the light conditions of the Markermeer, the experimental results were not conclusive whether or not the light field of the Markermeer is the limiting factor for growth of *Oscillatoria agardhii* in the long run.

### **Model development and applications**

The model development was performed in three steps. At first a model that describes sediment transport, resuspension and sedimentation in shallow lakes was developed and calibrated on the Markermeer data set (*STRESS-2d*). Secondly a routine was added, in which light attenuation by suspended solids and *Oscillatoria agardhii* was described (*CLEAR*). Finally, the *Oscillatoria agardhii* growth model ALGA has been integrated with the other models. Prior to the integration, each model was calibrated and validated separately.

#### *Sediment Transport, Resuspension and Sedimentation (STRESS-2d)*

The two-dimensional model for Sediment Transport, Resuspension and Sedimentation in Shallow lakes (*STRESS-2d*) is developed by Blom and Van Duin for lakes in the IJsselmeer area. The model is based on an existing two-dimensional horizontal hydrodynamic model, *WAQUA*. In *WAQUA* the studies area is divided in many compartments, for which the advection diffusion equation is solved. In *STRESS-2d* this advection diffusion equation is expanded with an additional source term (resuspension) and an additional sink term (sedimentation).

The sedimentation flux is estimated from a linear relationship between the suspended solids concentration and the settling speed. To account for variation in the settling speed, different fractions are used, distinguished by differences in fall velocity. In the Markermeer application four different fractions were used, each representing a different part of the fall velocity distribution.

The resuspension flux is related to the bottom orbital velocities produced by wind waves. Bottom orbital velocities are computed from the significant wave height and the significant wave period, which are estimated with a semi-empirical model based on the Sverdrup, Munk and Bretschneider method. In this steady state model, wave height and period are either fetch or depth limited. The agreement between simulated wave characteristics and measured ones was very good. The equation of Lam and Jaquet is used to relate the resuspension flux to the maximum orbital velocity. In this equation, resuspension occurs if the maximum orbital velocity exceeds a certain threshold value, the critical orbital velocity. In *STRESS-2d*, the same fractions, based on fall velocity that are used for the computation of the sedimentation flux, are used in the computation of the resuspension flux. Different critical orbital velocities are assigned to each fraction. The values of these critical orbital veloci-

ties and the concomitant proportionality constants are obtained by parameter optimization, using measured suspended solids concentrations and sedimentation fluxes.

The lake sediment is modelled with two layers: a thin non-cohesive watery top layer with a critical thickness of a few millimetres overlying a layer representing the IJsselmeer deposit. During periods with nett sedimentation, the thickness of the top layer will exceeds the critical value and surplus material is transported to the lower layer (consolidation). During the periods with nett resuspension, sediment is transported from the lower layer to the top layer (erosion). Additional mass transport between both layers is incorporated (turbation). The velocity of mass transport by consolidation, erosion and turbation is fixed. Different values of these velocities are compared in the parameter optimization runs.

Values of the resuspension parameters, the critical thickness of the sediment top layer and of the consolidation, erosion and turbation velocity were assessed by formal parameter optimization, using the *STRESS-2d* equations while ignoring horizontal transport. The best parameter sets were compared in the *STRESS-2d* model. With the final parameter set, the suspended solids concentration in the water of the Markermeer could be simulated rather accurately for at least 85% of the occurring weather conditions. With extreme wind speeds, the accuracy of the model decreases somewhat as the simulated suspended solids concentrations is sometimes lower than the measured values. As extreme wind events occur generally outside the growing season, these events are less important within the scope of this project.

#### *Light field (CLEAR)*

To estimate the available light energy for phytoplankton growth in the water phase, a Combined Light Energy Attenuation Routine (*CLEAR*) is developed, which could easily be integrated in the *STRESS-2d* model.

In the model, time series of light energy obtained from the KNMI, are transposed to under water irradiance values in the range of the Photosynthetically Available Radiation (PAR). A depth averaged value of the (vertical downward) attenuation coefficient, which describes the decrease of light energy with the depth, is estimated from the various light scattering or absorbing components. The contribution of each component to the total vertical downward light attenuation is modelled as a linear relationship between the concentration of the component and its specific attenuation coefficient. In this model five components are distinguished: four suspended solids fractions and the number of cells of *Oscillatoria agardhii*. The four suspended solids fractions are the same fractions used in the *STRESS-2d* model. Their specific attenuation coefficients are measured in the fall velocity distribution experiments. Although these measurements are not very accurate, results of these

measurements are consistent and the agreement between measured and simulated light attenuation is good.

With a depth integrated version of the Lambert-Beer equation, the total under water irradiance is estimated from the under water irradiance and the attenuation coefficient.

### *Algal growth*

The modelling of the growth of *Oscillatoria agardhii* in the Markermeer is based on non-equilibrium concepts. Hence, competition with other algae is excluded but time scales and environmental fluctuations are considered to be important. With two dynamic non-equilibrium models, the production of *O. agardhii*, measured in the experiments, was simulated. With a relatively simple model (SIMPLE), which simulates light limited production with fixed growth parameters, the representation of the measured production is poor. Differences between the light dependent growth parameters, obtained by calibration on the separate experiments, are large. Therefore it has been concluded that adaptation of the production parameters to the light conditions occurs and this adaptation should be incorporated in an *O. agardhii* growth model.

In the model ALGA, developed by Vermij, adaptation of growth parameters is incorporated. An upper and lower boundary are set for the maximum productivity and the light utilization efficiency. If the under water irradiance is higher than a threshold value, these parameters approach the lower boundaries (high light conditions). With under water irradiance levels below this threshold value, these parameters approach the upper limits (low light conditions). This construction accounts for the fast adaptation of growth parameters observed in the experiments. When the model is applied to the results of the field experiments, the calibrated values of the threshold values are that low, that the growth parameters are equal to the lower boundaries for most of the time. Although, the modelling of adaptation of growth parameters in ALGA is an improvement compared to fixed parameter models, the model ALGA does not succeed in an accurate simulation of the production measured in the experiments in its present form. The slow adaptation of growth parameters to the light conditions, as observed in the experiments, is not incorporated in ALGA. Simulation of the growth of algae for periods of months in the deeper parts of the lake showed rather good results. Unfortunately, the fact that the growth of *O. agardhii* is less in the shallower parts of the lake than in the deeper parts, could not be simulated with the model. Although the modelling of adaptation of growth parameters in ALGA is an improvement compared to fixed parameter models, the model ALGA does not yet result in an accurate simulation of the production measured in the experiments.

Simulation of the growth of *O. agardhii* by combination of the model ALGA with the models STRESS-2d and CLEAR has led to rather poor re-

sults, which is mainly due to imperfections in the biological part of the model, e.g.: the constant loss rate, the absence of slow adaptation, the exclusion of competition with other species, etc. A high loss rate, as calibrated by Vermij, led to a dramatic decrease of cell numbers in winter, which was not compensated by growth in summer. The use of a lower loss rate led to some improvement of the simulation results.

#### *Application of the integrated model*

With the integrated model, the present situation is simulated with time series of 1988 and 1989. As precipitation and evaporation are not included in the model WAQUA, discharges of water and concentrations of phytoplankton in these discharges are adjusted in order to obtain realistic water balances. Long term simulation of the suspended solids concentration led to acceptable results but some changes in the simulated location of the IJsselmeer deposit were unrealistic. The agreement between measured and simulated *Oscillatoria agardhii* concentrations was rather poor.

Simulation of the Markermeer after construction of the Markerwaard was conducted. The effect of the construction of the Markerwaard on the simulated suspended solids content and the attenuation coefficient is considerable. In general, lower suspended solid concentrations and attenuation coefficients are simulated in the areas remaining after the construction, due to reduction in fetch lengths and changes in flow patterns. The Gouwzee, IJmeer and Gooimeer are hardly affected. Although some care should be taken with the interpretation of the simulation results of the biological model, it can be concluded that the growth of *Oscillatoria agardhii* in the water areas remaining after the construction of the Markerwaard will probably increase compared to the present situation. Hence, this seems to agree with the conclusions of the IJff committee, that the possibility of the temporary blooms of *Oscillatoria agardhii* is expected to increase.

The effect of increased flushing with water from the IJsselmeer on the suspended solids concentration and the attenuation coefficient is minimal, even though the residence time of the water is halved in this scenario. Increased flushing causes a small increase in the numbers of *Oscillatoria agardhii*, as the concentration of *Oscillatoria agardhii* is usually higher in the IJsselmeer than in the Markermeer. This effect is noticed especially near the discharging sluices, but this effect diminishes at some distance of the sluices because it is absorbed in the larger water body.



# 1 Introduction

The Markermeer is a large shallow fresh water lake in the centre of the Netherlands. The water quality of the lake, with respect to micro pollutants, phytoplankton blooms and eutrophication, is good, compared to other lakes in the area. The lake sediment consists mainly of very fine silty material. Therefore processes in the lake are dominated by the intensive resuspension and subsequent settling of sediment. This results in a highly fluctuating suspended solids content of the water. The concomitant variability of the under water light field of the lake is held responsible for the absence of permanent blooms of troublesome blue-green algae (cyanobacteria) like *Oscillatoria agardhii* (Commissie IJff, 1984).

The regional development of the area is still proceeding and several possible management measures are being considered, varying from water level alterations to the reclamation of a polder of 41,000 hectares. As most measures will influence the extent of sediment transport and therefore the under water light field, the execution of such measures may lead to unfavourable phytoplankton conditions. Hence, additional information was needed, concerning the relationships between sediment transport, the under water light field and the growth of *Oscillatoria agardhii* and the impact of possible measures on these processes. A research project was set up to study these processes and to develop an operational model to simulate the effects of the proposed measures. The research was conducted by the Agricultural University Wageningen, Nature Conservation Department, and by Rijkswaterstaat, directorate Flevoland (former IJsselmeerpolders Development Authority), Scientific Department. The results of this study are presented in this thesis.

## 1.1 History

Until 1976, the Markermeer used to be part of the IJsselmeer, when the Houtribdijk, the dike between Enkhuizen and Lelystad, was closed (Figure 1.1). Like the other lakes in the area, its history and possible its future are determined by the realisation of the Zuider Zee project.

### 1.1.1 The Zuiderzee Project

Until 1932, the Zuiderzee in the centre of the Netherlands had an open connection with the Waddenzee (Figure 1.1), which is connected to the Noordzee. Hence, the water was saline. Plans to dam the Zuiderzee were first launched in the 17<sup>th</sup> century, but it was not until 1918, after the major floods of 1916, the Zuiderzee Act passed parliament. The Zuiderzee Project involved the damming of the Zuiderzee, the creation of a large fresh water lake, named the IJsselmeer, and the reclamation of over 200,000 hectares of new land. The initial aims of this project encom-

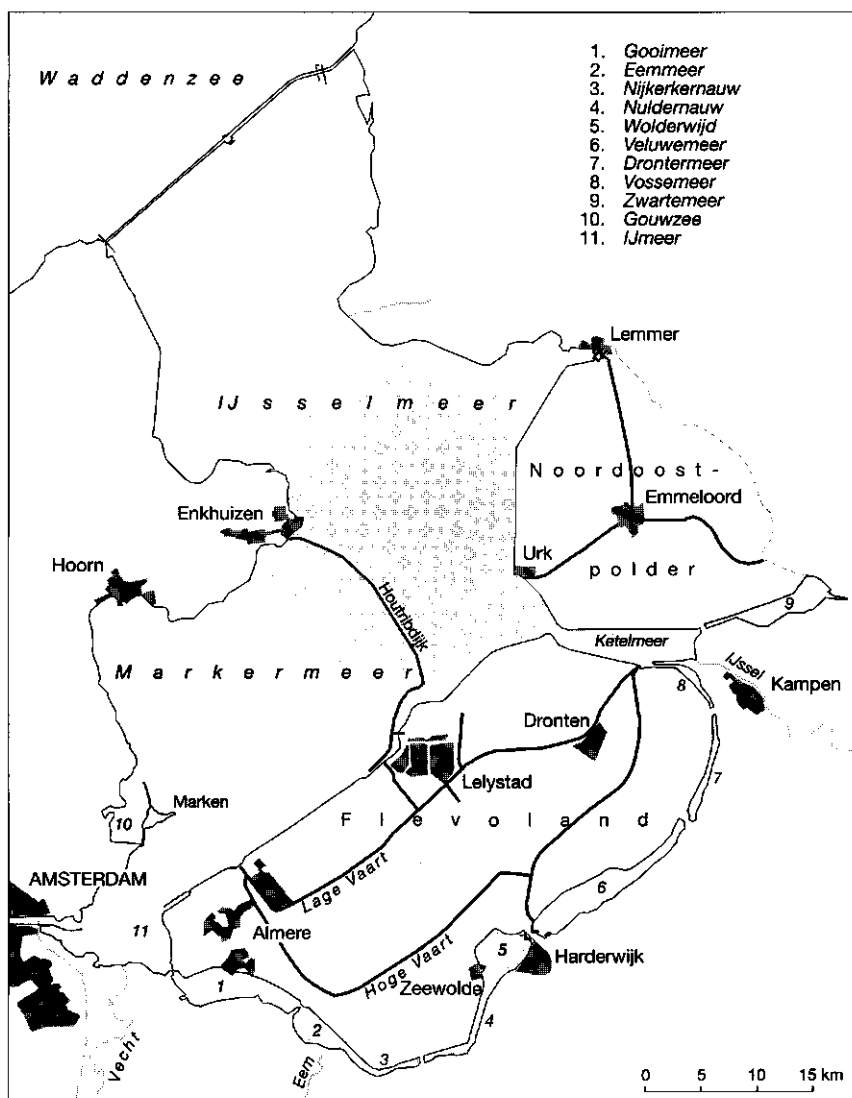


Figure 1.1 The IJsselmeer area

passed improving the water management of the surrounding areas and protecting them against flooding, the reclamation of fertile agricultural land and the provision of new employment opportunities. With the sharp rise of the population and the extensive industrialization, other aims were included with respect to nature preservation, urban expansion and recreation (Van Duin and De Kaste, 1985). In Zuidelijk Flevoland, reclaimed in 1967, the agricultural areas cover only 50 % of the land area

and a wetland, with a total area of 5,500 hectares, is preserved, which is called the Oostvaardersplassen.

In 1976 the Houtribdijk was completed, separating the Markermeer from the IJsselmeer. This dike was meant to be the first step towards the reclamation of the last polder; the Markerwaard. The increased consciousness of the environmental value of open water areas like the Markermeer and the growing agricultural surpluses in Europe, gradually changed the Dutch attitude towards the reclamation of the Markermeer. The reclamation of the Markerwaard was postponed and further studies were commissioned. In 1985, the Dutch cabinet decided to reclaim the Markerwaard as soon as certain conditions were met. Two complete alternative proposals were put forward, involving the reclamation of polders of 41,000 hectares and 23,000 hectares (the Markerwaard and Westelijk Flevoland) respectively. Both plans were not accepted by parliament, mainly for financial and ecological reasons. Several further studies concerning these objections were issued. One of the objections was the possible negative effect on the water quality of the remaining fresh water areas.

In 1990, the cabinet stated that reclamation of the Markerwaard would not be realised during its governing period. However, the possibility of the inpoldering of the Markermeer in the future was kept open.

#### 1.1.2 Water quality in the IJsselmeer area

The IJsselmeer is a very large eutrophic lake. The major water input is through the river IJssel, a branch of the river Rijn. Enrichment with nutrients and pollution with heavy metals and organic micro pollutants, is mainly caused by this river. Nutrient concentrations in the IJsselmeer are usually  $> 0.10 \text{ gP.m}^{-3}$  and  $> 2.2 \text{ gN.m}^{-3}$  (de Rijk, 1990). Chloride concentrations seldom exceed the standard of  $200 \text{ gCl.m}^{-3}$ . In general, green algae make up more than half of the biomass in the IJsselmeer ( $100 \text{ mgChla.m}^{-3}$ ), mainly *Scenedesmus* species. In spring, temporary blooms of diatoms are found, sometimes followed by blooms of cyanobacteria in late summer or autumn. Most often blooms of *Microcystis aeruginosa* occur, but sporadically blooms of *Oscillatoria agardhii*, *Oscillatoria redekeii*, *Aphanizomenon flos-aquae* or *Aphanocapsa delicatissima* have been observed (Berger and Sweers, 1988).

With the reclamation of the polders of Flevoland, a string of interlinked lakes was created between these polders and the main land on the East and South sides (Figure 1.1). The annual influx of phosphorus and nitrogen varies from one lake to the other but is generally high, up to  $30 \text{ gP.m}^{-2}$  and  $90 \text{ gN.m}^{-2}$  for the Eemmeer and Gooimeer (Berger, 1987). This initially led to a substantial increase in submerged water plants in the end of the sixties. After the first bloom in 1971, the cyanobacterium *O. agardhii* has been more or less continuously dominant in these lakes and the area covered with macrophytes gradually lessened. To over-

grow other species, *O.agardhii* needs a restricted but well regulated daily energy supply. As *O.agardhii* grows relatively slowly, the residence time in the lakes is probably also an important factor that determines the possibility of blooming (Berger, 1987).

The water quality of the Markermeer, with average phosphate and nitrogen concentrations of  $0.11 \text{ gP.m}^{-3}$  and  $1.6 \text{ gN.m}^{-3}$  respectively and average chlorophyll-a concentrations of  $0.7 \text{ mgChla.m}^{-3}$  (Chapter 3), is usually better than the water quality of the other lakes in the area. Still, on the basis of nutrient concentration, the lake is classified as eutrophic and a higher phytoplankton biomass was expected than is actually found. The often high and fluctuating suspended solids content, which causes the characteristic light field of the Markermeer, is held responsible for the absence of blooms of *O.agardhii* in this lake (Berger et al, 1986). Temporary the growth of algae is also nutrient-limited in the Markermeer (Vermij and Janissen, 1991).

## 1.2 Study outline

The present reasonable water quality situation of the Markermeer and the fear for a deterioration due to the various proposed regional developments, led to an increased interest in the specific water quality characteristics of the Markermeer by the involved authorities.

### 1.2.1 Background

With the reclamation of the Markerwaard still under consideration and the growing consciousness of the environmental value of the Markermeer, more knowledge was required on the impact of regional planning features on the water quality in the area. In 1984 a special committee, the 'Commissie Algenbloei Westelijke Randmeren' (Commissie IJff), was installed to assess the effect of the reclamation of the Markerwaard on the water quality of the remaining lakes, paying special attention to the growth of the cyanobacterium *Oscillatoria agardhii*. This committee concluded (Commissie IJff, 1984);

- 'the possibility of a permanent dominance of blue-green algae (cyanobacteria) in the lakes, which would remain after the reclamation of the Markerwaard, is not basically different from the probability for this to occur in a situation without the reclamation;
- the possibility of the occurrence of temporary blooms of blue-green algae is expected to increase compared with the current situation. The committee presumed that a change in the frequency of temporary blooms of blue-green algae would be possible. Especially the possibility of temporary blooms of *O.agardhii* is expected to increase.'

This increasing possibility of temporary blooms of *O.agardhii* after reclamation of the Markerwaard, depends on the measures that will be taken to prevent the occurrence of these blooms. Several measures were

suggested, including a decrease in residence time by enhanced flushing with water from the IJsselmeer and a change in the size and shape of the planned Markerwaard. To assess the effects of the different potential measures, more detailed knowledge was needed on the characteristic physical conditions of the Markermeer and their specific effect on the growth of *O.agardhii*. Furthermore, a tool was needed to simulate the effect of the alternative measures. Therefore, in 1984 a study was commissioned by the IJsselmeerpolders Development Authority (later named RWS, Directorate Flevoland) to assess the consequences of regional developments for the water quality in the Markermeer area, especially on the growth of *O.agardhii*, and the effect of possible measures to improve the water quality. In 1986 the Agricultural University Wageningen, Department of Nature Conservation, became involved in this study and in close cooperation a four year study was launched (Van Duin et al, 1989<sup>1</sup>).

### 1.2.2 Approach

In principle, mathematical models are best suited to assist the water manager in evaluating the effectiveness of lake eutrophication control measures (Van Straaten, 1986). Statistical models, including black box models, may be useful for control but have no predictive value if radical changes in lake characteristics are considered. Thus a conceptual model is required, preferably with a theory oriented character in order to predict phenomena that have not yet been observed. To account for stochastic variations in processes, parameters and variables, stochastic behaviour should be incorporated in the model. Furthermore, to include seasonal variability, the model should be dynamic. Based on the classification of Van Straaten (1986), to assess the effect of management measures on the light field and phytoplankton growth in the Markermeer a conceptual (theory oriented), stochastic, dynamic model is suited best. However, the development of such a model was not an easy task, because the processes affecting phytoplankton growth in the Markermeer are complex and available data were limited. A conceptual (partly theory oriented, partly data oriented), deterministic, dynamic model has been developed, which comprises three separate models;

- a model to simulate suspended solids concentrations (*STRESS-2d*),
- a model to characterize the under water light field (*CLEAR*) and
- a model to simulate phytoplankton growth, focusing on the growth of *Oscillatoria agardhii* (*ALGA*).

Each model is calibrated separately. Finally the models are linked, and the growth of *O.agardhii* in the Markermeer is simulated for the period January 1988 – December 1989. To guide both the model development and the calibration and validation of the models, an extensive field study was included in the project.

The basic features and the origin of the three models are summarized below, the flow chart of the model approach is presented in Figure 1.2.

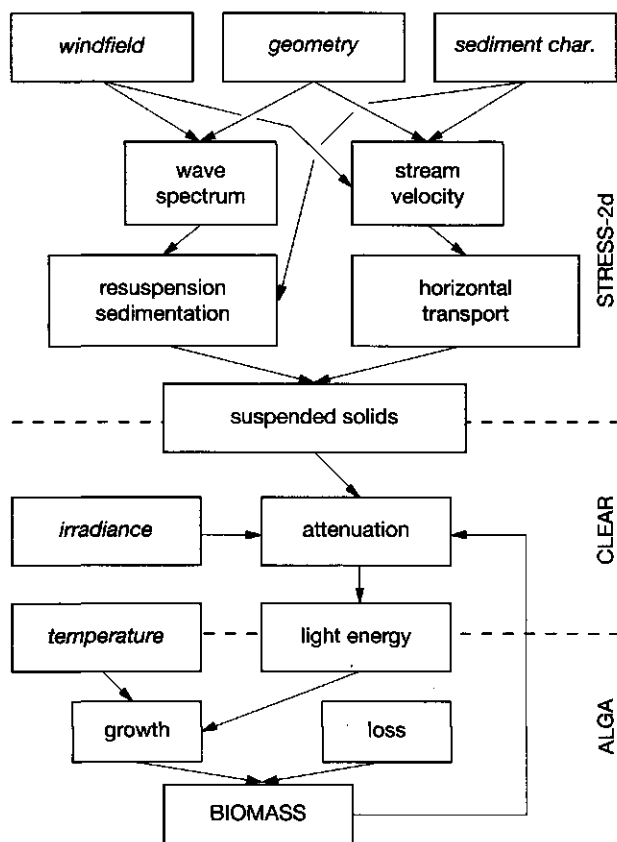


Figure 1.2 Flow chart

**STRESS-2d**, a two-dimensional model for Sediment Transport, Resuspension and Sedimentation in Shallow Lakes (Van Duin and Blom, 1992; Chapter 4). With the sediment transport model, the effect of management measures on the suspended solids concentration in the Markermeer, focusing on wind induced resuspension of sediment, is simulated. As large spatial variations in the process rate were expected and development measures often involve changes in the morphometry of the lake, the model had to be at least two-dimensional. A two-dimensional water transport model (WAQUA; Stelling, 1984) was available and is used as a basis of the model. The sediment transport model is basically conceptual and theory oriented, but some specific processes are modelled data oriented if no radical changes in these processes, parameters or input variables are expected. Part of the stochastic

character of weather data is included by the simulation of two different years of weather data.

*CLEAR*,

a Combined *Light Energy Attenuation Routine* (Van Duin et al, 1992). In this model irradiance, suspended solids and phytoplankton concentrations are transposed into a characterization of the under water light field. The model is developed simultaneously with the *STRESS-2d* model. In the Markermeer study the models are linked, producing a spatial distribution of the under water light field. In this model, for lack of theory oriented descriptions, relationships are based on field data (Chapter 5). Hence, application of the model is restricted to the Markermeer and extrapolation should be considered with care if the effect of management measures are to be predicted.

*ALGA*,

a light limited growth model for *O.agardhii* (Vermij, 1992). The development of the phytoplankton growth model forms no part of this thesis. An existing model, *ALGA*, developed especially for the Markermeer situation, has been used. Hence, the discussion of this model is limited to a model description, simulation and validation (Chapter 6).

The field study included the measurement of variables related to sediment transport and to the characteristics of the under water light field and phytoplankton growth in the Markermeer. Measurements had to serve both process studies and model calibrations (Chapter 3). Besides, a variety of field experiments was conducted to assess the specific conditions of the light field essential for the growth of *O.agardhii* and to study the growth of *O.agardhii* under Markermeer conditions. As the extrapolation of laboratory experiments to field conditions is hazardous, experiments were conducted in the Markermeer itself (Chapters 3 and 6).

## **2 The Markermeer**

The Markermeer is an extensive open water area, in the centre of the Netherlands. Besides, the ecological functions, social functions are attached to the lake, among which agricultural water supply, recreation, fishery and shipping (Ministerie van Verkeer en Waterstaat et al, 1990).

### **2.1 Morphometry and morphology**

The lake is characterized by a large open shallow area with a limited amount of inflow and outflow compared to its volume. The lake boundaries consist mainly of dikes. Only locally in the South and West there are some beaches.

#### **2.1.1 Topography**

The Markermeer is separated from the larger IJsselmeer by a dike in the North-east of the lake, the Houtribdijk. In this dike, ship locks and discharge sluices are constructed near Lelystad: the Houtribsluizen, and near Enkhuizen: the Krabbersgatsluizen (Figure 2.1). The southern part of the lake is called the IJmeer. Near Amsterdam the IJmeer is separated from the IJ by the Oranjesluizen. The IJmeer is connected in the East to a string of three lakes bordering Flevoland; the Gooimeer, the Eemmeer and the Nijkerkernauw (Figure 1.1). The IJmeer and the Gooimeer and the Eemmeer are connected by channels with a width of less than 100 metres. The surface area of the Markermeer, including the IJmeer and Gouwzee, is estimated at 68,000 hectares, the volume at 2,5 billion m<sup>3</sup>.

#### **2.1.2 Sediment**

The Markermeer, including the IJmeer, is a shallow lake with a mean water depth of 3.6 metres. The lake bottom is rather flat, sloping gently towards the Northeast, (Figure 2.2). Less than 9 % of the lake area has a depth less than 2.0 metres (Berger et al, 1986). Local sand pits and shipping channels have depths over 4.5 metres. In the IJmeer, a very large sand suction pit is located with an area of more than 500 hectares and a depth of more than 30 metres.



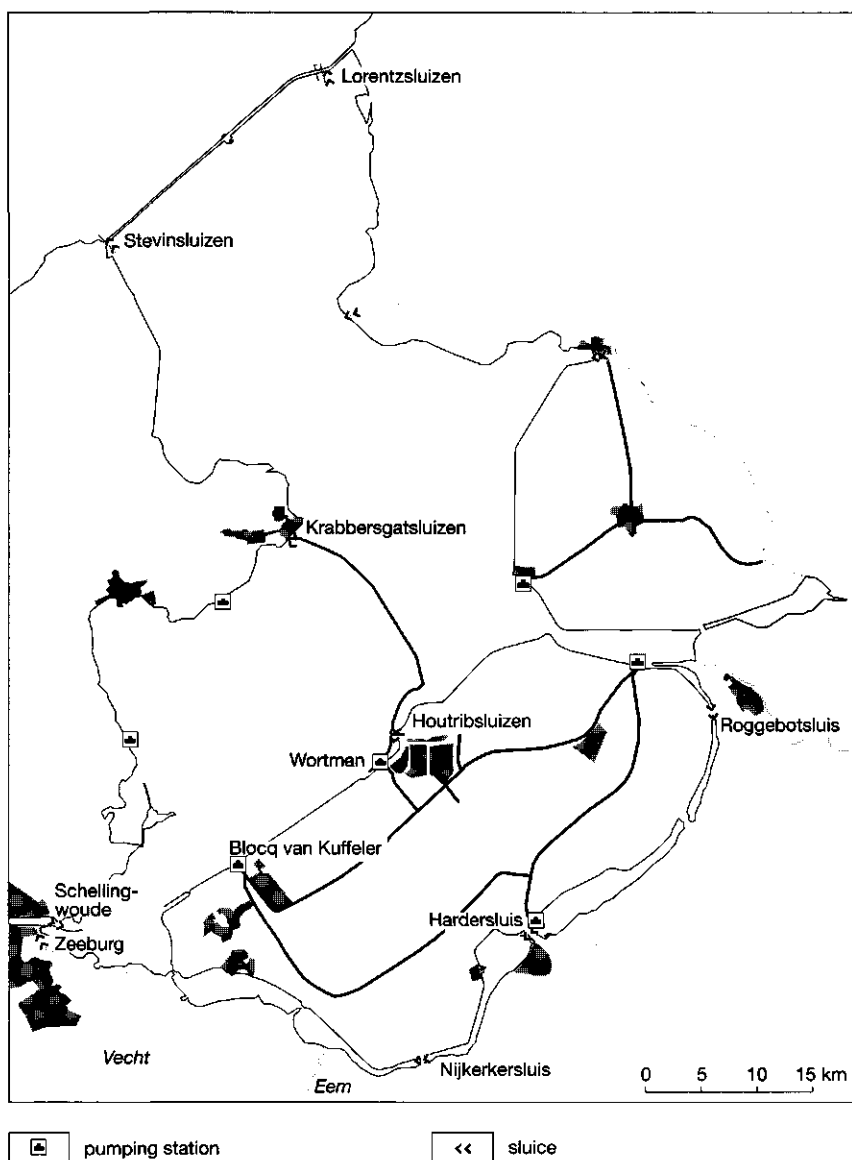


Figure 2.1 Location of main inflows and outflows

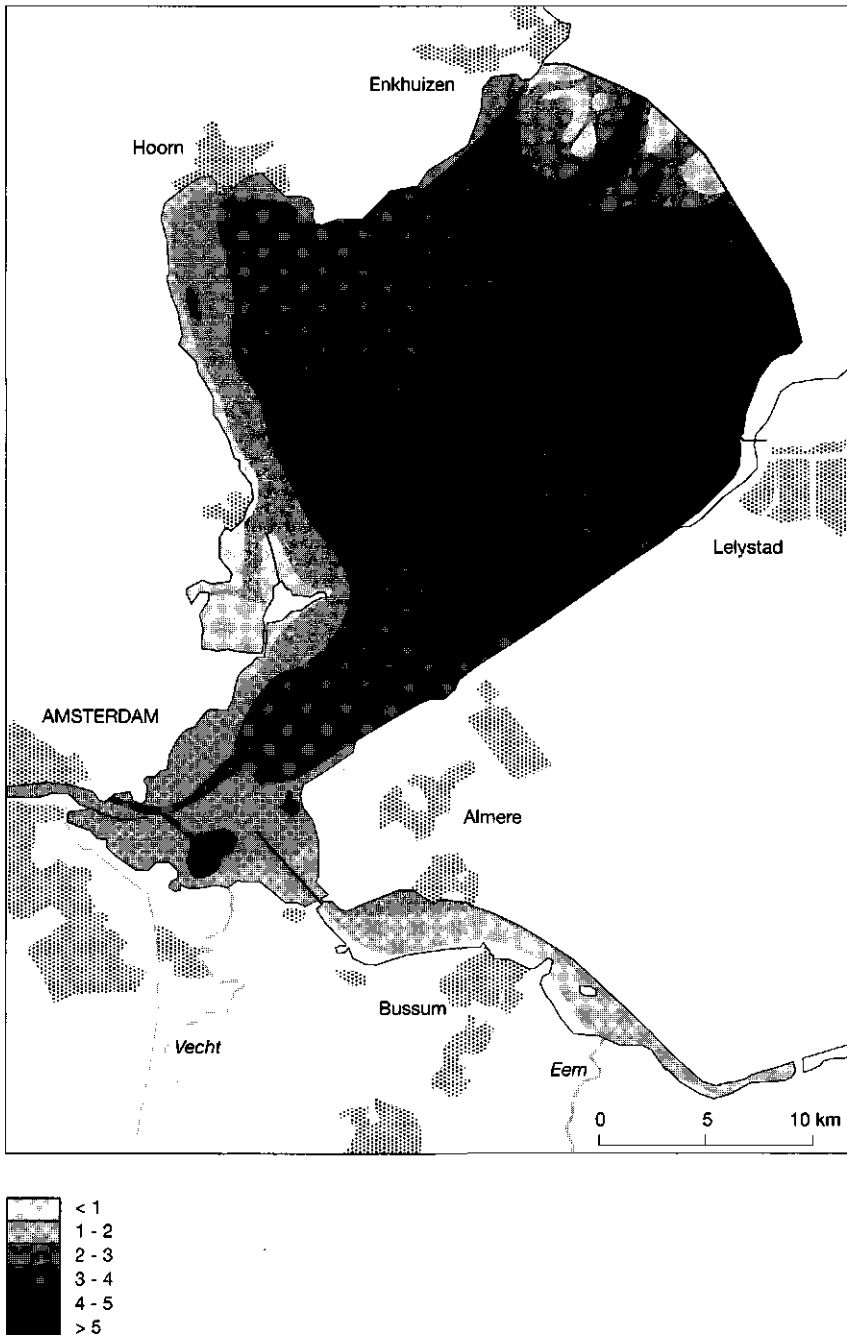


Figure 2.2 Depth in the Markermeer area (in metres)

The lake bottom dates from the Holocene and mainly consists of clay layers. In the western part of the lake, layers of fine and coarse sand have been deposited between the clay layers. Near Enkhuizen, the lake bottom consists of both fine and coarse sand. This sand, called the Enkhuizerzand, locally reaches a thickness of approximately 5 metres. Around the isle of Marken, peat is found in the top layers of the lake bottom. On top of the older deposits, a layer of fine silts is found on sixty percent of the lake bottom. This layer is called the IJsselmeer deposit. The water and lutum content of this deposit is high (Winkels et al, 1989). This material consists partly of material eroded from older deposits and partly of material supplied by the river IJssel, after the closing of the Afsluitdijk (§ 1.1.1). While no marine shells are found in the IJsselmeer deposit, this deposit can be easily distinguished from the older Holocene deposits. The extent and thickness of the IJsselmeer deposit is presented in Figure 2.3. Before the construction of the dike Enkhuizen-Lelystad almost the entire lake was covered with a layer of this IJsselmeer deposit. After the construction of this dike, the main flow patterns in the lake changed dramatically and the IJsselmeer deposit has been relocated (Winkels et al, 1989).

On top of all geological deposits, a thin ( $< 0.01$  metre) oxic silt layer is found over the entire surface of the lake. This layer consists of freshly deposited sediment with a water content in the order of 95 %.

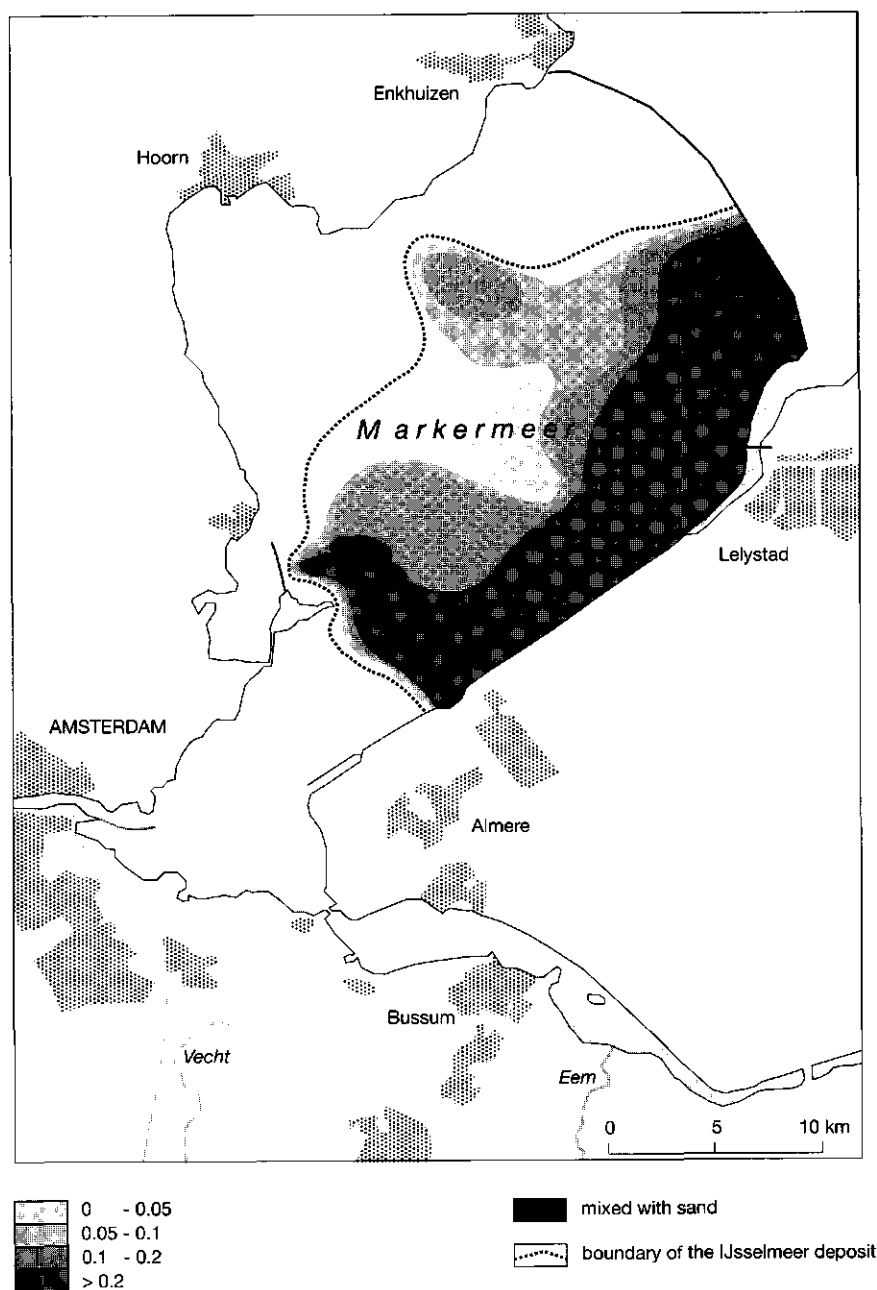


Figure 2.3 Thickness of the IJsselmeer deposit (in metres)

## 2.2 Limnology

### 2.2.1 Water balance

In order to preserve a large fresh water reserve and to enable water supply to the surrounding rural areas, the target water level of the Markermeer is set at 0.20 m -NAP (Nieuw Amsterdams Peil) during the summer period, from the first of April until the first of October. During the winter period, the target water level is set at 0.40 m -NAP in order to facilitate the drainage of the surrounding polder areas.

The water balance of the Markermeer, including the IJmeer, Gouwzee, Gooimeer, Eemmeer and Nijkerkernauw, is determined by precipitation and evaporation, the in- and outflow of water, infiltration and storage. The values for 1988 are presented in Figure 2.4. The average precipitation in the Netherlands amounts to an average of 750 millimetres per year (550 million m<sup>3</sup> in 1988 and 460 million m<sup>3</sup> in 1989 for the Markermeer area) and the average open water evaporation (Penman) to 650 millimetres per year (450 million m<sup>3</sup> in 1988 and 520 million m<sup>3</sup> in 1989 for the Markermeer area). Under the current water management, the main input to the lake are precipitation, the inlet of water from the IJsselmeer through the Houtrib- and Krabbersgatsluices, the discharge by the pumping stations of Flevoland, de Blocq van Kuffeler and the Wortman and the river Eem. The main output are evaporation and the outlet of water to the IJsselmeer by the Houtrib- and Krabbersgatsluizen and to the sluices to the Noordzeekanaal, near Zeeburg and Schellingwoude and the inlet of water for agricultural purposes in Noord-Holland. Detailed water balances for 1988 and 1989 are presented in Appendix II. In these water balances storage is estimated from water level alterations. In the initial water balance of 1988, the input is overestimated or an output of 138 million m<sup>3</sup> is missing. This could be accounted for by infiltration, which is not incorporated in the balances. This corresponds to a mean infiltration for the entire area of 0.56 mm·day<sup>-1</sup>, which seems not an unreasonable value (Hebbink, 1991). In the water balance of 1989 the input is underestimated with 76 million m<sup>3</sup>, excluding infiltration. Including the same amount of infiltration as estimated for 1988, would even worsen differences. The accuracy in the estimated values of inlet and outlet of water by sluices is rather low, as these values are estimated from opening hours of sluices. Besides, precipitation and evaporation values are obtained from a weather station near Lelystad, but values may differ locally.

With a water level of 0.20 m -NAP, the total volume of water in the area is estimated at 2.4 billion m<sup>3</sup> (De Rijk, 1990). With a total discharge of 1.8 billion m<sup>3</sup> per year, the residence time of the water in the Markermeer area is estimated at 1.5 year.

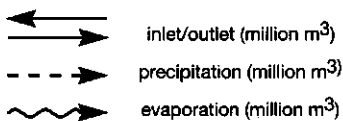
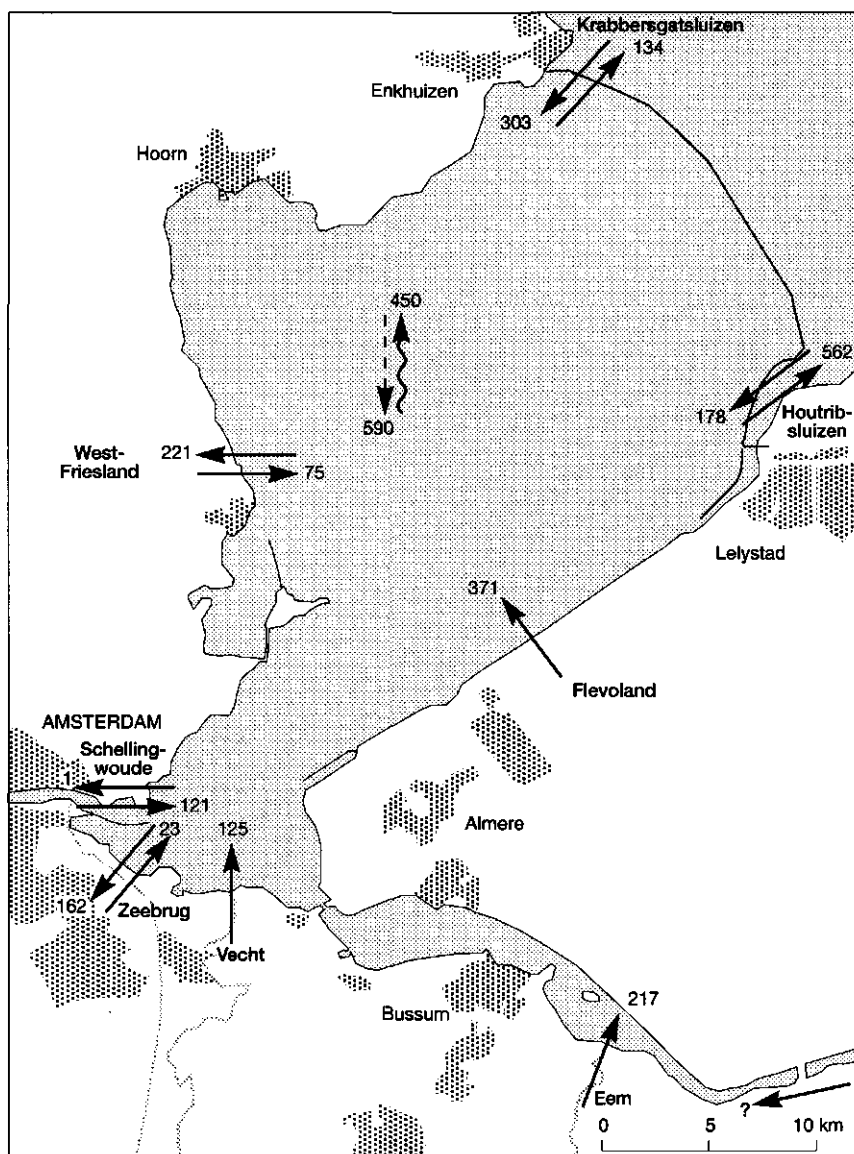


Figure 2.4 Water balance of the Markermeer area of 1988 (in  $10^6 m^3$ )

### 2.2.2 Water quality characteristics

An important reason for the suppletion of water from the IJsselmeer into the Markermeer is to dilute the salt content of the Markermeer. The water discharged by the Blocq van Kuffeler, contains a chloride concentration of approximately  $350 \text{ gCl}\cdot\text{m}^{-3}$ , resulting in a load of 150 million kgCl per year. Several smaller pumping stations along the coast of Noord-Holland discharge water with a high salt content as well. By flushing the Markermeer with water from the IJsselmeer, the chloride concentration is kept below  $200 \text{ gCl}\cdot\text{m}^{-3}$ .

The phosphate load of the Markermeer is in the order of  $1.4 \text{ gP}\cdot\text{m}^{-2}\cdot\text{year}^{-1}$ , half of it originating from the IJsselmeer. Other major contributors are the Eem and Vecht and the pumping stations of Flevoland and Noord-Holland. In 1987, 1988 and 1989 the phosphate concentration varied around  $0.11 \text{ gP}\cdot\text{m}^{-3}$  and the nitrogen concentration around  $1.6 \text{ gN}\cdot\text{m}^{-3}$ . Though the water is rather eutrophic, it usually still meets the Dutch basic minimal water quality standards of  $<0.15 \text{ gP}\cdot\text{m}^{-3}$  and  $<2.2 \text{ gN}\cdot\text{m}^{-3}$  respectively. The concentration of micro pollutants in the lake is very low and the sediment of the Markermeer is among the least polluted in the Netherlands.

The optical depth of the lake is low with an average of 0.4 m, though occasionally values of above 1 m are measured. This low transparency is caused by the high suspended solids content of the water, varying between 10 and  $200 \text{ g}\cdot\text{m}^{-3}$ , with an average value of  $50 \text{ g}\cdot\text{m}^{-3}$ . Due to the large fetch (up to 30 kilometres), the limited depth (up to 4.5 m), the flat bottom and the silty sediment, resuspension and sedimentation of sediment are the most prominent processes in the lake. They induce high and fluctuating suspended solids concentrations. Hence, the optical depth and the availability of light energy is fluctuating as well and generally low. This is an important factor in the ecology of the area.

### 2.2.3 Ecological aspects

The phytoplankton composition in the Markermeer is dominated by green-algae (Chlorophyta), mainly *Scenedesmus*-species with small blooms of diatoms (Chrysophyta) in spring. Occasionally, blooms of cyanobacteria (Cyanophyta) occur, mainly of *Aphanizomenon flos-aquae*. *Oscillatoria agardhii* is found regularly, but abundant blooms do not occur. Although blooms of *Microcystis aeruginosa* do occur very regularly in the IJsselmeer, they are not found in the Markermeer, except occasionally near the Krabbersgat- and Houtribsluizen. Due to the relatively small optical depth of the water, the growth of epiphytes and submersed macrophytes is limited to the near shore areas and the Gouwzee.

The macro zoobenthos mainly consists of fresh water mussels (*Dreissena polymorpha*), insect larvae (Diptera, Chironomidae), worms

(Vermes, Oligochaeta) and crustaceans (Crustacea, Gammaridae) (Van Eerden and Zijlstra, 1986). Fresh water mussels are found throughout the entire Western part of the lake, where the sediment is stable enough for their attachment. Fish species are dominated by smelt (*Osmerus eperlanus*), ruffe (*Gymnocephalus cernuus*), bream (*Abramis brama*), perch (*Perca fluviatilis*), pike perch (*Stizostedion lucioperca*) and eel (*Anguilla anguilla*) (Van Eerden and Zijlstra, 1986). The lake is important for birds to rest, to moult and to forage. In winter, assemblies of great crested grebes, smew and goosander prey on small fish, while thousands of tufted duck, pochard and seaup prey on mussels. In spring and summer, cormorants, breeding in the nearby nature reserves the Oostvaardersplassen, the Lepelaarsplassen and the Naardermeer and in summer large numbers of common and black terns as well, are committed to the Markermeer and the southern part of the IJsselmeer for foraging. Large numbers of diving ducks visit the area in the summer to moult.



### 3 Measurement methods and data analysis

Water quality monitoring is the effort to obtain quantitative information on the physical, chemical and biological characteristics of water via statistical sampling (Sanders et al, 1987). The results of this effort, the water quality data, are the base of water quality management and in environmental research. Only recently, has the random nature of water quality and the complexity of monitoring water quality characteristics been recognized. Two major steps can be defined in water quality monitoring: the design of the measurement program and the execution of the water quality monitoring. Usually, both steps have the limitation of financial resources in common.

In the design of water quality monitoring programs the time scales of the processes to be studied and the spatial variations expected in these processes are the key factors. Unfortunately, not much time is spend on this design and often studies are conducted with data that happen to be available. A rule of thumb could be that at least three to four samples should be taken within the time constant of the studied process in order to perceive its dynamics. On the other hand, the sampling period should be at least three to four times the time constant of the process to reveal significant trends. As in most studies several processes are studied, sampling of various variables at different time intervals and for different lengths of periods might be advisable. For example, for the IJsselmeer area Van Urk et al (1990) remarked that monthly sampling gave no representative view of the actual chlorophyll-a variations. To account for spatial variations is even more difficult. The number of sites to be sampled is also dependent upon the processes that are studied and often not clear until the data are analyzed.

Ward et al (1990) distinguish six components in the total water quality monitoring system, necessary to generate water quality data, i.e. sample collection, laboratory analysis, data handling, data analysis, reporting and information utilization. Traditionally, the first three components have been viewed as the total system, because the acquisition of data was viewed as the end point. In studies in which the data collection is not performed by the same person handling the information utilization, it is even harder to check, whether data are truly reliable and well interpreted. Reproducibility, often a good touchstone of data reliability, is often impossible in field experiments. A well known method to improve reliability is to work with duplicates; if possible by using different devices and methods. However, this will increase costs and is not necessary conclusive. The problem remains when results disagree; which of the two data is correct, should the mean value be used or are both data unreliable? To enhance reliability samples could be taken in threefold with triple analyses and measurements and if possible, using three different devices and methods. Evidently, this will increase costs even more. As money and time are often limited, retrenchments have to be made on the data collection. This means if measurements are done in

duplicate or triplicate, this affects the design of the monitoring program as less sites can be sampled or the sites are sampled less frequently. Besides the inherent inaccuracy in data collection, there is the problem of the human component. In principle the devices used may be capable to produce good results, but they may be used incorrectly or not be maintained well: A sensor may not be calibrated as frequently as needed, the samples taken may be disturbed or not representative. As human failure is inevitable, it is important to account for this when data are analyzed. Again, this is even more difficult when data analysis and data collection are performed by different persons.

### **3.1 Sampling Strategy**

In the Markermeer project a major effort in data collection and analysis has been made. Time and again, corrections were made for device failures, inaccuracies in calibration, mistakes in interpretation, etc. Many of these mistakes could not be anticipated, and possibly several more remained unobserved. The effort resulted in a data base with 'apparently' reliable data.

#### *3.1.1 Sampling sites*

For the calibration of the spatially segmented model, data are collected with high frequencies at two different sites, referred to as Y111 and Y112. Site Y111 is situated in the middle of the lake, in a region with only small spatial variations in sediment composition and water depth. The bottom depth is 4.2 m-NAP, which results in an average water depth of 4.0 m in the summer. Site Y112 is situated near the island Marken in an inhomogeneous area with a bottom depth of 3.2 m-NAP, which results in an average water depth of 3.0 m in the summer. After construction of the polder Markerwaard, this spot would be situated in the middle of one of the remaining lakes. The location of both sites is presented in Figure 3.1. As the final goal of the model is the simulation of the growth of *Oscillatoria agardhii*, measurements are limited to the main primary production period; from April until November. During these periods platforms or poles were mounted in the lake, which had to be removed in the winter to avoid damage by ice. Eight additional sites were visited every few weeks, in order to gain more information about the spatial distribution for a limited validation of the phytoplankton model.

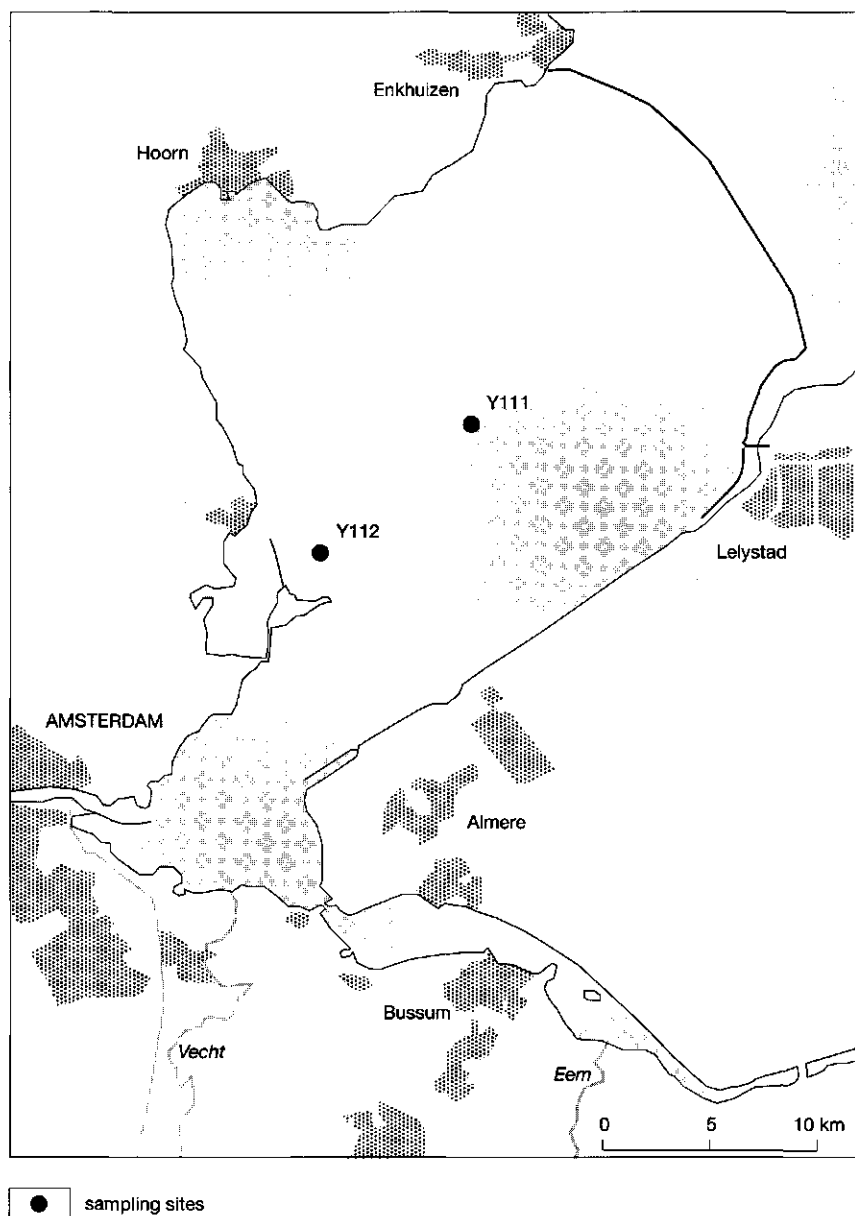


*Figure 3.1 Location of the sampling sites in Markermeer*

### 3.1.2 Sampling frequencies

The temporal resolution needed for the 2-dimensional water quality model is high for the suspended solids concentration and the under water light conditions. A good model requires a rather high frequency of measurement of the variables controlling these factors, as their values may change drastically within hours. If the direct response of phytoplankton to the available light energy is to be modelled, variables controlling this response should be measured with the same frequencies. To trace seasonal variations, weekly measurements may be sufficient.

The measurement program consisted of basically four types of measurements, which are:

regular water quality measurements,

like temperature, dissolved oxygen, pH, Secchi-depth, attenuation coefficient, nutrient concentration, suspended solids concentration, chlorophyll-a and phytoplankton numbers. These measurements were generally performed on a weekly basis, but during the high frequency sampling periods on a daily basis. To account for stratification, temperature, pH, dissolved oxygen and chlorophyll-a were measured at two depths, 0.5 m below the surface and at half the depth;

continuous measurements of water quality variables,

with automatically recording equipment. Sensors were mounted on platforms and values were recorded of temperature, dissolved oxygen, irradiance, wind speed and direction, water level and flow velocity and direction;

sediment and light attenuation characteristics,

besides well known measurements, like suspended solids concentration analysis in samples from automatic samplers and the use of sediment traps to measure sedimentation fluxes, fall velocity experiments were performed and the sediment top layer was sampled. Furthermore specific attenuation coefficients of various sediment fractions were measured;

primary production experiments,

experiments were performed in the field with classic light and dark bottle experiments and with a modified version of these experiments, in which bottles travel up and down the water column. Furthermore, growth experiments with *Oscillatoria agardhii* were performed in a perspex cylinder placed in the Markermeer for a couple of weeks.

Although, the first measurements for this project were done in 1984, the main effort in data collection and problem analysis as described above, started in 1987. During 1987, 1988 and 1989, the platforms posted at Y111 and Y112 were visited weekly from April until November to take samples, for maintenance of the equipment and to replace data loggers. During four two week periods in 1988, the sites were visited 5 days a week for high frequency sampling and some maintenance. During three two week periods in 1989, the sites were visited three times a week.

These high frequency periods are specified in Appendix 5. In 1990 some additional primary production experiments were done, some preliminary experiments were done already in 1988. A summary of the measurement program and frequency is presented in Table 3.1.

*Table 3.1 Summary of the measurement program*

| Variable               | Manual/<br>cont. | Weekly/<br>high-f | Depth |                 | 1987 | 1988 | 1989 | 1990 |
|------------------------|------------------|-------------------|-------|-----------------|------|------|------|------|
|                        |                  |                   | srf   | $\frac{1}{2} z$ |      |      |      |      |
| Temperature            | +/+              | +/+               | +     | +               | +    | +    | +    | +    |
| Dissolved Oxygen       | +/+              | +/+               | +     | +               | +    | +    | +    | -    |
| PH                     | +/-              | +/+               | +     | +               | +    | +    | +    | -    |
| Secchi                 | +/-              | +/+               |       |                 | +    | +    | +    | -    |
| Attenuation coeff.     | +/+              | +                 |       |                 | +    | +    | +    | -    |
| Chlorophyll-a          | +/-              | +/+               | +     | +               | +    | +    | +    | +    |
| Phytoplankton counts   | +/-              | +/-               | +     | -               | -    | +    | +    | -    |
| Nutrients              | +/-              | +/-               | -     | +               | +    | +    | +    | -    |
| Organic carbon         | +/-              | +/-               | -     | +               | -    | +    | -    | -    |
| Suspended solids       | +/+              | +/+               | +     | +               | +    | +    | +    | -    |
| Sediment traps         | +/-              | +/-               |       |                 | -    | +    | +    | -    |
| Fall velocity distr.   | +/-              | +/+               | -     | +               | -    | +    | +    | -    |
| Sp. attenuation coeff. | +/-              | +/+               | -     | +               | -    | +    | +    | -    |
| Light and dark bottles | +/-              | -/+               |       |                 | -    | +    | +    | +    |
| Cylinder experiment    | +/+              | -/+               |       |                 | -    | -    | +    | +    |

### 3.2 Regular water quality measurements

During the sampling season, Y111 and Y112 were visited at least weekly, but often more frequently. During each visit, some manual water quality measurements were done as summarized in Table 3.2. Usually the ship engine is brought in reverse to slow the ship and some manoeuvring is needed to land the ship at the platform or pole. By this action, large amounts of sediment are resuspended. Depending on the stream velocity and dispersion, sampling ought to be postponed for at least half an hour or more, before representative samples could be obtained. If no visit to the platform was needed, sampling could be done while the ship was drifting. High peaks in measured concentrations are often due to a lack of carefulness in this respect.

Sampling is usually done with a centrifugal submersible pump with a capacity of 1 m<sup>3</sup> an hour, which was let down at the prescribed depth. At the main sampling sites, samples were taken at two depths; at 0.5 m below the surface (srf) and at mid water depth, referred to as  $\frac{1}{2}z$ , which is set at 1.5 m and 2.0 m for Y112 and Y111 respectively. Unless stated otherwise, the data at half the depth are used. In Table 3.2 the mean results of the weekly measurements are summarized, while in the

following paragraphs the measurement methods are described in some detail.

**Table 3.2** *Summary of results of regular measurements at Y111 and Y112, performed from April till November in 1987, 1988 and 1989*

| Variable                                |                                     | Y112 |                  |      |       | Y111 |                  |      |       |
|---|-------------------------------------|------|------------------|------|-------|------|------------------|------|-------|
|   |                                     | mean | std <sup>1</sup> | min  | max   | mean | std <sup>1</sup> | min  | max   |
| Temperature-srf                         | (°C)                                | 14.9 | 4.2              | 5.0  | 22.4  | 14.6 | 4.2              | 5.2  | 23.4  |
| Temperature- $\frac{1}{2}z$             | (°C)                                | 14.8 | 4.2              | 5.0  | 22.5  | 14.4 | 4.4              | 5.2  | 23.0  |
| Dissolved oxygen-srf                    | (g·m <sup>-3</sup> )                | 11.0 | 1.3              | 8.9  | 14.3  | 10.8 | 1.3              | 8.5  | 14.5  |
| Dissolved oxygen- $\frac{1}{2}z$        | (g·m <sup>-3</sup> )                | 10.9 | 1.2              | 8.9  | 14.2  | 11.0 | 1.3              | 8.9  | 14.3  |
| PH-srf                                  | (-log[H <sup>+</sup> ])             | 8.5  | 0.3              | 7.8  | 9.8   | 8.4  | 0.3              | 7.5  | 9.1   |
| PH- $\frac{1}{2}z$                      | (-log[H <sup>+</sup> ])             | 8.5  | 0.3              | 7.8  | 9.3   | 8.4  | 0.2              | 7.9  | 9.1   |
| Secchi-depth                            | (m)                                 | 0.43 | 0.24             | 0.10 | 1.2   | 0.47 | 0.37             | 0.10 | 1.4   |
| Kd <sup>2</sup>                         | (m <sup>-1</sup> )                  | 3.8  | 3.0              | 0.4  | 11.5  | 3.4  | 2.3              | 0.5  | 10.6  |
| Suspended Solids-srf                    | (g·m <sup>-3</sup> )                | 47.9 | 39.1             | 7.0  | 180.4 | 42.8 | 32.5             | 7.0  | 130.8 |
| Suspended Solids- $\frac{1}{2}z$        | (g·m <sup>-3</sup> )                | 48.0 | 37.9             | 8.6  | 179.9 | 42.7 | 31.0             | 7.2  | 125.0 |
| Ash Free Dry Weight-srf                 | (g·m <sup>-3</sup> )                | 14.5 | 8.1              | 2.4  | 42.0  | 14.2 | 7.8              | 2.4  | 42.0  |
| Ash Free Dry Weight- $\frac{1}{2}z$     | (g·m <sup>-3</sup> )                | 14.3 | 8.0              | 2.4  | 38.6  | 14.4 | 7.8              | 1.9  | 34.8  |
| AFDW/SS- $\frac{1}{2}z$                 | (%)                                 | 36   | 12               | 15   | 70    | 40   | 12               | 21   | 76    |
| Chlorophyll-a-srf                       | (mg·m <sup>-3</sup> )               | 62   | 33               | 13   | 161   | 65   | 32               | 7    | 151   |
| Chlorophyll-a- $\frac{1}{2}z$           | (mg·m <sup>-3</sup> )               | 63   | 32               | 14   | 155   | 68   | 31               | 17   | 148   |
| Phaeophytine <sup>2</sup>               | (mg·m <sup>-3</sup> )               | 20   | 17               | 0    | 63    | 21   | 17               | 0    | 66    |
| Cell number <sup>2</sup> 1988           | (10 <sup>6</sup> ·m <sup>-3</sup> ) | 86   | 60               | 28   | 343   | 95   | 90               | 30   | 665   |
| 1989                                    | (10 <sup>6</sup> ·m <sup>-3</sup> ) | 43   | 33               | 6    | 148   | 44   | 32               | 9    | 154   |
| O.agardhii <sup>2</sup> 1988            | (10 <sup>9</sup> ·m <sup>-3</sup> ) | 1.1  | 1.6              | 0    | 7.4   | 1.1  | 1.1              | 0    | 3.6   |
| 1989                                    | (10 <sup>9</sup> ·m <sup>-3</sup> ) | 3.0  | 3.1              | 0    | 11.0  | 4.5  | 3.5              | 0    | 12.6  |
| O.agardhii <sup>2</sup> 1988            | (%)                                 | 4    | 3                | 1    | 14    | 2    | 2                | 1    | 7     |
| 1989                                    | (%)                                 | 14   | 10               | 1    | 35    | 17   | 12               | 1    | 39    |
| Particulate Organic Carbon <sup>3</sup> | (g·m <sup>-3</sup> )                | 7.1  | 3.4              | 2.0  | 14.0  | 7.1  | 3.4              | 3.0  | 15.0  |
| Dissolved Organic Carbon <sup>3</sup>   | (g·m <sup>-3</sup> )                | 6.9  | 0.5              | 6.2  | 8.9   | 6.8  | 0.3              | 6.2  | 7.8   |
| P-tot                                   | (g·m <sup>-3</sup> )                | 0.11 | 0.07             | 0.01 | 0.48  | 0.11 | 0.06             | 0.02 | 0.29  |
| P-PO <sub>4</sub>                       | (g·m <sup>-3</sup> )                | 0.01 | 0.02             | 0.00 | 0.12  | 0.01 | 0.01             | 0.00 | 0.06  |
| N-Kjeldahl                              | (g·m <sup>-3</sup> )                | 1.4  | 0.4              | 0.7  | 3.0   | 1.5  | 0.4              | 0.7  | 2.3   |
| N-NO <sub>x</sub>                       | (g·m <sup>-3</sup> )                | 0.15 | 0.27             | 0.00 | 1.30  | 0.14 | 0.26             | 0.00 | 1.10  |
| N-NH <sub>4</sub>                       | (g·m <sup>-3</sup> )                | 0.05 | 0.04             | 0.00 | 0.21  | 0.06 | 0.06             | 0.00 | 0.39  |
| SiO <sub>2</sub>                        | (g·m <sup>-3</sup> )                | 0.65 | 0.66             | 0.00 | 2.30  | 0.78 | 0.76             | 0.00 | 2.49  |
| <sup>1</sup>                            | standard deviation                  |      |                  |      |       |      |                  |      |       |
| <sup>2</sup>                            | in 1988 and 1989 only               |      |                  |      |       |      |                  |      |       |
| <sup>3</sup>                            | in 1988 only                        |      |                  |      |       |      |                  |      |       |

### 3.2.1 On site measurements

With portable equipment some water quality parameters were measured on site: dissolved oxygen, temperature, pH, Secchi disk depth and the attenuation of under water irradiance. The assumed precision of measuring instruments is usually provided by the manufacturer.

#### Dissolved oxygen

The concentration of dissolved oxygen and the saturation value were measured with amperometric oxygen electrodes (54-ARC, Yellow Springs, USA). In 1987 and 1988 calibration was done every week. The precision attained was apparently within  $1 \text{ g} \cdot \text{m}^{-3}$ . In 1989 a new oxygen electrode (OXI 196, Wissenschaftlich Technische Werkstätten, BRD) was used. This electrode was calibrated daily with a supplied calibration bottle. With this electrode the precision of the measurements improved up to  $0.1 \text{ g} \cdot \text{m}^{-3}$ . In general, the oxygen saturation was close to 100 %. Usually, the dissolved oxygen concentration was measured at two depths; -0.5 m surface and at mid water depth. Oxygen gradients were observed only on days with temperature stratification and high chlorophyll-a concentrations.

#### Temperature

The temperature was measured with the same devices used for dissolved oxygen measurements. With the equipment used initially, errors of  $\pm 1^\circ \text{C}$  were experienced, but with the new electrodes these decreased to  $\pm 0.1^\circ \text{C}$ . The temperature was measured at the same depths as dissolved oxygen. Stratification was detected a few times a year, during calm, windless days. The temperature difference between the surface and mid depth at such days was no more than  $1^\circ \text{C}$ .

#### pH

The pH was measured with an electrode, calibrated for the range from 7 to 10. The weekly calibration was rather cumbersome and not very accurate. The measurement precision was probably  $\pm 0.5$ . In 1989, new electrodes (PH 196, Wissenschaftlich Technische Werkstätten, BRD) were introduced, which were also calibrated during each visit for the range of 7 to 10. Because the calibration fluid with a pH of 10 was not very stable, in 1990 the calibration was done for the range of 4 to 7. According to the manufacturer, measurements in the range of 7 to 10 are still reliable. With these new electrodes errors decreased till  $\pm 0.01$ . pH varied normally between 8 and 9, with an occasional peak between 9 and 10 in mid summer.

#### Secchi disk depth

Secchi disk depth was measured with a white disk with three large circular holes. The results varied strongly between 0.2 and 1.5 metres.

#### Irradiance

All irradiance measurements were done with submersible irradiance sensors (Li-Cor 192S Under Water Quantum Sensor, Li-Cor inc., USA). In

these sensors a photoelectric detector is placed below a flat disk of translucent diffuse plastic, which is projected slightly upwards from the surrounding housing. According to the manufacturer, these sensors are cosine corrected for the angle of irradiance and a further correction factor is used for the immersion effect. The sensor responds equally to all quanta within the wave band between 400 and 700 nm, thus measuring the Photosynthetically Available Radiation (PAR). These sensors are widely used for measurements of irradiance (Kirk, 1983). According to the manufacturer linearity is guaranteed between 0 and  $10000 \mu\text{E}\cdot\text{m}^{-2}\cdot\text{s}^{-1}$ , the sensitivity of the instruments is  $0.001 \mu\text{E}\cdot\text{m}^{-2}\cdot\text{s}^{-1}$  and the relative error is less than 5 %. In 1987 manual measurements were done with sensors that had been used for several years. They were calibrated in July by the manufacturer. Two sensors were used simultaneously to measure the global irradiance and the irradiance below the surface respectively. Irradiance was measured during 10 s and averaged. The underwater irradiance was measured at 0.1 m depth intervals for the first metre, at 0.2 m intervals for the second metre and every 0.5 m thereafter. Afterwards the whole routine was repeated. If the global irradiance was more or less constant during these measurements, the vertical attenuation coefficient for PAR was estimated from Beers' Law:

$$\ln[E_d(z)] = -K_d \cdot z + \ln[E_d(0)] \quad (3.1)$$

$$\begin{aligned} E_d &= \text{downward irradiance} \\ &\quad (\text{photon flux density}) \quad (\mu\text{E}\cdot\text{m}^{-2}\cdot\text{s}^{-1}) \\ z &= \text{depth} \quad (\text{m}) \\ K_d &= \text{vertical downward attenuation} \\ &\quad \text{coefficient} \quad (\text{m}^{-1}) \end{aligned}$$

The linear regression coefficient of  $\ln[E_d(z)]$  versus  $z$ , gives the value of  $K_d$ . In Appendix 6, the measured  $E_d$  and estimated  $K_d$  are presented for some example days.

In 1989 new sensors of the same type were used but the measurement method was altered. As  $K_d$  turned out to be essentially constant with the depth, the method was simplified in 1989. Two sensors were mounted at a steel pipe at a distance of 0.2 m. The pipe is lowered in the water, in such a way that the upper sensor was at a depth of 0.5 m approximately. For 10 s the irradiance was measured with both sensors and recorded by the portable data logger. The vertical attenuation coefficient is estimated with equation 3.2. The effect of this change is discussed in Chapter 5.

$$K_d = \frac{\ln[E_d(z_1)] - \ln[E_d(z_2)]}{z_1 - z_2} \quad (3.2)$$

The measured vertical attenuation coefficient varied between 0.4 and  $12 \text{ m}^{-1}$ , but the reliability of values below  $1 \text{ m}^{-1}$  is very low, due to relatively small differences in  $\ln[E_d(z_1)]$  and  $\ln[E_d(z_2)]$ . High values are usually



measured during stormy events, not during periods with high productivity of algae.

### 3.2.2 Sample analysis

Samples taken on board, were usually placed in white containers when the air temperatures rose above 20° C, otherwise they were left outside on the deck of the ship. The time between sampling and arrival in the harbour was at least one and a half hour, but often more. Hence, some algal production or decay of organic material may have occurred during transport. Upon arrival on shore, the bottles were transported in a little van to the laboratory, where they were stored in a refrigerator or preserved by the addition of formalin (a 35-40 % aqueous solution of formaldehyde). In 1987, 1988 and 1989 formalin was added in a volumetric ratio of 1:10. Due to its toxic nature, in 1990 this ratio was decreased to 1:20. The method of laboratory analysis of samples was performed for most variables according to the Dutch standard (NEN-methods). In case other methods are used, this is mentioned.

The differences between measurements at Y111 and Y112 were usually very small, except for the suspended solids content and ash free dry weight (Table 3.2). Part of the data analysis is described in § 6.1.3, relating the growth of *Oscillatoria agardhii* to the physical characteristics of the Markermeer.

#### Total and ash free dry weight

Samples preserved with formalin were used for the analysis. The total dry weight measured in samples from the Markermeer during the weekly manual measurements, varied between 7 and 180 g·m<sup>-3</sup>. Ash free dry weight concentrations varied between 2 and 40 g·m<sup>-3</sup>. The ash free dry weight/ suspended solids concentration, representing the fraction of organic material, varied between 15 and 76 % with a mean value of 36 % at Y112 and 40 % at Y111. High organic contents occurred during long periods of very calm weather, when the contribution of resuspended sediment was minimal. This is illustrated in Figure 3.2. The mean suspended solids concentration was significantly higher at Y112 than at Y111. As the AFDW/SS ratio was smaller at Y112, the higher suspended solids concentration at Y112 was probably due to resuspension of sediment and not to biological production. In general, the suspended solids concentration near the surface equals that at the mid water depth. Hence, vertical gradients do not often occur.

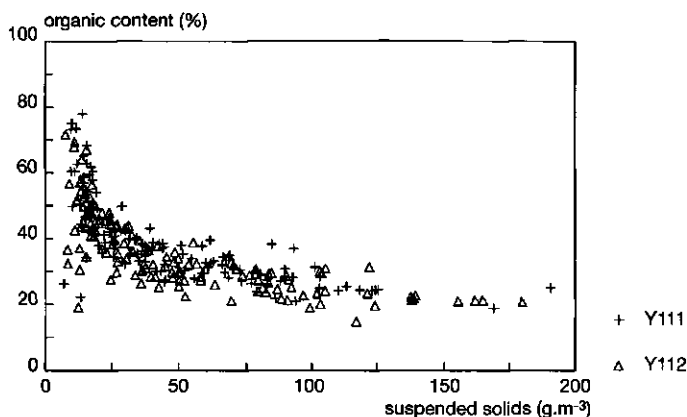


Figure 3.2 The ash free dry weight/ suspended solids ratio versus the suspended solids content at Y111 and Y112 in 1987, 1988 and 1989

#### Particulate and dissolved organic carbon

Particulate organic carbon (POC) is the difference between the total organic carbon (TOC) and the dissolved organic carbon (DOC). The DOC content varied little between 6.5 and 7.5  $\text{g}\cdot\text{m}^{-3}$ , except for some peaks in 1988. POC values varied between 2 and 16  $\text{g}\cdot\text{m}^{-3}$ . The trends in the POC concentration are very similar to the trends in the AFDW concentration. Therefore, at the end of 1988 the measurements of both POC and DOC were stopped.

#### Chlorophyll-a and phaeophytine

The chlorophyll-a concentration, varied between 10 and 200  $\text{mg}\cdot\text{m}^{-3}$ . The variations in chlorophyll-a concentrations are similar to those found in the suspended solids concentration. This is illustrated in Figure 3.3, which shows the relationship between the chlorophyll-a content and the inorganic solids content measured at Y111. As the main source of inorganic solids in the water phase is the resuspension of sediment, increases in chlorophyll-a concentrations are often due to the resuspension of sediment too (§ 6.1.3).

The chlorophyll-a concentration (Chla) is measured according to the NEN-6520 method. The NEN-6520 method is known for its tendency to exaggerate the actual values of chlorophyll-a, even though reproducibility is high. Van Urk et al (1990) recommend to separate algal pigments by high pressure liquid chromatography (HPLC) prior to quantification. In the Markermeer, the chlorophyll-a values measured according to the NEN-6520 method, were at least twice the values measured with HPLC (Van Urk et al, 1990).

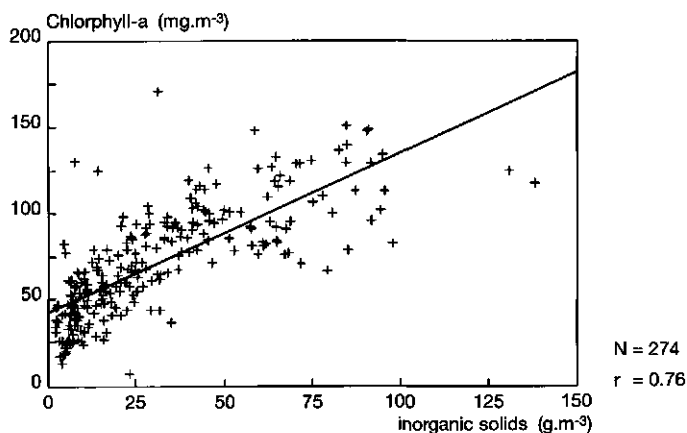


Figure 3.3 Chlorophyll-a content versus the inorganic solids content at Y111 in 1987, 1988 and 1989

#### Phytoplankton composition

In 1987, 1988 and 1989 the ratio of the numbers of different phytoplankton species were counted in samples taken near the surface at Y111 and Y112, preserved with formalin. In 1988 and 1989 the absolute cell number was counted as well, the results are presented in Figures 3.4 and 3.5. Individuals were counted in a haemocytometer (Fuchs-Rosental), the method is discussed extensively by Vermij and Janissen (1991). In every sample at least 100 individuals were counted. Unfortunately, the handled definition of an individual is not a cell, but a secluded cell or group of cells (Vermij and Janissen, 1991). Hence, a phytoplankton colony is counted as one individual. Especially for phytoplankton spe-

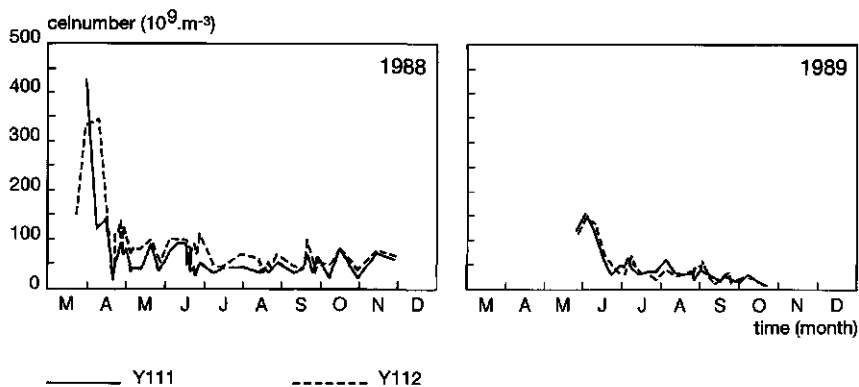


Figure 3.4 Measured phytoplankton cell numbers in 1988 and 1989 at Y111 and Y112

cies with a strongly varying number of cells per colony like *Microcystus* or *Aphanizomenon*, this method gives only an indication of the presence of the species. For the filamentous *O.agardhii*, the length of the filaments was usually measured as well.

From Figure 3.4 it is obvious that the numbers were highest during the spring. Unfortunately, in 1989 cell counts started not until May. The differences between the two sites are small, even though the water depth at site Y111 is about 1 m higher than the depth at site Y112. The species composition at Y111 is presented in Figure 3.5. In both years no blooms of blue-greens occurred and the total percentage of blue-green algae stayed well below 20 % in 1988 and below 50 % in 1989, with small absolute cell numbers during both years (Figure 3.4). In 1988 some growth of *Aphanizomenon* species occurred, whereas in 1989 some growth of *Oscillatoria* species was observed. In general green algae were the dominant species, but in 1988 in the summer a temporary increase of *Xanthophyllae* was observed.

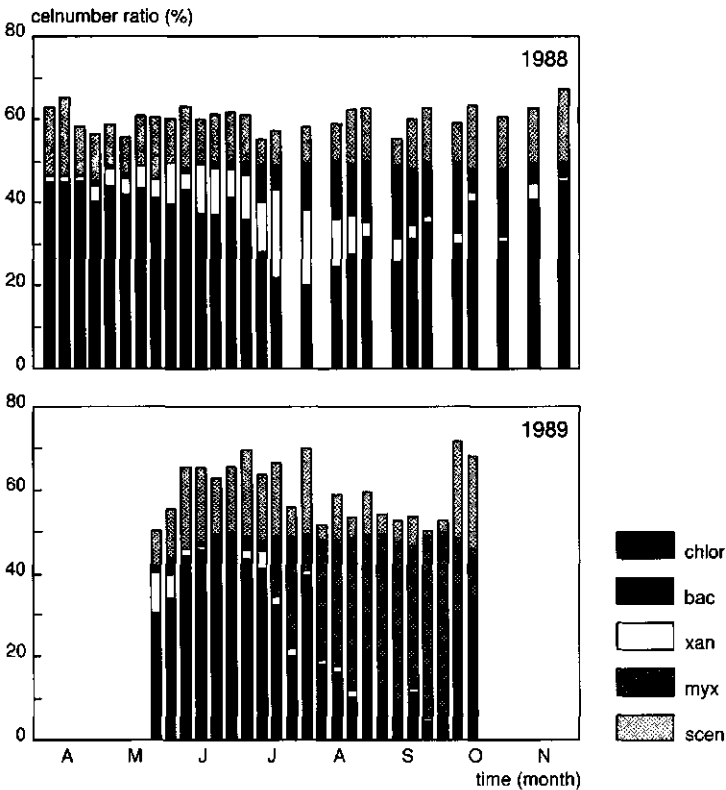


Figure 3.5a Measured cell ratios in 1988 and 1989 at Y111

Nutrients

Phosphorus was measured as total phosphorus (P-tot) and soluble phosphate (P-PO<sub>4</sub>). Due to the high partition coefficients of phosphate for sediment, the measured total phosphate concentrations are correlated with the suspended solids concentrations. This is illustrated in Figure 3.6. Hence, resuspension of sediment is an important factor controlling the concentration of total phosphate (Jagtman and Van Urk, 1988). The ortho-phosphate concentrations were lowest during the summer. In 1987 both in spring and in summer the measured ortho-phosphate concentration was below the detection limit.

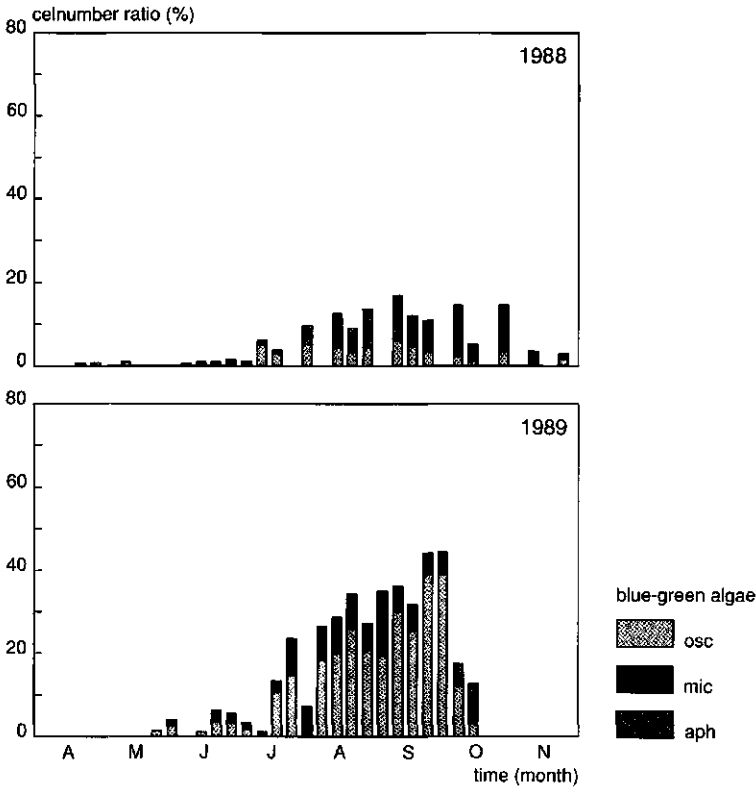


Figure 3.5b Measured cell ratios of blue-green algal in 1988 and 1989 at Y111

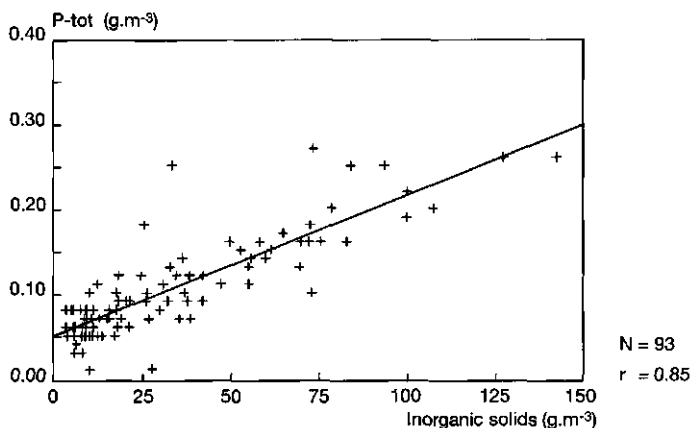


Figure 3.6 Total phosphate concentration versus the inorganic solids content at Y111 in 1987, 1988 and 1989

The N-Kjeldahl concentrations varied during the season between 0.7 and 3.0 (g.m<sup>-3</sup>). No relation was found with the inorganic solids concentration or any other variable. The concentration of NO<sub>x</sub> was high in early spring and autumn but below the detection limit in June, July, August and the first weeks of September in all three years, which is illustrated in Figure 3.7. The ammonium concentration were very variable, except for 1987, when concentration were below 0.02 g.m<sup>-3</sup> in the period from July till November.

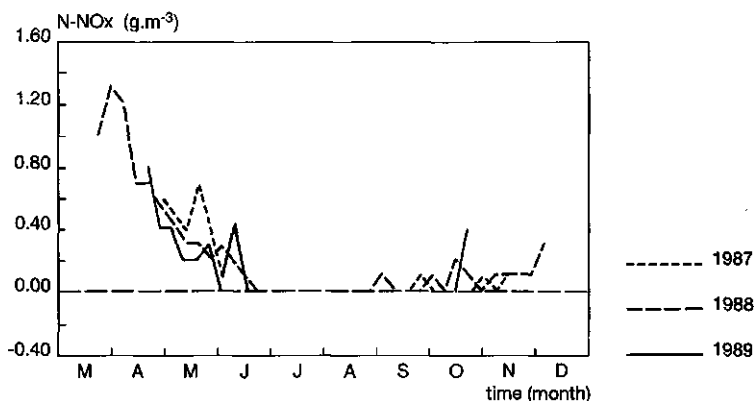


Figure 3.7 Measured NO<sub>x</sub> concentration at Y112 in 1987, 1988 and 1989

The concentrations of phosphate and nitrogen are important in the identification of the limiting factors of phytoplankton growth. As during the growth season ortho-phosphate, NO<sub>x</sub> and NH<sub>4</sub> are temporary very low,

phytoplankton growth in the Markermeer may be partially phosphate or nitrogen limited (Chapter 6).

The silica concentration showed the same pattern in each year. Concentrations decrease very fast in spring and increase a few months later, a second decrease is noticed at the end of the season. In 1989 this pattern may be related to the occurrence of Bacillariophyceae (diatoms), which were dominant during April and May but decreased in June. However, no increase in diatom number was found in September. No correlation between  $\text{SiO}_2$  concentrations and diatom number is found.

### **3.3 Automatic measurement of water quality variables**

The automatic measurement of variables offers an opportunity to collect data with a very high frequency and at moments when on site visits are not feasible. For variables reflecting dynamic processes with time scales of fluctuations less than a day, automatic measurement is often the only way to obtain a sufficient number of data. However, the technical requirements are considerable. Stations have to be mounted, which are entirely self sufficient for at least short periods of time. Even electricity is often not available. So, besides the installation of platforms, batteries must be provided which have to be changed regularly or electricity has to be generated on site. Valuable and sensitive equipment is installed at the platform and is subject to all weather conditions, fluctuating voltages and inquisitive tourists. If equipment transmission to data loggers functions properly, an immense number of data is generated, which has to be saved by the logger either in the original form (amperes or volts) or in a processed form. The conduct of simple computations on the raw data before saving, generally decreases the number of data to be saved, but unfortunately also destroys information on the individual data. For example if data measured with a 4 Hertz frequency are averaged for each hour, the memory capacity needed decreases substantially but information on both regular and irregular errors is lost. If data are transported from the station to the office, the heaps of data have to be processed to manageable files with transparent values. Prior to application, expert scanning of the data is necessary to detect device errors or procedural errors. This processing and scanning of data is very time consuming and therefore the period between the actual measurement and the scrutiny tends to be long. If errors in the devices or the procedures are observed at that stage, erroneous measurement may have been continued for very long periods. In studies involving automatic measurements, useless data are often obtained or more time is spend on data collection than on data analysis (Luettich, 1987, this study).

In the Markermeer study problems and errors occurred with almost all the equipment, including the batteries and the data loggers. Hence, sometimes only fragmented time series are available or none at all. On the other hand, the ultimate available data set has been scrutinized very carefully and is presumably reliable, nevertheless hidden errors cannot

be precluded. The data collection and processing and an overview of the available data for respectively 1987, 1988 and 1989 are described by Mugie et al (1989<sup>1</sup>), Mugie et al (1989<sup>2</sup>) and Bruinsma et al (1992). The main differences between the three years in the measurement strategies are:

- In 1987 most measurements were done from a platform at Y112 and some from a pole nearby Y112, no automatic measurements were done at Y111;
- In 1988 the same combination was used at Y112 as in 1987, but at Y111 a pole was placed on which the same equipment was mounted as used on the platform at Y112;
- In 1989 on both sites the equipment was mounted on poles. The platform at Y112 was only used for additional experiments, (paragraph 3.5).

Pictures of the platform used in 1988 and the pole used in 1989 used at Y112 are presented in Figure 3.8. A schematic representation of the stations is presented in Appendix 3.

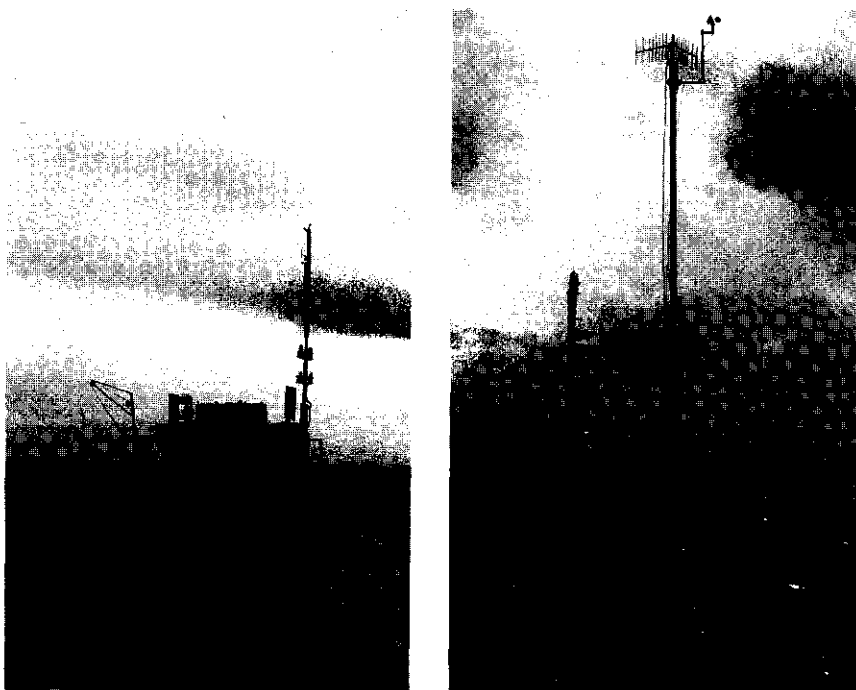


*Figure 3.8 Platform used in 1988 and the pole used in 1989 at Y112*

All equipment was fixed at a certain distance from the lake bottom. If necessary, the exact measurement depth was established afterwards, using the water level measurements (§ 3.3.3). All equipment was connected to 12 volt micro loggers (Campbell 21x, micro logger, Campbell Scientific Inc. USA) with 40 Kbyte memory and were extended with an



eprom. Data were transported with a Husky Hunter micro computer, which could also be used as additional memory for the micro logger or to load new programs in the micro logger.

### 3.3.1 *Suspended solids*

As the total suspended solids concentration in the Markermeer may change within the hour during stormy periods, an effort was made to measure the suspended solids content automatically.

In the field of water treatment and river sedimentology, turbidity meters are widely used to detect relative increases in suspended solids concentrations. To test the usefulness of these meters for the turbidity range observed in the Markermeer, some laboratory experiments were conducted with a MEX-3 Suspended solids meter and two different probes (RD-25 and RD-120/25, EUR-control). In these probes radiance is emitted at a wave length of 880 nm by diodes, the beam extinction is measured with silica photo diodes. According to the manufacturer, corrections are made for atmospheric influence and fouling. For the calibration of the meters suspensions with different concentrations of sediment of the Markermeer were made. Unfortunately the meters proved to be very susceptible to other sources of light and only the RD-120/25 probe seemed sensitive enough for measurements in the range of 0. to 500.  $\text{g}\cdot\text{m}^{-3}$  (Van Duin et al, 1988, Kuijpers and Van Duin, 1988). In the field, three RD-120/25 probes were fixed to a frame on a post mounted near the platform at Y112, approximately at depths of 0.5, 1.5 and 2.5 metre below the water surface. In contrast to the manufacturers guarantee, the probes were susceptible to pollution and therefore were cleansed weekly with a brush. Due to an error in the logger programs, values were registered only once per hour. When the measurement results were examined it became evident that the data displayed very arbitrary fluctuations. After recalculation the suspended solids concentration appeared 5 to 50 times larger than the data obtained from a direct analysis of water samples. After the measurement season the calibration of the meters was repeated over and again. It turned out that the sensors were very sensitive to the type of sediment used. Each type of sediment dilution series produced its own regression line, but for every individual sediment sample the scale was different. The meters were consistent only for a single well defined material like kaolinite, but not for natural sediments with variable composition. Therefore no data of these measurements are presented here nor used in the modelling work.

In 1988 a large sampling device was mounted at the platform at Y112. The sampler needed 380 Volt, which was delivered by a generator. The cooling system worked rather to well and the door of the container had to be kept open to prevent the samples from freezing. As after a few days the pump broke down and the control unit was flooded with water, new samplers were used in the third and fourth high frequency measuring period. These samplers (ISCO 2100 portable automatic sampler)

worked on 12 volt batteries, which were recharged by a wind generator. In the fourth period a similar sampler was mounted on the pole at Y111. Here the batteries were recharged by solar energy. These samplers worked well, except for some minor mechanical and electric problems. Grab samples were taken every 2 hours during work days and every 8 hours during the weekend in all four periods. Some data were omitted from the fourth period when the tube inlet apparently had sunk in the sediment instead halfway the water column.

In 1989 at both sites a new automatic sampler was mounted during the three high frequency sampling periods of two weeks. Apparently these samplers (PB-Mos, Edmund Bühler GMBH, BRD) were not equipped for grab sampling, so instead, mixed samples over a four hour period were taken by pumping a 150 millilitre sample every 40 minutes. Hence, peaks in the suspended solids concentration were smoothed. Although one sampler suffered from a short circuit and samples of one week were mixed up once, a few time series with reliable data are obtained, which are included in Appendix 5. Suspended solids concentrations varied between 10 and 150  $\text{g}\cdot\text{m}^{-3}$ . From these graphs it is obvious that the time scales for processes that determine suspended solids concentrations are small, for values may change dramatically within hours.

### *3.3.2 Wind speed and direction*

In 1987 and 1988 a Thies anemometer was mounted at 10 m above the water level at the platform at Y112. Once per minute the wind speed and direction were measured and averaged per hour by the micro logger. To average wind direction measurements may introduce large errors, if the direction within an hour is changing drastically. However, comparison with KNMI data of station the Houtrib exhibited a large similarity. As expected, wind speed values were higher at the Houtrib during winds from the South or the West, but lower with winds from the North-East (Mugie et al, 1989<sup>2</sup>). The meter was maintained well but not calibrated in 1987. Before the season of 1989 the wind speed meter was calibrated. If the average wind speed per hour is less than 3  $\text{m}\cdot\text{s}^{-1}$ , both wind speed and direction measurements are not reliable, for higher values the error in wind speed values is probably less than 2  $\text{m}\cdot\text{s}^{-1}$  and the error in wind direction about 5 degrees. In Appendix 5 the data are presented for the high frequency periods of 1988.

In 1988 wind speed was measured at Y111 as well with an anemometer (A110M, Vector Instruments). The meter produced a digital signal, unlike the analog signal produced at Y112. Unfortunately, the micro logger was not capable to count the pulses accurately during high wind speeds and no reliable data were obtained.

In 1989 the same wind speed meter was used as before at Y112. Mysteriously, no credible wind speed values were recorded and the wind direction proved to be very dissimilar from the direction measured at the

KNMI station, the Houtrib (Bruinsma et al, 1992). At Y111 the same anemometer was installed as in 1988, which produced very similar data compared to the Houtrib data (Bruinsma et al, 1992). Because no wind direction data are available of either sites, the wind speed data of Y111 are neglected and both wind speed and direction as measured at the Houtrib are used. In Appendix 5 the data of the Houtrib for the high frequency periods are presented.

At the KNMI station, wind speed and direction is measured during the entire year. For each hour the wind direction is defined as the mean value of the wind direction measured during the last ten minutes. In Figure 3.9, a detailed wind frequency table is presented of hourly wind speed and direction values measured in 1989, which is compared in Figure 3.10 with the other two years. During more than 50 % of 1989, the mean hourly wind speed varied between 5 and 10 m·s<sup>-1</sup>. Another third of the year the wind speed was less than 5 m·s<sup>-1</sup>. As is well known, wind from westerly directions is most common, and heavy storms originate from these directions too. In 1987 mean hourly values of more than 20 m·s<sup>-1</sup> were measured for 7 hours. In 1988 this occurred only once and it was never recorded in 1989. During each of the high frequency sampling periods of 1988 and 1989, wind speeds over 10 m·s<sup>-1</sup> were measured, but wind speeds over 15 m·s<sup>-1</sup> are only experienced once, during the last period of 1988 (88-4).

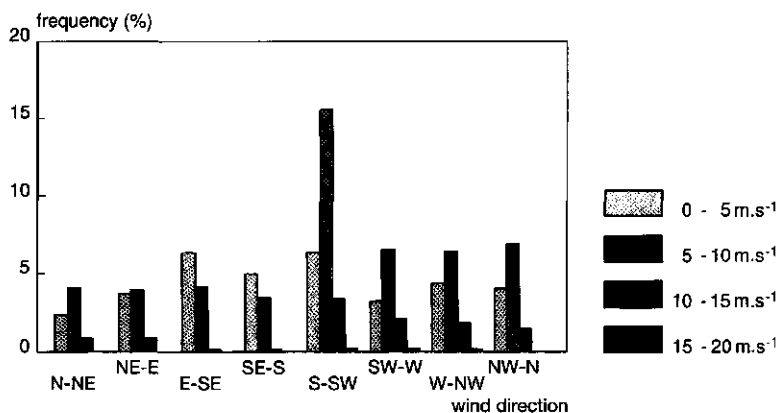


Figure 3.9 Wind frequency table of 1989 (data KNMI)

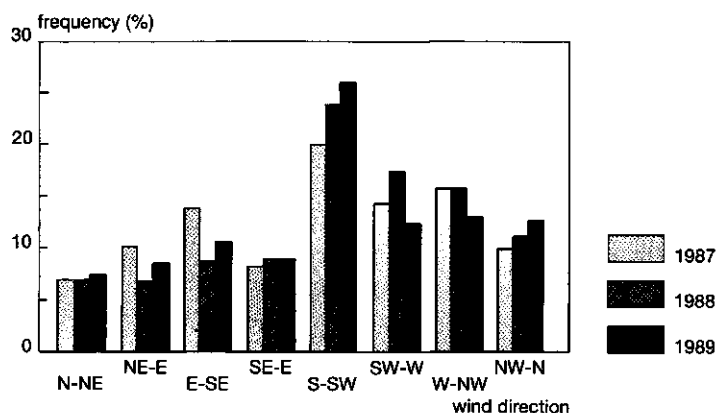


Figure 3.10 Comparison of the wind frequency table of 1987, 1988 and 1989 (data KNMI)

### 3.3.3 Water level and wave characteristics

In 1987 water level variations were measured by RWS-ZZW with a standard RWS digital wave staff at site Y112. Over 3 metres of the pole, electrodes were placed every 0.05 m. Ten times every second the resistance over the electrodes was measured and the water level was assessed twice per minute. The information was transmitted to a station at Lelystad-Haven. The data are processed automatically into hourly values of significant wave height and mean water level. The processing program was stored in an eprom built in the computer in an executable form, but the original software was unknown to the operators. The computed mean water level and significant wave height were printed every hour, the original data were lost.

In 1988 the same procedure for the measurement of water level variations was used in the beginning of the season. In the summer another receiving station was installed on the office roof, where all data were stored on diskettes first and processed afterwards. From these data significant wave height and wave period have been estimated (paragraph 4.2.2). After an initial mistake in the processing procedures a correct method was developed (Mugie, 1989). After comparison of this new method with the old (unknown) method, the old method appeared to be partly erroneous. Although the mean water level estimated with the old method proved to be credible, wave heights estimated with the old method are about 30 % lower than those estimated with the new method. The new measuring procedure was used for both Y112 and Y111. Unfortunately, the transmitted signal was often interrupted, because the over land distance was relatively long for the rather weak signal. Particularly, the signal of Y112 was frequently received poorly. Therefore the remaining set of reliable water level, significant wave height and wave period

data is limited and discontinuous. The data available from the high frequency sampling periods of 1988 are displayed in Appendix 5.

In 1989 water level, significant wave height and period were measured similar to the 'new' method of 1988, but the receiving station now was located in the building 'de Trekvogel'. Because this station is much closer to both transmitters and the travelling distance over land is short, the frequency of disturbance was less than in 1988.

As the distance between electrodes is 0.05 m, the step size of the measurements is 0.05 m. Hence, the relative error of wave height measurements, decreases with increasing wave height values. The obtained data set of 1989 is the most reliable one, unfortunately it is discontinuous. Water levels, registered by sluice attendants, were used to determine the NAP-level of both the wave staffs. These data were also used to calibrate the hydraulic model (§ 4.4.2)

#### *3.3.4 Flow velocity and direction*

In 1987 an attempt has been made to measure currents, both horizontal and vertical with acoustic flow velocity meters known as vector-aqua's (Rijkswaterstaat, Dienst Getijde Wateren). The principle of these meters is that high frequency acoustic signals are transmitted in four directions both ways. From the differences in delay of the receipt of the signal, the flow velocity and direction are estimated. Two meters were installed at the pole at Y112, one at an approximate depth of 0.5 metres and the other at an approximate depth of 2.5 metres below the water surface. Six times a day, flow velocity and direction measurements were done at a frequency of 2 Hertz for 3 minutes. The meters were susceptible to pollution and seemed very sensitive to vibrations in the pole as well. Therefore, part of the frame was lowered into the sediment. After the measurement season the meters were tested indoors and it became evident that calibration of the meters failed. Every time the power was switched off and on again, the sensitivity of the meters was different and calibration was necessary. Because on the measurement site the power was switched off and on, six times a day, the produced data evidently are worthless and had to be disregarded.

In 1988 a new attempt was made to measure horizontal flow velocity and direction with meters, based on electromagnetic methods (Marsh Mac-Birney, electromagnetic current meters, Rijkswaterstaat, Meetkundige Dienst). The sensor consisted of a spherical transmitter, generating an electromagnetic field and four electrodes, placed perpendicularly to the sphere in a horizontal field. From the difference in voltage measured by the four electrodes, the flow velocity and direction are estimated. The range of the meter is either 0.6, 1.5 or 3.0 m s<sup>-1</sup>, which not very suitable for measuring currents in Markermeer, which are estimated in the range of 0 to 0.1 m·s<sup>-1</sup>. Twice a day, for 3 minutes measurements were done with a frequency of 2 Hertz. Problems occurred with the power supply

and the meters were susceptible to corrosion. After data analysis it became evident that the data were not reliable and they were abandoned.

In 1989 no further attempts have been made to measure flow velocity and direction.

### *3.3.5 Irradiance and irradiance attenuation*

The nature of the underwater light field and the modelling of attenuation of light energy in water are described extensively in Chapter 5. In this paragraph, theoretical considerations are limited.

For the measurements of solar irradiance and underwater irradiance, the same underwater quantum sensors were used as described in § 3.2.1. During the three years of measurements, one underwater sensor was placed above the water surface at site Y112, in order to compare the KNMI method with the method used in the field and to obtain data to compare the various models for light reflection. For this sensor no immersion corrections were made, but further it was treated similar to the sensors placed under water.

In 1987 the old sensors of the RIJP, that had been used for years, were sent to the manufacturer for maintenance and calibration. After calibration they were placed on the platform at Y112, one above water and three under water at an approximate depth of 0.4, 0.7 and 1.0 m below the water surface. The three underwater sensors were placed on a mobile frame, each rotated about 30 degrees from the one above. These sensors were not functioning properly from the start and were replaced in August by brand new sensors. The cells were treated with translucent anti-fouling paint before instalment. Irradiance was measured for ten seconds every minute and averaged per hour. The mean value was stored each hour in the data logger. Every week the cells were cleaned. In the last month the cells were compared with the portable cell. Comparison was done by drawing them above water, these data seemed to agree rather well. Comparing the cells underwater was infeasible, because it was impossible to bear them at the same depth. Comparison of signals during the dark, was done by covering them with small lids. These measurements were useless as the lids appeared to be perforated. The measurements seemed rather reliable, but systematic differences in sensitivity can not be ruled out.

From the underwater irradiance measurements, the vertical downward attenuation coefficient  $K_d$  is estimated using equation 3.2. A threshold value of  $8 \mu\text{E}\cdot\text{m}^{-2}\cdot\text{s}^{-1}$  has been used for the computation of the attenuation coefficient as at night usually values of 2 to  $4 \mu\text{E}\cdot\text{m}^{-2}\cdot\text{s}^{-1}$  were measured. As measurements were done at three depths, both the attenuation between 0.4 and 0.7 metres and the attenuation between 0.7 and 1.0

metres can be estimated. In Figure 3.11, the estimated attenuation coefficients at Y112 are presented for a ten day period in October.

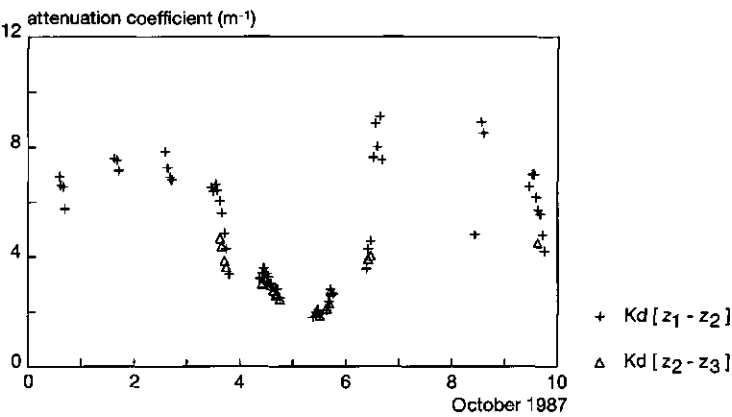


Figure 3.11 Estimated downward attenuation coefficient at Y112, October 1987.

The variation in the attenuation coefficient was large in this period. The attenuation coefficient estimated for the two deepest sensors is often not available, especially when the attenuation is high, because the sensors were not sensitive enough for such conditions. In Figure 3.12 both attenuation coefficients are compared.

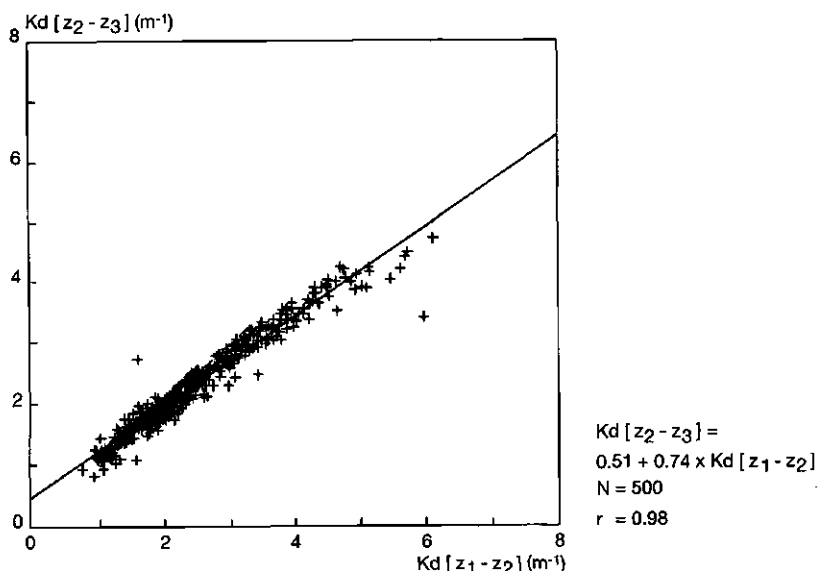


Figure 3.12 Comparison of the attenuation coefficient of -0.4 and -0.7 metres ( $K_d[z_1-z_2]$ ) and of -0.7 to 1.0 metres ( $K_d[z_2-z_3]$ ), estimated from measurements at Y112 in 1987

The correlation between both attenuation coefficients is very high, but it seems that the  $K_d[z_2-z_3]$  is slightly lower than the attenuation coefficient computed from the measurements nearer to the surface. This is in agreement with present theoretical insights (§ 5.2.2).

In 1988, the same four sensors were used as in 1987, but the distance between the underwater sensors was changed; they were placed at approximately 0.4, 0.65 and 0.9 metres below the water surface. The frequency of measurement was kept at once per minute and averaged at the hour. The sensitivity of the sensors was plainly lower than it was in 1987, in 1988 no irradiance was recorded any more when attenuation increased above  $6 \text{ m}^{-1}$ , even though the meters were placed closer to the surface than in 1987. At night values higher than  $6 \mu\text{E} \cdot \text{m}^{-2} \cdot \text{s}^{-1}$  were found. In Appendix 5, time series of the attenuation coefficients are presented for the high frequency sampling periods of 1988. In Figure 3.13 the relation between the two estimated attenuation coefficients is drawn. The slope of the curves of Figure 3.12 and 3.13 is identical, the increment is slightly smaller.



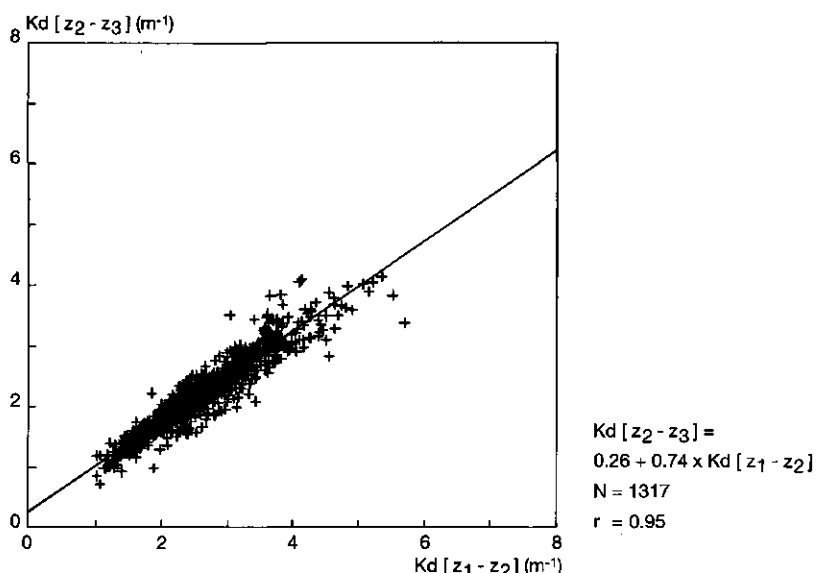


Figure 3.13 Comparison of the attenuation coefficient of -0.4 and -0.65 metres ( $K_d[z_1-z_2]$ ) and of -0.65 to 0.9 metres ( $K_d[z_2-z_3]$ ), estimated from measurements at Y112 in 1988

In January 1989 the sensors used at Y112 in 1988 were returned to the manufacturer for calibration. The total calibration drift in 18 months varied between 1 and 8 %. In April at each site three sensors were placed underwater; at 0.4, 0.6 and 0.8 metres below the surface. The individual resistances of each sensor, the calconnectors, were exchanged for other resistances, to produce higher voltage values in order to improve the reliability of the measurements. In the estimation of irradiance from the measured voltage values, a correction was made for the newly used resistances. At Y112 problems occurred time after time with the sensor at 0.8 metres, therefore was replaced at the end of August and again at the beginning of September. Useful measurements are virtually absent. At site Y111, problems occurred with the sensor at 0.4 meters until mid July. During each visit, the sensors were cleaned and irradiance measurements with all three cells above water were made to detect discrepancies in the sensitivity between the sensors. Discrepancies were found between the different sensors, but the discrepancies were not systematic and the deviations could not be attributed to one specific sensor. The downward attenuation coefficients of the layer between 0.4 and 0.6 metre and between 0.6 and 0.8 metre were estimated for all the data of Y111. For site Y112, the attenuation coefficient was estimated from the irradiance measurements from 0.6 and 0.8 metres only. The attenuation coefficients estimated for the high frequency sampling periods are presented in Appendix 5. The relation between the two coefficients estimated with data from Y111 is presented in Figure 3.14. Obviously the discrepancy between both attenuation coefficients is large and not sys-

tematically at all. Apparently, the effort made to improve data reliability had the reverse effect.

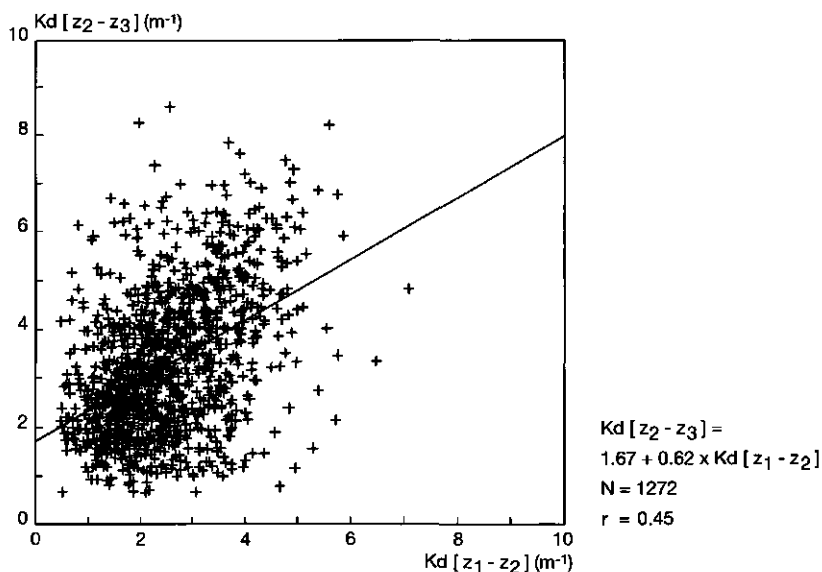


Figure 3.14 Comparison of the attenuation coefficient of -0.4 and -0.6 metres ( $K_d[z_1 - z_2]$ ) and of -0.6 to 0.8 metres ( $K_d[z_2 - z_3]$ ), estimated from measurements at Y111 in 1989.

In order to check the sensitivity of the different sensors a year after the calibration, all sensors were placed at the roof of the office for a few days. The discrepancy between the different values was much larger than expected. Apparently upon aging, discrepancies increase and regular calibration is no longer sufficient. Considering the newest sensor the most accurate, correction factors were estimated for all other sensors.

The decrease in the attenuation coefficient with the water depth may be quantified from the difference between the layers 0.4 to 0.65 or 0.7 and 0.65 to 0.9 or 0.7 to 1. The exact demarcation of the second layer did not seem to influence the ratio between the two attenuation coefficients, which can be seen by comparing Figure 3.12 with 3.13. To learn more about the decrease of the attenuation coefficient with depth, in 1990 nine sensors were mounted at the poles placed at Y112. Each 0.1 m a sensor was placed, starting at 0.3 m below the surface. Using the new factors, the measured irradiance is corrected and the downward attenuation coefficient is estimated for each ten centimetre layer. The result was unpleasant; no consistency between the estimated attenuation values was found and often the estimated values were below zero. By omitting

the data from two sensors and recomputing the attenuation coefficients, a more reasonable set of attenuation coefficients was found. But in fact there was no obvious reason to omit those two particular sensors, one was only two years old. Unfortunately, these data are not reliable enough to quantify the decrease of the downward attenuation coefficient with depth. In September the experiment was repeated with 8 sensors. After three weeks the entire frame with the sensors was placed above water and measurements were continued for a week. The global irradiance measured by the eight different sensors differed substantially: differences up to 50 % were recorded. A recalibration of the sensors was done until all the estimated irradiance values were the same for all sensors. With the new correction factors the underwater irradiance was recomputed for the three weeks of measurements. The values varied in an inconceivable way. Changing the way the sensors were grounded neither improved the results and the attempts were terminated.

### Conclusions

In the reliable data of 1987 and 1988, a decrease in the value of the downward attenuation coefficient with the depth has been observed. To quantify the exact value of the downward attenuation coefficient irradiance measurements have to be done at as many depths as feasible. The change in measurement procedure from manual irradiance measurements at every ten centimetres to a parallel measurements at only two depths is certainly no improvement (§ 3.2.1). To improve the new method with parallel measurement, either the distance between the sensors should be extended, measurements should be repeated at every site at different depths or at the pole two cells should be mounted at each depth. With the measurement of irradiance the utmost care is needed in the method of sensor instalment, calibration and measurement. In the manner the sensors were installed in 1989 and 1990, some still unidentified errors must have been made. Thorough and frequent calibration is of the utmost importance, which is confirmed in literature (Jewson et al, 1984).

### Scalar irradiance

The irradiance data needed as input for the simulation model, have to be approximately uninterrupted. For this purpose, the measurement data described above, are useless as no measurements were performed during the winter months. Hence, the continuous time series of solar radiance of the KNMI have been used instead. These were measured with a pyranometer at de Bilt, some 100 kilometres from the centre of the lake. This is a cosine collector measuring the total downward radiant flux at a flat circular area, for the range of 300 to 3000 nm. According to Tilzer (1983) the radiant flux can be converted to the photon flux density for PAR, using equation 3.3. This relationship is empirical and at different latitudes and with different ratios of cloud coverage results may diverge.

$$E_s = 2.11 \cdot I_s \quad (3.3)$$

$$\begin{aligned} E_s &= \text{scalar irradiance (PAR)} & (\mu\text{E} \cdot \text{m}^{-2} \cdot \text{s}^{-1}) \\ I_s &= \text{total incident solar radiation} & (\text{W} \cdot \text{m}^{-2}) \\ & \quad (300\text{-}3000 \text{ nm}) \end{aligned}$$

In Figure 3.15 the estimated global irradiance computed by equation 3.3 is compared with the global irradiance measured at site Y112 for 1988. As in Figure 3.15 there is some disagreement between the estimated and measured data that can not be attributed to systematic errors in the irradiance sensor, it can be concluded that some care should be taken when the KNMI data are used for simulations of the light field in the Markermeer.

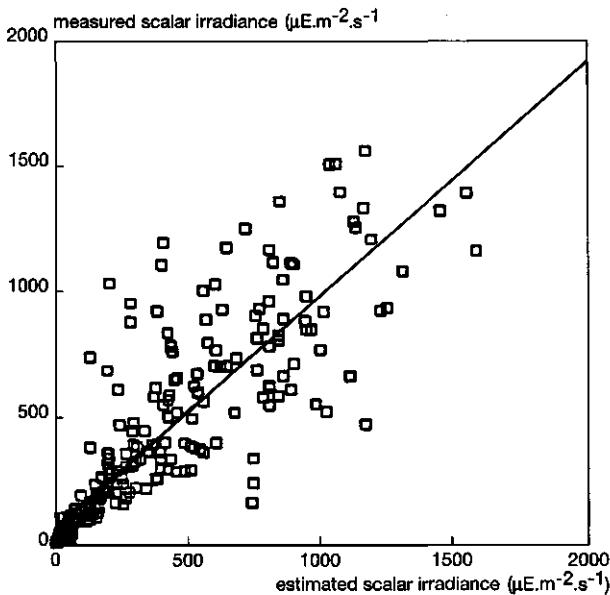


Figure 3.15 Comparison of the estimated and the measured scalar irradiance (PAR) of two weeks in June 1988 at Y112.

### 3.3.6 Dissolved oxygen concentration

In 1987 the dissolved oxygen concentration was measured at Y112 at 0.5 m below the surface, once every hour with an oxygen electrode (KCI-electrode 9200-032, Electrofact). Water in front of the membrane is renewed continuously by an oscillator. Weekly the membrane was cleaned or replaced and the value compared with the dissolved oxygen concentration measured manually (§ 3.2.1). If both values diverged more than  $0.5 \text{ g} \cdot \text{m}^{-3}$ , the electrode mounted on the platform was adjusted. Hence, the measured values are most reliable immediately after a visit and di-

verge slowly towards the end of the week. In general, the reliability of the measurements is not high and errors of at least  $1 \text{ g} \cdot \text{m}^{-3}$  are expected. In September no correct calibration was possible any more and these measurements were abandoned.

In 1988 the same procedure was used again, except for the oscillator, that was replaced by a small membrane pump. Every hour a cleansing fluid was pumped past the membrane of the electrode. The cleansing fluid, a solution of hydrochloric acid, worked well. Weekly the same calibration procedure was followed as described before, but the membrane was replaced more frequently than in 1987. The measurements seemed more reliable than those of 1987. At Y111 the same procedure was used for a similar electrode. However, due to a malfunction in the control unit, no reliable data are obtained.

In 1989 the same procedure was used again at both sites. Because the values showed inconceivable variations new electrodes (OXI 196, Wissenschaftlich Technische Werkstätten, BRD) were installed in August. These electrodes were cleaned weekly and calibrated. However comparison with the manually measured dissolved oxygen concentrations, still showed deviations. Apparently, the trend was measured well enough but absolute values are not always accurate.

### 3.3.7 Temperature

Temperature was measured at Y112 in 1987 with a temperature resistance metre (PT100 SM60, Electrofact) at two depths; 0.5 and 2.5 metres below the surface. Though hardly calibrated, measurements seem reliable and were relatively effortless. In 1988 the depths of measurement was changed to 0.5 and 1.5 metre below the surface. Calibration was attempted, but the laboratory calibration proved useless for equipment placed outdoors provided with a different power supply. Hence, the values were adjusted to the weekly manual measurements. At Y111 meters were placed in September at 0.5 and 2.0 metre below the water surface. These meters functioned well. A similar calibration procedure was used as for Y112.

In 1989 measurements continued at both sites at the same depths, but different electrodes (OXI 196, Wissenschaftlich Technische Werkstätten, BRD) were used. As the calibration of the electrodes produced the same problems as in 1988, corrections were made afterwards by comparison with the manual temperature measurements (§ 3.2.1). Apparently the electrodes diverged slowly. Linearly interpolated corrections were made for every 14 day period.

Short periods with temperature stratification have been detected every year, usually no longer than one day with differences in temperature between the measurements at the two depths up to  $1^{\circ} \text{C}$ . Again, for the simulation model time series of temperature had to cover the winter

period as well. For this purpose the daily measurements are used, that are conducted by the lighthouse-keeper of the island Marken. During periods with considerable changes in air temperature, the temperature near Marken may be slightly different from the water temperature in other areas of the lake.

### **3.4 Sediment characteristics and relationships with light attenuation**

In the Markermeer, the attenuation of light under water is mainly caused by suspended solids (§ 5.2.1). The contribution to the attenuation depends upon the physical, chemical and biological characteristics of the suspended solids. A distinction is made between suspended solids produced in the water column (living phytoplankton) and suspended solids brought into the water phase by resuspension of sediment. Phytoplankton characteristics and relationships with light attenuation are described in Chapters 5 and 6. Sediment is now defined as all material, both organic and inorganic which is for some period of time deposited on the bottom of the lake. Further characterisation and classification is made purely on physical characteristics of the sediment found on the lake bottom and in the lake water. Chemical differences are partly accounted for, as long as they affect physical characteristics.

#### **3.4.1 Sampling of sediment layers**

The composition of lake sediments varies both horizontally and vertically. Vertically many layers can be distinguished with different densities, porosities, pHs, oxygen concentrations, biological activity, etc. In the Markermeer study this was simplified to a distinction in two layers, a thin aerobic top layer, with a depth of less than one centimetre and a bottom layer composed of IJsselmeer deposit (§ 2.1.2).

Because the top layer is a very thin watery, aerobic silt layer of less than 0.01 m, undisturbed sampling of this layer is difficult. The thickness of the bottom layer varies, but may be as thick as 0.5 m. Hence, the sampling of this layer is easier. Håkanson and Jansson (1983) listed the requirements needed to take undisturbed samples. For loose and fine sediments they recommended core samplers. Five samplers, commonly used in the Netherlands, including three core samplers and two grab samplers, were tested on the lake (Winkels et al, 1989). Based on manageability and the fact that the samples were fairly undisturbed, two core samplers were selected; the Jenkin mud sampler, Figure 3.16 and the 'Vrij-wit-boor', Figure 3.17.



*Figure 3.16 Jenkin mud sampler*

When the Jenkin mud sampler was lowered on the lake bottom, the perspex tube slowly penetrated the top silt layer. By a hydraulic system the perspex tube is closed slowly at the upper side and the bottom side, whereafter the sampler is raised. The length of the tube is 0.5 m and the diameter 0.07 m. In loose sediments, usually 0.05 to 0.15 m silt was obtained, with a layer of water on top of it. If the sediment is too coarse, the tube could not penetrate the sediment and sampling fails. Afterwards the tube was removed from the sampler and the top lid was opened. A mixer was placed in the tube and during 30 seconds the water was stirred vigorously ( $\pm 370$  rotations per minute) and then left to settle. After 30 seconds the water with the suspended top layer is siphoned off. Hence, a suspension with sediment is obtained, except for particles with a very high fall velocity like sand or gravel. In order to improve the representativeness, at each site at least three samples were taken. In 1988 samples with the Jenkin mud sampler were taken at 12 sites, in 1989 at an additional 12 sites.



Figure 3.17 *Vrij-wit-boor*

The Vrij-wit-boor consists of two parts. A conical shaft, which is lowered in the sediment by manpower, using as many connecting rods as needed to reach the sediment. The second part is a rectangular lid, which is pushed down, using connecting rods again. Because the bottom side of the tube is closed, no sediment gets lost when the tube is raised. On board the Vrij-wit boor is placed horizontally and the lid is pushed open, giving displaying the sediment layers and the thickness of the layer containing IJsselmeer deposit was measured (§ 2.1.2). In 1988, 34 sites were sampled with the Vrij-wit-boor and in 1989 an additional 100 sites. The thickness of the silt layer is presented in Figure 2.3.

#### 3.4.2 *Sediment traps*

Compared to many other measurements, sediment traps are comparatively simple, cheap and easy to use. Gross sedimentation fluxes measured with traps give information about the mean fluxes for the



exposure period. For the construction of sediment traps Håkanson and Jansson (1983) formulated three basic rules:

- cylinders are the best form;
- cylinders should have aspect (height/diameter) ratios over 3 and in very turbulent waters this value should be increased to 10;
- cylinders should have diameters larger than .04 m.

For this study cylindric tubes were used, with a length of 0.5 m and a diameter of 0.048 metres, designed by the Agricultural University Wageningen, department of Nature Conservation. Around the tube two plastic rings are placed, to keep the tube floating in an upright position. The bottom of the tube is connected to a big street tile by a chain, to keep the tube in place. A small buoy is used as location mark.

In 1988 and 1989 sediment traps were placed each weekly visit at Y111 and Y112. In the next week the traps were removed and emptied. At each site three or four traps were placed, but at return traps were missing regularly. The number of traps, the total volume and the exposure time were registered, whereafter the contents of the traps at one site were mixed. This suspension was analyzed for total suspended solids and ash free dry weight. The sediment composition was analyzed as well (§ 3.4.3). For each site the mean sedimentation flux (SST) for that week was computed from the data. In 1988 the sedimentation flux of chlorophyll-a (ChlaT) and phaeophytine (PhaeoT) was measured as well. In Table 3.3 a summary of the computed data for 1988 and 1989 is presented.

*Table 3.3 Summary of sediment trap data of Y111 and Y112 in 1988 and 1989*

| Variable |  | Y111 |      |    | Y112 |      |    | Y111 & Y112 |       |
|----------|--|------|------|----|------|------|----|-------------|-------|
|          |  | mean | std  | N  | mean | std  | N  | min         | max   |
| 1988     |  |      |      |    |      |      |    |             |       |
| SST      | (g·m <sup>-2</sup> ·h <sup>-1</sup> )  | 15.9 | 13.1 | 32 | 29.4 | 13.4 | 33 | 4.6         | 165.1 |
| AFDW/SS  | (%)                                    | 23   | 2    | 32 | 18   | 4    | 33 | 9           | 29    |
| ChlaT    | (mg·m <sup>-3</sup> ·h <sup>-1</sup> ) | 6.9  | 2.3  | 34 | 6.7  | 3.1  | 33 | 2.4         | 15.6  |
| PhaeoT   | (mg·m <sup>-3</sup> ·h <sup>-1</sup> ) | 4.2  | 2.2  | 34 | 5.0  | 3.8  | 33 | 0.1         | 17.7  |
| 1989     |  |      |      |    |      |      |    |             |       |
| SST      | (g·m <sup>-2</sup> ·h <sup>-1</sup> )  | 10.8 | 5.8  | 26 | 16.0 | 9.6  | 26 | 1.5         | 37.8  |

Corresponding to the fact that the average wind speed in 1988 is higher than in 1989, the average sedimentation flux is higher as well. Partly this can be attributed to the shorter sampling period in 1989, when measurements were ceased in the second week of October, whereas in 1988 measurements were continued until the last week of November, including an additional six weeks in the storm season. Y112 is located in

the South-West of the lake and Y111 in the middle. Therefore during storms, which most often blow from the West or South-West (§ 3.3.2), Y111 might be expected to exhibit higher suspended solids concentrations and higher sedimentation fluxes. However, in both years the suspended solid concentrations (Table 3.2) and the sedimentation flux (Table 3.3) measured at Y112 are much higher than those measured at Y111. Obviously, not only fetch controls suspended solids concentrations and the sedimentation fluxes, but other factors as well (Chapter 4).

Due to the dynamic conditions in the Markermeer, sedimentation fluxes vary widely in space and time. As measurements were limited to part of two years and two sites, it was hard to estimate the absolute sedimentation flux for the whole lake. Concluding from the measurements, sedimentation fluxes over the lake may vary between 1.0 and 200  $\text{g}\cdot\text{m}^{-2}\cdot\text{h}^{-1}$ . Using  $0.36 \text{ kg}\cdot\text{m}^{-2}\cdot\text{day}^{-1}$  as a mean value for the entire lake, the internal load of the lake will be in the order of magnitude of a billion tons per year.

Two problems were encountered when the relationship between suspended solids concentration and sedimentation flux were formulated. Firstly, the suspended solids concentration of water is sampled with time intervals of several hours, whereas the sedimentation flux is the cumulative figure for the entire exposure period. During the exposure time at least two samples were taken and six at most. Hence, carefulness is needed with the comparison of both figures. The second problem is the occurrence of mineralisation processes in the sediment trap during the exposure time. Brinkman and Van Raaphorst (1986) found a mineralisation of 80 % in 14 days for the detritus of the Veluwemeer (Figure 1.1). They proposed a first order relation between mineralisation of particulate matter and the surface area available for colonization, stating that mineralisation of particulate matter is not limited by the availability of substrate. A measure for mineralisation might be the difference in organic content (AFDW/SS-ratio) between water samples and sediment trap samples, assuming that the sedimentation of organic and inorganic solids is comparable. The mean AFDW/SS ratio of the water samples is estimated from all the available data of the period the trap is exposed. In Figure 3.18 the difference between the AFDW/SS ratio of water samples and of sediment trap samples is related to the AFDW/SS ratio of water samples, but no significant correlation is observed. As mineralisation involves bacterial activity a relation between the water temperature and the mineralisation is expected. The mean water temperature during the sedimentation period is computed in a similar way as the mean AFDW/SS ratio in water samples is computed. But again no significant correlation was observed.

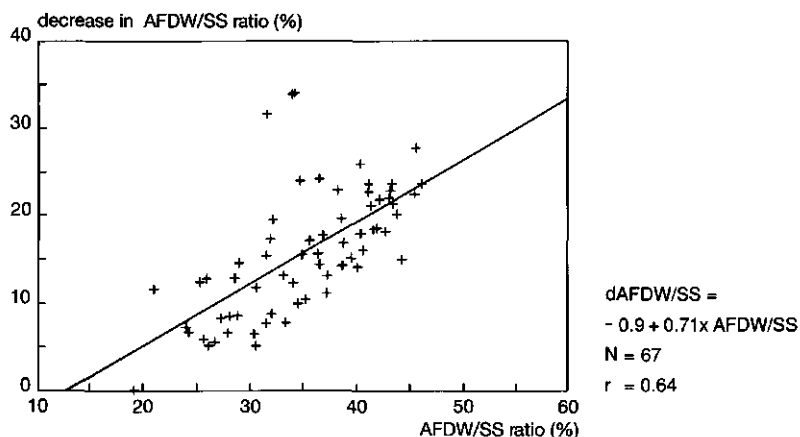


Figure 3.18 Difference in AFDW/SS ratio of water samples and sedimentation trap samples versus the AFDW/SS ratio in water samples of 1988

Though it is realized that the measured sedimentation fluxes are probably lower than the actual fluxes, due to the occurrence of mineralisation, no corrections are made for the occurrence of mineralisation. Hence, some care should be taken when the measured sedimentation fluxes are used.

### 3.4.3 Fall velocity distribution experiments

For the classification of sediments, an experimental method is used based on differences in fall velocities. The experiments were started in 1988. Due to problems with the data interpretation, a modified method was used in 1989 (Van Duin et al, 1992). During the experiments irradiance attenuation coefficients were measured as well, the results of those measurements are discussed in § 3.4.4.

The method to measure the fall velocity distribution of one sample used in 1988, is as follows. In nine cylindric glass tubes one litre of the suspension is brought and after stirring is left to settle. After a specific time, at 0.15 m below the water surface a pipette is inserted and the entire overlying layer is siphoned off in three out of the nine glass tubes. The same is done for the other six glass tubes, but for each group of three tubes a different settling time is used. The three samples of one group are mixed providing 1.3 litre of sample. In this sample no particles are present with a fall velocity larger than the sampling depth divided by the settling time. In the samples the total dry weight, ash free dry weight and the beam attenuation coefficient (§ 3.4.4) are measured. By subtraction of the analyzed dry weight contents of each group of tubes, the mass of a fraction is estimated. With the results, four classes of solids are dis-

tinguished by boundaries of settling velocities. The fraction with the smallest fall velocity, thus taking the longest settling time, is symbolized with  $SS_1$ . Fractions 2 to 4 are fractions with increasing fall velocities. This method has much in common with the particle size distribution method used for the classification of soil characteristics, except that now untreated fresh material is used. The boundary fall velocity values that are used in the Markermeer study are presented in Table 3.4. It is assumed that no coagulation or flocculation occurs during the experiment. In dilution series, no non-linearity was observed for concentrations below  $300 \text{ g}\cdot\text{m}^{-3}$ . Hence, in the experiments samples of sediment traps or top layer material were diluted to concentrations below  $300 \text{ g}\cdot\text{m}^{-3}$ .

*Table 3.4 Definition of fractions by fall velocity*

|        | minimum ( $\text{m}\cdot\text{s}^{-1}$ ) | maximum ( $\text{m}\cdot\text{s}^{-1}$ ) | mean ( $\text{m}\cdot\text{s}^{-1}$ ) | mean ( $\text{d}^{-1}$ ) |
|--------|--|--|---------------------------------------|--------------------------|
| $SS_1$ | 0  | $2.5\cdot 10^{-6}$                       | $3.4\cdot 10^{-6}$                    | 0.30                     |
| $SS_2$ | $2.5\cdot 10^{-6}$                       | $40.0\cdot 10^{-6}$                      | $25.5\cdot 10^{-6}$                   | 2.20                     |
| $SS_3$ | $40.0\cdot 10^{-6}$                      | $160.0\cdot 10^{-6}$                     | $109.0\cdot 10^{-6}$                  | 9.42                     |
| $SS_4$ | $160.0\cdot 10^{-6}$                     | ?  | $412.0\cdot 10^{-6}$                  | 36.6                     |

Theoretically, an infinite thin layer should be sampled from a settling tube with a pipette in order to obtain a sample with sharp boundaries in terms of fall velocities. Practically, a minimum quantity is needed for laboratory analysis. Because in the method used in 1988, the sampled layer is the entire 0.15 m layer above the pipette depth, which is not even close to the infinite layer condition, the interpretation of the data is complicated. The distribution of fall velocities over the samples is displayed in Figure 3.19. No particles with a fall velocity larger than the upper boundary are left in the sample and are therefore excluded, but the samples also contain varying proportions of material with a settling rate below the lower boundary.

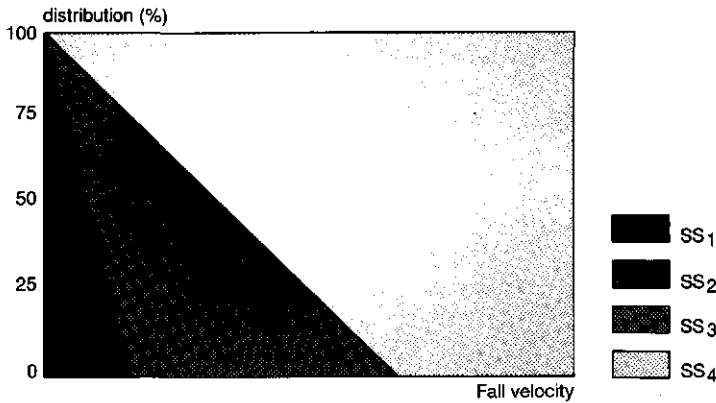


*Figure 3.19 Distribution of fall velocities over the different fractions in the experimental method of 1988*

In 1989,  $0.01 \text{ m}^{-3}$  samples were brought in cylindric glass tubes of 0.35 m in height and a diameter of 0.2 m. After a predetermined time at a predetermined depth a layer of two centimetres is obtained with a pipette, yielding the 1.3 litres needed for further analysis (Figure 3.20). The subsequent sample and data processing (Van Duin et al, 1992) is similar to the method used in 1988. Although the water level decline is two centimetres, the sample itself comes from an undefined space around the immersion point of the pipette. Hence, the fractions are still not absolutely defined, but compared to the method of 1988, they are much closer within the estimated range of settling rates.

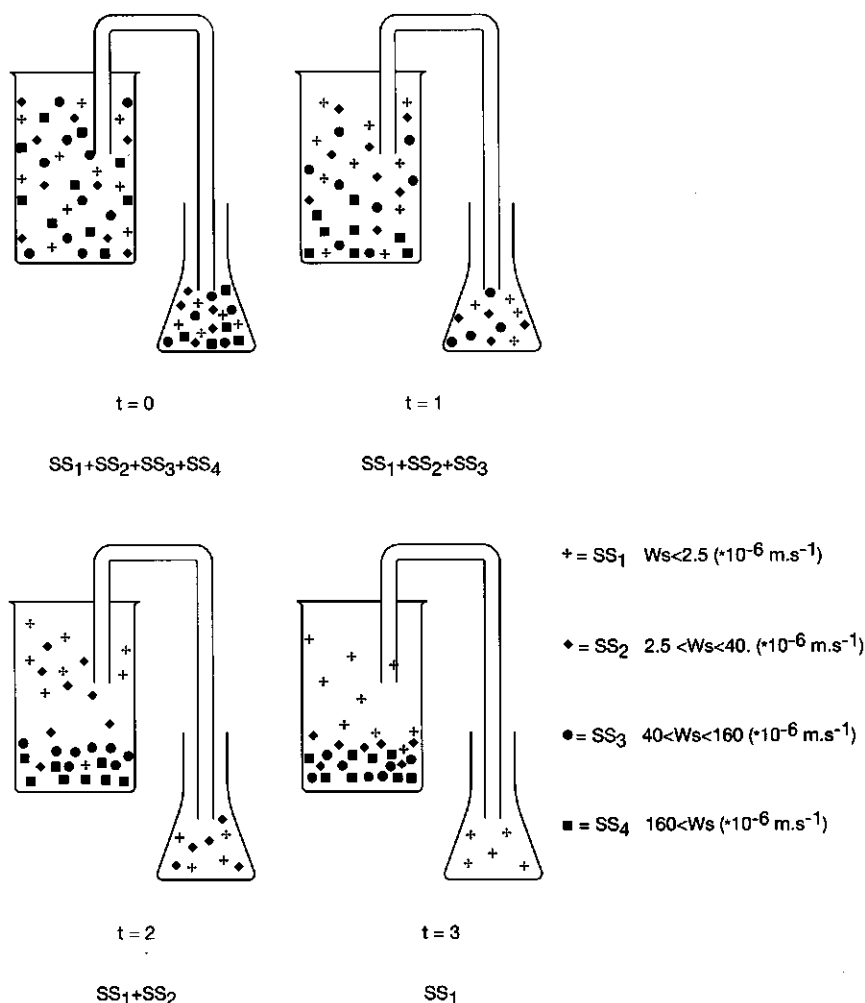


Figure 3.20 Fall velocity distribution experiments; the method used in 1989

The specific fall velocity of each fraction is estimated as the weighted mean of the boundary velocities. The background of this method is explained in § 4.1.2.

Samples of lake water, from sediment traps and from the sediment top layer have been analyzed for their fall velocities. Sediment top layer samples were taken with the Jenkin mud sampler (§ 3.4.1). In Table 3.5 the data of the fall velocity experiments are summarized for both years. Although difference were found between data of Y111 and Y112, not enough reliable data were available to discriminate systematically be-

tween these sites. Therefore in Table 3.5, data of site Y111 and site Y112 are averaged.

*Table 3.5 Summary of fall velocity distribution data of 1988 and 1989*

| (% of SS)     | SS <sub>1</sub> |     | SS <sub>2</sub> |     | SS <sub>3</sub> |     | SS <sub>4</sub> |     | N  |
|---------------|-----------------|-----|-----------------|-----|-----------------|-----|-----------------|-----|----|
|               | mean            | std | mean            | std | mean            | std | mean            | std |    |
| 1988          |                 |     |                 |     |                 |     |                 |     |    |
| Water samples | 37              | 13  | 34              | 10  | 10              | 5   | 18              | 14  | 63 |
| Sediment trap | 8               | 4   | 16              | 7   | 20              | 9   | 57              | 18  | 32 |
| Top layer     | 9               |     | 15              |     | 15              |     | 61              |     | 9  |
| 1989          |                 |     |                 |     |                 |     |                 |     |    |
| Water samples | 44              | 15  | 29              | 9   | 11              | 7   | 16              | 12  | 25 |
| Sediment trap | 22              | 8   | 34              | 13  | 16              | 7   | 28              | 15  | 35 |
| Top layer     | 7               | 5   | 18              | 11  | 12              | 4   | 63              | 18  | 7  |

| (% of SS <sub>i</sub> ) | AFDW <sub>1</sub> /SS <sub>1</sub> |     | AFDW <sub>2</sub> /SS <sub>2</sub> |     | AFDW <sub>3</sub> /SS <sub>3</sub> |     | AFDW <sub>4</sub> /SS <sub>4</sub> |     | N      |
|-------------------------|------------------------------------|-----|------------------------------------|-----|------------------------------------|-----|------------------------------------|-----|--------|
|                         | mean                               | std | mean                               | std | mean                               | std | mean                               | std |        |
| 1988                    |                                    |     |                                    |     |                                    |     |                                    |     |        |
| Water samples           | 35                                 | 9   | 33                                 | 10  | 33                                 | 14  | 32                                 | 15  | 29-125 |
| Sediment trap           | 21                                 | 6   | 24                                 | 6   | 24                                 | 5   | 18                                 | 5   | 34     |
| Top layer               | 24                                 |     | 25                                 |     | 20                                 |     | 16                                 |     | 9      |
| 1989                    |                                    |     |                                    |     |                                    |     |                                    |     |        |
| Water samples           | 49                                 | 16  | 40                                 | 16  | 30                                 | 12  | 40                                 | 14  | 8-57   |
| Sediment trap           | 37                                 | 13  | 27                                 | 12  | 26                                 | 14  | 23                                 | 21  | 22-36  |
| Top layer               | 36                                 | 12  | 20                                 | 10  | 19                                 | 7   | 9                                  | 6   | 6-12   |

As expected, in water samples the fractions with a low settling velocity dominated, whereas in samples taken from the sediment top layer, the fraction with the largest fall velocity dominated. In samples of sediment traps, fall velocities were distributed more homogeneously. This is illustrated in Figure 3.21. However, material left in the sediment traps for several days and material deposited in the sediment top layer is subject to chemical and physical processes like mineralisation and consolidation, modifying the characteristics of the material and thus their settling behaviour. Hence, the fall velocity distribution measured for sediment trap and top layer samples are used only as indicative values. Besides, in both years the sediment top layer samples are collected during a few days in March and no more than ten samples were taken. It is possible that the fall velocity distribution in the sediment top layer is quit different in autumn or in summer. Besides in the experiments, breakage of flocs or an additional aggregation may have occurred, which would have altered the fall velocity distribution (Van Leussen, 1986).

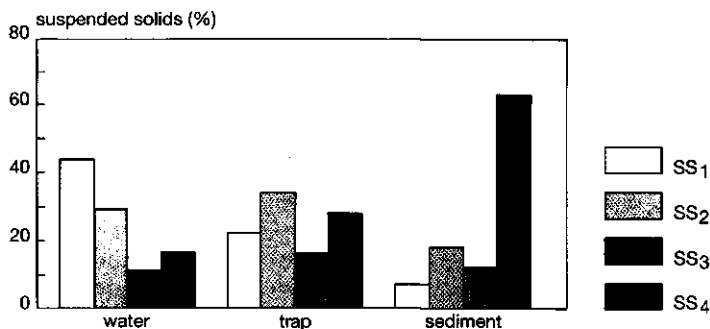


Figure 3.21 Mean fall velocity distribution in 1989 (Van Duin et al, 1992)

Considering the percentage of sediment within the various fractions of the water samples for both 1988 and 1989, the mean fall velocity of the suspended solids ranges between  $10 \cdot 10^{-6}$  and  $100 \cdot 10^{-6} \text{ m} \cdot \text{s}^{-1}$ . For estimations of the mean sedimentation flux the range of fraction 2 is used; a fall velocity around 2 metres per day. Combining this with a mean suspended solids concentration of  $50 \text{ g} \cdot \text{m}^{-3}$ , the mean sedimentation flux is estimated at  $0.1 \text{ kg} \cdot \text{m}^{-2} \cdot \text{day}^{-1}$ , instead of  $0.36 \text{ kg} \cdot \text{m}^{-2} \cdot \text{day}^{-1}$  estimated in § 3.4.2. This is caused by the fact that the impact of a few stormy events is much higher on the sediment trap data than on the suspended solids data. Probably, the value of  $0.36 \text{ kg} \cdot \text{m}^{-2} \cdot \text{day}^{-1}$  is the most realistic, as the sedimentation flux obtained from sediment trap data is based on a cumulative measurement instead of grab samples.

The results from the method of 1988 and of the method of 1989 are hard to compare. In October 1988, the fall velocity distribution of 27 samples was measured by both methods and the results were compared. With the improved method of 1989 the proportion of fraction 2 was increased with about 50 %, whereas the share of fraction 4 decreased with almost 50 %. For both fractions linear relationships with high correlations ( $> 0.9$ ) were derived. The proportion of fraction 1 decreased with about 10 % for the method of 1989 and the correlation between both methods was high for this fraction as well. Due to very low concentrations, measurements of fraction 3 failed regularly and only 12 data were left. With linear regression no relationship was found between the two methods for fraction 3. In 1988 the contribution of fraction 2 in water was roughly the same as the contribution of fraction 1 (Table 3.5), even though the method of 1988 tends to underestimate the contribution of fraction 2. In 1989, the contribution of fraction 2 was much smaller. This is probably due to the fact that suspended solids concentrations in general were higher in 1988 than in 1989 and this is probably due to a greater contribution of resuspended material in 1988. Accounting for the difference in method, the contribution of fractions 3 and 4 in sediment trap material, was also greater in 1988 than in 1989. The similarity in the fall velocity distribution of the sediment top layer of both years is remarkable.



In the different sediment samples, the AFDW/SS ratio is greatest for fraction 1 and smallest for fraction 4. In general the AFDW/SS ratio was smaller in 1988 than in 1989, caused by the smaller contribution of resuspended sediment in 1989. The difference between both years are most pronounced for fraction 1.

A major handicap of the used settling tube methods is the fact that many results are inaccurate, because concentrations and absolute quantities are very small. Hence, small errors in the analyzing procedure affect the estimated fraction values dramatically. Often data sets had to be discarded, because a negative quantity of a fraction resulted after subtraction.

#### 3.4.4 Specific attenuation coefficient

As the scattering and absorption of irradiance by particulate matter is partly determined by the physical and chemical characteristics of the particulate matter and partly by the spectrum of the irradiance itself, a light attenuation model including both aspects is needed. In Chapter 4 the relation between both aspects is discussed extensively. In this section a description of the experimental methods and a discussion of the data are presented. The underlying theory is presented as far as needed to understand the interpretation of the measurements.

The downward attenuation coefficient can be estimated by addition of the contribution of the different components, Kirk (1983):

$$K_d = K_{d,0} + K_{d,1} + \dots + K_{d,n} \quad (3.4)$$

If the contribution per unit of weight of a component to the attenuation coefficient is considered to be independent of the concentration, the downward attenuation coefficient of that component can be estimated :

$$K_{d,i} = k_{d,i} \cdot C_i \quad (3.5)$$

$$\begin{aligned} k_{d,i} &= \text{specific downward attenuation} \\ &\quad \text{coefficient of component } i \quad (\text{m}^2 \cdot \text{g}^{-1}) \\ C_i &= \text{concentration of component } i \quad (\text{g} \cdot \text{m}^{-3}) \end{aligned}$$

If the contribution of each component to the total attenuation is considered constant as well, except for the contribution of suspended solids, the relationship between the downward attenuation and the suspended solids content can be obtained by linear regression. In Figure 3.22 the relationship between the downward attenuation coefficient measured in the field (§ 3.2.1) and the suspended solids concentration is estimated for 1988 and 1989. The correlation between the suspended solids concentration and the attenuation coefficient is high, even though the variable composition of the suspended solids was not considered.

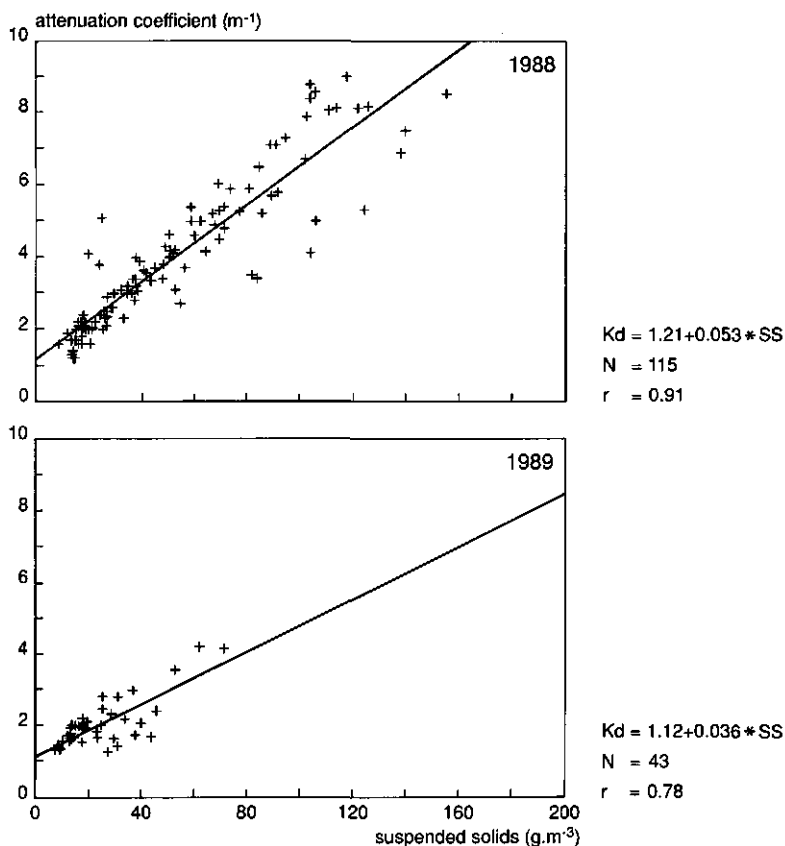


Figure 3.22 Measured downward attenuation coefficient versus the suspended solids concentration in 1988 and 1989

Besides the in situ measured vertical attenuation coefficient, the beam attenuation coefficient of water samples has been measured with a laboratory spectrophotometer. The spectrum between 400 and 700 nm was scanned in 50 nm steps. The mean beam attenuation coefficient,  $\epsilon$ , was calculated as the mean value. With a spectrophotometer, the combined effect of scattering and absorption is measured, whereas in the field mainly the effect of absorption is measured. Hence the mean beam attenuation coefficient measured with a spectrophotometer,  $\epsilon$ , is larger than the attenuation coefficient,  $K_d$ , estimated from underwater irradiance measurements. With linear regression a relationship is derived between the in situ measured  $K_d$  and  $\epsilon$ , this is presented in Figure 3.23. This relation is based on 103 measurements of 1988 and the estimated correlation coefficient is 0.94.

$$K_d = 0.68 + 0.29 \cdot \epsilon \quad (3.6)$$

$\epsilon$  = mean beam attenuation coefficient  
(PAR) ( $\text{m}^{-1}$ )

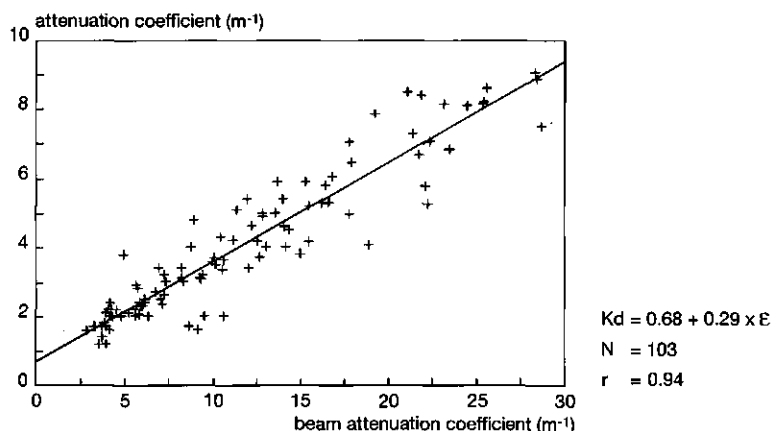


Figure 3.23 Downward attenuation coefficient  $K_d$  versus the mean beam attenuation coefficient  $\epsilon$

Apart from the distinction in different fractions of suspended solids by fall velocity, an attempt has been made to use these same fractions to model the attenuation coefficient. The method is based on the assumption that both the attenuation of light by particles (Baker and Lavelle, 1984) and the settling velocity of particles are related directly to the cross sectional area of the particles and not to their volume (§ 5.2). As most phytoplankton species settle slowly, the contribution of phytoplankton to the attenuation coefficient is incorporated in the attenuation of the fractions  $SS_1$  and  $SS_2$ .

In the fall velocity distribution experiments, the specific beam attenuation coefficient was estimated as follows. For each sample taken during the experiment, the beam attenuation coefficient is measured with a spectrophotometer. As the total beam attenuation coefficient of a suspension can be estimated from the contribution of its components, the beam attenuation coefficient is obtained for each fraction after a similar estimation procedure as used to compute the mass of each fraction: The beam attenuation coefficient of fraction 2,  $\epsilon_2$ , is computed by subtracting the beam attenuation coefficient of the sample with the smallest fall velocity from the beam attenuation coefficient of the sample with the smallest but one fall velocity. This is repeated for fraction 3 and 4. The specific beam attenuation coefficient of each fraction is obtained by dividing the beam attenuation coefficient of a fraction by the mass of that

fraction. In Table 3.6 the results of this method are presented for both 1988 and 1989. The specific attenuation coefficients  $k_{d,2}$ ,  $k_{d,3}$  and  $k_{d,4}$  were estimated from the results presented in Table 3.6, using equation 3.6 without the increment.

*Table 3.6 Summary of the specific beam attenuation coefficient measurements of 1988 and 1989 ( $m^2 \cdot g^{-1}$ )*

|                   | mean | std | min | max | N   |
|-------------------|------|-----|-----|-----|-----|
| <b>1988</b>       |      |     |     |     |     |
| $\epsilon_2/SS_2$ | .21  | .07 | .06 | .66 | 116 |
| $\epsilon_3/SS_3$ | .16  | .10 | .05 | .70 | 50  |
| $\epsilon_4/SS_4$ | .15  | .10 | .04 | .51 | 34  |
| <b>1989</b>       |      |     |     |     |     |
| $\epsilon_2/SS_2$ | .18  | .08 | .08 | .34 | 21  |
| $\epsilon_3/SS_3$ | .13  | .06 | .05 | .19 | 4   |
| $\epsilon_4/SS_4$ | .07  | .06 | .03 | .18 | 5   |

The results for fraction 1 are not presented in Table 3.6. Fraction 1 contains the dissolved substances and the slowly settling particles, including most of the phytoplankton cells. Hence for the computation of the attenuation coefficient, the background attenuation by water itself and the dissolved substances is incorporated in the attenuation of fraction 1. To distinguish between the contribution of phytoplankton and the contribution of the suspended solids in fraction 1, both the mass and the measured extinction coefficient are corrected for phytoplankton occurrence measured as chlorophyll-a content.

$$K_{d,1'} = K_{d,1} - k_{d,phyt} \cdot Chla \quad (3.7)$$

$$AFDW' = AFDW - C_1 \cdot C_2 \cdot Chla \quad (3.8)$$

$$\begin{aligned} K_{d,phyt} &= \text{specific attenuation coefficient of a} \\ &\quad \text{mixed Blue-green/Diatom popula-} \\ &\quad \text{tion} \\ &= 0.015 \text{ (Kirk, 1983)} \quad (m^2 \cdot mg^{-1}) \\ C_1 &= \text{Carbon/chlorophyll-a ratio} \\ &= 35 \text{ (Stutterheim and Smits, 1985)} \quad (-) \\ C_2 &= \text{organic content/ carbon ratio} \\ &= 2.0 \text{ (Werkgroep Normering, 1986)} \quad (-) \end{aligned}$$

The distinction between the background attenuation, including the contribution of dissolved substances, and the attenuation by fraction 1 was made by linear regression. The values of  $K_{d,1}$  were estimated from the measured beam attenuation coefficient,  $\epsilon_1$ , using equation 3.6. The results for both years are displayed in Figure 3.24.

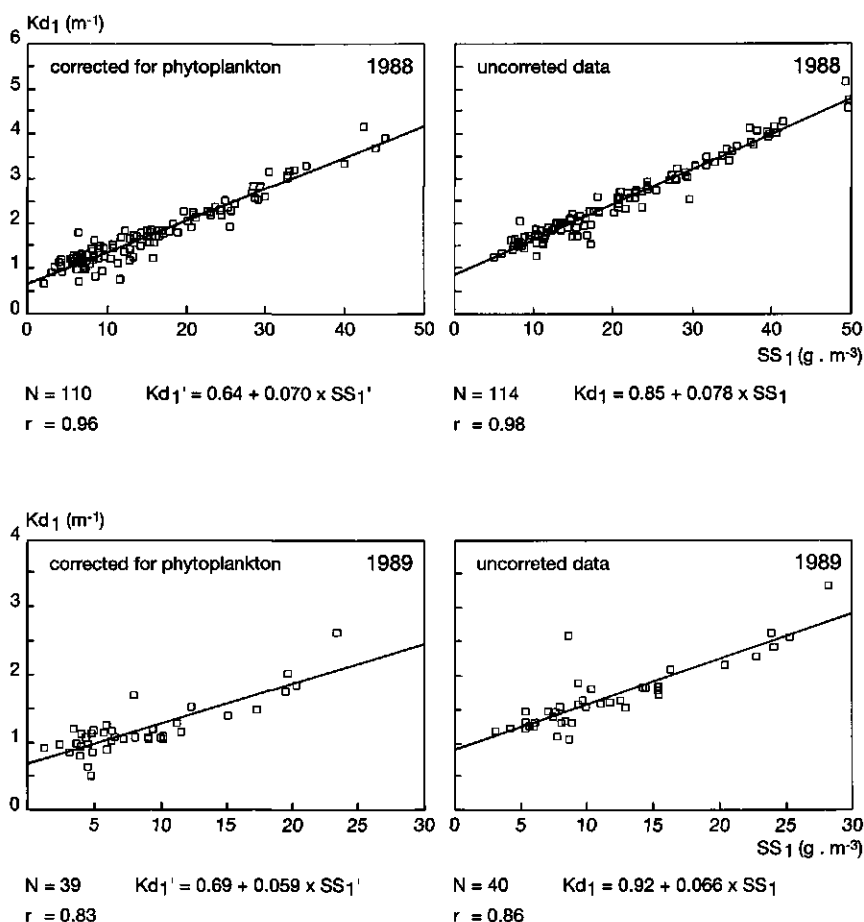


Figure 3.24 Attenuation coefficient of fraction 1 versus the mass of fraction 1 in 1988 and 1989

The total vertical attenuation by suspended solids is described by equation 3.9. The equation is corrected for the contribution of phytoplankton, hence the contribution of phytoplankton itself is *not* incorporated in this equation. The overall estimation procedure, including phytoplankton is presented in § 5.2.2.

$$1988: K_d = 0.64 + 0.070 \cdot SS_1 + 0.060 \cdot SS_3 + 0.045 \cdot SS_3 + 0.037 \cdot SS_4 \quad (3.9a)$$

$$1989: K_d = 0.69 + 0.059 \cdot SS_1 + 0.052 \cdot SS_3 + 0.038 \cdot SS_3 + 0.021 \cdot SS_4 \quad (3.9b)$$

The variability in the results is considerable and the number of data is limited, especially for the data set of 1989 (Table 3.6). The standard deviation is in the order of 50 % of the mean value and for the computation of the specific attenuation coefficient for fraction 3 and 4 of 1989, no more than 5 respectively 6 pair of data were available. This is due to frequently low concentrations in the samples, prohibiting a reliable analysis. Because the methods of fall velocity distribution measurements for both years were different, a comparison of the results is difficult (Van Duin and Kuipers, 1989). In 1988, particles with a smaller fall velocity than the defined boundaries were still present in the samples. Because solids with a small fall velocity have a larger specific attenuation coefficient, the estimated specific attenuation coefficients for 1988 are higher than those for 1989.

### 3.5 Primary production experiments

The objective of the Markermeer study centred on the growth of the cyanobacterium *Oscillatoria agardhii*. The typical light field of the Markermeer is mainly held responsible for the absence of blooms of *Oscillatoria* species (§ 6.1). Therefore, field experiments have been performed in the Markermeer itself with *O. agardhii*, to test the postulated hypotheses on primary production. A modified version of the light and dark bottle technique and a perspex tube have been used. The background and final interpretation of the experimental research is described in § 6.1.4.

#### 3.5.1 General lay-out of the experiments

The primary production experiments had to meet many requirements:

- a experiments had to be carried out with the characteristic light field of the Markermeer;
- b experiments had to be carried out with *Oscillatoria agardhii* organisms;
- c no other physical factors except the available light energy should be limiting during the experiments;
- d enough experiments should be carried out to test the reproducibility of the experiments and
- e the vertical movement of the algae should be reproduced.

To meet the first requirement, all experiments were carried out in glass or perspex containers, which were placed in the water of the Markermeer at site Y112. Assuming that the effects of scattering and absorption by the glass and perspex are negligible, the organisms will experience the natural light field of the Markermeer.

As blooms of *O. agardhii* are absent in the Markermeer, *O. agardhii* species had to be sampled elsewhere or grown in the laboratory. Because laboratory cultures may differ essentially from natural phytoplankton cultures and our experience with laboratory cultures was

limited, it was decided to obtain *O. agardhii* samples from another lake; the Nijkerkernauw (Figure 1.1). Blooms of *O. agardhii* have dominated the phytoplankton community in this lake for years (Berger, 1987). Before the start of the experiments, this dominance was checked. During the experiments, at least once a week, the Nijkerkernauw was visited and plastic containers were filled with water at the 'Laakse Strand'. The suspension was filtered through a 100  $\mu\text{m}$  net, to filter out most of the zooplankton species. In the laboratory the content of these containers was poured in a plastic 0.2 m<sup>3</sup> basin. A provisional light/dark cycle was provided by placing the basin below a lamp (Day light lamp, 400 – 700 nm, 250 Watt, Phillips), which was lighted during office hours. In the weekend it was lighted from friday morning until saturday afternoon and then switched off until monday morning. At days when site Y112 in the Markermeer was visited, the basin was moved aboard of the ship and placed on deck. The basin was shielded from the sun by a plastic lid. As the lid and basin were translucent and light and temperature on deck were often high, photosynthetic activity in the basin was often high, causing the suspension to be highly over-saturated with oxygen.

To eliminate the effect of limiting nutrients, a solution containing nutrients and macro-ions was added to the suspension in the basin. The composition of the solution is presented in Appendix 7.

In order to obtain enough experimental results to test the reproducibility, the experiments were conducted during both the second and third high frequency sampling periods of 1989 and during two high frequency sampling periods in 1990. The results of the second period of 1990 are described elsewhere (Visser, 1991).

### 3.5.2 Light and dark bottle experiments

The classical method of measuring photosynthesis *in situ* proceeds through the enclosure of water samples in glass bottles with ground glass stoppers (Vollenweider, 1974). In order to determine the total production in a given water column, it is necessary to run a series of vertical measurements, exhibiting the variation of photosynthetic activity per unit volume with depth. From this relationship (depth-profile), the activity below a unit area of surface can be calculated as the integral. The mean productivity is estimated as the integral divided by the depth. When an exposure has been made with sub-samples of a phytoplankton population in clear ('light') and darkened bottles, the initial concentration of dissolved oxygen can be expected to decrease in the darkened bottles by respiration. In the light bottles, the nett production will be measured, i.e. the photosynthetic oxygen production minus the respiration. This is true as long as other processes involving oxygen are absent or can be neglected, like respiration by zooplankton or fish. Bacterial decay of organic material may not be negligible in a dense phytoplankton population and will effect the estimated respiration. The conditions experienced by the phytoplankton cells within the experimental vessel may

be at variance with those in the lake in various ways and this may affect the activity being measured. This includes the absorption and scattering by the material of the vessel, the lack of turbulence within the vessel causing wall effects and sedimentation, the exposure of cells to excessive turbulence or strong light during manipulations and their maintenance at a fixed point rather than a circulation in the water column (Voltenweider, 1974). The relative influence of the manipulation is diminished by the extension of the immersion period. On the other hand, by decreasing the immersion time the influence of over or under saturation and settling within bottles, will subside. A duration of one to four hours of the experiments is chosen as a compromise for both.

By keeping the bottles at a fixed depth, the light field experienced by the algae will be different from the light field experienced in the open water. Hence, instead of fixed bottles, a string of bottles was used, which could be circulated through the water column. Two types of closed strings were used, short and long strings. A long string is 6 metres, with 6 bottles distributed evenly over the string. A short one is 3 metres, again with 6 bottles evenly distributed. All bottles are 1 litre glass bottles. Between every pair of bottles a loop of rope is fixed. On the platform in the Markermeer, a pipe with 7 hooks is attached, immediately above the water surface. When a loop of one of the strings of bottles is attached to a hook, the bottles will sink into the water and hang in three pairs at three different depths (Appendix 3). After a certain time interval, the next loop is placed on the hook and so the string is rotated. After 6 movements the string has made a full circulation and the bottles are back in their original position. By changing the time interval between movements, the migration of the alga across the water column can be slackened or accelerated. As the bottles on the long string reach almost to the lake bottom, a completely mixed system is simulated by rotating these strings. With the short string a partly stratified situation is simulated. If the string is not moved, a classical light and dark bottle experiment is conducted. The bottles of one long string are obscured by covering them with aluminum-paper.

At the start of the experiment the bottles are filled with the *O. agardhii* suspension from the basin on deck of the ship, which is brought to an oxygen saturation level by vigorous stirring. As soon as all bottles of one string are filled this string is placed on a hook at the platform. An effort is made to lower them in the water as quickly as possible, to prevent them from exposure to direct sunlight. First the string with dark bottles is placed. Second and third are a long and a short string with light bottles that are not moved. The other strings are two long and two short strings with different rotational speeds. At the end the strings are raised one by one. In all bottles the oxygen concentration is measured electrochemically (§ 3.2.1).

In 1989, two strings were not moved, strings F and G, which were the short and long string respectively. String A and B, were short strings that were moved every five minutes. Hence, the bottles travelled up and



down the water column twice every hour. String C and D were the long strings, with a similar rotation time. The bottles of string E were covered with aluminum paper.

In 1989, six successful experiments were completed. The results of the experiments are summarized in Table 3.7. Respiration and nett production at a certain depth are estimated by dividing the measured change in oxygen concentration by the duration of the experiment and the biomass. The total gross production over the depth of the strings with the fixed bottles is estimated by multiplying the gross production of each bottle by the thickness of the water layer it represents and adding the results of the individual bottles. The mean production is estimated by dividing the gross production with the depth of the experiment. The production measured in the bottles of the rotated strings are all more or less the same. The mean production of these strings is estimated by averaging the production measured in the individual bottles.

*Table 3.7 Summary of the results of bottle experiments of 1989*

| Date                          |   | 30/6  | 7/7   | 12/7    | 6/9   | 8/9   | 15/9    |
|-------------------------------|---|-------|-------|---------|-------|-------|---------|
| Duration of rotation (h)      |   | 2.0   | 2.0   | 2.0     | 1.5   | 1.0   | 1.0     |
| Duration of fixed bottles (h) |   | 2.25  | 2.0   | 2.0     | 1.33  | 1.60  | 1.12    |
| $t_{\text{halfway}}$          |   | 13.00 | 13.00 | 14.30   | 13.30 | 12.15 | 11.30   |
| $E_{d,0}$                     | ( $\mu\text{E}\cdot\text{m}^{-2}\cdot\text{s}^{-1}$ )       | 1515  | 1390  | 907     | 1073  | 1115  | 603     |
| $K_d$                         | ( $\text{m}^{-1}$ )   | 1.8   | 2.4   | 1.2     | 1.5   | 1.2   | 1.9     |
| $E_{\text{mean,top}}$         | ( $\mu\text{E}\cdot\text{m}^{-2}\cdot\text{s}^{-1}$ )       | 621   | 444   | 481     | 498   | 591   | 238     |
| $E_{\text{mean,deep}}$        | ( $\mu\text{E}\cdot\text{m}^{-2}\cdot\text{s}^{-1}$ )       | 333   | 231   | 287     | 280   | 353   | 126     |
| Sky                           |   | clear | clear | clouded | clear | clear | clouded |
| PH                            |   | 9.9   | 10.3  | 9.8     | 9.8   | 9.7   | 9.2     |
| T                             | ( $^{\circ}\text{C}$ )                                      | 22.0  | 22.0  | 20.3    | 23.0  | 18.5  | 16.7    |
| AFDW                          | ( $\text{g}\cdot\text{m}^{-3}$ )                            | 61.4  | 53.3  |         | 89.2  | 42.5  | 55.     |
| Chla                          | ( $\text{mg}\cdot\text{m}^{-3}$ )                           | 367.  | 462.  | 229.    | 541.  | 248.  | 250.    |
| N-Osc                         | ( $10^6\cdot\text{m}^{-3}$ )                                | 4518  | 5693  |         | 10374 | 5634  |         |
| PP                            | ( $\text{gO}_2\cdot\text{gChla}^{-1}\cdot\text{h}^{-1}$ )   |       |       |         |       |       |         |
| top-rot                       | A,B   | 7.4   | 6.3   | 4.8     | 8.4   | 13.2  | 5.8     |
| top-fix                       | F   | 5.8   | 5.3   | 3.2     | 7.2   | 10.1  | 7.9     |
| deep-rot                      | C,D   | 7.0   | 4.8   | 3.0     | 8.2   | 12.2  | 4.8     |
| deep-fix                      | G   | 5.8   | 4.1   | 2.4     | 6.6   | 9.6   | 5.0     |
| RESP                          | ( $\text{gO}_2\cdot\text{gChla}^{-1}\cdot\text{h}^{-1}$ ) E | 1.9   | 2.4   | 2.6     | 1.6   | -1.4  | -0.4    |

Differences in production between the various rotation regimes are significant, but no systematical variations are observed. The differences in production per day vary much more than differences in production between fixed and rotating bottles.

In 1990 a construction of three poles was used instead of the platform. The experiments are described in detail by De Groote (1992). The place

of the loops was changed to one third of the distance between two bottles. When the string is placed in the water the depth of all the bottles is different, which prevents the breakage of bottles. Strings A and B were the short strings, which were moved every 2.5 and 5 minutes respectively. Hence, the number of rotations of string A is 4 times per hour, and for string B, 2 times per hour. String C and D were long strings, moving every 5 and 10 minutes respectively. E is the long string with dark bottles, which is rotated every 10 minutes in order to compensate for potential temperature variations. F and G are the short and long strings that are not moved. After a string of bottles is filled, the oxygen concentration in each bottle was measured. At the end of the experiment the oxygen concentration and the temperature is measured in each bottle.

During the first high frequency sampling period of 1990, 5 successful experiments were conducted. The results are summarized in Table 3.8. Respiration and gross production are estimated similar to the experiments of 1989.

*Table 3.8 Summary of the results of bottle experiments of 1990*

| Date   |   | 18/6   | 20/6  | 27/6  | 29/6  | 16/7    |
|--|---|--------|-------|-------|-------|---------|
| Duration of rotation (h)                               |   | 2.0    | 2.5   | 2.5   | 2.5   | 2.5     |
| Duration of fixed bottles (h)                          |   | 3.08   | 2.75  | 3.45  | 3.67  | 3.90    |
| $E_{d,o}$ ( $\mu E \cdot m^{-2} \cdot s^{-1}$ )        |   | 994    | 624   | 1062  | 1327  | 887     |
| $K_d$ ( $m^{-1}$ )                                     |   | 1.3    | 1.3   | 1.5   | 1.5   | 1.8     |
| $E_{mean, top}$ ( $\mu E \cdot m^{-2} \cdot s^{-1}$ )  |   | 511    | 321   | 515   | 646   | 378     |
| $E_{mean, deep}$ ( $\mu E \cdot m^{-2} \cdot s^{-1}$ ) |   | 298    | 187   | 292   | 361   | 202     |
| Sky  |   | clouds | hazy  | hazy  | sunny | clouds  |
| PH   |   | 9.5    | 9.6   | -     | 10.3  | 8.3/9.3 |
| T ( $^{\circ}C$ )                                      |   | 21.0   | 19.7  | 20.2  | 19.8  | 22.5    |
| AFDW ( $g \cdot m^{-3}$ )                              |   | 44.3   | 42.5  | 64.2  | 31.1  | 39.8    |
| Chla ( $mg \cdot m^{-3}$ )                             |   | 254    | 281   | 399   | 271   | 304     |
| N-Osc ( $10^6 \cdot m^{-3}$ )                          |   | 21820  | 23747 | 27357 | 30432 | 30980   |
| PPgross ( $gO_2 \cdot gChla^{-1} \cdot h^{-1}$ )       |   |        |       |       |       |         |
| top-rot-slow   | A | 9.3    | 9.8   | 11.6  | 5.1   | 8.9     |
| top-rot-fast   | B | 10.2   | 9.8   | 11.1  | 5.8   | 8.4     |
| top-fix  | F | 9.0    | 11.4  | 10.0  | 4.2   | 6.3     |
| deep-rot-slow  | C | 7.1    | 8.9   | 13.0  | 5.5   | 4.8     |
| deep-rot-fast  | D | 8.8    | 8.6   | 11.0  | 3.8   | 4.9     |
| deep-fix   | G | 7.5    | 9.6   | 8.8   | 4.5   | 3.9     |
| RESP ( $gO_2 \cdot gChla^{-1} \cdot h^{-1}$ )          | E | 1.4    | 1.3   | 2.0   | 1.7   | 1.7     |

The strings with bottles had to be rotated by hand, replacing the loops every 2.5, 5 or 10 minutes. This was time consuming and required much patience. Hence, the duration of the experiments was kept as short as possible. For all experiments, each string had to be moved at least one full circle and preferably two. Hence, the time needed for one exper-

iment was at least two hours in 1989 and one hour in 1990. The rotation of the strings had to be done with utmost care, to prevent bottles from smashing each other or the string from becoming one big knot. Wave action complicated the work and often the experiment had to be cancelled because waves were too high. The accuracy of the experiments was dependent on several factors, including the accuracy of the oxygen measurements, the carefulness in the manipulation of the bottles, the state of the phytoplankton suspension, etc. Thus, the experiments were not as easy as anticipated at first.

From the experiments of 1989, when all experiments were done with at least two duplicate bottles, it was estimated that deviations of 10 % were standard. But occasionally deviations of 25 percent were found. Hence, the accuracy of the experiments is moderate.

### *3.5.3 Cylinder experiments*

By moving the bottles during the light and dark bottle experiments, one of the major disadvantages of the traditional method is removed or at least reduced. Unfortunately, application of the new method is limited to short duration experiments. Hence, processes with larger time scales such as slow adaptations to changing light conditions can not be studied with this set up. For long term primary production experiments, mixing within the experimental vessels is necessary. Also on-line process registration is desirable to enhance the quantity and quality of the data obtained. Therefore an experimental method was designed that accommodated these requirements. A perspex tube of 2.8 m in height was constructed, which is the water depth at Y112 at low water levels. The diameter of the cylinder is 0.3 m. The cylinder was lowered in the water of the Markermeer at site Y112 using a winch, the construction of the cylinder is presented in Appendix 3.

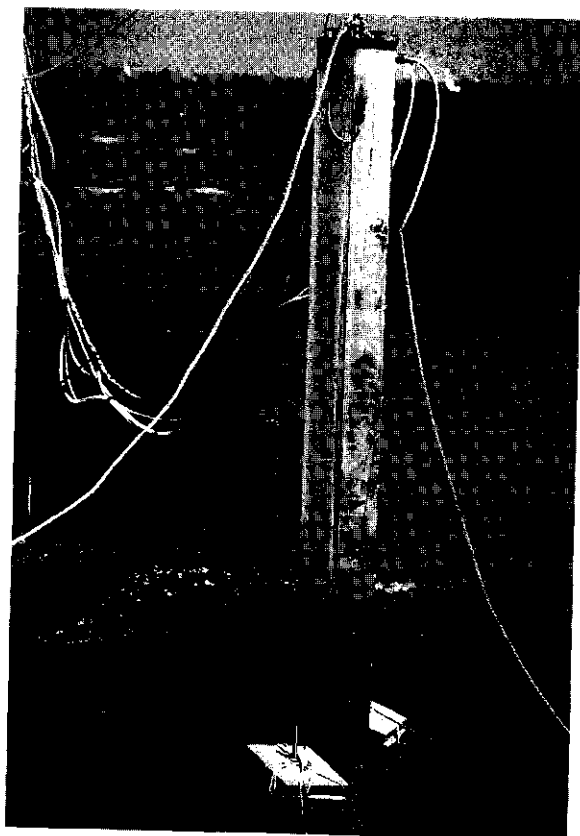
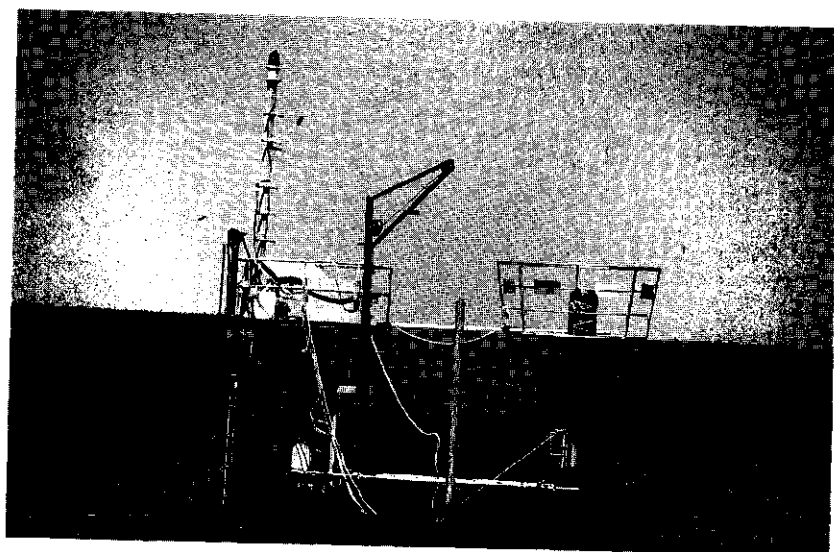


*Figure 3.25  
Configuration  
of the cylinder used  
in 1990*



Within the cylinder three thin plastic tubes were placed, with a length of 0.9, 1.8 and 2.7 metres. The tubes were connected through the top of the perspex cylinder jacket to thin hoses leading to a switchboard. One connector was let through a pump, from which the outlet with a hose is connected to the top of the cylinder. With this system of pump and hoses, the water in the cylinder was circulated. By shutting one or two of the inlet hoses on the switchboard, the water circulation in the cylinder could be changed, from circulating the top third of the cylinder, the top two thirds or the entire content of the cylinder. By opening the lower plastic tube or all three tubes, the entire cylinder content was circulated, but with the second method the top third of the cylinder was recirculated more intensively than the lower third. Because the turbulence was highest near the top of the cylinder, an oxygen-temperature sensor (OXI-196) was placed here, opposite the water inlet. During the experiment, the sensors were connected to a small logger (Campbell 21X, micro-logger) on the platform. Oxygen concentration and temperature were registered every 15 minutes. A fifth hose was connected to a hole in the top of the cylinder, to prevent significant over or under pressure. At the switch board a tap was placed to take samples from the water in the cylinder. These samples could be withdrawn from the three depths 0.9, 1.8 and 2.7 metres by opening one of the three inlet tubes on the switch board. At the start of each experiment the cylinder was filled with the *Oscillatoria agardhii* suspension and lowered into the lake. In general for each experiment, the cylinder was operated for a week, with samples taken every second day. If the *O. agardhii* population inside the cylinder seemed unhealthy or seriously injured, the cylinder was cleaned and filled with a fresh phytoplankton suspension, and the membrane of the oxygen sensor replaced. This happened for example when the pump broke down for one or two days and stratification occurred in the cylinder with strong oxygen depletion in the lower part of the cylinder. Generally, after a week the experiment had to be stopped to replace the oxygen membrane and to clean the walls of the cylinder. After three weeks the experiments had to be stopped for some time anyway, to clean all the instruments and the plastic tubes as well.

For the comparison of the under water light field inside the cylinder with the under water light field in the Markermeer itself, two light cells (Li-cor under water quantum cells) were placed inside the cylinder at a depth of 0.4 and 0.6 m and connected to the micro logger. Unfortunately, immediately after installation of the cylinder, algae settled on the surface of the light cells, rendering the measurements useless. Therefore, careful comparison of both light fields is impossible.

In 1989 a membrane pump was used to circulate the water. This was done after careful comparison of the damage by different pumps on the *O. agardhii* suspension as measured by the primary production. From these experiments it was concluded that the membrane pump had the least effect as long as it was operated at a low pressure. The effect of continuous pumping by a tube or centrifugal pump was devastating. In spite of several attempts with flow meters it was not possible to measure

the mixing rate of the cylinder at a pump pressure of 1.5 bar. In 1989 the cylinder was operated during the second (89-2) and third (89-3) high frequency sampling period. During period 89-2, only the top hose was opened. Hence, only the top third of the cylinder was circulated and a partly stratified situation was simulated. During the period 89-3, only the lower hose was opened to simulate a completely mixed situation. Samples were taken every two days and analyzed for biomass. The measured oxygen concentration and temperature inside the cylinder are presented in Figure 3.26. In the first week of 89-2, the cable, which attached the cylinder to the winch, broke and the cylinder disappeared

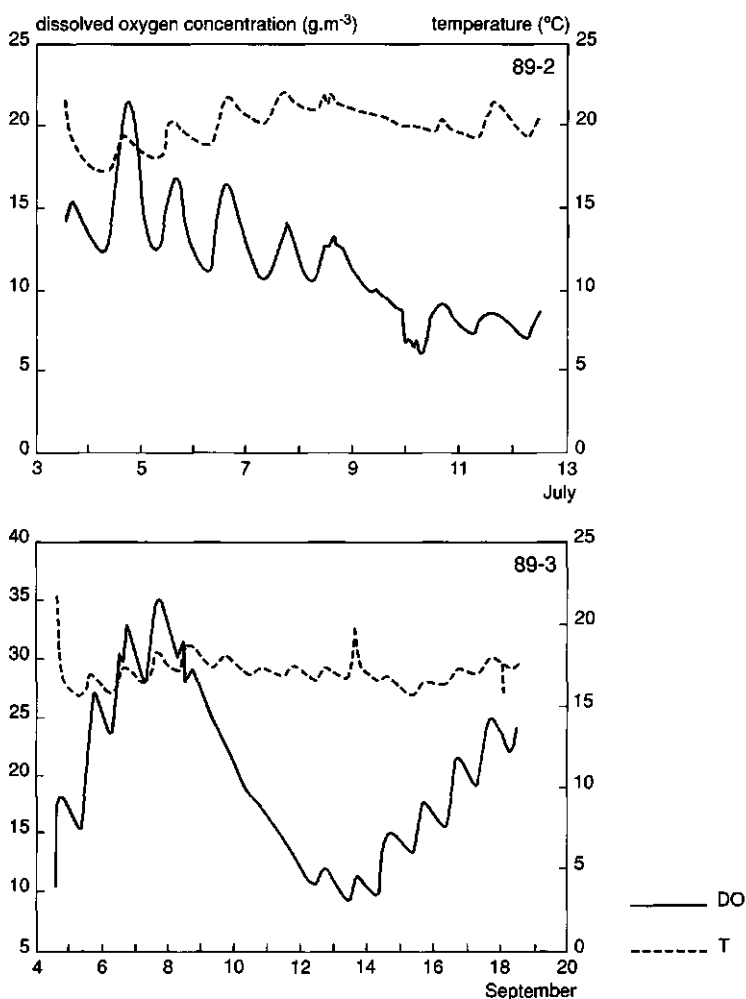


Figure 3.26 Measured oxygen concentration (DO) and temperature (T) in the cylinder experiments in 1989

into the mud. After repair one day later, the pump broke down and two days later this happened again. Hence, continuous measurements did not start until the 3<sup>rd</sup> of July and data interpretation is restricted to nine days from July 3<sup>rd</sup>. In period 89-3, the instruments functioned very well.

In 1990 new laboratory tests were done with several pumps and the effects on the length of the *O. agardhii* filaments and on the shape of their vacuoles were studied (De Groote, 1992). The effect of continuous pumping with a membrane pump on the vacuoles of the algae seemed critical, as the number and size of vacuoles decreased drastically. The effect of small submersible pumps was small. Hence, during the experiments of 1990 small submersible pumps were fixed on the mouth of the three inlet tubes in the cylinder. In the experiments of 1990 the oxygen temperature sensor was placed in a small vessel in the connector hose on the switchboard to improve maintenance possibilities. Pictures of the 1990 experiment are shown in Figure 3.25. The cylinder was operated from June 25 till July 18 and functioned rather well. During 5 days the aggregate, delivering the electricity for the small pumps, did not function well and results were discarded. The measured oxygen concentration and temperature are presented in Figure 3.27.

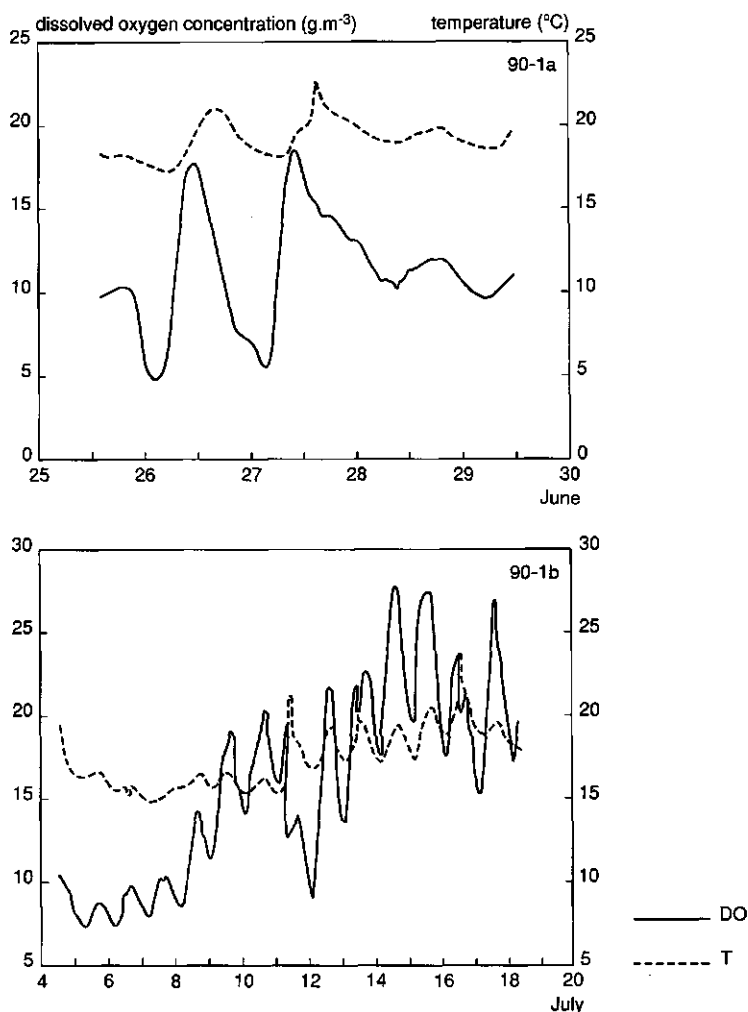


Figure 3.27 Measured oxygen concentration (DO) and temperature (T) in the cylinder experiments in 1990

After some typical start-up problems, the cylinder experiments functioned well. Attempts to measure the light field and the mixing rate inside the cylinder all failed. This complicated the interpretation and the transferability of the experimental results. The theoretical interpretation of the experiments is described in § 6.1.4.



## 4 Sediment transport, resuspension and sedimentation

The transport of fine-grained cohesive sediments enters in several ways in the management of natural and artificial shallow water bodies. The attenuation of light, which affects the ecosystem in various ways (Chapter 5), is dependent on the concentration of suspended sediments. As fine grained sediments have a relatively large surface to mass ratio, they have large adsorbent capacities and consequently are an important factor in the transport of contaminants, like micro-pollutants, heavy metals or phosphate (Lick, 1982). Additionally, sediment transport may result in navigational problems or aggravate the dilemmas around the disposal of dredging sludge. In large shallow lakes the internal loads by resuspension of sediments may be much larger than the input by rivers. Although measurement data are not very accurate and extrapolation of available data is difficult, the gross sedimentation flux in the Markermeer is estimated in the order of billions of tons a year (§ 3.4). Hence, a thorough understanding of the processes of sediment-water interactions and the availability of mathematical models capable of predicting the origin, fate and quantities of suspended sediment in a lake after a single meteorological event and after longer periods of time will be extremely useful in lake management (Sheng and Lick, 1979).

The lakes in the IJsselmeer area, Figure 1.1, are shallow, wind exposed lakes with soft fine-grained sediments. In these lakes, water quality problems are often related to sediment composition and transport. Realizing this, many studies have been issued by government authorities, concerning aspects of sediment transport in parts of the area. In the same period as the Markermeer study has been initiated, a second study concerning the modelling and simulation of internal transport of phosphate rich silt in the Veluwemeer has been started. In both systems, flow patterns are induced by the wind, whereas flow velocities are small. The distribution of suspended sediment in both systems is highly affected by horizontal transport. The external loads of solids are small, compared to internal loads by resuspension of sediments. As both systems are dominated by similar processes, both studies required a similar modelling approach. The model *STRESS-2d* was developed for this purpose by Van Duin and Blom (1992). *STRESS-2d* is a two-dimensional model for Sediment Transport, Resuspension and Sedimentation in Shallow lakes and was applied separately in both studies (Blom, 1989; Van Duin et al, 1992). In a third case study concerning the simulation of the resuspension and distribution of contaminated sediment in the Ketelmeer, the model *STRESS-2d* has been used. In this study some adaptations were made to the model *STRESS-2d* to cope with the load conditions of this lake (Blom and Toet, 1991).

Several processes affect the transport of sediment and the sediment composition in shallow lakes. These include production, decay, resuspension, sedimentation, internal and external transport. This study focuses on suspended solids. Sediment is defined as the non-living

solids, including mineral (clay particles, calcite, sand) and dead organic material. The production and decay of phytoplankton is modelled separately. In this study, the role of production and decay of sediment is neglected. Hence, the production of calcite is neglected, which is acceptable for simulations over shorter periods of time (years instead of decades). For dead organic material it is assumed that the decay of organic material is balanced by the production and that the composition of the total bulk of organic material is steady.

Although the amount of water discharged on the Markermeer is considerable, the external suspended solids load is relatively unimportant. Firstly, because the input concentration of solids is low. Secondly, because the detention time of solids in the water phase is small. Consequently most of the solids will settle near the discharge location. In this study, the modelling of sediment transport is limited to the processes of resuspension, sedimentation and internal transport.

*STRESS-2d* is based on an existing two-dimensional horizontal hydrodynamic model, WAQUA (Stelling, 1984), which is developed and placed at our disposal by Rijkswaterstaat and Delft Hydraulics Laboratory. In WAQUA a studied area is divided in many compartments. For each compartment the advection diffusion equation is solved. In *STRESS-2d*, the advection-diffusion equation is expanded with an additional source term (resuspension) and an additional sink term (sedimentation). A schematic representation of the mass balance of a water compartment in *STRESS-2d* is presented in Figure 4.1. The nett sedimentation flux is the difference between the resuspension flux,  $\Phi_r$ , and the gross sedimentation flux,  $\Phi_s$ .

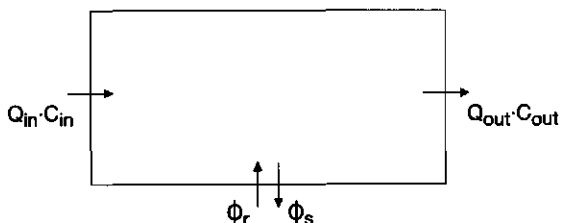


Figure 4.1 Sediment mass balance for each compartment of water in *STRESS-2d*

#### 4.1 Gross sedimentation

The gross sedimentation flux is defined as the mass transported downwards across the sediment-water interface per unit of time and area. The most important factors determining the sedimentation flux are the settling speed or fall velocity and the sediment concentration.

#### 4.1.1 Estimation of the fall velocity distribution

In calm waters particles more dense than water will assume a constant fall velocity, in which the force of downward motion is equal to the drag force resisting motion. If the total suspended solids concentration is modelled with one single mass transfer equation, the fall velocity,  $w_s$ , can be expected to vary as a function of time for each site, due to changes in the particle size distribution. Alternatively, the total suspended solids concentration can be broken up in different size classes, with each its own specific fall velocity (Lick, 1986). For laminar flow conditions, Stokes' law states the relationship between particle size, settling velocity and density deviations:

$$w_s = \frac{(\sigma_s - \sigma) \cdot g \cdot d_s^2}{18 \cdot \sigma \cdot V \cdot O} \quad (4.1)$$

|                                       |   |                                    |
|---------------------------------------|---|------------------------------------|
| $w_s$                                 | = settling velocity or velocity of particles relative to the fluid            | (m·s <sup>-1</sup> )               |
| $\sigma_s$                            | = particle density  | (g·m <sup>-3</sup> )               |
| $\sigma$                              | = density of water  | (g·m <sup>-3</sup> )               |
| $g$                                   | = acceleration due to gravity   | (m·s <sup>-2</sup> )               |
| $d_s$                                 | = diameter of a sphere having the same volume as an irregular shaped particle | (m)                                |
| $V$                                   | = kinematic viscosity   | (m <sup>2</sup> ·s <sup>-1</sup> ) |
| $O$                                   | = coefficient of form resistance  | (-)                                |
| $O$ equals 1 for spherical particles. |   |                                    |

Natural suspensions contain particles of many different sizes, shapes and densities. Particle size distributions may be measured with particle counters, but in case of natural sediments these are expensive and time-consuming measurements. Measurements of particles in ocean waters, ocean sediments, waste waters and sludge digesters have indicated that distribution functions of particle size frequently follow a power law of the form (Lerman et al, 1977):

$$n(d_s) = A \cdot d_s^{-B} \quad (4.2)$$

|          |   |                                       |
|----------|---|---------------------------------------|
| $A$      | = coefficient related to particle concentration             | (m <sup>B-1</sup> · m <sup>-3</sup> ) |
| $B$      | = experimentally determined coefficient ranging from 2 to 5 | (-)                                   |
| $n(d_s)$ | = particle size distribution function of diameter           | (-)                                   |

In natural systems the particle size distribution is not fixed as particles aggregate or disaggregate. Aggregation and disaggregation of fine-grained particles in lake water are complex processes. The rate of aggregation depends upon the particle contact rate and on particle attachment. The particle contact rate is determined by three different

physical processes: Brownian motion, fluid shear and differential settling (O'Melia, 1985). The probability of particle attachment depends on the particle concentration, particle size, salinity and ionic strength. However, a large experimental effort is needed to quantify the probability of attachment. Hence, the particle size distribution is not only difficult to measure but is also variable.

For suspended lake sediments, the fall velocity distribution is more easily determined experimentally than the particle size distribution. As flocs or aggregates will generally settle more rapidly in water than the individual particles would (Håkanson and Jansson, 1983), the fall velocity distribution is not stable. If the sedimentation flux is more important than the exact particle size distribution, measurement of the fall velocity distribution may be sufficient. In the fall velocity experiments it is then assumed that aggregation and disaggregation of particles are similar as under field conditions. In the fall velocity experiments carried out in the Markermeer project, differences with the field situation are mainly due to the undisturbed settling in the laboratory tubes (§3.4.3). For samples taken at the Markermeer, the fall velocity distribution is measured in four intervals defined in Table 3.4. As minimum and maximum settling speeds are unknown, the settling speed ranges over at least three orders of magnitude. The mean fall velocity for each interval depends on the particle size distribution, because the fall velocity is related to  $d_s^2$ , whereas the particle mass is related to  $d_s^3$ . If particle sizes are evenly distributed, a numerical mean of the fall velocity boundaries would underestimate the fall velocity. The mass of spheres is related to the settling velocity to the power 1.5. The average fall velocity of a certain fraction is estimated as the numeric average, of the boundary values to the power 1.5, raised to the power 2/3. The fall velocity of fraction 1 and 4 is a rough estimate, as the upper and under boundary of the fall velocity distribution are not measured.

In lake sedimentology many other methods to classify grain sizes exist. Often sediments are classified in four categories (Håkanson and Jansson, 1983):

- \* sand, diameter  $> 63 \mu\text{m}$ ;
- \* silt, diameter  $2 - 63 \mu\text{m}$ ;
- \* clay, diameter  $< 2 \mu\text{m}$ ;
- \* organic content.

In this approach, fractions are treated as completely separate components. In lakes components will often aggregate, due to surface interactions. The results of the fall velocity experiments showed that the organic content of all fractions of suspended solids in water samples varies between 30 and 50 % (Table 3.5). Though they may have different origins, the behaviour of the different components is the same. Therefore, the distinctions in sand, silt, clay and organic content may be useful for comparison with other systems, but not for models of sedimentation processes.

#### 4.1.2 Description of the sedimentation flux

In the field of sedimentology there is considerable agreement on the modelling of sedimentation fluxes. Both Partheniades (1971) and Sheng and Lick (1979) proposed a linear relationship with the settling velocity,  $w_s$ , and the suspended solids concentration SS. In its simplest form:

$$\Phi_s = w_s \cdot SS \quad (4.3)$$

If the range of the fall velocity distribution is large, a background concentration of non-settling material may be used (Lam and Jaquet, 1976; Luettich, 1987):

$$\Phi_s = w_s \cdot (SS - SS_b) \quad (4.4)$$

$$SS_b = \begin{array}{l} \text{background suspended solids} \\ \text{concentration} \end{array} \quad (\text{g} \cdot \text{m}^{-3})$$

Lick (1982) suggested that besides settling, Brownian motion may be significant especially near the sediment water interface. He describes sedimentation fluxes with:

$$\Phi_s = \beta \cdot SS \quad (4.5a)$$

$$\beta = w_s / (1 - e^{-w_s/\beta_d}) \quad (4.5b)$$

$$\begin{array}{ll} \beta & = \text{coefficient of proportionality} \quad (\text{m} \cdot \text{s}^{-1}) \\ \beta_d & = \text{limiting value of } \beta \quad (\text{m} \cdot \text{s}^{-1}) \end{array}$$

Where  $\beta_d$  is the limiting value of  $\beta$ , if only Brownian diffusion is considered important. As the particle size decreases, Brownian diffusion becomes more important and  $\beta$  approaches  $\beta_d$ . For large particles  $\beta$  is approximately equal to the settling velocity and 4.5a merges into 4.3. As particle sizes are not constant and therefore complex to estimate, the effect of Brownian diffusion is often neglected in the modelling of sedimentation fluxes. But it should be noticed that the use of equation 4.3 instead of 4.5 will lead to an underestimation of the sedimentation flux of the smaller particles.

#### 4.2 Resuspension

Compared to the modelling of sedimentation fluxes, much more disagreement is displayed concerning the modelling of resuspension of sediment and on the question whether erosion and deposition occur simultaneously or alternating.

is incorporated, the usage of these models in two dimensional models requires a lot of computing time and memory capacity. Hence, this study was confined to the semi-empirical models.

Wind waves grow as a result of a flux of momentum and energy from the air to the water body. Most theories, including the semi-empirical models, relate the impact of energy and momentum to the surface stress, which is highly dependent upon the wind speed. In most wave models, the wind velocity measured at an elevation of ten metres above the surface,  $U_{10}$ , is used. In wave hindcasting models, either the wind speed is used directly or a wind stress factor,  $U_a$ , is used.  $U_a$  is an adjusted wind speed:

$$U_a = C_1 \cdot U_{10}^{C_2} \quad (4.8)$$

Besides wind speed, wave growth is determined by the fetch, the duration of the wind event and the water depth. The fetch generating area is the unobstructed area of water over which the wind blows in an essentially constant direction. The fetch length,  $F_l$ , is the length of the generating area in the direction of the wind. The fetch width,  $F_w$ , is the width of the generating area, perpendicular to the fetch length. In general, lake fetches are limited by the lake shores. At irregular shaped lakes, small variations of the wind direction may induce large fluctuations in the estimated fetch length. That is the reason why the effective fetch,  $F$ , which is related to both fetch length and width, is often used in lake models. Usually, the effective fetch is estimated as the weighted mean value of the fetch length exactly in the direction of the wind and sections on both sides of the central radial. The larger the angle between the central radial and a section, the lesser its contribution to the effective fetch (Saville et al, 1962, Håkanson and Jansson, 1983). In this study, the compass-card is divided in 16 sections of 22.5 degrees. For every section the fetch length is estimated for a specific site with wind direction intervals of 4 degrees. The mean value of these fetch lengths is used as the effective fetch, for every wind with a direction within that section. This approach is less accurate than the method described by Saville et al. (1962), but was necessary to save computer memory (§ 4.5).

The wind duration,  $t_d$ , is the time the wind acts on the water surface. The minium wind duration is the time required to establish steady state conditions for a particular wind speed, fetch and depth.

The significant wave method was introduced originally by Sverdrup and Munk and after some extensions became known as the SMB-method (Bretschneider, 1966). The wave forecasting parameters evolved from theoretical considerations, but the actual relationships required certain basic data for the determination of various constants and coefficients. They developed wave forecasting equations based on dimensionless parameters.

$$TT = g \cdot T_s / U_a = \text{wave period parameter} \quad (4.9a)$$

$$HH = g \cdot H_s / U_a^2 = \text{wave height parameter} \quad (4.9b)$$

$$FF = g \cdot F / U_a^2 = \text{effective fetch parameter} \quad (4.9c)$$

$$zz = g \cdot z / U_a^2 = \text{depth parameter} \quad (4.9d)$$

$$tt = g \cdot t_d / U_a = \text{wind duration parameter} \quad (4.9e)$$

In most models based on the SMB-method, steady state conditions are assumed. In these models waves are therefore either fetch or depth limited but never duration limited. Equations of these models all have the same form, but the parameters have different values (CERC, 1977; Bouws, 1986; Groen and Dorrestein, 1976). In these models TT and HH are related to depth and fetch, according to:

$$TT = C_3 \cdot f_z^i \cdot \tanh[f^F_i / f_z^i] \quad (4.10)$$

$$HH = C_4 \cdot f_z^2 \cdot \tanh[f^F_2 / f_z^2] \quad (4.11)$$

$f_z^i$  = function of depth parameter

$f^F_i$  = function of effective fetch parameter

A summary of models, constants and wind speed modifications is presented in table 4.1. In variable wind fields, stationary conditions are not reached as assumed in equations 4.10 and 4.11. Duration limited wave generation will occur when the wind speed increases rapidly. Hence, measured wave heights and periods are sometimes smaller than computed wave characteristics. On the other hand, when the wind speed decreases fast, wave characteristics will be higher than computed. CERC (1984) presented an experimental equation for wind duration limited wave period computation:

$$TT = 0.0677 \cdot tt^{0.429} \quad (4.12)$$

The wave period is computed for both fetch limited and duration limited conditions. If the wave period, computed with the duration limited equation, is smaller than the fetch limited wave period, wind duration is limiting the wave growth. Using equation 4.10, a wind duration corrected fetch is estimated, which in combination with equation 4.11 produces the matching wave height. Groen and Dorrestein (1976) proposed a method to expand the use of equations 4.10 and 4.11 to dynamic wind fields, without introducing the wind duration in the equations. They assumed that there is only a limited time lag between changes in wind and the adaptation of the wave characteristics to the new wind field. If the time step between computations is small, so will generally be the changes in the wave field. The wave field at time  $t$  minus 1 affects the wave field at time  $t$ . Hence, the wind field at time  $t$  minus 1, affects the wave field at time  $t$ . They suggested that the wind field at time  $t$  should be a weighted wind speed combined from both the wind field at time  $t$  and time  $t$  minus 1. For the correction of the wind speed equation 4.13 is formulated (Groen and Dorrestein, 1976):

$$U_{10} = C_5 \cdot U_{10}^t - (1 - C_5) \cdot U_{10}^{t-1} \quad 0.5 \leq C_5 \leq 1.0 \quad (4.13)$$

$$C_5 = \text{weight factor} \quad (-)$$

This concept is used to produce semi-dynamic versions of in principle stationary models and is included in table 4.1.

*Table 4.1 Summary of constants of different wave models*

|                | CERC1s                      | CERC2s - CERC2d              | BOUWSs - BOUWSd             |
|----------------|-----------------------------|------------------------------|-----------------------------|
| C <sub>1</sub> | 1.0                         | 0.71                         | 0.537                       |
| C <sub>2</sub> | 1.0                         | 1.23                         | 1.23                        |
| C <sub>3</sub> | 7.54                        | 7.54                         | 7.54                        |
| C <sub>4</sub> | 0.283                       | 0.283                        | 0.283                       |
| f <sub>1</sub> | 0.833 · zz <sup>0.375</sup> | 0.833 · zz <sup>0.375</sup>  | 0.833 · zz <sup>0.375</sup> |
| f <sub>2</sub> | 0.530 · zz <sup>0.75</sup>  | 0.530 · zz <sup>0.75</sup>   | 0.530 · zz <sup>0.75</sup>  |
| f <sub>1</sub> | 0.077 · FF <sup>0.25</sup>  | 0.0379 · FF <sup>0.333</sup> | 0.077 · FF <sup>0.25</sup>  |
| f <sub>2</sub> | 0.0125 · FF <sup>0.42</sup> | 0.00565 · FF <sup>0.5</sup>  | 0.0125 · FF <sup>0.42</sup> |
| duration       | -                           | - 4.12                       | - 4.13                      |
| C <sub>5</sub> | 1                           | 1 1                          | 1 0.75                      |

The models summarized in Table 4.1 are very much alike. Bouws used the same model as CERC1s, except that he used an adjusted wind speed. Some constants of CERC2s and CERC2d differ from the other models. To assess the efficiency of the different models, simulation runs with all the models were done, using the data sets of 1988 and 1989. Bouws model was used in its original form (BOUWSs) and used in an extended form, including the duration concept of Groen and Dorrestein (BOUWSd, equation 4.13). A value of 0.75 was used for constant C<sub>5</sub>. The latest CERC model was used with (CERC2d) and without (CERC2s) the wind duration limitation. If the increase in wind speed was more than 1.0 m·s<sup>-1</sup> in one hour, both the duration and fetch limited period were estimated. If the duration limited period was the smaller one, wave growth was assumed to be duration limited and wave height computations were omitted.

The wave characteristics measured at the Markermeer in 1988 and 1989 are used to validate the simulation results. The estimated values of significant wave height and period are compared to the measured values, if the measured wave height was at least 0.1 m (H<sub>c</sub>). The behaviour of the models was described by the mean value of the sum of square roots of the difference between estimated and observed values (SSQ) and the mean relative error, MRE. A summary of the simulation results is presented in Appendix 9. For all five models the significant wave height measured at Y111 in 1988 was simulated best and wave height measured at Y111 in 1989 worst. The latter is probably caused by the faltering



data transmission (§ 3.3.3). The original model, CERC1s, produced credible results with relative errors around 20 % or less. Especially the wave period estimations seem reliable. The introduction of the new growth curves in 1984 does not seem an improvement, although differences in behaviour are small. Considering model behaviour Bouws introduction of an adapted wind speed in the original equations, seems an improvement. Considering the relative error it is a relapse. In about 20 % of the simulated events, limitation of wave growth by wind duration occurred. During the same number of events, the wind speed increased  $1.0 \text{ m}\cdot\text{s}^{-1}$  or more within an hour. During every event with an increased wind speed, wave growth is observed to be duration limited. However, the estimated wave periods with this method do not agree with the measure values and consideration of this effect does not improve the hindcasting of wave heights. Hence, the inclusion of duration limitation, as described with CERC2d, is another relapse in wave hindcasting. The method of weighting of wind speed to include dynamics, as is done in BOUWSd, does not seem to have much effect on model behaviour.

As the relative error in the measured wave heights is larger for small wave heights (§ 3.3.3) and very small waves are not important in the estimation of resuspension fluxes, a minimum value of  $H_s$  for model behaviour estimation is defined,  $H_c = 0.1$ . To test the sensitivity of the model behaviour for the value of  $H_c$ , simulation runs were done with the BOUWSs model for different minimum values of  $H_c$ ; 0.0 and 0.2 (m). When the value of  $H_c$  was lowered, model accuracy actually increased.

The models neglecting any aspect of duration limitation of wave growth, like CERC1s, CERC2s and BOUWSs, produce the best results for this data set. The difference between the behaviour of the models is small, although the relative errors in BOUWSs are bigger. Still, the BOUWSs model is used in STRESS-2d, mainly caused by historical reasons: A first comparison of the five models was done in 1988, using the data sets of 1987 and 1988 of Y112. BOUWSs model produced the best results, other models overestimated the wave characteristics. As this agreed with the findings of Bouws (1986) for the Markermeer, BOUWSs model was adopted for use in the STRESS-2d model. As in 1989 it appeared that the measured wave data were unreliable (§ 3.3.3), a quick check-up was done on the behaviour of the BOUWSs model, using the new data of 1988 of site Y111. As model behaviour seemed unchanged, the model was still used further. Not until 1990 it was realized that the same measurement mistakes might have been made in the collection of the data set used by Bouws. Hence, the extensive study on the behaviour of the different models with the data of 1988 and 1989 was repeated in the end of 1990. The results are presented in Appendix 9. Because the results of the BOUWSs model are still acceptable, it is still used. Furthermore, changing the wave model in STRESS-2d to CERC1s or CERC2s would mean a time-consuming recalibration of the entire resuspension model.

### 4.2.3 Relationships for wave induced resuspension

With the identification of wind induced waves as the major force for resuspension in Markermeer, a quantitative relationship between this force and the resuspension flux has to be formulated. Many other factors affect the resuspension as well, among which the physical and chemical characteristics of both the water and the sediment, the availability of sediment for resuspension, the activity of benthos and the covering of sediment with macrophytes. As surface waves are hard to simulate in laboratory experiments, presently experiments are limited to the entrainment of sediment by steady flow (Partheniades, 1965; Mehta and Partheniades, 1975; Fukuda and Lick, 1980; Lee et al, 1981) or by tide. Tsai and Lick (1986) developed a portable device (shaker), in which turbulence was generated by an oscillating grid. In both cases, the generated turbulence is quite different from the turbulence induced by surface waves. Due to the complicity of the process and the limited information from experiments, the best results are still obtained with semi-empirical models (Brinkman and Van Raaphorst, 1986).

Numerous relationships have been proposed, relating the resuspension flux either directly to the wind speed (Gons, 1989), wave height (Luettich, 1987), the maximum orbital bottom velocity (Lam and Jaquet, 1976) the squared maximum orbital bottom velocity (Migniot, 1966) or to the bottom shear stress related to surface waves (Sheng and Lick, 1979). A direct relationships between the resuspension flux and wind speed is incapable of simulating the effect of measures concerning lake geometry or depth on the resuspension of sediment. In studies relating either the maximum orbital velocity or the bottom shear stress to the resuspension flux, a critical minimum value of either has been observed. Below this critical value no resuspension occurs. If the critical value is exceeded, erosion rates increase very rapidly. The relationship between the maximum bottom wave orbital velocity and the wave characteristics is described by Phillips (1966).

$$U_b = [\pi \cdot H_s / T_s] \cdot \sinh(2 \pi \cdot z / L) \quad (4.14)$$

$$U_b = \begin{array}{l} \text{maximum bottom wave orbital} \\ \text{velocity} \end{array} \quad (\text{m} \cdot \text{s}^{-2})$$

A comparison of existing relationships is presented by Aalderink et al. (1984). Three commonly used models including these phenomena are:

Lam and Jaquet (1972):

$$\Phi_r = 0 \quad U_b < U_{b,cr} \quad (4.15a)$$

$$\Phi_r = K_1 \cdot K_2 \cdot [U_b - U_{b,cr}] / U_{b,cr} \quad U_b > U_{b,cr} \quad (4.15b)$$

Migniot (1966):

$$\phi_r = 0 \quad U_b < U_{b,cr} \quad (4.16a)$$

$$\phi_r = K_1 \cdot [U_b^2 - U_{b,cr}^2] / U_{b,cr}^2 \quad U_b > U_{b,cr} \quad (4.16b)$$

Sheng and Lick (1979)

$$\phi_r = 0 \quad \tau_w < \tau_{w,cr1} \quad (4.17a)$$

$$\phi_r = K_1 \cdot [\tau_w - \tau_{w,cr1}] \quad \tau_{w,cr1} < \tau_w < \tau_{w,cr2} \quad (4.17b)$$

$$\phi_r = K_1 \cdot [\tau_w - \tau_{w,cr2}] \quad \tau_{w,cr2} < \tau_w \quad (4.17c)$$

$$K_2 = \sigma_s \cdot \sigma_w / (\sigma_s - \sigma_w)$$

$$K_1 = \text{constants} \quad (-)$$

$$U_{b,cr} = \text{critical maximum orbital bottom velocity} \quad (m \cdot s^{-1})$$

$$\tau_{w,cr} = \text{critical maximum bottom stress} \quad (N \cdot m^{-2})$$

In the model STRESS-2d, the use of both equations 4.15 and 4.16 is optional. As  $\tau_w$  is related to the square of  $U_b$ , equations 4.16 and 4.17 lead to more extreme values of the resuspension flux, than computed with equation 4.15. A comparative study between 4.15 and 4.17 with the Veluwemeer data set favoured the use of equation 4.15 (Blom, 1989). A comparison of model behaviour between 4.15 and 4.16 with the Markermeer data set, also favoured the use of 4.15 (Raap and Buis, 1988). Hence, equation 4.15 (Lam and Jaquet, 1976) was used in the Markermeer study.

The value of  $U_{b,cr}$  depends on the mineral composition and particle size distribution of the sediment, the absence or presence of benthic fauna and bacteria (Fukuda and Lick, 1980), the ionic strength (chloride), (Terwindt, 1977), vegetable cover (Partheniades, 1972), etc. Migniot (1966) found that for various types of sediments, the critical shear velocity may be expressed adequately as an inverse function of the water content in the sediment. By Lam and Jaquet this was accounted for in the description of  $K_2$ . As the variation in the named factors that affect the value of  $U_{b,cr}$  may be large for different lakes and sediments but may even change with different seasons, the value of  $U_{b,cr}$  may be different for different lakes, different kinds of sediments and for different periods of the year. The effect of seasonal variations is mainly due to differences in biological activity. As these processes are hard to assess for an entire lake, either a simple temperature relation may be used or the effect may be neglected at all. The latter is done in this study, leaving differences in sediment composition as the only cause for differences in  $U_{b,cr}$ . In many other studies differences in  $U_{b,cr}$  for different sediments are neglected as well (Lam and Jaquet, 1976, Sheng and Lick, 1979). The omission of variability in  $U_{b,cr}$  in combination with the disregard of differences in fall velocity may cause, from a modelling perspective, the need to define a background concentration (Luettich et al, 1990). The definition of a background concentration is a hidden method to introduce differences in sediment characteristics. In the sedimentation model,

sediments were discriminated by ranges of fall velocity. Assuming that larger flocs require more energy for resuspension and settle faster as well, the same classification is used for both the resuspension and the sedimentation model. Therefore equation 4.15 is redefined to include different sediment classes:

$$\phi_r = \sum \epsilon_r^i = \sum K^i [U_b - U_{b,cr}^i] \quad (4.18)$$

$$K^i = \frac{K_1^i \cdot \sigma_s^i \cdot \sigma_w}{(\sigma_s^i - \sigma_w) \cdot U_{b,cr}^i}$$

Values have to be obtained for both  $K^i$  and  $U_{b,cr}^i$  of each fraction, which is described into detail in § 4.5.2).

### 4.3 Modelling of the sediment layers

Not only the sediment characteristics and the bottom stress, but also the limited availability of sediment for resuspension may be an important factor controlling the resuspension fluxes. Sediment characteristics may vary within the different layers of sediment. Hence, the modelling of the lake sediment is as important as the modelling of the wave characteristics and sedimentation rates. Unfortunately, less information is available on the processes controlling the erodability of sediments and these characteristics may vary enormously from lake to lake.

#### 4.3.1 Different concepts for sediment modelling

If the lake bottom is an inexhaustible source of solids for the considered time scale, a model of the lake bottom is not necessary (BOT0). More often, the thickness of the lake sediment varies within the lake and varies within the considered time and is a function of deposition and erosion rates. In the Markermeer, the silt layer varies in thickness at different parts of the lakes and is transported during the years. Beneath the silt layer a coarse sand layer is located, which is hardly affected by wind waves. Hence, depletion of the silt layer will actually occur and limit the resuspension of sediment (BOT1).

Laboratory experiments have shown that erosion of a cohesive sediment occurs until a depth is reached, where the bed strength is equal to the erosive force (Mehta and Partheniades, 1975). The bed strength depends on the degree of consolidation that has occurred since the bed was deposited, the make-up of the bed, bioturbation, etc (Fukuda and Lick, 1980, Lee et al, 1981). Hence, the critical maximum orbital velocity for resuspension is not constant for each sediment layer, but increases with depth and with time as consolidation of the deposited sediment occurs. At any time, a certain fraction of the available sediment is deposited as surficial sediment and overlays sediment, which is more difficult to entrain, while the rest of the available sediment is suspended in

the overlying water (Lick, 1982). For a lake bottom with a high silt content, Luettich et al (1990) suggested the existence of a thin non cohesive top layer. The contents of this layer never become cohesively bound to the bed and resuspension of this layer is relatively easy. Possible mechanisms to restrain this layer from becoming a part of the bed, include bioturbation and bottom shear exerted by the mean current and small waves. Although the latter may be weak in comparison to the stress necessary to cause resuspension, it is nearly always present. In samples taken with the Jenkin mud sampler (§ 3.4.1), such a layer was actually detected. Above a grey sediment a thin yellowish layer with a thickness of a few millimetres to a centimetre was spotted. Although the layer was often disturbed by the sampling, its existence could be observed readily with the eye by its different colour. This layer is assumed to be aerobic in contrast with the layer beneath, causing the colour difference. Hence, the concept of a thin non-cohesive top layer is plausible for the Markermeer. The water content of this layer is assumed to be 95 %, the same value as assumed by Luettich et al. (1990). The exact thickness of this layer is variable as sediment is resuspended or consolidated. If the thickness of the top layer becomes too high, the forces that are keeping the silt in the non cohesive layer may not reach deep enough and sediment consolidates. This part of the top layer will become cohesive and therefore will become part of the lower layer.

The cohesive part of the sediment will vary in bed strength with sediment depth. It may be approached as a number of sub-layers, each defined by its own bed strength and thus describing erosion as a discontinuous process (Vlag, 1992). On the other hand, if the top layer is partly or completely removed, the sediment below is subject to the same processes as the top layer was before and therefore will acquire the same properties. In the latter approach, one lower layer is sufficient to attribute for the variability in bed strength within the sediment (BOT2).

#### *4.3.2 Numerical implications*

Although model equations have been formulated in the former paragraphs for resuspension and sedimentation, it has not been discussed yet whether both processes appear simultaneously or exclude each other. Partheniades (1965) observed simultaneous occurrence of deposition and erosion in rivers with coarse sediments, but a much more complicated situation for rivers with fine cohesive sediments. He stated that erosion and deposition of cohesive sediments are different and exclusive processes, as the shear stress required to erode deposited fine sediment is considerably higher than the stresses under which the same sediment may deposit (Mehta and Partheniades, 1975, Partheniades, 1972). In one study Partheniades (1972) observed that for deposited flocs to be resuspended, the flow induced lift and drag forces will have to overcome its chemical bonds with the bed in addition to the submerged weight. Consequently, higher shear stress would be required to resuspend deposited sediments than those under which the same sedi-

ment deposits. In later work he stated conclusively that erosion and deposition will not occur simultaneously in rivers with cohesive sediments and sedimentation fluxes were modelled likewise (Mehta and Partheniades, 1975). A similar approach was used by Krone (1972).

$$\begin{aligned}\phi_s &= 0 & \tau_c &\geq \tau_{cr} & (4-19a) \\ \phi_s &= w_s \cdot SS \cdot (1 - \tau_c / \tau_{cr}) & \tau_c &\leq \tau_{cr} & (4-19b)\end{aligned}$$

Although the studies of Partheniades and Krone are on cohesive sediments, they are all done in rivers or in laboratory experiments, where erosion is flow induced. Flow induced shear stress to erode sediments has to be much higher than wave induced shear stress to erode the same sediment (§ 4.3.1). In similar experiments, using cohesive lake sediments in a rotating circular flume, Fukuda and Lick (1980) and Lick (1982) observed in every experiment a steady state concentration, which they reasoned to be due to a dynamic equilibrium between entrainment and deposition. Hence, with similar experiments they reached the opposite conclusion. As in the Markermeer study the top layer is assumed to be non-cohesive, the simultaneous occurrence of resuspension and sedimentation is a logical result. Hence, in the STRESS-2d model resuspension and sedimentation may occur simultaneously. In other studies, resuspension and sedimentation of cohesive sediments was modelled by simultaneously occurring processes as well, with reasonable results (Lam and Jaquet, 1976; Sheng and Lick, 1979; Aalderink et al, 1986).

In § 4.3.1 different concepts for the modelling of the sediment layers are presented:

- BOT0: One layer of infinite depth;  
It implies that no mass balance of the lake bottom has to be kept as the source is unlimited and the composition constant. The applicability of this model is limited to short term simulations.
- BOT1: One single well mixed layer of finite depth;  
A mass balance of this layer should be kept for each fraction. As the exhaustion of lake sediment is included in this model, it is more versatile than the first. Still, as variability in bed strength within the sediment depth is neglected, limitations in its applicability is expected.
- BOT2: Two layers of variable depth. The top layer a thin layer, its thickness the nett result of sedimentation and resuspension. The lower layer acting as a source for the upper layer. In this model, the consolidation of the top layer is modelled as a mass transport from the top layer to the lower layer. This transport occurs when the thickness of the top layer exceeds a critical value. This process will be further referred to as consolidation, although it is not exactly the same because no gradients are considered. The transport of material from the lower layer to the top layer is defined likewise. If the thickness of the upper layer is less than the critical value, mass transport from the lower layer to the top layer occurs. This transport is referred to as erosion but is not dependent on the shear stress. The flux from one layer to

another is not dependent on the thickness of any layer, but is modelled as a constant. The magnitude of these fluxes is therefore arbitrary.

In the STRESS-2d model, the sediment bottom model with two layers of variable depth is used (BOT2). The thickness of the sediment top layer is computed with equation 4.20

$$z_t = \frac{MSS_t}{\sigma_s(1-e)} \quad (4.20)$$

$$\begin{aligned} z_t &= \text{thickness of the sediment top layer} & (\text{m}) \\ MSS_t &= \text{total sediment mass in the sediment top layer} & (\text{g} \cdot \text{m}^{-2}) \\ \sigma_s &= \text{sediment density} & (\text{g} \cdot \text{m}^{-3}) \\ e &= \text{porosity} & (-) \end{aligned}$$

At each time step, mass transfer between the top and the lower layer occurs by turbation. Besides this either erosion or consolidation occurs, dependent on the thickness of the sediment top layer. If the thickness of the top layer is larger than the critical thickness of the top layer, sediment is transported to the lower layer by consolidation and turbation and to the upper layer by turbation:

$$\frac{\delta(MSS_{t,i})}{\delta t} = M_t \cdot \frac{(1-e_l)}{(1-e_t)} \cdot SS_{t,i} - (M_t + M_c) \cdot SS_{t,i} \quad (4.21a)$$

$$\frac{\delta(MSS_{l,i})}{\delta t} = -M_t \cdot \frac{(1-e_l)}{(1-e_t)} \cdot SS_{t,i} + (M_t + M_c) \cdot SS_{t,i} \quad (4.21b)$$

If the thickness of the top layer is less than the critical thickness, mass is transported from the lower layer to the top layer by turbation and erosion and vice versa by turbation:

$$\frac{\delta(MSS_{t,i})}{\delta t} = (M_t + M_e) \cdot \frac{(1-e_l)}{(1-e_t)} \cdot SS_{t,i} - M_t \cdot SS_{t,i} \quad (4.22a)$$

$$\frac{\delta(MSS_{l,i})}{\delta t} = - (M_t + M_e) \cdot \frac{(1-e_l)}{(1-e_t)} \cdot SS_{t,i} + M_t \cdot SS_{t,i} \quad (4.22b)$$

$$\begin{aligned} MSS_{t,i} &= \text{sediment mass of component i in the top layer} & (\text{g} \cdot \text{m}^{-2}) \\ MSS_{l,i} &= \text{sediment mass of component i in the lower layer} & (\text{g} \cdot \text{m}^{-2}) \\ M_t &= \text{mass transport by turbation} & (\text{m} \cdot \text{s}^{-1}) \\ M_c &= \text{mass transport by consolidation} & (\text{m} \cdot \text{s}^{-1}) \\ M_e &= \text{mass transport by erosion} & (\text{m} \cdot \text{s}^{-1}) \end{aligned}$$

|            |  |                    |
|------------|--|--------------------|
| $SS_{t,i}$ | = sediment concentration of component i in the top layer   | $(g \cdot m^{-3})$ |
| $SS_{l,i}$ | = sediment concentration of component i in the lower layer | $(g \cdot m^{-3})$ |
| $e_t$      | = porosity of the top layer                                | $(-)$              |
| $e_l$      | = porosity of the lower layer                              | $(-)$              |

#### 4.4 Sediment transport

The equation for the conservation of mass of suspended sediment describes the advective and dispersive transport of sediments in a turbulent system:

$$\frac{\delta SS}{\delta t} + \frac{\delta(uSS)}{\delta x} + \frac{\delta(vSS)}{\delta y} + \frac{\delta(w + w_s)SS}{\delta z} = \frac{\delta(D_h \cdot (\delta SS / \delta x))}{\delta x} + \frac{\delta(D_h \cdot (\delta SS / \delta y))}{\delta y} + \frac{\delta(D_v \cdot (\delta SS / \delta z))}{\delta z} + S \quad (4.23)$$

|        |  |                                 |
|--------|--|---------------------------------|
| $x, y$ | = horizontal coordinate                              | $(m)$                           |
| $z$    | = vertical coordinate<br>(positive = upward)         | $(m)$                           |
| $u$    | = fluid velocity in x direction                      | $(m \cdot s^{-1})$              |
| $v$    | = fluid velocity in y direction                      | $(m \cdot s^{-1})$              |
| $w$    | = fluid velocity in z direction                      | $(m \cdot s^{-1})$              |
| $w_s$  | = velocity of suspended solids relative to the fluid | $(m \cdot s^{-1})$              |
| $D_h$  | = horizontal eddy diffusivity                        | $(m^2 \cdot s^{-1})$            |
| $D_v$  | = vertical eddy diffusivity                          | $(m^2 \cdot s^{-1})$            |
| $S$    | = source (or sink) term                              | $(g \cdot m^{-3} \cdot s^{-1})$ |
| $t$    | = time   | $(s)$                           |

It has been assumed that the concentration of suspended solids is sufficiently small, so that the dynamics of the flow are not appreciably affected by the suspended solids. A numerical model based on this mass balance implies the use of a three-dimensional model. If gradients in either horizontal or vertical directions are small, the role of transport in this direction may be ignored and the dimensionality of the model can be reduced.

##### 4.4.1 Vertical transport

The occurrence of vertical gradients of suspended solids in lakes is dependent on the transport induced by wind waves, the effect of currents, dispersion and sedimentation. The sedimentation process tends to create gradients, whereas most other processes tend to smooth gradients. The effect of advective transport by downward seepage on concentration gradients in the water column is nil in the Markermeer area as



the seepage rate is less than  $1 \text{ mm} \cdot \text{day}^{-1}$ . The relative impact of at one side sedimentation and on the other side the effect of currents and waves may be compared by matching the characteristic time scales of the processes (Sheng and Lick, 1979). The characteristic time for settling and the characteristic time for turbulent diffusion are defined as (Lick, 1982):

$$t_s = z/w_s \quad (4.24)$$

$$t_t = z^2/2D_v \quad (4.25)$$

$$t_s = \text{characteristic time for settling} \quad (\text{s})$$

$$t_t = \text{characteristic time for turbulent diffusion} \quad (\text{s})$$

When the settling time is much less than the diffusion time,  $t_t \gg t_s$ , settling is the dominant mechanism for vertical transport of sediment. When  $t_t \ll t_s$ , turbulent diffusion is the dominant mechanism and gradients will be smoothed. In the Markermeer the mean settling velocity varies between  $10 \cdot 10^{-6}$  and  $100 \cdot 10^{-6} \text{ m} \cdot \text{s}^{-1}$  (§ 3.4.3). The depth of the lake varies between 2.0 and 4.5 m. Hence,  $t_s$  varies between  $2 \cdot 10^4$  and  $45 \cdot 10^4 \text{ s}$ . The vertical dispersion coefficient in shallow Dutch lakes is in the order of  $2 \cdot 10^{-4}$  and  $10^{-3} \text{ m}^2 \cdot \text{s}^{-1}$  (DiGiano et al, 1978). Therefore,  $t_t$  lies between  $0.2 \cdot 10^4$  and  $5 \cdot 10^4$ . During stormy weather both  $w_s$  and  $D_v$  increase, whereas during calm weather both decrease. As  $t_t$  is usually much smaller than  $t_s$ , normally gradients due to settling can be ignored. This corresponds with the results obtained from measurements at different depths (§ 3.2.2). Differences in concentrations measured at different depths were rare and usually less than 5 %. Because usually vertical gradients are of minor importance, this third dimension is omitted from equation 4.23 and a two-dimensional horizontal approach for the sediment transport model is used.

#### 4.4.2 Horizontal transport (WAQUA)

Horizontal transport of constituents is related to the horizontal water movement. The depth averaged horizontal currents are described by the so called Shallow Water Equations (SWE) or the long period wave equations (Leendertse, 1987), which are valid if vertical flow velocities and accelerations are small and also the vertical gradients in horizontal velocities are small.

$$\frac{\delta \xi}{\delta t} + \frac{\delta(h + \xi)u}{\delta x} + \frac{\delta(h + \xi)v}{\delta y} = 0 \quad (4.26)$$

$$\begin{aligned} \frac{\delta u}{\delta t} + u \cdot \frac{\delta u}{\delta x} + v \cdot \frac{\delta u}{\delta y} + g \cdot \frac{\delta \xi}{\delta x} - f \cdot v + \frac{g}{Ch^2 \cdot (h + \xi)} \cdot u \sqrt{(u^2 + v^2)} \\ - \frac{\tau_u^x}{(h + \xi)} - r \cdot \left( \frac{\delta^2 u}{\delta x^2} + \frac{\delta^2 u}{\delta y^2} \right) = 0 \end{aligned} \quad (4.27a)$$

$$\begin{aligned} \frac{\delta v}{\delta t} + u \cdot \frac{\delta v}{\delta x} + v \cdot \frac{\delta v}{\delta y} + g \cdot \frac{\delta \xi}{\delta y} + f \cdot u + \frac{g}{Ch^2 \cdot (h + \xi)} \cdot v \sqrt{(u^2 + v^2)} \\ - \frac{\tau_u^y}{(h + \xi)} - r \cdot \left( \frac{\delta^2 v}{\delta x^2} + \frac{\delta^2 v}{\delta y^2} \right) = 0 \end{aligned} \quad (4.27b)$$

|            |   |                                      |
|------------|---|--------------------------------------|
| $\xi$      | = water level elevation relative to the reference plane | (m)                                  |
| $h$        | = distance from the reference plane to the bottom       | (m)                                  |
| $u$        | = vertically averaged fluid velocity in x-direction     | (m·s <sup>-1</sup> )                 |
| $v$        | = vertically averaged fluid velocity in y-direction     | (m·s <sup>-1</sup> )                 |
| $\tau_u^x$ | = component of the wind stress in x-direction           | (m <sup>2</sup> ·s <sup>-2</sup> )   |
| $\tau_u^y$ | = component of the wind stress in y-direction           | (m <sup>2</sup> ·s <sup>-2</sup> )   |
| $f$        | = Coriolis parameter                                    | (s <sup>-1</sup> )                   |
| $r$        | = velocity diffusion coefficient                        | (m <sup>2</sup> ·s <sup>-1</sup> )   |
| $Ch$       | = Chézy coefficient                                     | (m <sup>1/2</sup> ·s <sup>-1</sup> ) |

The three dimensional equation of conservation of mass, 4.23, can be replaced by a two-dimensional equation (§ 4.4.1):

$$\begin{aligned} \frac{\delta(z \cdot SS)}{\delta t} + \frac{\delta(z \cdot u \cdot SS)}{\delta x} + \frac{\delta(z \cdot v \cdot SS)}{\delta y} + \frac{\delta(z \cdot D_h \cdot (\delta SS / \delta x))}{\delta x} \\ + \frac{\delta(z \cdot D_h \cdot (\delta SS / \delta y))}{\delta y} + \phi_r - \phi_s = 0 \end{aligned} \quad (4.28)$$

Horizontal currents and the solution of the advection-diffusion equation are computed with the model WAQUA, which is the core of STRESS-2D (§ 4.5.1). WAQUA is a two-dimensional horizontal hydrodynamic model, which has been developed by Rijkswaterstaat and the Delft Hydraulics Laboratory (Leendertse, 1967; Stelling, 1984). For the numerical solution of the advection diffusion equation in WAQUA, an Alternating Direction Implicit (ADI) method with finite differences is applied, using a staggered grid. With the ADI-method the solution of the equations is done in two steps; during the first half time step an implicit solution is estimated in x-direction and an explicit solution in y-direction. During the second half time step an explicit solution is estimated in x-direction and an implicit solution in y-direction. A staggered grid means, that  $\xi$ ,  $h$ ,  $u$  and  $v$ , are not computed for the same coordinates, but for coordinates shifted half

a grid size. Stelling (1984) claims that using a staggered grid leads to a 75 % reduction of the computation time, when solving the SWE equations. Furthermore he states that the numerical method is unconditionally stable and the numerical dispersion is low. As numerical dispersion, stability and computation time is usually a problem in two-dimensional modelling, these were the main reasons for the use of the WAQUA model in STRESS-2d. Besides, experiences with WAQUA in several previous projects seemed good and the program source was available. Extensive descriptions and discussions of the model are available (Leendertse, 1967; Stelling, 1984). The specification of characteristics and parameters as described in this paragraph, apply to the rectangular WAQUA version used in STRESS-2d.

The most important parameters for the application of the model for a specific water system are;

- \* the grid size,  
the size of the grid determines the extent of details described by the model and has an important influence on numerical dispersion, computation time and computer memory use;
- \* the time step,  
the size of the time step is related to the grid size and has a major effect on computation accuracy and computation time;
- \* the wind stress coefficient,  
the wind stress coefficient relates the transfer of energy from the wind field to the water body. In WAQUA the wind stress coefficient is constant for all conditions;
- \* the bottom friction,  
the bottom friction is described by the Manning-coefficient,  $M$ , which is related to the Chézy-coefficient:

$$Ch = z^{1/6} \cdot M \quad (4.29)$$

- \* the velocity diffusion coefficient,
- \* the Coriolis coefficient,  $f$ ,  
the Coriolis effect depends on the latitude,  $\phi$ :

$$f \approx 1.46 \cdot 10^{-4} \cdot \sin(\phi) \quad (4.30)$$

#### 4.5 Model outline and parameter optimization

The numerical implications and the calibration procedures used in complex models are often misty for outsiders, no matter how extensive publications are. In a fresh attempt, a review of the entire model structure and the calibration effort is made in these paragraphs.

#### 4.5.1 Model outline

A summary of the model equations is presented in Table 4.2. Only the equations used in the Markermeer study are listed. Except for the expanded advection-diffusion equation, specific WAQUA equations are omitted.

Table 4.2 Summary of STRESS-2d equations

$$\frac{\delta(z \cdot SS_i)}{\delta t} + \frac{\delta(z \cdot u \cdot SS_i)}{\delta x} + \frac{\delta(z \cdot v \cdot SS_i)}{\delta y} + \frac{\delta(z \cdot D_h \cdot (\delta SS_i / \delta x))}{\delta x} + \frac{\delta(z \cdot D_h \cdot (\delta SS_i / \delta y))}{\delta y} + \phi_{r,i} - \phi_{s,i} = 0$$

$$\frac{\delta(MSS_{t,i})}{\delta t} - \phi_{r,i} + \phi_{s,i} = 0$$

$$z_t = \frac{MSS_t}{\sigma_s(1-e)}$$

$$z_t < z_c : \quad \begin{aligned} \frac{\delta(MSS_{t,i})}{\delta t} + (M_t + M_s) \cdot \frac{(1-e_i)}{(1-e_t)} \cdot SS_{t,i} - M_t \cdot SS_{t,i} &= 0 \\ \frac{\delta(MSS_{t,i})}{\delta t} - (M_t + M_s) \cdot \frac{(1-e_i)}{(1-e_t)} \cdot SS_{t,i} + M_t \cdot SS_{t,i} &= 0 \end{aligned}$$

$$z_t > z_c : \quad \frac{\delta(MSS_{t,i})}{\delta t} + M_t \cdot \frac{(1-e_i)}{(1-e_t)} \cdot SS_{t,i} - (M_t + M_s) \cdot SS_{t,i} = 0$$

$$\frac{\delta(MSS_{t,i})}{\delta t} - M_t \cdot \frac{(1-e_i)}{(1-e_t)} \cdot SS_{t,i} + (M_t + M_s) \cdot SS_{t,i} = 0$$

In STRESS-2d, the advection-diffusion equation of WAQUA is expanded with a source term, describing the resuspension flux, and a sink term describing the sedimentation flux. As referred to in §4.4.2, suspended solids concentrations are computed partly implicitly and partly explicitly in the WAQUA model. The sedimentation and resuspension flux are computed every half time step. As the sedimentation flux,  $\phi_{s,i}$ , is dependent on the suspended solids concentration,  $SS_i$ , and vice versa, the result of the computation of the sedimentation flux is added to the implicit part of the solution of the advection-diffusion equation. The resuspension flux is independent of the suspended solids concentration and is added to the explicit part. For each grid cell, this equation is solved for all fractions used, which is four in the Markermeer study.

After the mass balance of the water layer and the sediment top layer have been estimated, the mass transport between the layers by consolidation, erosion and turbation is estimated. These processes are controlled by the thickness of the sediment top layer.

#### 4.5.2 Calibration of the water movement model

The calibration and testing of the water movement model, the WAQUA part of STRESS-2d, was done by M.J.M. Scholten. A summary of the final parameter values is presented in Table 4.3.

Table 4.3 Summary of WAQUA parameters

| parameter  | value              | dimension              |
|------------|--------------------|------------------------|
| $dx$       | 500                | m                      |
| $dt$       | 600                | s                      |
| $N$        | 3600               | —                      |
| $\alpha$   | 34                 | °                      |
| $\Gamma_u$ | 0.021              | $m^2 \cdot s^{-2}$     |
| $f$        | $0.015 \cdot 10^3$ | $s^{-1}$               |
| $M$        | 0.026              | $m^{1/2} \cdot s^{-1}$ |
| $T$        | 1.0                | $m^2 \cdot s^{-1}$     |

The grid orientation,  $\alpha$ , and the grid size,  $dx$ , are chosen in order to minimize the number of grid cells and the boundary effects on one hand and on the other hand to maximize the amount of detail for the area. In Figure 4.2 the depth schematisation of the Markermeer area is presented. The small inset in the lower right corner of the figure, represents

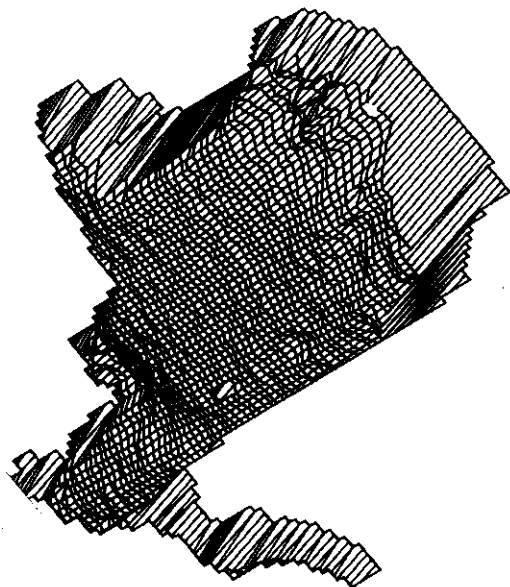


Figure 4.2 Depth schematisation of the Markermeer

the Gooimeer and part of the Eemmeer. These two small lakes are not represented very accurately, but are merely used to model the input of the river Eem and of the Randmeren to the IJmeer, the southern part of the Markermeer area.

For the calibration of the water movement part, water level measurements at five sluices have been used. Three periods of a few days to a week in 1988 were used, to optimize the model. Unfortunately, no stream velocity data were available. In the calibration of the model no sources or sinks of water, like flow through sluices, rivers and rain or evaporation, were considered and the calibration was focused on internal transport.

The time step is an important factor to determine both the accuracy and the computation time of the model. The optimal ratio between the grid size and the time step is given by the Courant-number (Langerak et al, 1987);

$$Cr = 2 \cdot dt \cdot \sqrt{(2 \cdot g \cdot z)} / dx \quad (4.31)$$

For the Markermeer study a time step of 10 minutes is used. Hence,  $Cr$  is plus minus 20, which is very high. However, results seemed reliable. The results of computations with a time step of 5 minutes, were very similar. Results of simulations with three different values of the wind stress coefficient were compared, 0.016, 0.021 and  $0.026 \text{ m}^2 \cdot \text{s}^{-1}$ . The best results were obtained with a wind stress coefficient of 0.021. Three values of the Manning coefficient were used, 0.021, 0.026 and 0.031. The results of water level simulations were very similar, but estimated flow velocities decreased with 0.02 to  $0.03 \text{ m} \cdot \text{s}^{-1}$ , with increasing values of the Manning coefficient. Hence, the data did not allow an accurate discrimination between the values for  $M$  and a value of 0.026 has been used. The sensitivity of the model to the velocity diffusion coefficient is very small as far as the computed water level are concerned. Virtually no differences were detected in the simulated water level when a value of 0.1 or  $10.0 \text{ m}^2 \cdot \text{s}^{-1}$  was used instead of  $1.0 \text{ m}^2 \cdot \text{s}^{-1}$ .

#### 4.5.3. *Optimization of the parameters of the sedimentation/resuspension model*

In order to use the resuspension-sedimentation model for the Markermeer, the value or range of many parameters had to be assessed. Using the field data series, the values of these parameters can be assessed by parameter optimization. During parameter optimization procedures, the results of model simulations, using a specific parameter set, are compared with observed values. Based on this comparison, parameter values are slightly modified and the comparison is repeated. In formal parameter optimization procedures the changes in the parameters values are directed by a mathematical search method. For both formal and

informal parameter optimization methods, usually a large number of simulation runs are made. As systematic formal parameter optimization with a two-dimensional model like WAQUA is not feasible with the accessible computer hardware and STRESS-2d is completely integrated with the WAQUA model, so that each run of STRESS-2d involves a run of WAQUA as well, parameter optimization with STRESS-2d is not feasible. This is one of the unfavourable consequences of merging both models. Hence, formal parameter optimization was done using a zero-dimensional version of STRESS-2d, ignoring horizontal transport. The best parameter sets were tested in the 2d model and compared.

The formal parameter optimization was conducted using a Rosenbrock-scheme, using optimization routines developed by Wolters (Wolters, 1992). The least sum of squares (SSQ) was used as the minimization criterium. For the parameter optimization data of both Y111 and Y112 of 1988 and 1989 were used:

- the concentration of total suspended solids (SS) collected with the automatic samplers during the high frequency sampling periods. Data of 1988 are grab samples, data of 1989 are the average of 4 hours each. Additionally the total suspended solids data collected during the incidental measurements at both sites were used (§3.3.1);
- the ratio of the different fractions ( $SS_i$ ) obtained from the fall velocity distribution experiments were used (§3.4.3);
- the total sedimentation flux (SST) obtained from sediment trap data were used (§3.4.2).

As the frequency and the accuracy of the three types of data is different, the influence of the different types on the minimization criterium was weighted as described in equation 4.32)

$$SSQ = \sqrt{\sum_{t=1}^{Nt} \frac{[C_1 \cdot (SS^c - SS^m)^2 + C_2 \cdot \sum (SS_i^c - SS_i^m)^2 + C_3 \cdot (SST^m - SST^c)^2]}{N_t}} \quad (4.32)$$

To account for the fact that the value of SST expressed in  $g \cdot m^{-2} \cdot s$  is somewhere between  $10^{-5}$  and  $10^{-4}$ ,  $C_3$  is much higher than  $C_1$ . As  $SS_i$  data are relatively scarce but less accurate than suspended solid concentration data or sedimentation flux data,  $C_2$  is higher than  $C_1$  but less than  $C_3$ . Thus:  $C_1 < C_2 < C_3$ . In the optimization procedure values for  $C_1$ ,  $C_2$  and  $C_3$  of respectively 1, 4 and  $230 \cdot 10^3$  ( $230 \cdot 10^3 \approx 3600 \cdot 64$ ) were used.

In the Markermeer study four sediment fractions were defined by fall velocity and these same fractions have been used in the resuspension model. Hence, for each fraction values of  $U_{bcr,i}$  and  $K_i$  had to be assessed. The values of  $U_{bcr,i}$  and  $K_i$  for each fraction are dependent, if  $U_{bcr,i}$  increases, usually  $K_i$  increases too. Besides, the values of  $U_{bcr,i}$  and  $K_i$  of the fractions are mutually dependent. Hence, for each optimization period, a few sets of values of  $U_{bcr,i}$  and  $K_i$  were found with the same value of SSQ. However, the definition of  $U_{bcr}$  is based on the assumption, that the critical energy needed for resuspension depends on the characteristics of each fraction. In the Markermeer,  $U_b$  varies between 0.0 and 0.5

$\text{m}\cdot\text{s}^{-1}$ . Assuming that larger particles require more energy for resuspension, it is assumed that  $0.0 < U_{\text{bcr},1} < U_{\text{bcr},2} < U_{\text{bcr},3} < U_{\text{bcr},4} < 0.5 \text{ m}\cdot\text{s}^{-1}$ . The ratio of  $U_{\text{bcr}}$  of the different fractions is unknown. In this study it has been assumed that the ratio between  $U_{\text{bcr}}$  of each fraction is the same as the ratio in averaged fall velocities of each fraction. Hence:  $w_{s,1}:w_{s,2}:w_{s,3}:w_{s,4} = U_{\text{bcr},1}:U_{\text{bcr},2}:U_{\text{bcr},3}:U_{\text{bcr},4}$ . This evidently is an arbitrary choice but expresses at least the reasonable conception that heavier particles settle faster and need more energy for resuspension. Now, the optimization of the resuspension-sedimentation model was limited to the resuspension constants  $K_i$  and the thickness of the top layer  $z_c$ . The results are presented in Appendix 10. Earlier attempts to optimize more parameters simultaneously produced unstable calculations. From a global survey of the optimization results it becomes clear, that within the ranges of the predetermined parameters, the model is rather insensitive to the exact values. Hence, most of the optimization runs produced good and comparable results and sifting is complex. Apart from the previous defined SSQ, the mean relative error MRE was used for the final sifting of parameter sets. Generally, results are better if the data of Y112 are used, instead of the data of Y111. Period 89-3 generally produced better results than period 89-2.

For both sites data of day 120 (30 April) until day number 270 (27 September) are used, excluding the high frequency sampling period of April 1989. For this period the measured suspended solids concentrations were much higher than found during the rest of the year, even though the wave induced energy, expressed as  $U_b$ , was in the same range. Hence, either the suspended solid data of that particular period are incorrect or the model is not capable to simulate suspended solid concentrations during this period. The latter could be caused by the assumption that the resuspension parameters  $U_{\text{bcr}}$  and  $K$  are constants and no aggregation of particles occur. With this temperature effects or other seasonal variations are ignored.

Four sets of  $U_{\text{bcr}}$  have been tested in the parameter optimization runs as described in Table 4.4. Using the set with the highest values of  $U_{\text{bcr},i}$ , virtually no resuspension of  $\text{SS}_4$  occurs, even though this fraction is found regularly in the fall velocity distribution experiments. The high set of  $U_{\text{bcr}}$  leads to the underestimation of the sedimentation flux. The results of both sets with small values of  $U_{\text{bcr}}$  are very similar. The set with  $U_{\text{bcr},1}$  of  $0.002 \text{ m}\cdot\text{s}^{-1}$  ( $U_b$ -K) and  $U_b$ -M were used for further optimization.

During most optimization runs a certain order in the values of  $K_i$  is detected;  $K_1 < K_2 < K_3 < K_4$ . Hence higher values of  $U_{\text{bcr}}$  produce higher values of  $K$ .



Table 4.4 Used sets of  $U_{bcr}$  ( $m \cdot s^{-1}$ )

|           | $U_{bcr,1}$ | $U_{bcr,2}$ | $U_{bcr,3}$ | $U_{bcr,4}$ |
|-----------|-------------|-------------|-------------|-------------|
| $U_b$ -G  | 0.0008      | 0.0060      | 0.0260      | 0.1000      |
| $U_b$ -M  | 0.0004      | 0.0030      | 0.0130      | 0.0500      |
| $U_b$ -K  | 0.0002      | 0.0015      | 0.0065      | 0.0100      |
| $U_b$ -K' | 0.0000      | 0.0015      | 0.0065      | 0.0100      |

The critical thickness of the sediment top layer was estimated in the range of a few millimetres to less than one centimetre. This range was obtained through a visual inspection of the samples of the Jenkin mud sampler. Besides, if the porosity in the top layer is assumed to be 95 % (Luettich et al., 1990) and the water depth is between 3 and 4 m, the sediment concentration caused by direct resuspension of the top layer may vary between 80 and 300  $g \cdot m^{-3}$ . Higher suspended solids concentrations then must be caused by erosion of the bottom layer. Values of 0.006 and 0.008 m both produce adequate optimization results. With lower values, the optimization results deteriorate as the top layer became immediately depleted from the smaller fractions.

Quantitative knowledge about the erosion ( $M_e$ ), consolidation ( $M_c$ ) and turbation ( $M_t$ ) velocities between sediment top and bottom layer is limited. Hence, the values of these constants have been estimated with a so called educated guess and tested in a few runs. Assuming that the effect of a storm on the thickness and composition of the sediment top layer is erased within a week, two values of  $M_c$  were used; a value of  $1.0 \cdot 10^{-7} m \cdot s^{-1}$  and a value of  $0.5 \cdot 10^{-8} m \cdot s^{-1}$ . For lack of any quantitative data about  $M_e$  it was assumed  $M_e$  equals  $M_c$ . Hence, any relationship between bottom stress and  $M_e$  is ignored. With a value of  $z_c$  of 0.006 m the small value of  $M_e$  and  $M_c$  produce better results (Appendix 10). The same tendency was found using the set of  $U_{bcr}$  with the medium values. For the small  $U_{bcr}$  or  $z_c$  of 0.008 m, no clear differences were found. Suspecting a preference of the small values of  $M_c$  and  $M_e$ , the parameter optimization is focused on them.

Further optimization has been done with the two-dimensional model using the same data sets and using the data sets of 1988 of both sites. The parameter sets that were compared are presented in Table 4.5. A summary of the results is presented in Table 4.6.

*Table 4.5 Selected parameter sets*

| id  | $U_{bcr}$ | $z_c$ | $M_c \& M_b$        | $K_1$                | $K_2$                | $K_3$                | $K_4$                |
|-----|-----------|-------|---------------------|----------------------|----------------------|----------------------|----------------------|
| 3b  | $U_b-M$   | 0.006 | $1.0 \cdot 10^{-8}$ | $6.13 \cdot 10^{-7}$ | $8.04 \cdot 10^{-6}$ | $4.17 \cdot 10^{-5}$ | $1.04 \cdot 10^{-4}$ |
| 8b  | $U_b-M$   | 0.006 | $0.5 \cdot 10^{-8}$ | $7.15 \cdot 10^{-7}$ | $9.17 \cdot 10^{-6}$ | $3.57 \cdot 10^{-5}$ | $1.10 \cdot 10^{-4}$ |
| 9a  | $U_b-M$   | 0.008 | $0.5 \cdot 10^{-8}$ | $7.56 \cdot 10^{-7}$ | $8.49 \cdot 10^{-6}$ | $8.34 \cdot 10^{-5}$ | $1.04 \cdot 10^{-4}$ |
| 11b | $U_b-K$   | 0.006 | $0.5 \cdot 10^{-8}$ | $6.34 \cdot 10^{-7}$ | $9.37 \cdot 10^{-6}$ | $2.67 \cdot 10^{-5}$ | $8.98 \cdot 10^{-5}$ |
| 12b | $U_b-K$   | 0.008 | $0.5 \cdot 10^{-8}$ | $5.77 \cdot 10^{-7}$ | $1.16 \cdot 10^{-5}$ | $1.00 \cdot 10^{-5}$ | $8.59 \cdot 10^{-5}$ |

*Table 4.6 Optimization results of STRESS-2d runs*

| id  | 1988        |             | 89-2        |             | 89-3        |             |
|-----|-------------|-------------|-------------|-------------|-------------|-------------|
|     | Y111<br>MRE | Y112<br>MRE | Y111<br>MRE | Y112<br>MRE | Y111<br>MRE | Y112<br>MRE |
| 3b  | 34          | 55          | 26          | 23          | 20          | 16          |
| 8b  | 31          | 46          | 27          | 24          | 18          | 17          |
| 9a  | 26          | 37          | 30          | 27          | 19          | 23          |
| 11b | 32          | 45          | 27          | 24          | 18          | 17          |
| 12b | 34          | 43          | 26          | 23          | 19          | 18          |

The results of the two dimensional model with the selected parameter sets are again very similar and it is difficult to discriminate between the sets. Parameter set 8b and 11b give on average the best results, so a critical sediment toplayer thickness of 0.006 gives the best results. In the further simulation parameters set 8b has been used, the set with the moderate values of  $U_{bcr}$ .

#### 4.5.4 Validation of the STRESS-2d model

In the previous paragraphs, a part of the model validation has already been discussed. This paragraph is limited to a general overview.

In the STRESS-2d model, the driving force of the resuspension model is wind waves, which are simulated with the SMB-based relationships. In Figure 4.3, the simulated and the available observed wave heights of the high frequency sampling periods are compared. It is obvious that in general the behaviour of the model is very good. In period 89-3 at site Y111, simulated wave heights are higher than observed wave heights, but this might as well be caused by the wind data as by the wave model.

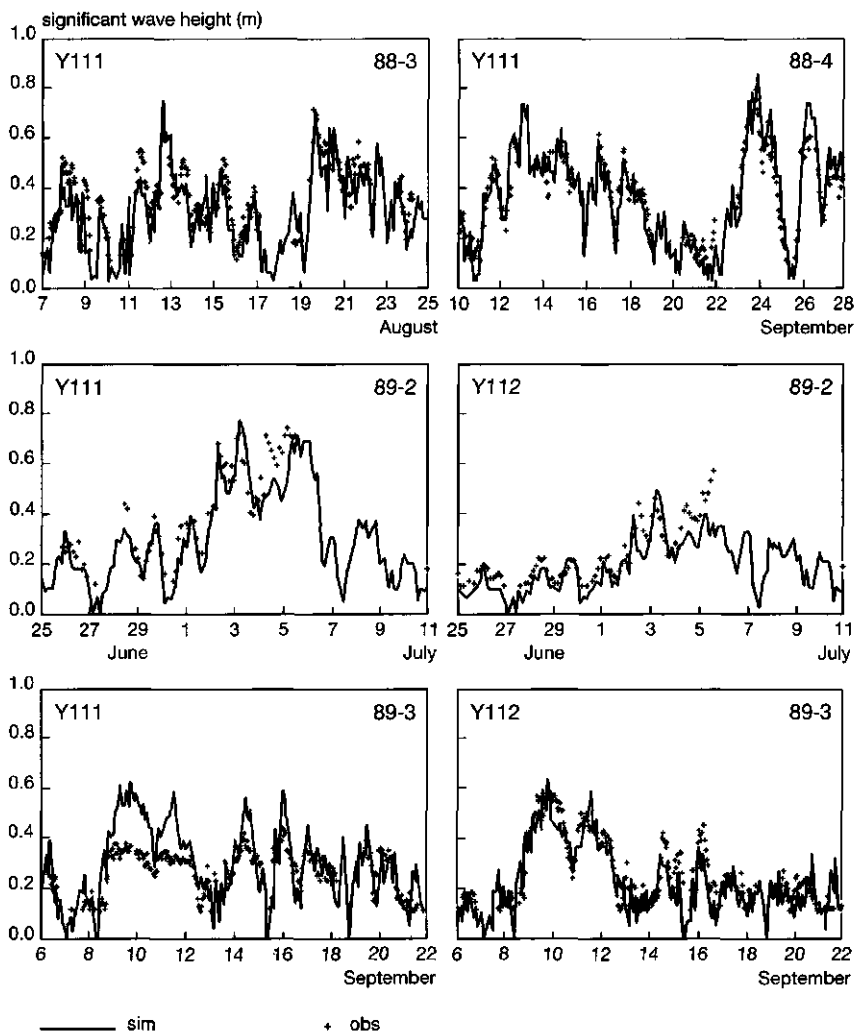


Figure 4.3 Observed and simulated wave heights

One of the most important assumptions in the STRESS-2d model and one of the most arbitrary too, is the fact that processes like aggregation and disaggregation of flocs is ignored. Although this seems disputable, the obtained model results are very good, which is shown in Figure 4.4 and Figure 4.5. The resuspension parameters  $K_i$  and  $U_{bcr,i}$  are mutually dependent: a higher fixed value for  $U_{bcr,i}$  results in a lower estimated value for  $K_i$  and vice versa. The model is insensitive to the value of  $U_{bcr,i}$  and  $K_i$  within the parameter space derived with optimization.

The simulated sedimentation flux can be validated by comparison with the measured sedimentation fluxes as obtained from sediment trap data.

The error in the simulated sedimentation flux with the final parameter set is less than 15 %, which is rather good. The suspended solids concentration at a certain site is the combined result of resuspension, sedimentation and sediment transport. Simulated and observed suspended solids concentrations are shown in Figure 4.4 for the high frequency sampling periods of 1988 and in Figure 4.5 for 1989. In general, the results for the Markermeer are rather good as trends are simulated rather well. Some observed peaks are not simulated precisely. The accuracy of the simulated values decreases when the average hourly wind speeds increase over  $10 \text{ m}\cdot\text{s}^{-1}$ . It should be noted that an average hourly wind speed higher than  $10 \text{ m}\cdot\text{s}^{-1}$  occurs during less than 15 % of the time (§ 3.3.3).

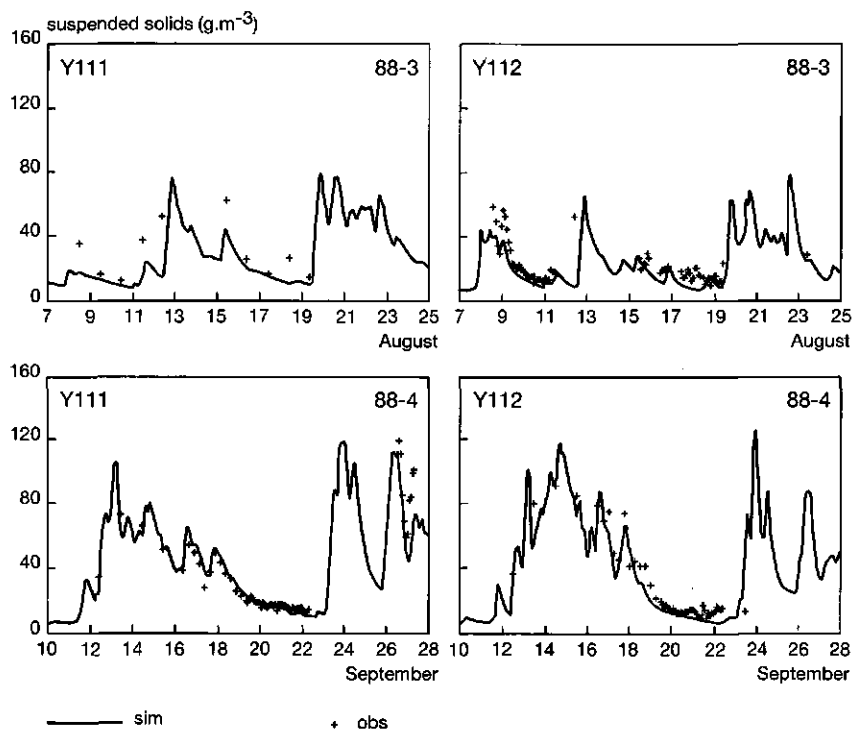


Figure 4.4 Observed and simulated suspended solids concentrations of the high frequency sampling periods of 1988

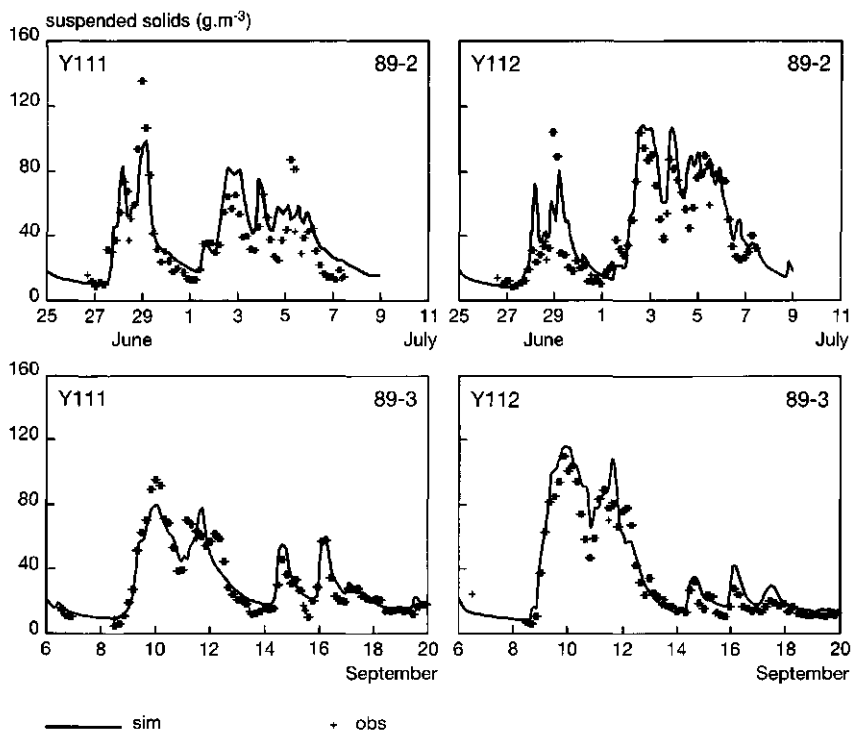
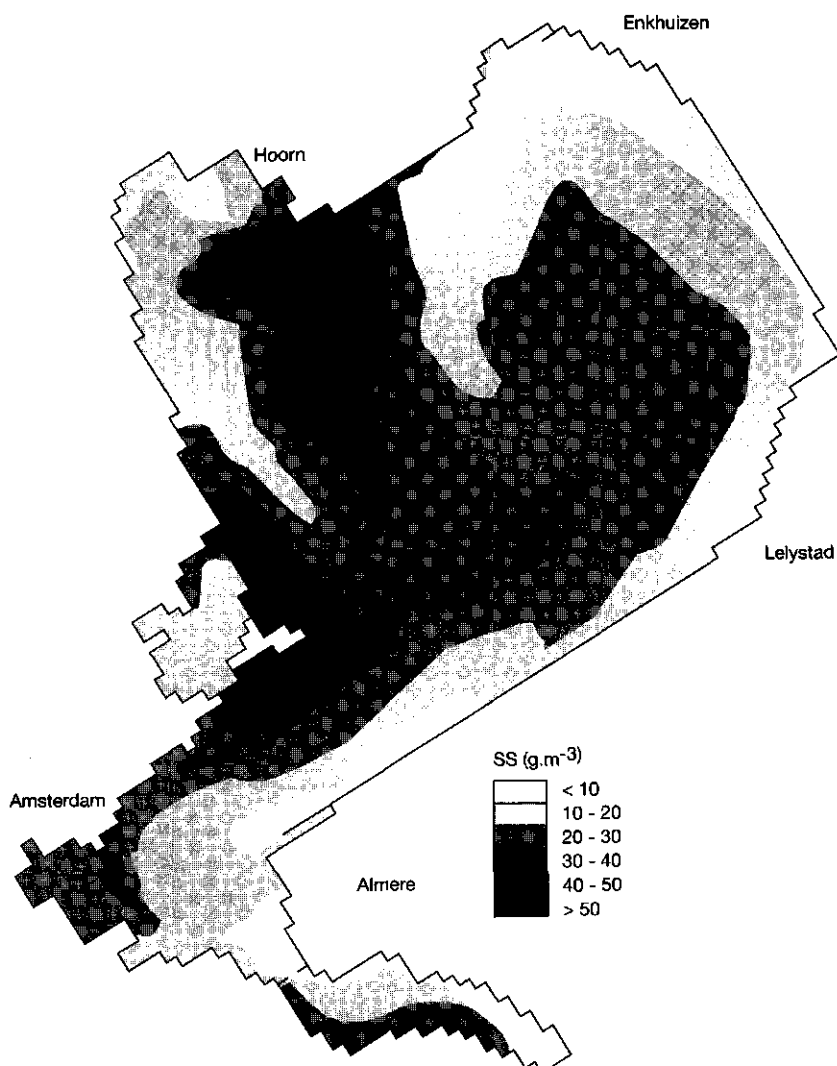


Figure 4.5 Observed and simulated suspended solids concentrations of the high frequency sampling periods of 1989

The model is very sensitive to the input time series of the wind speed and the wind direction, as these are the main driving forces for resuspension. The amount of sediment available for resuspension at the beginning of the simulation is an important factor determining the spatial distribution of suspended solids, due to characteristics of the bottom model. The description and calibration of the bottom model is still primitive. At this moment, it is considered the major weakness of the model STRESS-2d.

The modelling of the horizontal sediment transport is difficult to validate as data of more than the sites used for optimization are scarce. Comparison of simulated suspended solids concentration maps with concentration maps derived from satellite images was only of limited use (Buitenveld et al, 1990). This is mainly due to the fact that clear satellite images are available on clear, sunny, mostly windless days and the available set of images is not a representative selection of the occurring weather conditions. Besides, the estimated concentration maps from the images are based on limited measurement data of samples taken at the surface of the lake and are not very accurate near the boundaries of the lake. In Figure 4.6, maps of the total sediment concentration and the total



*Figure 4.6a Simulated total suspended solids concentration at 11 September 1989 at 12.00 a.m.*

sediment transport at 11 September 1989 at 12.00 a.m. are presented. At that particular day wind speeds over  $10 \text{ m.s}^{-1}$  were measured from the North-East. The effect on the distribution of suspended solids over the lake is clear: the suspended solids concentration increases towards the South-West. In Figure 4.7 the same maps are shown for 15 September 1989 at 0.00 a.m.. During that night, wind speed decreased from  $12 \text{ m.s}^{-1}$  to  $5 \text{ m.s}^{-1}$  and the wind direction was South-West. The simulated distribution patterns of the suspended solids concentration are very different from those in Figure 4.6.

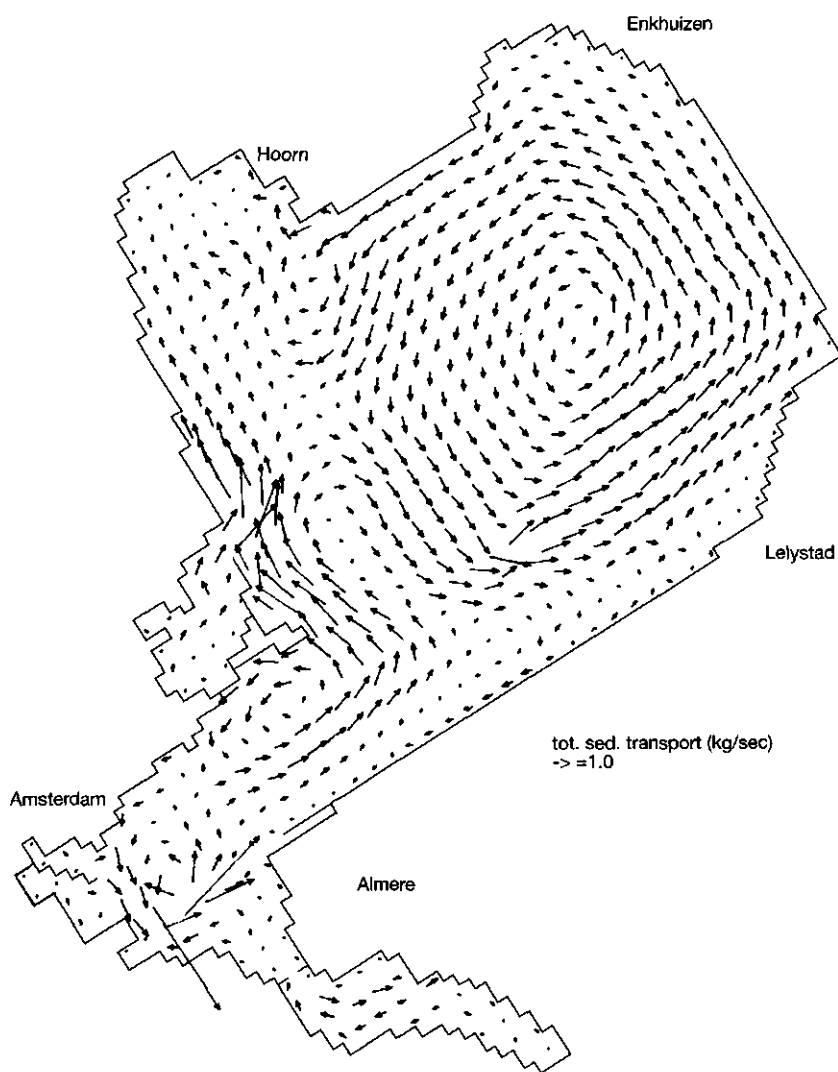


Figure 4.6b Simulated total suspended solids transport at 11 September 1989 at 12.00 a.m.

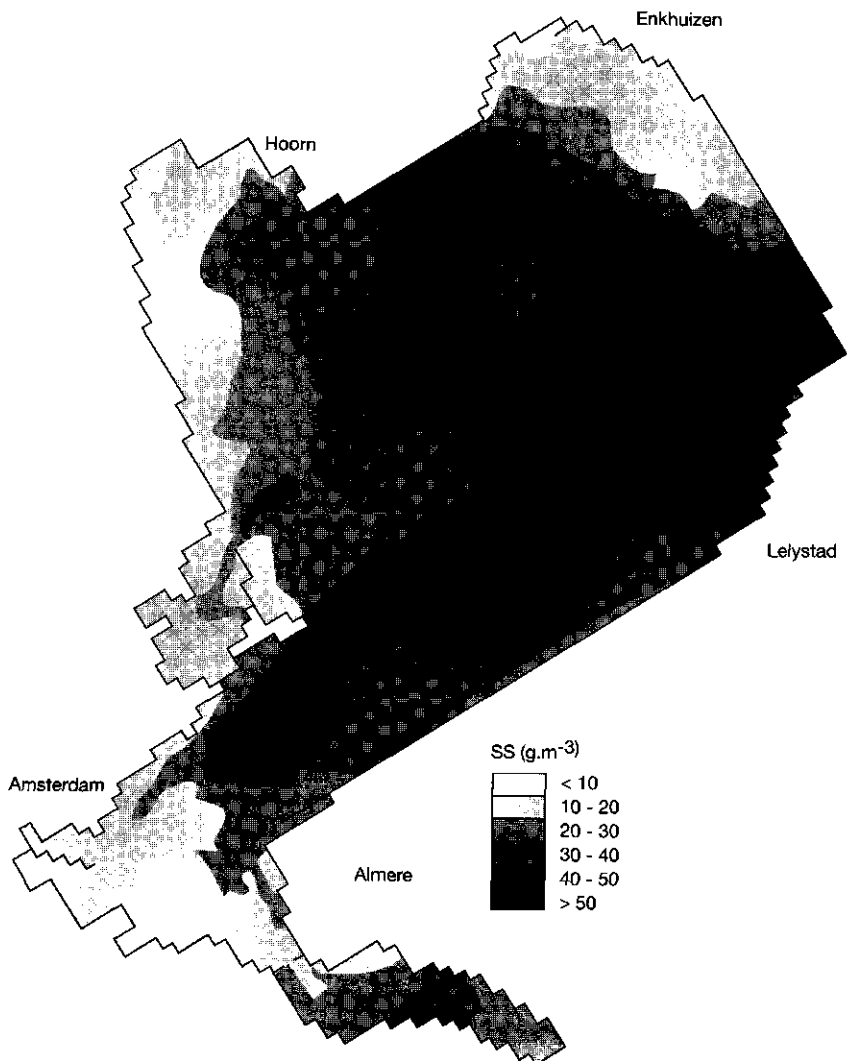


Figure 4.7a Simulated total suspended solids concentration at 15 September 1989 at 0.00 a.m.



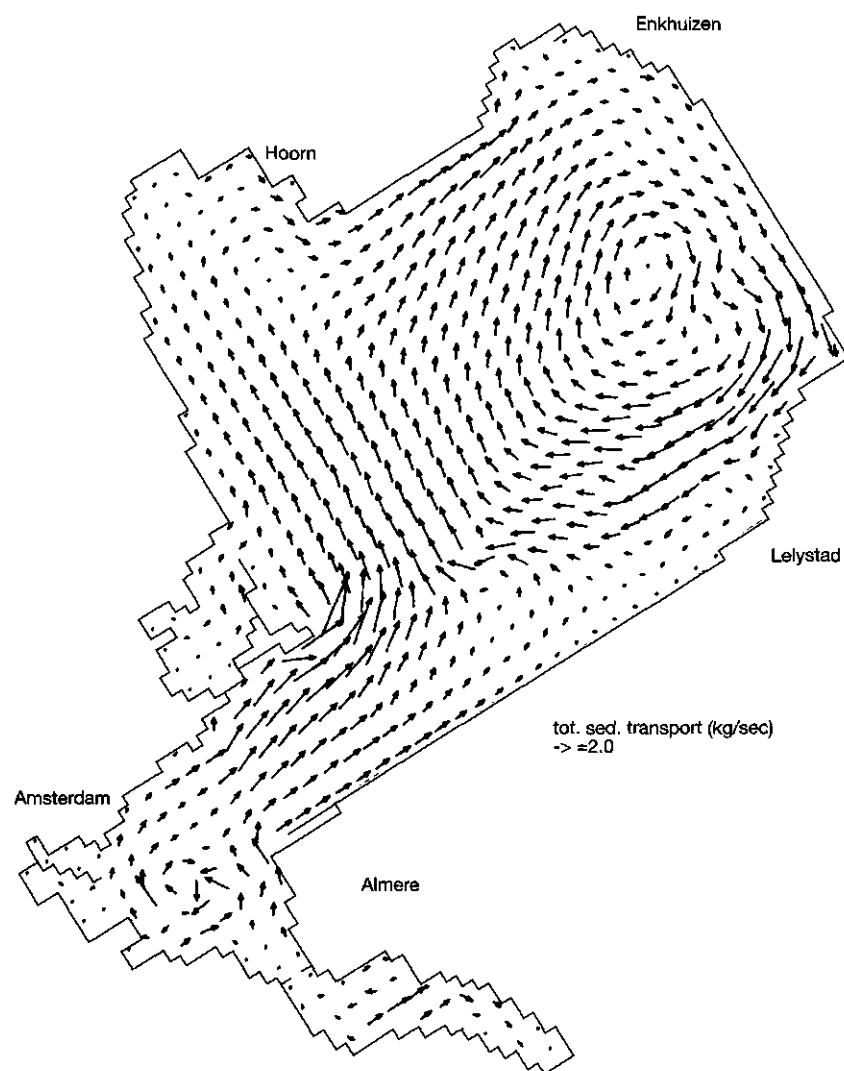


Figure 4.7b Simulated total suspended solids transport at 15 September 1989 at 0.00 a.m.

## 5 Under water light field

The under water light field is a very important factor in the ecology of water systems. It has a major influence on the growth of phytoplankton and macrophytes and affects the foraging possibilities of fishing birds and the mating and grazing possibilities of some fish by influencing the optical depth. Further, the optical depth is an important standard in the Dutch water quality assessment system. In this study, the main concern for the under water light field is its relation with phytoplankton growth. The light availability is of major importance, not only in determining how much plant growth there will be, but also which kind of species will predominate and which will evolve. Macrophytes and phytoplankton compete for solar radiation not only with each other, but also with all the other light-absorbing components of the aquatic medium.

Many factors determine the nature of the under water light field. Hence, the light conditions may be very site or time specific. The characteristics of the under water light field of the Markermeer have been stated to be the predominant cause of the absence of blooms of the blue-green algae *Oscillatoria agardhii* (§ 1.2.1). To simulate the under water light field of the Markermeer, the model *CLEAR* (Combined Light Energy Attenuation Routine) has been developed. The model may be useful for other lakes with a similar nature of the under water light field; shallow turbid water in which the attenuation of light is dominated by resuspended sediment.

The nature of the under water light field is determined by two categories of aspects: the properties of the radiation and the optical properties of the aquatic medium. Preisendorfer (1961) distinguished two types of optical properties of the aquatic medium:

- inherent optical properties,  
which are not affected by the prevailing distribution of the radiation;
- apparent optical properties,  
which depend on the prevailing distribution of the radiation.

### 5.1 Inherent optical properties

#### 5.1.1 Properties of the radiation field

The three most important properties of the radiation field are the irradiance, the spectral distribution and the angular distribution.

The irradiance is defined as the radiant flux per unit area. This radiant flux per unit area can be expressed either in terms of energy per unit area ( $\text{W}\cdot\text{m}^{-2}$ ) or in terms of quanta per unit area ( $\text{quanta}\cdot\text{m}^{-2}\cdot\text{s}^{-1}$ ). As the amount of energy of a photon depends on the wave length, one should be careful with the conversion between these two. To make a clear distinction between the two,  $I_s$  is defined as the radiation in  $\text{W}\cdot\text{m}^{-2}$  and  $E$  as the irradiance in  $\mu\text{E}\cdot\text{m}^{-2}\cdot\text{s}^{-1}$ , with  $1 \mu\text{E} = 6.02\cdot 10^{17}$  quanta. Photosyn-

thesis is a photochemical process. Although the probability of a photon to be absorbed is affected by its wavelength, each absorbed photon has basically the same contribution to photosynthesis, regardless of its wavelength (Kirk, 1977). Hence, in the context of photosynthesis, irradiance  $E$ , defined in terms of quanta per unit area per unit time, is the more important quantity in this study. The segment of solar radiation that can be used for photosynthesis is frequently called the Photosynthetically Active Radiation, PAR. Most commonly this is taken to be the waveband from 400 to 700 nm.

Normally, irradiance is measured on a horizontally placed flat surface. The downward irradiance,  $E_d$ , and the upward irradiance,  $E_u$ , are the respective values of the irradiance on the upper and lower face. The radiant flux traversing a unit area of this surface per second, is proportional to the cosine of the angle between the light beam and the perpendicular to the receiving surface: this is the Lambert Cosine Law. Due to these inherent geometric properties, Jerome et al (1990) stated that the scalar irradiance,  $E_s$ , is a better parameter in the study of photochemical or photobiological processes. The scalar irradiance is defined as the total energy per unit area arriving at a point from all directions when all directions are equally weighted, which is more similar to the radiation received by phytoplankton than the downward irradiance. Nevertheless, the downward irradiance is the more commonly measured and used variable and the data available in this study concerned only downward irradiance. Hence, in this study the downward irradiance is used.

The spectral distribution of the incident solar radiation, in terms of the proportion of irradiance of different wave lengths in the total solar radiation, is determined by the length of the path through the atmosphere and the atmospheric conditions. The atmospheric path length is determined by the solar altitude,  $\gamma$ , or the zenith angle. The solar elevation is the angle between the downward vertical (perpendicular) and the direction of the sun beam and can be estimated at any given latitude,  $\phi$ , from the following equations (Kirk, 1983):

$$\sin \gamma = \sin \phi \cdot \sin \alpha_1 - \cos \phi \cdot \cos \alpha_1 \cdot \cos \alpha_2 \quad (5.1a)$$

$$\alpha_1 = 0.396 - 22.91 \cdot \cos \alpha_3 + 4.03 \cdot \sin \alpha_3 - 0.39 \cdot \cos^2 \alpha_3 + 0.05 \cdot \sin^2 \alpha_3 \quad (5.1b)$$

$$\alpha_2 = 360 \cdot t_h / 24 \quad (5.1c)$$

$$\alpha_3 = 360 \cdot \text{dayn} / 365 \quad (5.1d)$$

$$\gamma = \text{solar elevation} \quad (^\circ)$$

$$\phi = \text{latitude} \quad (^\circ)$$

$$t_h = \text{time} \quad (\text{h})$$

$$\text{dayn} = \text{Julian day number} \quad (-)$$

In Figure 5.1, examples of solar elevation for the Netherlands are presented.

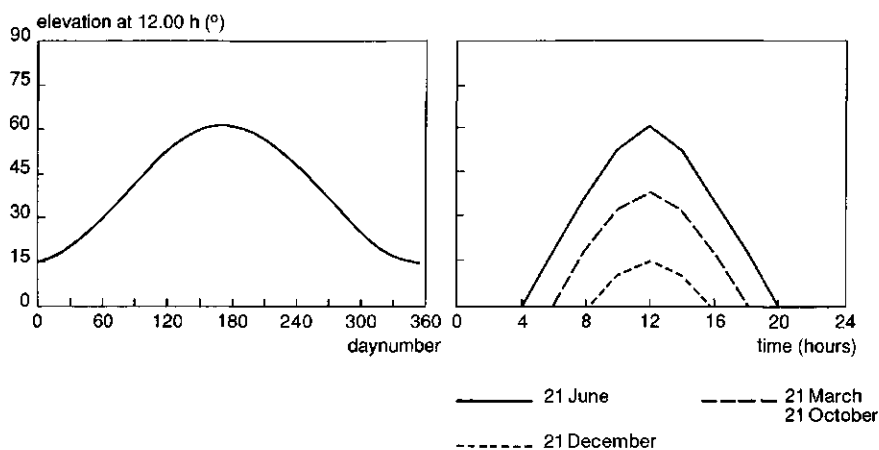


Figure 5.1 Examples of solar elevation for the Netherlands

At lower solar altitudes, there is relatively more blue light and less red. The composition of the atmosphere influences the absorption and scattering of incident radiation. The composition includes both gaseous and particulate components of the atmosphere and cloud coverage. The presence of a large water surface and consequently local high water vapour contents, may reduce the intensity of the solar radiation considerably. This is particularly likely to happen with large lakes, where much of the lower atmosphere may have been influenced by the presence of the lake. Scattering not only increases the path length and therefore the probability of absorption, but also the angular distribution of the radiation. One way to use such theories in the description of the light field is to add a stochastic atmospheric absorption to the theoretical maximum irradiance, which has the same statistical properties of cloud-cover, humidity, etcetera, as the meteorological records. However, for this study radiation data were available hourly averaged downward irradiance, covering the energy in the range of 300 to 3000 nm (§ 3.3.5). Hence, no detailed information about the spectral distribution was available. Lower values of irradiance are caused by cloud coverage, but no specific information was available and the angular distribution of the radiation is therefore hard to assess. This radiation sum was measured above land at more than 60 kilometres of the lake (de Bilt). Assuming a spectral distribution that is constant in time with 48 % of the total energy in the range of PAR, the downward irradiance,  $E_d$ , is estimated (Tilzer, 1984; § 3.3.5). As two years of rather different light conditions are used in the simulations, most differences in light conditions between De Bilt and the lake will be levelled out.

As the incident radiation crosses the air-water interface, a part of the radiation will be reflected. The proportion of the radiation that is reflected depends on the angular distribution of the radiation, and on the properties of the water surface. It varies from 2 % for vertically incident

light, to almost 100 % for horizontally incoming light at an undisturbed water surface (Kirk, 1983). In Table 5.1 reflectance values as presented by Kirk (1983) are summarized.

*Table 5.1 Percentage reflectance of unpolarized light from a flat surface (Kirk, 1983)*

| elevation | reflectance   |
|-----------|---------------|
| 45 - 90°  | < 3 %         |
| 30 - 45°  | 3 < R < 6 %   |
| 20 - 30°  | 6 < R < 14 %  |
| 10 - 20°  | 14 < R < 35 % |

Roughening of the water surface by wind has little effect on the reflectance of sun light from high solar elevations, but does significantly decrease reflectance at low solar elevations, since on average waves increase the angle between the incident light and the surface. Another important factor in the estimation of the reflectance is the cloud coverage, in relation to its effect on the angular distribution of the radiation. For overcast days with diffuse radiation, for low solar elevation reflection will be lower than listed in Table 5.1. Various empirical determinations indicate that 6 to 8 per cent of the light from an overcast sky returns from the surface (Hutchinson, 1957). Hence, there is no simple accurate relation between reflectance and solar elevation, wave height and irradiance. If one mean reflectance value is used for the entire year, reflectance will be overestimated during high noon in the summer months and underestimated around sunset and sunrise and in the winter months.

### *5.1.2 Properties of the aquatic medium*

The absorption and scattering properties of the aquatic medium for light of any given wave length are specified in terms of the absorption coefficient,  $a$ , the scattering coefficient,  $b$ , and the volume scattering function. The beam attenuation coefficient,  $\epsilon$ , is the sum of the absorption and the scattering coefficient. The volume scattering function describes the angular distribution of scattering. In all natural waters which have been examined, the volume scattering function is such that most of the scattering is in a forward direction, within a rather narrow angle relative to the incident beam (Kirk, 1977). Above a certain minimum level of turbidity, particle scattering is dominant over the scattering by other components at all angles. Since the shape of the volume scattering function is determined by the intrinsic scattering properties of the particles and not by their concentration, this shape is independent of the turbidity (Kirk, 1983).

The effect of scattering is to impede the vertical penetration of light. Scattering by itself does not remove light, but it increases the total path length of the photons and so increases the probability of a photon being absorbed. The main contributors to scattering are the suspended particles, including phytoplankton.

Most of the light energy absorbed in the aquatic system, after a very brief period as electronic excitation energy, ends up either as heat or as chemical energy in the form of photosynthetically produced biomass. The light absorption which takes place in natural waters can be attributed to four components of the aquatic ecosystem: water, dissolved yellow pigments (Gilvin), the photosynthetic biota (phytoplankton) and the inanimate particulate matter (suspended solids). The contribution of the various components to the absorption and scattering in natural waters is listed below, emphasizing the characteristics of the Markermeer.

Water itself absorbs light throughout the PAR spectrum, with absorption being strongest at the red end. The absorption coefficient varies between 0.02 and 0.65  $\text{m}^{-1}$  for PAR (Smith and Baker, 1981) or up to 0.68  $\text{m}^{-1}$  (Buiteveld and Donze, 1991). Water itself does scatter light but its contribution is dwarfed by that of particles. The contribution of water itself to the attenuation of PAR by absorption of quanta is of significance above 550 nm.

Gilvin or the dissolved yellow substance, is a complex mixture of plant degradation products, referred to as humic substances. As the concentration of Gilvin may be extremely variable, this also applies to the absorption of radiation by Gilvin. This absorption is highest for the short wave lengths and decreases to zero at wavelengths near 700 nm. The absorption of Gilvin as a function of wave length has been described by an exponential equation (Bricaud et al, 1981). The absorption coefficient at 375 nm (Bricaud et al, 1981) is a good measure for the concentration of Gilvin. According to Buiteveld and Donze (1991), the DOC concentration is not a good measure for the Gilvin content of a lake and the absorption coefficient at 380 nm  $a_g(380)$  should be used. Unfortunately, often only DOC concentrations are available. In the Markermeer  $a_g(380)$  ranges from 3 to 6  $\text{m}^{-1}$  (Buiteveld and Donze, 1991) and the DOC concentration from 6 to 9  $\text{g}\cdot\text{m}^{-3}$  with a mean value of 7  $\text{g}\cdot\text{m}^{-3}$  (§ 3.2.2).

Suspended solids, defined as resuspended sediment, contribute mainly to the scattering coefficient and the volume scattering function of water and in a lesser extent to the absorption. The absorption spectra of suspended solids all have much the same shape: absorption is low or absent at the red end of the spectrum and rises steadily as the wave length decreases towards the blue end (Kirk, 1983). Particle scattering is rather insensitive to wavelength, though shorter wavelengths are scattered slightly more intensely. Approximately linear relationships between the scattering coefficient and the concentration of suspended matter have been observed, although the proportionality constant varies from one

kind of suspended matter to another. The refractive index and the size distribution of the particles are properties that influence the relationship between the scattering coefficient and the sediment concentration. Baker and Lavelle (1984) reported a much more efficient attenuation of light per unit of mass by smaller particles ( $8.5 \mu\text{m}$ ) than by larger particles ( $48 \mu\text{m}$ ) and a dependency of the attenuation on the effective diameter rather than a semi-spherical one ( $d_s$ , § 4.1.1). These effects have been explained by the dependency of light attenuation on the cross sectional area of the particles and not directly on their volume or mass.

A significant contribution to the total absorption coefficient in productive waters is the absorption by phytoplankton, due to the absorption of light by the photosynthetic pigments. All photosynthetic plants contain chlorophyll-a and carotenoids. Most classes of plant contain in addition other chlorophyll pigments or biliproteins as well. The absorption spectrum of chlorophyll-a has absorption peaks in the blue and red part of the spectrum at 440 and 675 nm. Carotenoids absorb predominantly at the short wavelength end of the visible spectrum. One of the biliprotein chloroplasts found in blue-green algae are the phycocyanins, with their main absorption peak in the red end of the spectrum. As phytoplankton usually contains a mixture of pigments, their absorption spectra contain a number of absorption peaks. Hence, the whole range of visible light is affected by phytoplankton absorption. The amount of light harvested by the phytoplankton cells depends not only on the total amounts of photosynthetic pigments but also on the size and shape of the algal cells or colonies, similar to the scattering by sediment particles. For example, the light harvesting efficiency per unit of volume of long, thin cylindric filaments is much higher than the efficiency of spheres (Kirk, 1983). The contribution to the scattering of light by phytoplankton is similar to the contribution by sediment particles.

In the model *CLEAR* the beam absorption and beam scattering coefficient are not used independently. Instead the attenuation coefficient is used, in which the absorption and scattering properties of the aquatic medium are combined.

## 5.2 Apparent optical properties

To assess the available light energy at a certain depth and the attenuation of irradiance in natural waters, the properties of the light field and the aquatic medium have to be combined. Downward irradiance diminishes in an approximately exponential manner with depth, expressed by Beers' Law:

$$E_{d,\lambda}(z) = E_{d,\lambda}(0) \cdot e^{-K_{d,\lambda} \cdot z} \quad (5.2)$$

$$E_{d,\lambda} = \text{downward irradiance of wavelength } \lambda \quad (\mu\text{E} \cdot \text{m}^{-2} \cdot \text{s}^{-1})$$

$$K_{d,\lambda} = \begin{array}{l} \text{vertical downward attenuation} \\ \text{coefficient of wavelength } \lambda \end{array} \quad (\text{m}^{-1})$$

The vertical downward attenuation coefficient can be obtained from irradiance measurements at different depths. In principle, the irradiance at each secluded wavelength should be measured but in practise the downward irradiance of PAR is measured. Thus, instead of the vertical downward attenuation coefficient of wavelength  $\lambda$ ,  $K_{d,\lambda}$ , the vertical downward attenuation coefficient of the entire PAR range of the spectrum,  $K_d$  is estimated. This  $K_d$  value thus depends on both the composition of the aquatic medium and the properties of the irradiance and is therefore an apparent property. The effects of the averaging of  $K_d$  over the waveband of PAR is evaluated in § 5.2.2.

### 5.2.1 Contribution of individual components tot the attenuation coefficient

The vertical attenuation coefficient for downward irradiance in natural waters can be partitioned into a set of partial vertical attenuation coefficients, each corresponding to a different component of the medium:

$$K_d = K_{d,1} + K_{d,2} + \dots + K_{d,n} \quad (5.3)$$

$$K_{d,i} = \begin{array}{l} \text{partial vertical downward attenu-} \\ \text{ation coefficient of component } i \end{array} \quad (\text{m}^{-1})$$

Although the contributions of the different components of the medium to the total attenuation of irradiance can simply be added, the nature of their contribution can vary markedly. The partial attenuation coefficient is a function of both the irradiance distribution and the concentration of the component. The distribution of the irradiance is in turn affected by the presence of the component. Hence, the value of the partial vertical downward attenuation coefficient will not increase linearly with an increase in the concentration of the component. Nevertheless, such a linear relationship is often used, assuming that deviations are small (Kirk, 1983).

$$K_d = k_{d,1} \cdot C_1 + k_{d,2} \cdot C_2 + \dots + k_{d,n} \cdot C_n \quad (5.4)$$

$$k_{d,i} = \begin{array}{l} \text{specific partial vertical downward} \\ \text{attenuation coefficient of} \\ \text{component } i \end{array} \quad (\text{m}^2 \cdot \text{g}^{-1})$$

$$C_i = \text{concentration of component } i \quad (\text{g} \cdot \text{m}^{-3})$$

In many studies, attenuation by suspended solids is often based on a distinction of the suspended solids in inorganic material and an organic fraction (ash free dry weight) and the chlorophyll-a content for living plankton. Because the inorganic and organic material can not be separated physically, specific attenuation coefficients are estimated using



multiple regression methods (Verduin, 1982; DiToro, 1982, Bakema, 1988). Specific partial attenuation coefficients often differ between lakes, and even between years for the same lake. Also negative values may be obtained. With this method applied to the Markermeer data set, both problems occurred (Van Duin and Kuijpers, 1989). Therefore a new method has been developed in which different components are distinguished that can actually be separated physically, so that partial attenuation coefficients can be measured directly rather than estimated through regression (Van Duin et al, 1992). The method is based on the fact that both the attenuation of light by particles and the settling of particles is related to the cross sectional area of the particles. Hence, smaller particles show a relatively much higher attenuation of light than larger particles (§ 5.1.2) and in general the settling velocity of smaller particles is lower as well. Thus, particle classes defined by settling velocity are different in attenuation efficiency too. This distinction in settling rates is also more operational in the overall objectives of this study, notably for the suspended solids balance based on resuspension and sedimentation and also allows a direct, unbiased coupling between *STRESS-2d* and *CLEAR*. The laboratory aspects of the method and the results have been described extensively in § 3.4.4. The specific partial vertical downward attenuation coefficients of the sediment fraction are summarized in equation 3.10. In the experiments no distinction is made between the contribution of phytoplankton and that of suspended solids, but corrections for phytoplankton are made afterwards.

As phytoplankton families differ in pigment content, size, shape, etc, the specific partial attenuation coefficient of phytoplankton is very sensitive to the species composition. The specific partial attenuation coefficient of phytoplankton, expressed in  $\text{m}^2\text{-mg Chla}$ , may vary between 0.008 to 0.027 for different phytoplankton species. Kirk (1983) observed for an *Oscillatoria* population in Lough Neagh a specific partial vertical downward attenuation coefficient of 0.012-0.013  $\text{m}^2\text{-mgChla}$ . By expressing the attenuation of phytoplankton per unit chlorophyll-a, changes in phytoplankton composition may be overlooked. Therefore the attenuation of certain groups of phytoplankton species is better expressed in terms of attenuation per number of cells per volume. Unfortunately, cell number counts ( $N_{\text{Osc}}$ ) are very inaccurate (§ 3.2.2) and it was impossible to assess the value of  $k_{d,\text{Osc}}$  ( $\text{m}^2\text{-N}^{-1}$ ) from the sedimentation experiment data (§ 3.4.4). As the phytoplankton model simulates colony numbers, a value of  $k_{d,\text{Osc}}$  of  $0.045\cdot 10^{-9} \text{ m}^2\text{-colony}$  was used, as estimated by Vermij using field data of the Wolderwijd (Vermij, 1992). The specific attenuation coefficient of *O.agardhii* was estimated by linear regression between the measured vertical downward attenuation coefficient and the counted colony number of *O.agardhii* per unit of volume, for data from periods that *O.agardhii* was dominant in the lake. This value is probably not very accurate while the contribution of other components is ignored in the estimation and the counted colony number is rather inaccurate (§ 3.2.2).

In equation 5.5 the specific partial attenuation coefficients of suspended

solids fractions, back ground attenuation and phytoplankton as derived from the measurements are summarized.

$$K_d = 0.69 + 0.059 \cdot SS_1 + 0.052 \cdot SS_2 + 0.038 \cdot SS_3 + 0.021 \cdot SS_4 + 0.045 \cdot 10^{-9} \cdot N - Osc \quad (5.5)$$

The long term average contribution of the various components to the attenuation coefficient is estimated by combining the estimated specific partial attenuation coefficients with the mean concentration values. The results are presented in Table 5.2. The average estimated vertical downward attenuation coefficient of the Markermeer is  $3.9 \text{ m}^{-1}$ . The agreement between the computed value of  $3.9 \text{ m}^{-1}$  and the observed value of  $3.8 \text{ m}^{-1}$  (§ 3.2.2) is remarkable.

*Table 5.2 Average contribution of various components to the attenuation coefficient in the Markermeer*

|   | Component<br>( $\text{g} \cdot \text{m}^{-3}$ ) | $k_{d,i}$<br>( $\text{m}^2 \cdot \text{g}^{-1}$ ) | $K_{d,i}$<br>( $\text{m}^{-1}$ ) | $K_{d,i}$<br>(%) |
|---|---|---|----------------------------------|------------------|
| Chla  | 0.065 <sup>1</sup>                              | 15 <sup>3</sup>                                   | 0.98                             | 25               |
| SS <sub>1</sub>   | 20 <sup>2</sup>                                 | 0.059   | 1.18                             | 30               |
| SS <sub>2</sub>   | 13 <sup>2</sup>                                 | 0.052   | 0.68                             | 18               |
| SS <sub>3</sub>   | 5 <sup>2</sup>                                  | 0.038   | 0.19                             | 5                |
| SS <sub>4</sub>   | 7 <sup>2</sup>                                  | 0.021   | 0.15                             | 4                |
| Background  | -   | -   | 0.69                             | 18               |
| Total   | -   | -   | 3.87                             | 100              |
| <sup>1</sup> mean value at Y111 and Y112 in 1987-1989<br><sup>2</sup> mean value at Y111 and Y112 in 1987-1989, combined with observed ratio between SS <sub>1</sub> :SS <sub>2</sub> :SS <sub>3</sub> :SS <sub>4</sub> = 44:29:11:16 (§3.4.3)<br><sup>3</sup> mean value of 0.008 and 0.027 $\text{m}^2 \cdot \text{mg}^{-1}$ (Kirk, 1983) |   |   |                                  |                  |

According to the data in Table 5.2, the suspended solids cover more than 50 % of the average attenuation in the Markermeer. During storm events, this contribution will increase to 90 %. This result endorses the assumption that the light field in the Markermeer is dominated by the attenuation by suspended solids. Furthermore, the average contribution of suspended solids to the light attenuation is higher in the Markermeer than in many other lakes. In the Wolderwijd the contribution of suspended solids to the attenuation of light was estimated at 27 % and in the Veluwemeer at 33 % (Blom, 1991).

The major part of the attenuation by suspended solids in the Marker-

meer is caused by the fractions  $SS_1$  and  $SS_2$  (84 %). Hence, the average specific attenuation coefficient of the total suspended solids is about  $0.05 \text{ m}^2 \cdot \text{g}^{-1}$ . During storms this coefficient will decrease to  $0.03 \text{ m}^2 \cdot \text{g}^{-1}$ .

### 5.2.2 Depth dependency of the attenuation coefficient

The exponential decrease of the downward irradiance defines the vertical downward attenuation coefficient for PAR,  $K_d$ . In fact, the decrease of irradiance is only exponential for narrow bands of wavelengths. As some ranges are absorbed more intensely than others in the aquatic medium, the proportion of the most penetrating wavelengths of the irradiance increases with the depth. Hence, due to the changes in spectral distribution of irradiance within the aquatic medium, the vertical downward attenuation coefficient decreases with depth.

In natural waters, irradiance will not penetrate without deviation from its initial direction, but will suffer from scattering. The scattering of irradiance increases the path length of the photons. For turbid waters the average path length increases with a factor of 2 to 3 (Kirk, 1977). This amplification of the path length tends to increase with depth because the light becomes increasingly more diffuse. As the light absorption increases with an increase in path length, the attenuation coefficients will increase with depth in turbid waters.

The tendency of attenuation to increase with depth due to the scattering effect opposes the tendency of attenuation to decrease with depth due to changes in spectral distribution as described above. Kirk (1977) observed that in turbid, yellow, inland waters the attenuation of total photosynthetic available radiation closely obeyed the exponential law. The same behaviour may be expected for the Markermeer, due to its turbid character. This has been checked using the manual irradiance measurements of 1988 (§3.2.1). In some measurements a slight decrease of the vertical downward attenuation coefficient with depth was observed. Mostly this occurred at days with low values of the attenuation coefficient, but in most measurements the coefficient seemed constant with the depth. This is illustrated in Appendix 6, where a few examples of the measured exponential decrease of irradiance are presented. Thus, by using equation 5.5 in the model *CLEAR* for the computation of the available irradiance in the water column, a small error may be introduced, especially on calm days with low suspended solids contents. To assess the error made by assuming a constant vertical downward attenuation coefficient, a comparison has been made between the total irradiance in the water column as computed with a constant  $K_d$  and with the measured total irradiance. The estimated total irradiance was estimated from equation 5.6, which is the integrated form of equation 5.2.

$$E_T = \frac{E_{d,0}}{K_d} [1 - e^{(-K_d z)}] \quad (5.6)$$

$$\begin{array}{ll}
 E_T = \text{total under water irradiance} & (\mu\text{E}\cdot\text{m}^{-1}\cdot\text{s}^{-1}) \\
 E_{d,0} = \text{downward irradiance near the} & \\
 \quad \text{water surface} & (\mu\text{E}\cdot\text{m}^{-2}\cdot\text{s}^{-1})
 \end{array}$$

In Figure 5.2 results of the high frequency sampling periods of 1988 at Y111 are presented. The measured total irradiance is estimated by integration of the incidental measurements done at the 10 and 20 centimetre intervals. From this figure it is obvious that the results are very similar. The correlation coefficient is 0.99 ( $N=38$ ). The estimated total irradiance values tend to be slightly higher, but the average difference is small. Hence, the use of a constant attenuation coefficient for PAR, yields good results for the estimated total light energy in the water column.

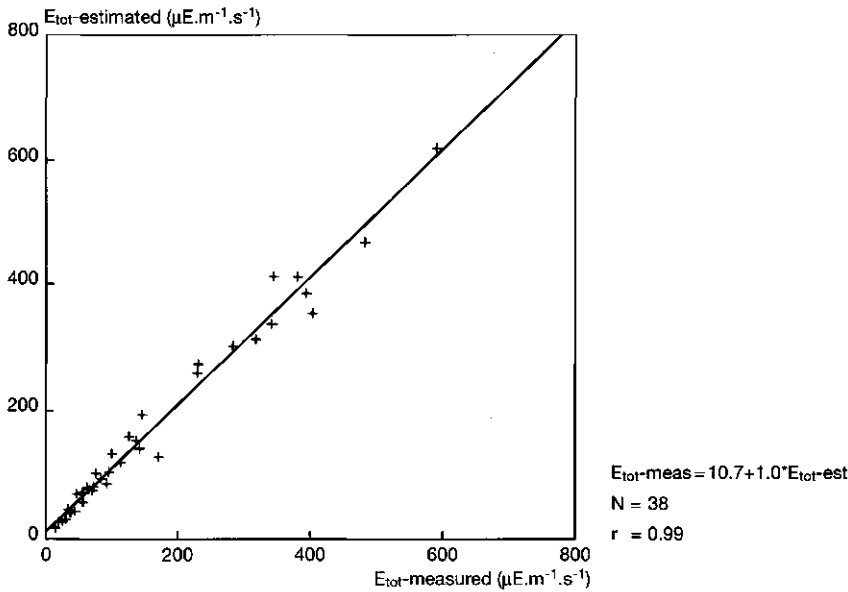


*Figure 5.2 Comparison of the estimated total irradiance using a constant  $K_d$  and the total irradiance estimated from measurements for the high frequency sampling periods of 1988 at Y111*

A very practical reason to ignore the spectral distribution effect on the attenuation coefficient, is the availability of input data for the simulation. Only the total radiation from 300 to 3000 nm is available on a regular basis (§ 3.3.5). These data are recorded at a rather distant station without any details about the spectral distribution. To account for small spectral variations within the water without specific knowledge about the spectral distribution of the irradiance itself, would be a waste of time.

Although an approximately constant value of  $K_d$  has been proven to be justified, this may not be true for other, less turbid, lakes in the IJsselmeer area. Therefore the change of the measurement method (§ 3.2.1) such that the irradiance is measured at only two depths, is beforehand not an improvement.

An additional factor related to the path length dependency is the effect of the solar elevation. As the solar altitude decreases, the path length of light travelling to a certain depth increases and thus the attenuation of light increases. On the other hand, when the sun sinks, the spectral distribution of the irradiance changes and the contribution of the red light to PAR increases. As red light is absorbed less than blue light, the attenuation coefficient may decrease when the solar altitude decreases. Again, two effects oppose each other and the remaining effect is hardly noticed. In continuous measurements, both u and n shaped variations in the attenuation coefficient during the day have been found, which may be attributed to the effects mentioned, but seemed merely caused by the measurement methods.

### 5.3 Combined Light Energy Attenuation Routine (CLEAR)

The Combined Light Energy Attenuation Routine (CLEAR) is a relatively simple model, available in FORTRAN 77 both for PC use or in combination with *STRESS-2d*. The model is developed especially for the Markermeer study (Van Duin et al, 1992).

#### 5.3.1 Model outline

In the model *CLEAR* the total incident radiation is converted to under water PAR. The vertical downward attenuation coefficient is assessed on the basis of the contributions of the suspended solids fractions and the number of *Oscillatoria agardhii* cells. Finally the total under water irradiance of PAR is estimated. The model equations are summarized in Table 5.3, including the values of the coefficients used.

Table 5.3 Summary of *CLEAR*-equations

---


$$E_d = 2.11 \cdot I_s$$

$$E_{d,0} = 0.92 \cdot E_d$$

$$K_d = 0.69 + 0.059 \cdot SS_1 + 0.052 \cdot SS_2 + 0.038 \cdot SS_3 + 0.021 \cdot SS_4 + 0.045 \cdot 10^{-9} \cdot N\text{-Osc}$$

$$E_T = \frac{E_{d,0}}{K_d} \cdot [1 - e^{(-K_d \cdot z)}]$$


---

### 5.3.2 Link with the STRESS-2d model

The link of the model *CLEAR* with the model *STRESS-2d* is simple, as suspended solids fractions calculated with the *STRESS-2d* model are used as input into *CLEAR* to assess the contribution of resuspended sediment to the vertical downward attenuation coefficient.

### 5.3.3 Validation of the light energy model

To validate the model the measured and estimated values of the vertical downward attenuation coefficient  $K_d$  are compared in Figure 5.3. The measured values of the suspended solids fractions were used to estimate the attenuation coefficient. Only the values for the high frequency sampling periods of 1989 are presented, as the suspended solids fraction analysis of 1988 is different (§ 3.4.3). As the number of complete data sets of fractions are small (§ 3.4.3) and the attenuation coefficient was not measured accurately at all days, the number of complete data sets to compare the estimated and measured attenuation coefficient is limited to twelve. The agreement between estimated and measured attenuation coefficients is very good.

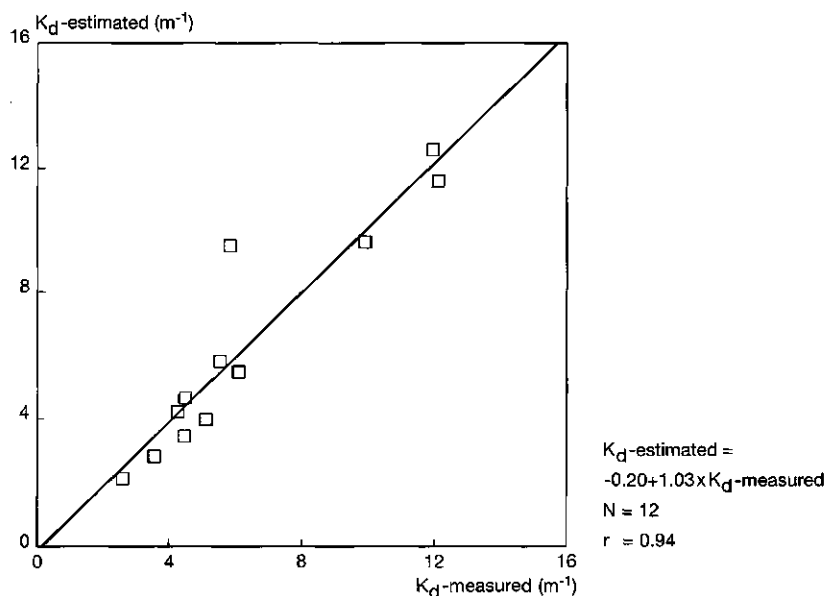


Figure 5.3 Comparison of measured and estimated values of  $K_d$  of 1989

The contribution to the attenuation coefficient of temporary blooms of other algae than *Oscillatoria agardhii* is not incorporated in the model. As the average contribution of phytoplankton to the total attenuation

coefficient is 25 %, the error in the computations may be as high as 25 %. Ignoring the contribution of other phytoplankton species than *Oscillatoria* is one of the major imperfections of the model and limits its applicability to specific case studies in the *Oscillatoria* dominated lakes of the IJsselmeer area. To implement the contribution of other species in the model is easy if cell numbers and specific attenuation coefficients are known. In the model *CLEAR* this was not done because other phytoplankton species are not incorporated in the phytoplankton model (§ 6.2).

The conversion of irradiance in the 300-3000 nm spectrum to the underwater irradiance of PAR is discussed in § 3.3.5 and produces agreeable results. The estimation of the reflection is appropriate for most hours of the day, but will be underestimated during sunrise and sunset and in the winter months (§ 5.1.1)

In the model *CLEAR*, the decrease in the attenuation coefficient with the depth, due to changes in spectral distribution, is not accounted for. Comparison of the total under water irradiance estimated from measurements and the total under water irradiance estimated from an attenuation coefficient independent of the depth, showed no significant differences. Hence, the use of an average vertical downward attenuation coefficient is justified.

## 6 Growth of *Oscillatoria agardhii*

In many lakes in the Netherlands, blooms of *Oscillatoria* species occur regularly (Hosper et al, 1980). These lakes are all shallow and eutrophic with little stratification. In lakes with *Oscillatoria* blooms transparency decreases and so did the macrophyte coverage of the lake bottom. The decrease in submerged vegetation had drastic consequences for the fish populations. Due to the diminished refuges, the pike population in these lakes declined which led to an explosive growth of prey fish. Bream, and to a lesser extent roach, are very successful in the turbid waters, with plenty of benthic organisms and little vegetation that hinder feeding (Gulati et al, 1989). Other consequences of *Oscillatoria* blooms are tainting of the fish and the formation of taste and smell compounds and toxins. Due to the nuisance of *Oscillatoria* blooms, several studies on the growth of *Oscillatoria* species have been done. Measures to overcome this phenomenon have been and are being tested, with varying success (Hosper et al, 1986; Meijer et al, 1990).

The growth of *Oscillatoria* species has been studied by the Scientific Department of Rijkswaterstaat, Directorate Flevoland (former RIJP) since 1971, when *Oscillatoria agardhii* became dominant in the lakes bordering Flevoland for the first time. These studies were conducted in order to investigate the causes of blooms of *Oscillatoria* species and to find measures to eliminate these blooms (Berger, 1987). Results of a habitat analysis of *O. agardhii* increased the insight in steering variables for the growth and blooming of *O. agardhii* (Berger, 1987; Vermij and Janissen, 1991). However, the effect of the proposed measures was always uncertain as no quantitative relationships were available. Quantitative relations obtained from laboratory experiments were difficult to translate into field conditions (Van Duin and Lijklema, 1989<sup>2</sup>; Vermij 1992).

To assess the effect of management measures two approaches may be followed, which are schematically presented in Figure 6.1:

- \* to simulate with deterministic models the effects of measures on the physical and chemical characteristics of the freshwater ecosystem and to assess whether these characteristics suit the habitat of *Oscillatoria*;
- \* to simulate the effect of measures on the growth of *Oscillatoria* with a deterministic *Oscillatoria* growth model, including the relevant physical and chemical processes affected by the measures.

The second approach varies from the first only for the biological component. Initially, the first option seemed easier to achieve and was therefore explored. However, as the assessment of quantitative limits of physical and chemical conditions in a dynamic environment for the growth of *Oscillatoria agardhii* seemed not yet feasible (Berger, 1988), the second pathway was followed as well (Vermij, 1992). Detailed relationships were studied by means of field experiments (§ 3.5).



## 6.1 Phytoplankton growth in the IJsselmeer area

The water quality of the Markermeer is closely linked to the water quality of the other lakes in the IJsselmeer area. Originally, these lakes formed one large lake. Presently, there is still a substantial exchange of water between the newly created subsystems. The development of water quality of the lakes, that would be induced by the construction of a Markerwaard, may be similar to the changes in water quality in the lakes bordering Flevoland. The algal community of these lakes is generally dominated by blooms of *Oscillatoria agardhii*. Berger (1987) stated that the habitat of *Oscillatoria agardhii* can be deduced from the characteristics of these lakes.

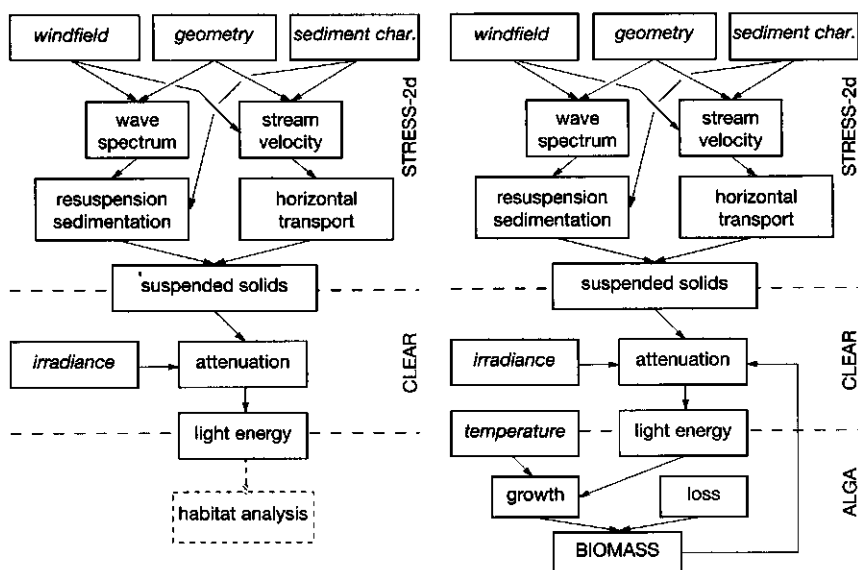


Figure 6.1 Flow chart of both path ways to assess the effect of management measures on the growth of *O. agardhii*

### 6.1.1 Phytoplankton succession in the IJsselmeer area

From 1927 to 1941 the effect on the flora and fauna in the area of the change of the brackish Zuiderzee into the freshwater IJsselmeer, was studied by the Zuiderzee-committee (De Beaufort, 1954). The first bloom of *Oscillatoria agardhii* in the IJsselmeer area is detected in the north-eastern part of the IJsselmeer in the summer of 1933, shortly after closing of the Barriërdam (§ 1.1.1). As far as known, this is also the first bloom of *O. agardhii* reported in the Netherlands (Berger, 1987). Growth of *Oscillatoria* species occurred in the IJsselmeer until 1936. From 1935 onwards blooms of *Aphanizomenon flos-aquae* were found and the

numbers of *Microcystis aeruginosa* increased (Wibaut-Isebree Moens, 1954). From 1941 till 1971, no detailed time series of the phytoplankton population in the IJsselmeer area are available. Since 1971, many surveys have been made (Berger, 1987).

In the large IJsselmeer, green algae (Chlorophyceae) in general make up more than half of the biomass, mostly *Scenedesmus* species. In spring, temporary blooms of diatoms (Bacillariophyceae) are found. Blooms of cyanobacteria often occur in late summer or autumn. Most often blooms of *M.aeruginosa* occur (1973, 1975, 1977, 1979, 1981, 1983) but also blooms of *O.agardhii* (1974, 1976, 1979, 1989), *A.flos-aquae* (1982) (Berger et al, 1986) *Oscillatoria redekeii* or *Aphanocapsa delicatissima* (Berger and Sweers, 1988) are found. In the Markermeer the same pattern, diatoms in spring and predominately green-algae during the rest of the year, is observed. Blooms of *M.aeruginosa* appeared shortly after closing the Houtribdijk (1977, 1979, 1982). Moderate blooms of *A.flos-aquae* occur occasionally (1982, 1983, 1988). In 1989 a bloom of *O.agardhii* was spotted for the first time (Vermij, 1991). The lakes bordering Flevoland (the Randmeren) suffer from virtually continuous blooms of *Oscillatoria* species since 1970 (Berger, 1987) and only intensive measures have recently improved the phytoplankton composition (Hosper et al, 1986).



Figure 6.2 *O.agardhii* filaments as seen through a microscope (250 x)

### 6.1.2 Habitat and growth characteristics of *Oscillatoria agardhii*

As the ultimate goal of the Markermeer project is to assess the effect of certain management measures on the suitability of the lake system as a habitat for growth of *Oscillatoria agardhii*, the characterization of the habitat of *O. agardhii* is of major importance for the structure and interpretation of the physical model. A characterization of this habitat has been made by Berger (1987; 1988) and Vermij and Janissen (1991). In this paragraph some of the characteristics of the habitat and of the growth of *O. agardhii* are summarized.

*Oscillatoria* species (*O. agardhii*, *O. redekeii*, *O. limnetica*, *O. rubescens*, etc.) belong to the family of the Oscillatoriaceae. *Oscillatoria* species are solitary filamentous cyanobacteria. Within the *O. agardhii* species different variants are distinguished. This study is limited to the species *O. agardhii* GOMONT. Each filament consists of a large number of cells. The length of the filaments of *O. agardhii* is extremely variable. In the IJsselmeer area the mean size usually varies between 200 and 400  $\mu\text{m}$ . The size of one single cell is rather constant: 4-6  $\mu\text{m}$  in width and 2.5-4  $\mu\text{m}$  in length (Huber-Pestalozzi, 1966). Besides the light harvesting pigments chlorophyll-a and various carotenoids, *O. agardhii* contains also c-phyco-cyanin, with its maximum absorption between 600 and 620 nm. The energy harvested by this pigment is transferred to the chlorophyll-a pigment system.

Based on growth strategies, two groups of species can be distinguished: the *r*-strategists and the *K*-strategists. The concept of *r*- and *K*-selection was introduced by MacArthur and Wilson and is based upon the logistic equation of growth, *r* being the intrinsic growth rate and *K* the upper asymptote of the hyperbolic growth curve (i.e. the point at which a resource is absolutely limiting) (Reynolds, 1984). In natural environments, there is competition both for the available space, for which rapid colonization and rapid growth as exhibited by *r*-strategists is advantageous, and for the available resources, where the ability to operate close to the environmental carrying capacity will be selecting the *K*-strategists. *r*-strategists, or the opportunists, are characterized by a short generation time, the large amount of energy they put into reproduction and their tendency to occur in unstable environments, where they respond quickly to the availability of environmental resources but cannot maintain there maximum density for long. *K*-strategists tend to grow and reproduce slowly and are able to tolerate or accommodate to periods of resource-stress. They tend to be good competitors (Reynolds, 1984; Harris, 1986). *Oscillatoria* species are considered to be *K*-strategists.

*O. agardhii* is photoautotrophic, even at very low light energy levels growth may occur (Berger, 1987). In continuous culture experiments it has been established that the relation between growth and irradiance can be divided roughly in three regions (Van Liere and Mur, 1979; Van Liere and Mur, 1980). At low irradiance growth is light limited. The light utilization efficiency  $\alpha$  (the initial slope of the productivity versus irra-

diance curve) is not constant. *O.agardhii* adapts to lower energy levels by increasing the value of  $\alpha$  per chlorophyll-a mass and increasing the c-phycocyanin/chlorophyll-a ratio (Post et al, 1985<sup>1</sup>; Post et al, 1985<sup>2</sup>).  $\mu_{\max}$ , the maximal photosynthetic productivity in the optimal energy region, is influenced by the temperature of the environment. This is attributed to the influence of temperature on the rate of the photosynthetic electron transfer (Post et al, 1985<sup>1</sup>). In the third and highest energy range, above  $85 \mu\text{E}\cdot\text{m}^{-2}\cdot\text{s}^{-1}$ , the growth rate of *O.agardhii* is photo-inhibited (Van Liere, 1979). These observations indicate that *O.agardhii* essentially adapts as a shade-plant that is particularly favoured by conditions of low irradiance and short day length. This phenomenon may contribute to the absence of *O.agardhii* in shallow, transparent lakes (Vermij and Janissen, 1991). The inhibition is less pronounced for high irradiance periods with a short duration or when nutrient levels or temperature are high (Berger et al, 1986). From experiments in continuous growth cultures, where *O.agardhii* was grown with a periodic supply of light energy, it was deduced that the pigment content increased with shorter light periods as did the growth yield on carbon and the dark growth yield (Post et al, 1985<sup>2</sup>).

Phytoplankton cells in lakes are not only exposed to a changing irradiance by the diurnal light-dark rhythm, but to other variations in light regimes as well. The relationships between photosynthetic responses and light are influenced by the time scale of the change in the light field. Falkowski (1984) distinguished a number of physiological responses to variations in the light regime:

|                   |  |
|-------------------|--|
| flicker effect    | these are fluctuations in light intensities with periods in the order of 0.1 s. Photosynthesis is sometimes increased and sometimes decreased by this effect. The overall effect on primary production is probably limited;  |
| turbulent mixing  | the time scale of fluctuations caused by turbulent mixing is highly variable and little is known about its effect on photosynthesis;   |
| state transitions | are brought about by the alternate phosphorylation and dephosphorylation of light harvesting chlorophyll-a protein complexes and they may last from seconds to minutes. State transitions are frequently studied under laboratory conditions but few studies have been made in natural phytoplankton communities or in cultures under natural light regimes;   |
| diurnal changes   | on time scales of a few hours to a few days, phytoplankton may adjust their physiological responses to low-frequency variations in irradiance. They include variations in the amounts and ratios of photosynthetic pigments, changes in photosynthetic responses, gross chemical composition, cell volume, respiration, etcetera. It may be due to negative feedback of photosynthesis by end product inhibition, changes in cellular chlorophyll content, |

|                  |   |
|------------------|---|
|                  | photorespiration, etcetera, and has potentially more influence on photosynthesis at high light intensities;       |
| photo-inhibition | photo inhibition is time dependent but careful kinetic analysis of the phenomenon are scarce;                     |
| respiration      | the occurrence of irradiance dependent respiration is observed, but little quantitative information is available. |

All processes have their own periodicity and interact in their influence on the growth of *O.agardhii*. Unfortunately quantitative knowledge about these processes and variations in light field are limited.

The conversion of photosynthetically fixed carbon into growth is particularly efficient at low irradiance levels, while the energy requirements for maintenance seem remarkably low. All combinations of light energy and light period that lead to a low daily irradiance favour the growth of *O.agardhii* over green algae (Van Liere and Mur, 1980, Foy and Smith, 1980). From competition experiments with *O.agardhii* and *Scenedesmus protuberans* it was concluded that low light conditions favour the dominance of *O.agardhii* due to its lower maintenance requirement (Mur et al, 1978). However, at light limiting conditions when loss rates are more or less equal, the *Scenedesmus* species grow faster than *O.agardhii* (Loogman, 1982). Hence, the low maintenance energy of *O.agardhii* is essential for the success of the species. From the patterns of adaptation to changes in light energy and temperature it may be concluded that these factors provide the basis for the survival of *O.agardhii* populations during the winter season, yielding a favourable position of *O.agardhii* at the start of the growing season (Post et al, 1985<sup>1</sup>). This may explain the observed phenomenon that lakes, once they have become dominated by *O.agardhii* for the first time, seem to be more subject to subsequent *O.agardhii* blooms than lakes in which no *O.agardhii* blooms did occur before. As *O.agardhii* grows rather slowly and the initial concentration seems important for its success during the summer season, the residence time of the water and the concentration of *O.agardhii* in the incoming water are very important for the occurrence of blooms. The importance of the long residence time was the starting point of some effective measures against *O.agardhii* blooming in the Netherlands (Hosper et al, 1986), which involved flushing.

*O.agardhii* is able to regulate its buoyancy with gas vacuoles. The sedimentation rate of algae depends on the density, size and shape of the organism and the density and viscosity of the water (Stokes' law, § 4.1.1). Both the size and the density differences are to some extent subject to adaptation of the filaments. The buoyancy regulation of *O.agardhii* becomes advantageous compared with green algae and diatoms when mixing consistently extends beyond the penetration depth of saturating irradiance (Reynolds et al, 1987) or when mixing is limited and sedimentation can be prevented by buoyancy regulation only (Vermij, 1992). In the fall velocity experiments (§ 3.4.3), in general *O.agardhii* filaments were observed not to settle but remained floating.

Loss of *O.agardhii* by grazing by zooplankton is very limited as filaments exceeding 100  $\mu\text{m}$  are virtually immune to ingestion (Reynolds, 1984).

*O.agardhii* has no nitrogen fixing capacities but may use ammonium, nitrate and ureum as nitrogen source. Although *O.agardhii* is usually found in very eutrophic lakes, it is able to achieve maximal growth rates at relatively low nutrient availabilities (Van Liere, 1979), which enables the species to inhabit waters with a wide range of trophic status (Reynolds, 1984).

In summary: the characteristics of *O.agardhii*, which are considered important for its occurrence, are: the low energy requirement for maintenance, the occurrence of photo-inhibition at high energy levels, the capability to adapt to low energy levels, the low specific growth rate, its high affinity for nitrogen and phosphorus, its small sedimentation losses and low predation pressure by zooplankton. Therefore *O.agardhii* lakes are characterized by long residence times, high turbidity and a high eutrophic level (Berger, 1987), but the high eutrophic level is more important in relation to the turbidity than to the actual available nutrient concentrations.

#### 6.1.3 Characteristics of the Markermeer in relation to growth of *Oscillatoria agardhii*

The Markermeer is a shallow eutrophic lake with a high turbidity and long residence times (Chapter 2). With this characterization the lake seems suitable for excessive growth of *Oscillatoria agardhii*. However, growth of *O.agardhii* in the lake happens only occasionally and blooms occur only temporarily and locally (Berger et al, 1986; Vermij and Janissen, 1991). The absence of significant growth of *O.agardhii* are imputed especially to the frequent fluctuations in the turbidity (Berger et al, 1986). Although *O.agardhii* is able to adapt to different light energy levels and fluctuations (§ 6.1.2), the adaptation is slow and not efficient when the variability is high.

In the Markermeer, the phytoplankton population is characterized by green algae and diatoms in spring. In the summer, the growth of cyanobacteria may increase, but the population is never dominated by *O.agardhii* and phytoplankton cell numbers remain low (Vermij, 1991). Temporarily the biomass may increase by wind induced resuspension of settled phytoplankton. This has been deduced from the high correlation between the chlorophyll-a content and the inorganic solids content in the field data (Figure 3.3). After settling into the sediment top layer, the plankton is subject to the resuspension processes as described in Chapter 4. After resuspension in the water, this plankton may participate again in the production process, if still alive. The influence of sedimentation and resuspension may be large on the biomass of phytoplankton in the Markermeer (Mur et al, 1990), but will be less for algae with a strong buoyancy regulation as *O.agardhii*, compared to green algae.

Jagtman and Van Urk (1988) stated that variations in the algal biomass in the water column of the Markermeer are mainly caused by resuspension of algae present in the bottom of the lake, instead of growth of algae in the water column itself. Their conclusion was mainly based on the linear relation they found between inorganic solids (SS-AFDW) and chlorophyll-a concentration at Y111 with data of 1985. However, their data set was not representative for the Markermeer in general; all chlorophyll-a concentrations were below  $100 \text{ mg} \cdot \text{m}^{-3}$ , whereas in 1987, 1988 and 1989 at Y111 at least 17% of the measured chlorophyll-a concentrations was higher than  $100 \text{ mg} \cdot \text{m}^{-3}$ . Although there is indeed a significant relation between the chlorophyll-a content and the inorganic content, the ratio between chlorophyll-a and suspended solids concentration tends to decrease when the suspended solids concentrations increase. This is illustrated in Figure 6.3. When no sediment is resuspended, the biomass concentrations can become relatively high due to production. The dramatic decrease between 0 and  $20 \text{ g} \cdot \text{m}^{-3}$  is caused by the resuspension of sediment with a lower average chlorophyll-a content than found in the suspended solids which are continuously present in the water phase. So at low turbidity growth also contributes to the algal biomass.

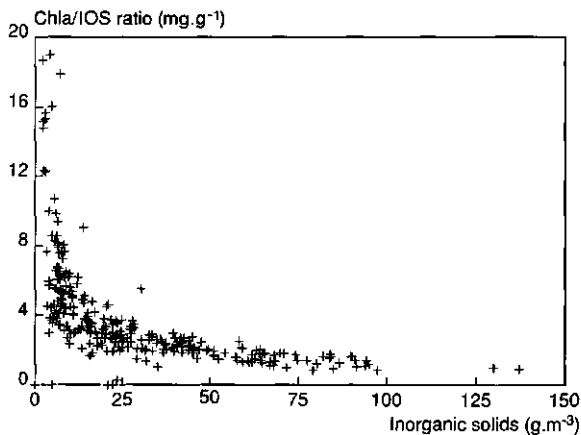


Figure 6.3 Chlorophyll-a/inorganic solids ratio versus the inorganic solids content at Y111 in 1987, 1988 and 1989

Occasionally, very low nutrient concentrations occur in the Markermeer, but nutrient limited growth of phytoplankton will not occur often. Mur et al (1990) considered the occurrence of nutrient limited growth in the Markermeer not likely for 1987 and 1988. They found very high growth rates during the summer season, but no relationship between the light field at 1 metre depth and the growth rate. They assumed that the phytoplankton in the sediment top layer adapted to the light limitation by increasing its light utilization efficiency. After resuspension of these

algae in the water, the growth rate of these algae will be high, even when the turbidity of the water is high.

As the adaptation rate and the growth rate of *O.agardhii* is lower than that of green algae, the absence of persistent *O.agardhii* blooms in the Markermeer is attributed to the very high and fluctuating turbidity. Hence, quantitative information on the extent of this turbidity and on the fluctuations in turbidity and insight in the effect of management measures on the turbidity are needed. To determine the effect of changes in the mean turbidity level and in the variations of the turbidity on the growth of *O.agardhii*, more knowledge is needed on the specific relations between turbidity variations, and the adaptation to these variations of the growth rates of *O.agardhii*.

#### 6.1.4 Field experiments

The ratio of the gross primary production and the sum of losses by respiration, the loss rate by mortality and nett sedimentation of organisms under specific environmental conditions, determines whether the biomass of these organisms increases or decreases. The large number of factors which operate simultaneously in nature, makes it very difficult to design and perform well defined representative experiments. Thus the relationship between theory and experiment in ecology is much less well defined than in many other sciences (Harris, 1986). The specific reaction of organisms on environmental conditions such as available light energy, changes in light-dark regime, temperature and nutrient concentration have been studied in laboratory experiments frequently (Van Liere and Mur, 1979; Loogman, 1982; Post et al, 1985<sup>1</sup>). From these studies relationships have been derived between growth rates and physical environmental factors. However, the translation of these relationships to quantitative relationships for field conditions, where all environmental factors vary, is complex (Van Duin and Lijklema, 1989). Furthermore it is often difficult to simulate physical factors like the under water light field in detail under laboratory conditions. Hence, field primary production measurements are often used to assess these relationships (Vollenweider, 1974; Berger, 1987).

After the habitat analysis of *Oscillatoria agardhii* in the IJsselmeer area (Berger, 1987) a few questions concerning the suitability of the Markermeer as a habitat, remained unanswered:

- 1 Is the under water light field in the long run really the limiting factor for the growth of *O.agardhii*, or is the absence of blooms of *O.agardhii* merely a matter of time (§ 6.2);
- 2 Is the growth of *O.agardhii* in the Markermeer possible for short periods and how is this related to the under water light field;
- 3 What is the maximal depth for growth of *O.agardhii* under different light conditions;
- 4 What is the influence of vertically mixing on the growth of *O.agardhii*;



- 5 What is the maximal production of *O.agardhii* for different light fields;
- 6 How fast do growth parameters of *O.agardhii* adapt to changes in the light field.

In order to answer these interrelated questions, experimental methods have been designed that can be carried out in the Markermeer itself, to ensure realistic light field conditions. The rotating light and dark bottle experiments are modifications of the well known light and dark bottle experiments (Vollenweider, 1974). The perspex cylinder experiments were newly designed for the Markermeer study. The general lay-out and procedures for the experiments are described in § 3.5.

Phytoplankton biomass can be measured as either filament numbers, filament length, chlorophyll-a content or ash free dry weight. Theoretically, the most accurate measure of phytoplankton quantity is produced by a combination of filament number and length, but due to the errors in the phytoplankton counts (Vermij and Janissen, 1991) filament counts have an indicative value of phytoplankton quantity only. Chlorophyll-a content is a good measure of living phytoplankton and plant tissue, but makes no distinction between various phytoplankton families or macrophytes. Another disadvantage of the chlorophyll-a content as a measure of biomass, is that the chlorophyll-a/cell biomass ratio is not only different for different phytoplankton families, but varies in time for a single species, due to adaptations to changes in the light field. Hence, to study the adaptation to changes in the light field, chlorophyll-a is not an objective measure for biomass. Ash free dry weight may be used as a measure for phytoplankton biomass, but is does not discriminate between phytoplankton, zooplankton, macrophytes, detritus, etc. In the designed field experiments, the enclosures are filled with *O.agardhii* suspensions of 95% or more. Hence, for the interpretation of these experiments, the biomass measure does not need to distinguish between phytoplankton families. Considering the pros and cons, chlorophyll-a seemed the biomass measure with the least disadvantages for these experiments and is generally used in this chapter. The chlorophyll-a/ash-free-dry-weight ratio was reasonably constant for the *O.agardhii* suspensions used in both years (Figure 6.4). In 1989 the estimated ratio was  $0.0065 \text{ gChla:gAFDW}^{-1}$  and in 1990  $0.0069 \text{ gChla:gAFDW}^{-1}$ . The average ratio for the two years is  $0.0068 \text{ gChla:gAFDW}^{-1}$  with a standard deviation of 0.0020.

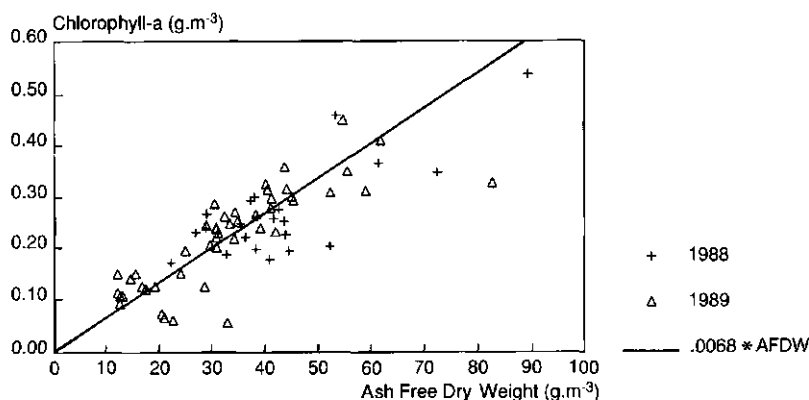


Figure 6.4 Chlorophyll-a concentration versus the ash free dry weight content of the *O. agardhii* suspensions used in 1989 and 1990

As light and dark bottle experiments can be conducted for short periods only, results of these experiments produce insight in questions 2, 3, 4 and 5 only. However they yield some additional information on growth and respiration parameters.

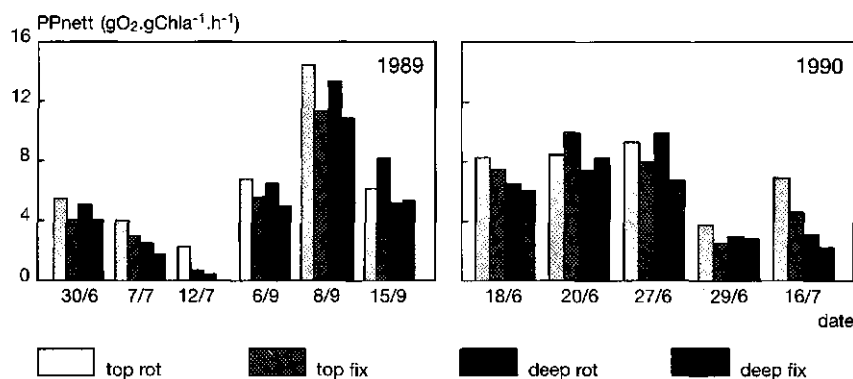


Figure 6.5 Mean nett production of the bottle experiments

The results of the bottle experiments are summarized in Tables 3.7 and 3.8. In Figure 6.5, the measured nett production averaged over the depth for both years are presented. Differences in production vary much more between days than differences in production between fixed and rotating bottles. In the experiments of 1989 the production rates in September are higher than those in July. In Figure 6.6 the gross production averaged over the depth of the rotating bottles is plotted versus the gross production over the depth of the fixed bottles for both years. Small differences between fixed and rotating bottles are observed and gene-

rally rotation of the bottles tends to enhance the production. However, as the accuracy and the number of the measurements is small and the differences between the values is small more data are needed to formulate significant relationships between rotation and production.

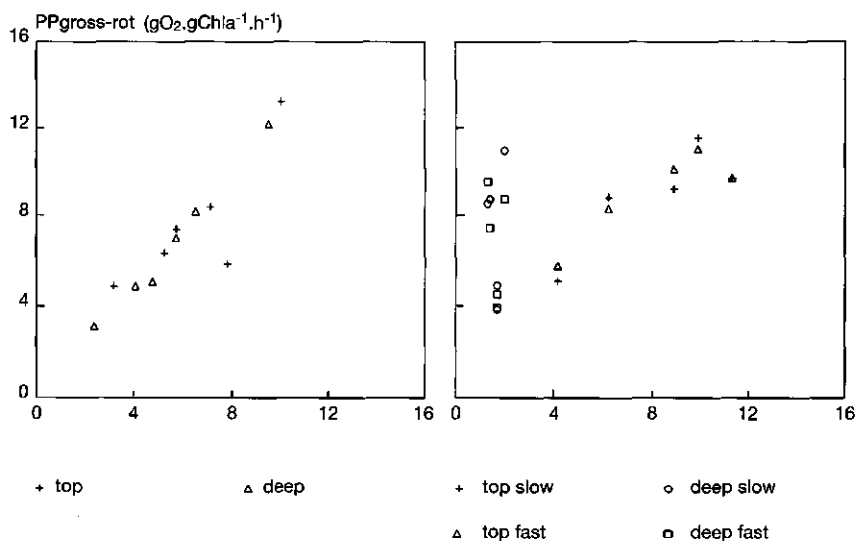


Figure 6.6 Mean gross production of the rotating bottles versus that of the fixed bottles for 1989 and 1990

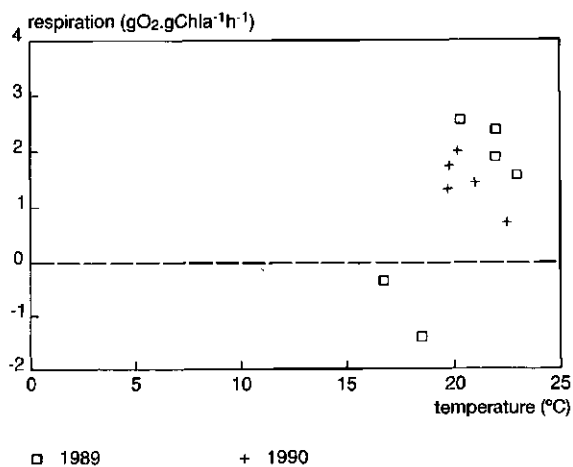


Figure 6.7 Respiration versus the temperature in the bottles experiments of 1989 and 1990

One of the most puzzling results of the experiments are the negative respiration values during two of the experiments in 1989. Negative respiration values means oxygen production in the dark bottles. Because the respiration is measured in 6 bottles, the increase in oxygen concentration was found in all six bottles and the procedure followed was the same as on the other measuring days, experimental errors are probably not the cause of this phenomenon. The negative respiration values are found in the experiments with a duration of less than two hours; 8-9-'89 and 15-9-'89. However, the duration of the respiration experiment of 6-9-'89 is just as short, without resulting in negative respiration values. In Figure 6.7 the relation between the respiration and the temperature is represented. The temperature was the lowest for the experiments with the negative respiration values, but no distinct relationship between the respiration and the temperature has been found, although this was expected (§ 6.2). Oxygen production in dark bottles has been reported by others as well (Nor, 1991; Pamatmat, 1988; Pennak, 1978) but no satisfactory explanation has been given thus far.

In Figure 6.8, the gross production versus the downward irradiance at the measuring depth is plotted, with a sketched line connecting the data of one day. At low irradiance values an increase in production is found with an increase in irradiance, but beyond a certain value a further increase tends to result in reduced production rates (inhibition). However, the magnitude of the transition value beyond which inhibition begins, differs from day to day. Production models for the simulation of the experiments are presented in § 6.2.

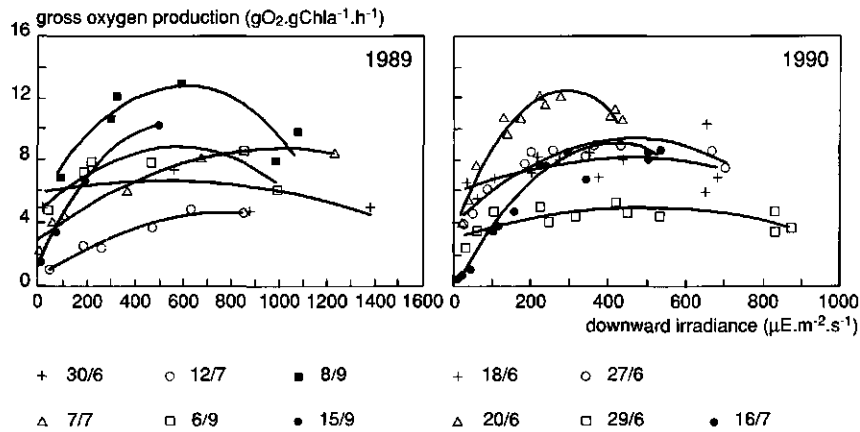


Figure 6.8 Gross production versus downward irradiance at depth *z* of the bottle experiments of 1989 and 1990

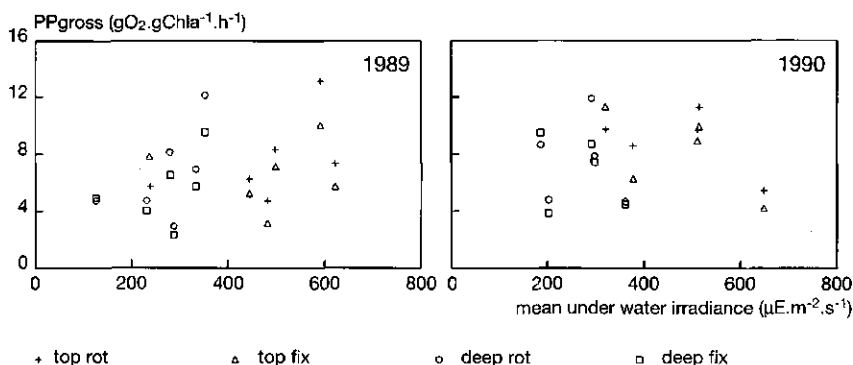


Figure 6.9 Mean gross production versus the mean under water irradiance of the bottle experiments of 1988 and 1989

In Figure 6.9 the relation between the mean gross production (averaged over the depth) and the mean under water irradiance (§ 5.3) is presented. No distinct overall relationship between the gross primary production and the total under water irradiance can be determined. This may be due to adaptation or inhibition or the inadequacy of chlorophyll-a to express the active cell material.

From the experiments some preliminary conclusions can be drawn. To judge these conclusions on their merits, some shortcomings of the experiments should be realized:

- \* all experiments were conducted on days with only small wave action. Hence the turbidity during the experiments was always low;
- \* experiments were done for short periods only (hours) around noon, when the irradiance is relatively high;
- \* the physical condition of the algae will be affected by the extensive manipulation and the preservation in the big basin aboard the ship or in the laboratory room.

Summarizing the results leads to the following conclusions:

- \* as the nett production measured in the bottles is always positive, growth of *O.agardhii* is possible for periods of hours under the light conditions of the Markermeer on all test days (question 2);
- \* no lower limit of the total irradiance for the growth of *O.agardhii* can be deduced from the experiments. The relationship between the production per unit chlorophyll-a and the available irradiance varies very much from day to day (questions 2 and 3);
- \* though some effect of vertical mixing on the growth of *O.agardhii* is found, no conclusive evidence for an increase or decrease of production has been found (question 4);
- \* the maximum gross production ( $P_{\text{max}}$ ) that has been measured lies in the range of  $14 \text{ gO}_2 \cdot \text{gChla}^{-1} \cdot \text{h}^{-1}$ , but the relationship with the light field is not unequivocal (question 5).

The estimated nett oxygen production per unit chlorophyll-a in the cylinder for both years is represented in Figure 6.10. During the period 89-2, the algae were transported through the upper metre of the cylinder only, whereas during the periods 89-3, 90-1 and 90-2 they were mixed through the entire length of the cylinder (§ 3.5.3). The temperature was slightly higher in the period 89-2 than in the other periods. Still, the maximum production rates of 89-2 and 89-3 are similar.

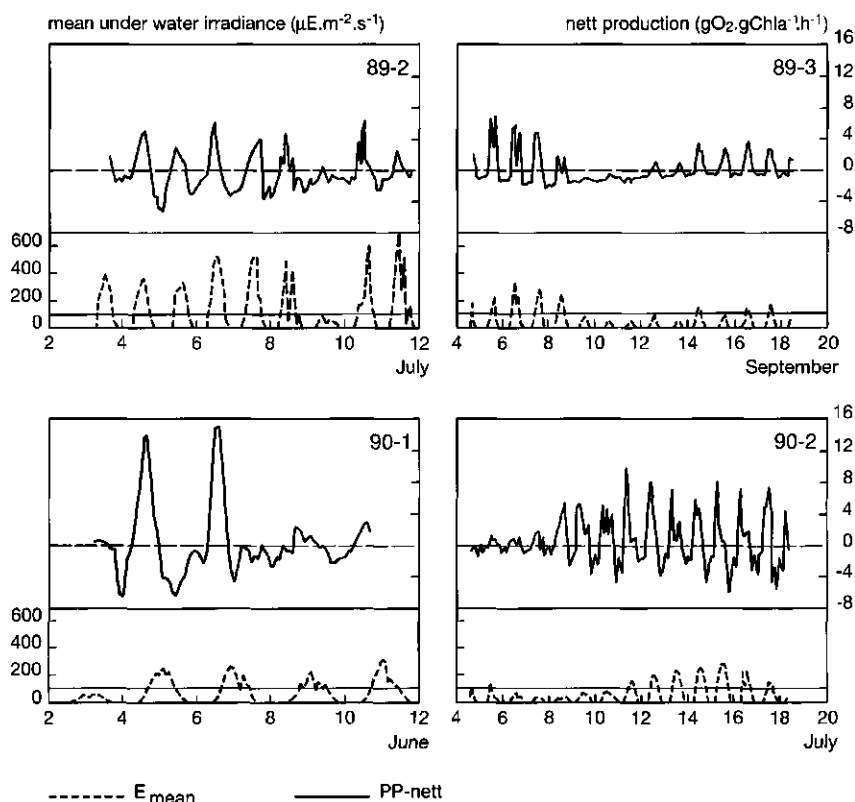


Figure 6.10 Measured nett production per unit chlorophyll-a and the mean under water irradiance in the cylinder in 1989 and 1990

The total under water irradiance (§ 5.2.2) at Y112 is comparable for all periods (Appendix 5), but the mean under water irradiance for the *O. agardhii* suspension in the cylinder is slightly higher for period 89-2, as the suspension is only rotated through the upper metre of the cylinder during this period. Figure 6.10 reveals that no nett production occurs at mean under water irradiance values of  $100 \mu\text{E}\cdot\text{m}^{-2}\cdot\text{s}^{-1}$  or less (July 9, September 9-11, 1989 and July 5-6, 1990), but that after prolonged

periods of low maximum irradiance values ( $> 2$  days), the production efficiency increases and the nett production may become positive even at a mean under water irradiance value of less than  $100 \mu\text{E}\cdot\text{m}^{-2}\cdot\text{s}^{-1}$  (September 12-13, 1989 and July 8-10, 1990). Hence, adaptation to low maximum energy levels does occur within a few days. This is referred to as slow adaptation.

The respiration in the cylinder at night is estimated as the average of the nett production values between two hours after sunset until two hours before sunrise. The relationship between the thus measured mean respiration rate and the temperature at night is presented in Figure 6.11. For the experiments of 1989 an increase in temperature tends to lead to an increase in respiration rate. For 1990, this tendency is less pronounced and some data seem rather out of range.

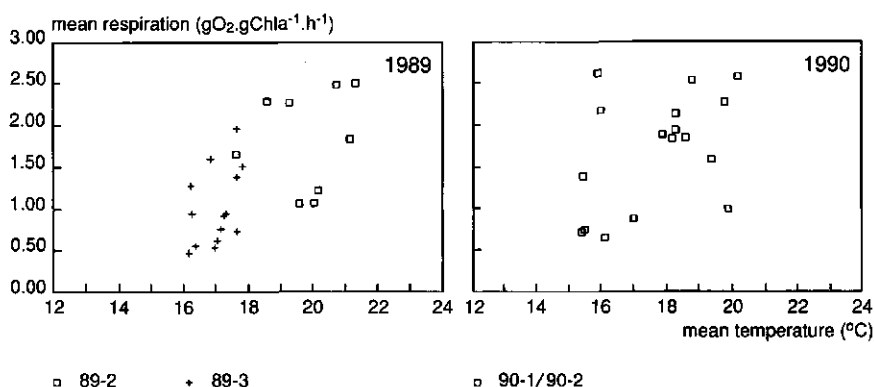


Figure 6.11 Mean respiration at night versus the mean temperature at night in the cylinder in 1989 and 1990

The respiration is assumed to be constant for each measurement day and is estimated as the mean of the average respiration of the previous and the following night. The gross production per hour is estimated as the sum of the nett production per hour and the mean respiration. Because the mean respiration is used and not the maximum measured decrease in oxygen, negative production values may occur at night.

In Figure 6.12, the relationship between the gross production rate and the mean under water irradiance is represented. For all periods the shape of the production curve is hard to distinguish and no significant patterns are observed. Differences in Pmax within each period can not be attributed to changes in the temperature as the temperature during each period is rather uniform.

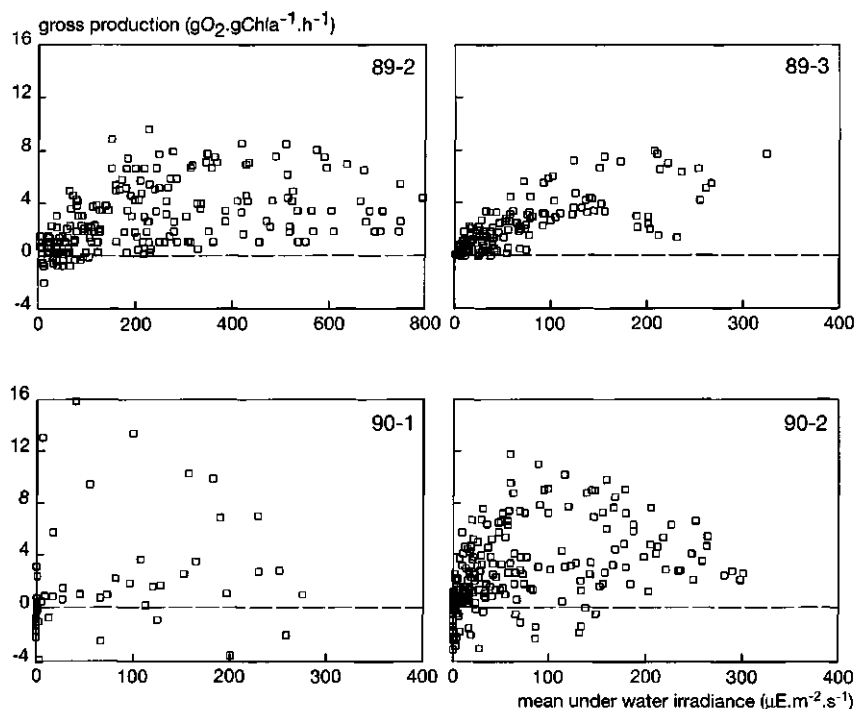


Figure 6.12 Estimated gross production per unit chlorophyll-a in the cylinder versus the mean under water irradiance

To assess the effect of adaptation of growth parameters of *O. agardhii* to the light field within hours, production data were studied in more detail (Appendix 8). From both years together, 30 days were selected with data sets that were not or hardly interfered by cylinder maintenance or malfunctioning problems. For each day, the gross production per hour is related to the total under water irradiance for that hour. If adaptation of growth parameters to available energy occurs within hours, production will be more efficient during hours with increasing irradiance (morning) than during hours with decreasing irradiance (afternoon), i.e. a hysteresis effect. Each day has been judged on the occurrence of this phenomenon. Based on an estimation of the accuracy of the production values, a threshold value of  $2 \text{ gO}_2 \cdot \text{gChla}^{-1} \cdot \text{h}^{-1}$  is defined. If the gross production in the morning was more than  $2 \text{ gO}_2 \cdot \text{gChla}^{-1} \cdot \text{h}^{-1}$  larger than the gross production in the evening, that particular day was labelled to the category on which adaptation of growth parameters occurred ( $\text{PP}_{\text{increase}} > \text{PP}_{\text{decrease}}$ ). If a data set was not conclusive, it is added to  $\text{PP}_{\text{increase}} \approx \text{PP}_{\text{decrease}}$ . The results are presented in Table 6.1. The expected hysteresis is observed in 14 of the 30 daily sets, the reverse is never observed. From the 16 data sets without conclusive adaptation, mean under water irradiance values stayed well below  $200 \mu\text{E} \cdot \text{m}^{-2} \cdot \text{s}^{-1}$  for 12 days (75%). From the data sets with adaptation, during only 3 out of



the 14 days mean under water irradiance values stayed below  $200 \mu\text{E}\cdot\text{m}^{-2}\cdot\text{s}^{-1}$  (21%). Hence, it may be concluded that in general adaptation of growth parameters of *O.agardhii* to the under water light field is observed for days with maximum mean under water irradiance values over  $200 \mu\text{E}\cdot\text{m}^{-2}\cdot\text{s}^{-1}$ . At days with maximum values below  $200 \mu\text{E}\cdot\text{m}^{-2}\cdot\text{s}^{-1}$ , adaptation usually does not occur or is imperceptible. The hysteresis effect is referred to as fast adaptation. The occurrence of hysteresis may be either due to diurnal changes or photo-inhibition (§ 6.1.2). In the latter, the representation of the nett primary production instead of the gross primary production in the curves of Appendix 8, would have been preferable. However, for the objectives of this study, the precise physiological cause for the fast adaptation is less important than the quantification of the light field causing the adaptation.

**Table 6.1** Experimental days with and without hysteresis

| PP <sub>increase</sub> > PP <sub>decrease</sub> |                   | PP <sub>increase</sub> ≈ PP <sub>decrease</sub> |                   |
|---|-------------------|---|-------------------|
| date  | E <sub>mean</sub> | date  | E <sub>mean</sub> |
| July 6, 1989                                    | 800               | July 11, 1989                                   | 708               |
| July 8, 1989                                    | 640               | September 5, 1989                               | 210               |
| July 10, 1989                                   | 747               | September 8, 1989                               | 229               |
| September 6, 1989                               | 323               | September 9, 1989                               | 74                |
| September 7, 1989                               | 266               | September 10, 1989                              | 39                |
| June 27, 1990                                   | 276               | September 11, 1989                              | 43                |
| July 8, 1990                                    | 28                | September 13, 1989                              | 77                |
| July 9, 1990                                    | 70                | September 14, 1989                              | 136               |
| July 12, 1990                                   | 206               | September 15, 1989                              | 93                |
| July 13, 1990                                   | 253               | September 16, 1989                              | 142               |
| July 14, 1990                                   | 264               | September 17, 1989                              | 155               |
| July 15, 1990                                   | 300               | June 28, 1990                                   | 252               |
| July 16, 1990                                   | 238               | July 5, 1990                                    | 132               |
| July 17, 1990                                   | 167               | July 6, 1990                                    | 65                |
|   |                   | July 7, 1990                                    | 34                |
|   |                   | July 10, 1990                                   | 76                |

Summarizing the results leads to the following conclusions:

- \* growth of *O.agardhii* for periods of weeks is possible in the Markermeer, at least for the characteristic light field of the summer months (question 2);
- \* a mixing depth of 2.8 metres is not prohibitive for growth of *O.agardhii* during days with maximum total under water irradiance values >  $200 \mu\text{E}\cdot\text{m}^{-2}\cdot\text{s}^{-1}$  (question 4);
- \* the maximum gross production rate for *O.agardhii* is in the range of  $12 - 14 \text{ gO}_2\cdot\text{gChla}^{-1}\cdot\text{h}^{-1}$  for temperatures around 20 °C, maximum respiration rates of  $2.5 \text{ gO}_2\cdot\text{gChla}^{-1}\cdot\text{h}^{-1}$  are found for the same temperatures (question 5);

- \* adaptation of growth parameters to low irradiance levels (mean under water irradiance  $< 100 \mu\text{E}\cdot\text{m}^{-2}\cdot\text{s}^{-1}$ ) occurs within a few days, this is referred to as slow adaptation (question 6);
- \* during dark periods (night) growth parameters adapt to low light conditions. During days with high maximum mean under water irradiance values ( $> 200 \mu\text{E}\cdot\text{m}^{-2}\cdot\text{s}^{-1}$ ) growth parameters of *O. agardhii* usually adapt in a few hours to high light conditions, this is referred to as fast adaptation. During days with lower maximum values, growth parameters tend to keep their high efficiency (question 6);
- \* though the experiments produced valuable information about the growth characteristics of *O. agardhii* under the light conditions of the Markermeer, the experiments were not conclusive whether or not the light field of the Markermeer is the limiting factor for the growth of *O. agardhii* in the long run.

These conclusions were based on experiments, with the following short comings:

- \* the physical condition of the algae will be affected by the extensive manipulation and the preservation in the big basin aboard the ship or in the laboratory room;
- \* Production and respiration rates are all expressing  $\text{O}_2$  per unit chlorophyll-a, but the chlorophyll-a content of the phytoplankton cells itself will be affected by the experiments;
- \* the light field inside the cylinder will be different from that in the lake itself, by influence of the perspex wall, differences in  $K_d$  inside and outside the cylinder and by growth of organisms on the cylinder wall. In the estimation of the under water irradiance, these effects are not accounted for.

## 6.2 Modelling the growth of *Oscillatoria agardhii*

In ecological theory, two fundamentally different concepts are distinguished: the **equilibrium** and the **non-equilibrium** theory. The acceptance of either one has major consequences for the interpretation of data and the development of the *Oscillatoria agardhii* model. A clear comparison between both models is presented by Harris (1986), and is summarized in the next subsection.

The equilibrium theory originates from nineteenth century naturalists like Darwin. In this theory it is assumed that species are in equilibrium with their environment and with other species present. In stable environments, population size and community structure depend upon population growth, competition and co-evolution. The equilibrium theory implies the following limiting assumptions:

- \* the population-environment system is in equilibrium;
- \* at least some resources are constantly limiting;
- \* the environment is fully occupied or saturated with species;
- \* the optimum is always the same in time;
- \* the theoretical optimum is always attainable;

- \* founder effects are not important

- \* and there is no effect from the past history of the population.

This led to the definition of the Gause axiom: one species- one niche. Hence, species must use the environment differently in order to coexist and the number of coexisting species is equal or less than the number of resources. The equilibrium theory views the world in terms of closed systems, where interactions take place in 'closed boxes' in equilibrium. Thus there is no concept of history or time and no migration or disposal. However, natural environments are not constant in time and the interactions between the environmental fluctuations and the ability of various species to cope with and to adapt to these fluctuations will determine the size of the population. This is the essence for the non-equilibrium theory. According to this theory it is possible that environmental patchiness occurs and patches may open and close faster than the species can migrate from one to the other. Non-equilibrium systems in ecology are assumed to be characterized by the following properties:

- \* environmental fluctuations;

- \* high mortality;

- \* lack of competition;

- \* absence of limiting resources;

- \* environments not saturated with species;

- \* adaptive optima that change with time;

- \* the presence of founder effects

- \* and a strong historical component.

A non-equilibrium model requires that environmental disturbances occur with sufficient frequency to disrupt the course of competitive exclusion. Hence, time is an explicit component. Furthermore, the environmental fluctuations themselves become a resource and thus characterization of the fluctuations is as important as the average magnitude of a resource. The contrast between equilibrium and non-equilibrium theory is summarized by the question whether a given community structure is the way it is because of present day (proximate) events like competition, or due to evolutionary (ultimate) causes that occurred in the distant past. The distinction between proximate and ultimate causes lies in the inevitable temporal component which pervades all ecological processes. Both models give extreme points of view and it is most likely that any given species may be limited by environmental factors at one time and by competition at others.

In this study, the modelling of the occurrence of *Oscillatoria agardhii* is based on the non-equilibrium concept, because from earlier studies on the growth of *O. agardhii* in the IJsselmeer area (Berger, 1987; Vermij and Janissen, 1991) it was deduced that competitive exclusion is not important for the development of *O. agardhii* dominance in the area (Vermij, 1992), even though *O. agardhii* is defined as a *K*-strategist. In general, in highly disturbed environments *r*-strategists should be favoured, but the presence of *K*-strategists does not necessarily imply equilibrium conditions. Vermij (1992) concluded that *O. agardhii* dominance in the IJsselmeer area occur in summer due to the increasing loss rates of green algae and diatoms caused by the changing weather

conditions. Sedimentation rates increase at the generally lower wind speeds and mortality increases by grazing. Thus the observed succession is the consequence of the environmental fluctuations and not of competition for light or nutrients between *O.agardhii* and other algae.

If the ecological system of the Markermeer is not in equilibrium, the occurrence of algae is mainly due to the suitability of the lake as a habitat and is not dependent on the occurrence of other phytoplankton species. If the Markermeer is not in equilibrium yet, this does not imply that this will never occur in future. In the final steady state *O.agardhii* may be the dominant phytoplankton species. This might be deduced from the fact that *O.agardhii* was not dominant in the Randmeren until 1971. After the first year of blooming, the bloom became persistent, suggesting the importance of the historical component. The temporary blooming of *O.agardhii* in 1989 may have been the first sign of this process in the Markermeer.

In models based on the equilibrium theory, competition is the dominant process, leading to the modelling of complex and partly unknown relationships between species. In models based on non-equilibrium concepts, the model structure becomes more complicated as time scales and environmental fluctuations have to be incorporated. Assuming a changing situation in a non-equilibrium state, other algal species do not have to be modelled, but the growth model itself is much more difficult. Besides, the calibration of the model on other lakes is objectionable because the presence of founder effects and the historical component are difficult, if not impossible, to compare. In subsequent paragraphs the development and application of models based on the non-equilibrium concept will be discussed.

#### 6.2.1 Model SIMPLE

For one of the Randmeren, the Wolderwijd, a simple primary production and respiration model has been developed during an earlier study and calibrated on measurements obtained during years with persistent blooms of *Oscillatoria agardhii* (Van Duin and Lijklema, 1989<sup>2</sup>). In spite of the simple nature of the model, inclusion of the production and respiration in a dissolved oxygen model yielded a good agreement between observed and simulated data. To examine whether a simple model approach would be sufficient for the simulation of growth of *O.agardhii* in the Markermeer, this model has been applied to the data of the field experiments. The model and its validation are described in detail elsewhere (Van Duin and Lijklema, 1989<sup>2</sup>). Its description here is limited to the basic concepts and formulas.

Primary production is modelled as a function of the specific maximum production rate and of limiting factors related to temperature and the available light energy. Respiration includes both maintenance and growth respiration and the oxygen used for bacterial decay. Temper-

ature dependencies are described according to modified Arrhenius relationships, with 20° C as the reference temperature. The photosynthetic light response is modelled using the mathematical formula of Steele. The model is summarized by equation 6.1 and integrated in depth in equation 6.2.

$$\frac{dDO}{dt} = Chla \cdot Y \cdot U_{max} \cdot \theta_p^{(T-20)} \cdot (E_{d,z}/E_{opt}) \cdot e^{(1-(E_d/E_{opt}))} - Chla \cdot Y \cdot R_{max} \cdot \theta_r^{(T-20)} \quad (6.1)$$

$$\frac{dDO^*}{dt} = z \cdot Chla \cdot Y \cdot U_{max} \cdot \theta_p^{(T-20)} \cdot (e/k_d \cdot z) \cdot [e^{(-E_{d,b}/E_{opt})} - e^{(-E_{d,o}/E_{opt})}] - z \cdot Chla \cdot Y \cdot R_{max} \cdot \theta_r^{(T-20)} \quad (6.2)$$

|                  |  |   |
|------------------|--|---|
| DO               | = dissolved oxygen concentration               | (gO <sub>2</sub> ·m <sup>-3</sup> )     |
| DO*              | = mass of dissolved oxygen in the water column | (gO <sub>2</sub> ·m <sup>-2</sup> )     |
| Chla             | = chlorophyll-a concentration                  | (gChla·m <sup>-3</sup> )                |
| Y <sub>p</sub>   | = yield coefficient of production              | (gO <sub>2</sub> ·gChla <sup>-1</sup> ) |
| U <sub>max</sub> | = maximum production rate at 20° C             | (h <sup>-1</sup> )                      |
| θ <sub>p</sub>   | = temperature coefficient for production       | (-)                                     |
| T                | = temperature                                  | (°C)                                    |
| E <sub>d</sub>   | = downward irradiance                          | (μE·m <sup>-2</sup> ·s <sup>-1</sup> )  |
| E <sub>d,b</sub> | = downward irradiance near the lake bottom     | (μE·m <sup>-2</sup> ·s <sup>-1</sup> )  |
| E <sub>d,o</sub> | = downward irradiance near the water surface   | (μE·m <sup>-2</sup> ·s <sup>-1</sup> )  |
| E <sub>opt</sub> | = optimal irradiance for production            | (μE·m <sup>-2</sup> ·s <sup>-1</sup> )  |
| R <sub>max</sub> | = maximum respiration rate at 20°C             | (h <sup>-1</sup> )                      |
| θ <sub>r</sub>   | = temperature coefficient for respiration      | (-)                                     |
| Y <sub>r</sub>   | = yield coefficient of respiration             | (gO <sub>2</sub> ·gChla <sup>-1</sup> ) |

The inclusion of the external phosphate concentration as a rate limiting factor in the model did not improve the results in the Wolderwijd study but rather caused a negative temperature coefficient. Therefore nutrient limitation was discarded. This was imputed to the temperature effect upon the cycling of phosphate. The values of the optimal parameter set for the Wolderwijd data (WW) are presented in Table 6.1. With the data obtained from the field experiments, the applicability of the model *SIMPLE* for the Markermeer is examined.

Table 6.2 Optimal parameter set of the model *SIMPLE* for the Wolderwijd data

| parameter           | value | dimension                            |
|---------------------|-------|--------------------------------------|
| $E_{opt}$           | 290   | $\mu E \cdot m^{-2} \cdot s^{-1}$    |
| $\theta_p$          | 1.030 | -                                    |
| $\theta_1$          | 1.081 | -                                    |
| $Y_p \cdot U_{max}$ | 7.65  | $gO_2 \cdot gChla^{-1} \cdot h^{-1}$ |
| $Y_1 \cdot R_{max}$ | 1.47  | $gO_2 \cdot gChla^{-1} \cdot h^{-1}$ |

Gross production curves were obtained from the primary production measurements in the fixed bottles of the dark and light bottle experiments. Simulated and observed production values are presented in Appendix 11 and summarized in Table 6.3. With the parameter set obtained with the Wolderwijd data the simulated DO-concentration is usually too low. Inhibition is simulated above  $300 \mu E \cdot m^{-2} \cdot s^{-1}$  but is usually observed at much lower energy values. As the observed and simulated values often matched poorly, the model *SIMPLE* was calibrated for each experiment using a Rosenbrock-scheme for optimization (§ 4.5.3). The parameters  $Y_p \cdot U_{max}$  and  $E_{opt}$  were optimized for the least mean of the sum of squares of the differences between simulated and observed values. The calibration results are included in the graphs of Appendix 11 and in Table 6.3. After calibration, the model *SIMPLE* produces rather good results for the individual experiments, but no uniform parameter set seems to be appropriate for all different circumstances encountered in the different individual tests. The optimum irradiance value for growth varied between 247 and  $769 \mu E \cdot m^{-2} \cdot s^{-1}$ , though effectively a value above  $500 \mu E \cdot m^{-2} \cdot s^{-1}$  means that no inhibition is found. The maximum production rate ( $Y_p \cdot U_{max}$ ) varied between 5.4 and  $13.5 gO_2 \cdot gChla^{-1} \cdot h^{-1}$ .

Table 6.3 Results of the model *SIMPLE* to the fixed bottle experiments

| data set   | Calibrated |                  |      | Wolderwijd set |
|------------|------------|------------------|------|----------------|
|            | Y-Umax     | E <sub>opt</sub> | SSQ  | SSQ            |
| Wolderwijd | 7.65       | 290              | -    | -              |
| 30/6/89    | 8.20       | 390              | 1.83 | 2.35           |
| 7/7/89     | 8.27       | 769              | 1.50 |                |
| 12/7/89    | 4.29       | 669              | 0.31 | 3.28           |
| 6/9/89     | 8.62       | 448              | 1.35 | 2.66           |
| 8/9/89     | 13.46      | 483              | 1.07 | 5.69           |
| 15/9/89    | 11.36      | 573              | 0.49 | 2.24           |
| 18/6/90    | 8.69       | 340              | 1.89 | 2.30           |
| 20/6/90    | 12.30      | 247              | 0.72 | 3.93           |
| 27/6/90    | 9.12       | 387              | 0.82 | 1.89           |
| 29/6/90    | 5.37       | 368              | 0.91 | 1.80           |
| 16/7/90    | 7.89       | 475              | 0.59 | 1.53           |

Similar to the simulations of the light and dark bottle experiments, the model *SIMPLE* was subsequently used to simulate the DO-concentration in the cylinder. The results of the simulations with the parameter set as estimated for the Wolderwijd are presented in Appendix 12. Simulated values are much too high for period 89-2 and much too low for period 89-3. Therefore the model was calibrated for each period separately and the obtained parameter set was used to simulate the other three periods. Simulation and calibration results are included in Appendix 12 and summarized in Table 6.4. With the model *SIMPLE* it is possible to simulate the mean trend in the measurements, but daily dynamics are not reproduced very well. The differences between the four periods are substantial. Period 89-2 is characterized by low growth rates and virtually no inhibition by light energy, 89-3 by high growth rates and inhibition, 90-1 by high growth rates without inhibition and 90-2 by low growth rates with inhibition. Hence, again from the calibration no general parameter set or model improvement can be deduced. The differences between the calibrated parameter sets are even larger than the variation found for the light and dark bottle experiments. part of the variation that is observed in the optimized parameter sets may be due to the dependency between  $Y_p \cdot U_{max}$  and  $E_{opt}$ .

Table 6.4 Results of the model SIMPLE for the cylinder experiments

| calibration period | Y-Rmax | Y-Umax | E <sub>opt</sub> | SSQ of period used for validation |       |       |       |
|--------------------|--------|--------|------------------|-----------------------------------|-------|-------|-------|
|                    |        |        |                  | 89-2                              | 89-3  | 90-1  | 90-2  |
| Wolderwijd         | 1.47   | 7.65   | 290.             | 8.80                              | 12.67 | 4.50  | 4.60  |
| 89-2               | 1.05   | 2.32   | 946.             | 2.47                              | 16.05 | 5.28  | 7.17  |
| 89-3               | 2.55   | 19.60  | 57.              | 10.23                             | 4.83  | 17.09 | 15.98 |
| 90-1               | 1.59   | 12.05  | 943.             | 18.60                             | 14.53 | 4.06  | 5.47  |
| 90-2               | 0.21   | 1.36   | 61.              | 3.91                              | 10.19 | 4.82  | 3.50  |

The model *SIMPLE* may be used to simulate the oxygen production and respiration in the enclosure experiments but the simulation results are poor. The parameter set calibrated for the *O.agardhii* population of the Wolderwijd is not transferable. This is not caused by the absence of nutrient limitation in the model as the experiments were conducted with nutrient rich *O.agardhii* suspensions. Calibration of the model for the Markermeer field experiments gives good results for the light and dark bottle experiments, but the results for the cylinder experiments were less good. The differences between the parameters found for individual experiments are large and no single set satisfying all experiments, could be established. Hence, it may be concluded that the model *SIMPLE* does not represent the processes that control the production of *O.agardhii* in enclosures in the Markermeer. The major weakness is evidently the absence of adaptation of growth parameters to the changes in light field.

### 6.2.2 Model ALGA

The model *ALGA* has been developed especially for the Markermeer project by Vermij (1992). The aim was to produce a model describing the growth of *Oscillatoria agardhii* as a function of the variable light field and the temperature. The model is designed to be incorporated in the model *STRESS-2d* and *CLEAR*, for the simulation of the growth of *O.agardhii* in the Markermeer under prevailing conditions and after possible management measures.

The model concepts, structure and calibration are described extensively elsewhere (Vermij, 1992; Visser, 1991). A summary of the basic concepts and formulas is given below. Starting point of the model is the non-equilibrium concept. The model describes the growth, respiration and decay of *O.agardhii*.



$$\frac{\partial \text{N-Osc}}{\partial t} = [\text{PP} - \text{RESP} - \text{DECAY}]/z \quad (6.3)$$

|       |   |                                  |  |
|-------|---|----------------------------------|--|
| N-Osc | = | <i>O. agardhii</i> concentration | ( <i>O. agardhii</i> ·m <sup>-3</sup> )                  |
| PP    | = | primary production               | ( <i>O. agardhii</i> ·m <sup>-2</sup> ·s <sup>-1</sup> ) |
| RESP  | = | respiration                      | ( <i>O. agardhii</i> ·m <sup>-2</sup> ·s <sup>-1</sup> ) |
| DECAY | = | decay                            | ( <i>O. agardhii</i> ·m <sup>-2</sup> ·s <sup>-1</sup> ) |
| z     | = | depth                            | (m)  |

The basic response of growth rates to light energy is described with Smith's model:

$$P = \frac{E_d \cdot \alpha}{\sqrt{[1 + (\alpha \cdot E_d / P_{\max})^2]}} \quad (6.4)$$

|                  |   |                                     |  |
|------------------|---|-------------------------------------|--|
| P                | = | productivity                        | (s <sup>-1</sup> )   |
| P <sub>max</sub> | = | maximum productivity                | (s <sup>-1</sup> )   |
| α                | = | light energy utilization efficiency | (s <sup>-1</sup> ·(μE·m <sup>-2</sup> ·s <sup>-1</sup> ) <sup>-1</sup> ) |
| E <sub>d</sub>   | = | downward irradiance                 | (μE·m <sup>-2</sup> ·s <sup>-1</sup> )                                   |

The temperature dependency is described with a correction factor with respect to the standard temperature of 20° C: T/20. The column productivity is obtained by integration of Smith's formula in depth using Beers' Law (equation 5.2), resulting in equation 6.5;

$$\text{PP} = - \text{N-Osc} \cdot \frac{P_{\max} \cdot T}{K_d \cdot 20} \cdot \ln \left( \frac{e^{-K_d \cdot z} + \sqrt{[e^{-2 \cdot K_d \cdot z} + \{P_{\max} \cdot T / (20 \cdot \alpha \cdot E_{d,o})\}^2]}}{1 + \sqrt{[1 + \{(P_{\max} \cdot T / (20 \cdot \alpha \cdot E_{d,o})\}^2]}} \right) \quad (6.5)$$

|                  |   |  |  |
|------------------|---|--|--|
| K <sub>d</sub>   | = | vertical downward attenuation coefficient        | (m <sup>-1</sup> )                     |
| z                | = | depth  | (m)                                    |
| E <sub>d,o</sub> | = | downward irradiance just below the water surface | (μE·m <sup>-2</sup> ·s <sup>-1</sup> ) |

The adaptation of the maximum growth rate (P<sub>max</sub>) and of the light utilization efficiency (α) to different levels of light energy, is based upon the transient state experiments performed by Post (1986), resulting in a first order kinetics description of the changes in P<sub>max</sub> and α. A threshold value, E<sub>crit</sub>, has been introduced. If the mean irradiance over the water column is below this threshold value, adaptation to low light conditions occurs and the values of P<sub>max</sub> and α increase. Above this threshold value adaptation to high light conditions occurs.

$$\begin{aligned} E_{\text{mean}} > E_{\text{cr}} : & P_{\max} = P_{\max,H} + (P_{\max} - P_{\max,H}) \cdot e^{(-C_p, LH \cdot dt)} \quad (6.6a) \\ & \alpha = \alpha_H + (\alpha - \alpha_H) \cdot e^{(-C_\alpha, LH \cdot dt)} \end{aligned}$$

$$\begin{aligned} E_{\text{mean}} < E_{\text{cr}} : & P_{\max} = P_{\max,L} + (P_{\max} - P_{\max,L}) \cdot e^{(-C_p, HL \cdot dt)} \quad (6.6b) \\ & \alpha = \alpha_L + (\alpha - \alpha_L) \cdot e^{(-C_\alpha, HL \cdot dt)} \end{aligned}$$

$$E_{\text{mean}} = \frac{E_T}{Z} = \frac{E_{d,0}}{K_d \cdot Z} [1 - e^{-K_d \cdot Z}] \quad (6.7)$$

|                    |  |  |
|--------------------|--|--|
| $E_{\text{mean}}$  | = mean under water irradiance over the depth           | $(\mu\text{E} \cdot \text{m}^{-2} \cdot \text{s}^{-1})$                            |
| $E_T$              | = total under water irradiance over the depth          | $(\mu\text{E} \cdot \text{m}^{-2} \cdot \text{s}^{-1})$                            |
| $E_{\text{cr}}$    | = critical threshold value for growth parameters       | $(\mu\text{E} \cdot \text{m}^{-2} \cdot \text{s}^{-1})$                            |
| $P_{\text{max,H}}$ | = Pmax at high irradiance values                       | $(\text{s}^{-1})$  |
| $P_{\text{max,L}}$ | = Pmax at low irradiance values                        | $(\text{s}^{-1})$  |
| $\alpha_H$         | = $\alpha$ at high irradiance values                   | $(\text{s}^{-1} \cdot (\mu\text{E} \cdot \text{m}^{-2} \cdot \text{s}^{-1})^{-1})$ |
| $\alpha_L$         | = $\alpha$ at low irradiance values                    | $(\text{s}^{-1} \cdot (\mu\text{E} \cdot \text{m}^{-2} \cdot \text{s}^{-1})^{-1})$ |
| $C_{p,LH}$         | = adaption rate Pmax, from low to high irradiance      | $(\text{s}^{-1})$  |
| $C_{p,HL}$         | = adaption rate Pmax, from high to low irradiance      | $(\text{s}^{-1})$  |
| $C_{\alpha,LH}$    | = adaption rate $\alpha$ , from low to high irradiance | $(\text{s}^{-1})$  |
| $C_{\alpha,HL}$    | = adaption rate $\alpha$ , from high to low irradiance | $(\text{s}^{-1})$  |

In the model *ALGA* it is assumed that the carrying capacity of *O.agardhii* of a water body is determined by the concentration of available nutrients. The possible productivity based on nutrient availability is computed using Equation 6.8, for total phosphorus and nitrogen. This simple nutrient limitation model is introduced to set an upper boundary to phytoplankton growth in order to simulate the actual data obtained for the lakes in the IJsselmeer area.

$$P_{\text{nut}} = P_{\text{opt}} \cdot \frac{(C_{\text{nut}}/N - \text{Osc}) - Q_{\text{nut}}}{(C_{\text{nut}}/N - \text{Osc})} \quad (6.8)$$

|                  |  |   |
|------------------|--|---|
| $P_{\text{nut}}$ | = productivity based on available nutrients        | $(\text{s}^{-1})$                         |
| $P_{\text{opt}}$ | = optimal productivity without nutrient limitation | $(\text{s}^{-1})$                         |
| $C_{\text{nut}}$ | = nutrient concentration                           | $(\text{g} \cdot \text{m}^{-3})$          |
| $Q_{\text{nut}}$ | = minimal internal nutrient concentration          | $(\text{g} \cdot \text{O.agardhii}^{-1})$ |

The first order loss rate of biomass by respiration is a function of the temperature only;

$$\text{RESP} = N - \text{Osc} \cdot R_{\text{max}} \cdot T/20 \quad (6.9)$$

$$R_{\text{max}} = \text{maximum respiration rate} \quad (\text{s}^{-1})$$

The loss rate of biomass by mortality, grazing and sedimentation are assumed to be constant. The value of the decay constant was obtained by calibration.

$$\text{DECAY} = N\text{-Osc} \cdot C_d \quad (6.10)$$

$$C_d = \text{decay constant} \quad (\text{s}^{-1})$$

Horizontal spatial heterogeneity of the studied water bodies is introduced by means of division of the water body into a limited number of compartments, distinguished by depth. The influence of wind is assessed for two extremes: total mixing of all the compartments for wind speeds above  $6 \text{ m} \cdot \text{s}^{-1}$  and total absence of mixing for lower wind speeds. Vertical mixing is assumed to be complete at all times.

The model has been applied to three lakes in the IJsselmeer area: the Markermeer, the IJsselmeer and the Wolderwijd (Figure 1.1). For the calibration, weekly measurements of numbers of *O. agardhii* were used. Parameters were varied at random over broad intervals, to obtain the best fitting set. Parameters were calibrated for each lake separately, as no uniform set for the three lakes could be found. For the Markermeer, data sets of 1988 and 1989 were used. The parameter set used by Vermij is summarized in Table 6.5. The parameters obtained by calibration are marked, the remaining parameters were obtained from literature.

Table 6.5 Parameter set of the model ALGA

| relative growth ( $\text{s}^{-1}$ ) |                   |  | O <sub>2</sub> -prod per Chla ( $\text{h}^{-1}$ ) |  |
|-------------------------------------|-------------------|--|---|--|
| parameter                           | value             | dimension  | value   | dimension  |
| $P_{\text{max}, H}$                 | $2.78 \cdot 10^5$ | ( $\text{s}^{-1}$ )  | 0.196   | ( $\text{gO}_2 \cdot \text{gChla}^{-1} \cdot \text{h}^{-1}$ )  |
| $P_{\text{max}, L}$                 | $2.50 \cdot 10^3$ | ( $\text{s}^{-1}$ )  | 17.65   | ( $\text{gO}_2 \cdot \text{gChla}^{-1} \cdot \text{h}^{-1}$ )  |
| $a_H$                               | $1.57 \cdot 10^5$ | ( $(\mu\text{E} \cdot \text{m}^{-2} \cdot \text{s}^{-1})^{-1} \cdot \text{s}^{-1}$ ) | 0.111   | ( $\text{gO}_2 \cdot \text{gChla}^{-1} \cdot (\mu\text{E} \cdot \text{m}^{-2} \cdot \text{s}^{-1})^{-1} \cdot \text{h}^{-1}$ ) |
| $a_L$                               | $6.70 \cdot 10^5$ | ( $(\mu\text{E} \cdot \text{m}^{-2} \cdot \text{s}^{-1})^{-1} \cdot \text{s}^{-1}$ ) | 0.473   | ( $\text{gO}_2 \cdot \text{gChla}^{-1} \cdot (\mu\text{E} \cdot \text{m}^{-2} \cdot \text{s}^{-1})^{-1} \cdot \text{h}^{-1}$ ) |
| $E_{cr}$                            | 10                | ( $\mu\text{E} \cdot \text{m}^{-2} \cdot \text{s}^{-1}$ )                            | 10  | ( $\mu\text{E} \cdot \text{m}^{-2} \cdot \text{s}^{-1}$ )  |
| $C_{p, LH}$                         | $2.78 \cdot 10^3$ | ( $\text{s}^{-1}$ )  | 0.100   | ( $\text{h}^{-1}$ )  |
| $C_{p, HL}$                         | $9.44 \cdot 10^4$ | ( $\text{s}^{-1}$ )  | 0.034   | ( $\text{h}^{-1}$ )  |
| $C_{d, LH}$                         | $1.08 \cdot 10^2$ | ( $\text{s}^{-1}$ )  | 0.389   | ( $\text{h}^{-1}$ )  |
| $C_{d, HL}$                         | $3.61 \cdot 10^4$ | ( $\text{s}^{-1}$ )  | 0.013   | ( $\text{h}^{-1}$ )  |
| $R_{\text{max}}$                    | $5.56 \cdot 10^5$ | ( $\text{s}^{-1}$ )  | 0.392   | ( $\text{gO}_2 \cdot \text{gChla}^{-1} \cdot \text{h}^{-1}$ )  |
| $C_d$                               | $7.22 \cdot 10^5$ | ( $\text{s}^{-1}$ )  | —   |  |

\*parameters obtained by calibration

The suitability of the model ALGA for the Markermeer conditions is examined with the data obtained from the field experiments analogous to the application of the model SIMPLE. As the duration of the bottle experi-

ments is too short to simulate adaptation of growth parameters, these experiments were used to validate the basic concept of the model, the response of the productivity to the available light energy based on Smith's model (Equation 6.4) and the temperature dependency. The value of the maximum gross production rate ( $P_{\max}$ ) and the initial slope of the production curve ( $\alpha$ ) are estimated. The simulation results are presented in Appendix 13 and parameter values are summarized in Table 6.6.

*Table 6.6 Results of the model ALGA for the fixed bottle experiments*

| data set | $P_{\max}$  | $\alpha$   | SSQ  |
|----------|---|--|------|
|          | ( $\text{gO}_2 \cdot \text{gChla}^{-1} \cdot \text{h}^{-1}$ ) | ( $\text{gO}_2 \cdot \text{gChla}^{-1} \cdot (\mu\text{E} \cdot \text{m}^{-2} \cdot \text{s}^{-1})^{-1} \cdot \text{h}^{-1}$ ) |      |
| 30/6/89  | 6.15  | 0.34   | 1.09 |
| 7/7/89   | 7.71  | 0.06   | 1.06 |
| 12/7/89  | 5.10  | 0.01   | 0.21 |
| 6/9/89   | 7.58  | 0.15   | 0.77 |
| 8/9/89   | 10.84   | 0.11   | 1.72 |
| 15/9/89  | 11.34   | 0.04   | 0.52 |
| 18/6/90  | 7.65  | 0.23   | 1.15 |
| 20/6/90  | 11.66   | 0.16   | 0.63 |
| 27/6/90  | 8.39  | 0.09   | 0.67 |
| 29/6/90  | 4.44  | 0.10   | 0.51 |
| 16/7/90  | 9.49  | 0.04   | 0.62 |

The gross production in the light bottles is simulated rather well by the model ALGA. One parameter set was obtained for all the different bottles at one day, thus adaptation to the mean circumstances is allowed for each experiment. As in Smith's production curve no inhibition is modelled, production rates at high irradiance values can be slightly overestimated. In the model ALGA, where adaptation of  $P_{\max}$  and  $\alpha$  is allowed,  $P_{\max}$  at the very high energy levels would be lower to account for inhibition. The value of  $P_{\max}$  and  $\alpha$  varies from experiment to experiment.  $P_{\max}$  varies within the range of  $P_{\max,H}$  and  $P_{\max,L}$  (Table 6.5).  $\alpha$  varies between 0.01 and 0.34, whereas the range of  $\alpha$  according to Vermij (1992) is from 0.111 to  $0.473 \text{ gO}_2 \cdot \text{gChla}^{-1} \cdot (\mu\text{E} \cdot \text{m}^{-2} \cdot \text{s}^{-1})^{-1} \cdot \text{h}^{-1}$ . In 6 out of 11 data sets the value of  $\alpha$  was calibrated to be lower than  $\alpha_H$ . Hence, the light utilization efficiency computed for the light and dark bottle experiments is lower than the efficiency found in the transient state experiments conducted by Post (1986).

Similar to the simulations of the light and dark bottle experiments, the model ALGA has been used to simulate the DO-concentration in the cylinder with the parameter set as proposed by Vermij (Table 6.5). The initial value of  $P_{\max}$  and  $\alpha$  were calibrated, but the initial value of  $\alpha$

seemed of little influence of the behaviour of the model. The results of the simulations are presented in Appendix 14 and the model behaviour is presented in Table 6.7. Because the simulated dissolved oxygen concentration in the cylinder differed much from the measured concentration, the calibration was done with data from the cylinder experiments. Three parameters were selected for calibration: the threshold irradiance,  $E_{crit}$ , the maximum respiration rate,  $R_{max}$  and  $P_{max}$  at time  $t=0$ . To the other parameters the values of Table 6.5 were assigned. The obtained parameter set for each period was subsequently used for simulation of the other three periods. The results are included in Appendix 14 and Table 6.7.

**Table 6.7 Results of the model ALGA for the cylinder experiments**

| calibration period | $E_{crit}$ | $R_{max}$ | SSQ of period used for validation |       |       |       |
|--------------------|------------|-----------|-----------------------------------|-------|-------|-------|
|                    |            |           | 89-2                              | 89-3  | 90-1  | 90-2  |
| ALGA               | 10         | 0.392     | 2.58                              | 9.26  | 3.44  | 3.97  |
| 89-2               | 2          | 0.479     | 2.12                              | 23.92 | 15.07 | 35.60 |
| 89-3               | 166        | 1.010     | 7.85                              | 7.09  | 2.97  | 5.39  |
| 90-1               | 164        | 1.124     | 10.16                             | 7.32  | 2.95  | 7.27  |
| 90-2               | 100        | 0.632     | 2.73                              | 8.29  | 3.28  | 3.66  |

The simulation results improved substantially by this calibration and the average trend in the dissolved oxygen concentration is simulated rather well. The daily fluctuations however are simulated poorly. Though the estimated parameter sets were very similar for period 89-3 and 90-1, they are very different for the other periods and no uniform parameter set is obtained. For period 89-2, when *O. agardhii* rotated through the top metre of the cylinder only, the calibrated parameters concern high light conditions almost continuously as can be seen from the low value of  $E_{crit}$  of  $2 \mu E \cdot m^{-2} \cdot s^{-1}$ . For the three periods with rotation of *O. agardhii* over the entire depth, much higher values of  $E_{crit}$  are estimated. This implies that with a value of  $E_{crit}$  of  $10 \mu E \cdot m^{-2} \cdot s^{-1}$ , the values of the growth parameters are much too low to simulate the high production and respiration in the cylinder. The same is true for the value of  $R_{max}$ . If  $R_{max}$  is set at the original value of ALGA, only little production is allowed to balance the low respiration and the high production and respiration rates measured in the cylinder are not reproduced. Partly this can be contributed to the bacterial respiration incorporated in the  $R_{max}$ .

The results of the calibration are slightly better than the results obtained with the model SIMPLE, but are still unsatisfying. Hence, including adaptation of growth parameters to changes in the light field according to the model ALGA in its present form is not sufficient to describe the production of *O. agardhii* in enclosures in the Markermeer. It should be noted however, that part of the differences between observed and simulated

production of *O.agardhii* may be caused by the differences between the light field inside the cylinder and the light field in the Markermeer. Further, the damage of *O.agardhii* in passing through the pumps may explain lower measured production rates. However, it can not explain higher measured production rates.

In the model ALGA an upper and lower boundary are set for the maximum productivity,  $P_{\max}$ , and the light utilization efficiency,  $\alpha$ . Depending on the average irradiance over the depth the value of the growth parameters varies between these boundaries. From the field experiments it may be concluded that the boundaries for  $P_{\max}$  are chosen well for the time being, but that the defined range for  $\alpha$  may be too narrow. The threshold value for adaptation obtained by calibration by Vermij is  $10 \mu E \cdot m^{-2} \cdot s^{-1}$ . For a mean depth of 3.6 m, a mean vertical downward attenuation coefficient of  $4 m^{-1}$  and a reflection of 10 %, this corresponds to an irradiance  $E_{d,0}$  of  $150 \mu E \cdot m^{-2} \cdot s^{-1}$ . This occurs during more than 77 % of the light hours in July. This is illustrated in Table 6.8. At site Y112 with a lower depth, the percentage of hours with a value of  $E_{\text{mean}} > 10 \mu E \cdot m^{-2} \cdot s^{-1}$  will be even higher. The calibrated values of  $E_{\text{crit}}$  in the cylinder experiments is therefore somewhat biased as the values of  $E_{\text{mean}}$  at Y112 in July are not very representative for the entire lake. However, the magnitude of these calibrated values for  $E_{\text{crit}}$  is important;  $E_{\text{crit}}$  is calibrated at a very low value of  $2 \mu E \cdot m^{-2} \cdot s^{-1}$  for *O.agardhii* in the upper metre of the column. Hence,  $P_{\max}$  and  $\alpha$  do not vary during most of the day, but are constantly kept at their lower limits. The high values of  $E_{\text{crit}}$  for *O.agardhii* mixed over the entire depth, imply that only low light conditions are simulated. Thus the growth parameters are invariable set on their upper boundary value and adaptation does (again) not occur.

Table 6.8 Distribution of mean under water irradiance in the Markermeer in 1989 (computed from  $E_{d,0}$   $z = 3.6$  m and  $K_d = 4 m^{-1}$ )

| month   | day light hours<br>% | total hours $E_m > 10$<br>% | day light hours $E_m > 10$<br>% |
|---------|----------------------|-----------------------------|---------------------------------|
| January | 36                   | 12                          | 34                              |
| April   | 59                   | 41                          | 70                              |
| July    | 68                   | 52                          | 77                              |
| October | 44                   | 28                          | 62                              |

The model ALGA describes general trends in production reasonably well, if parameter sets are modified. However, gross production and respiration are underestimated considerably, even with the modified parameters. Some concepts of the model can not be tested in the field experiments, among which of the rather crude division of the lake in compartments with different depths, the primitive concept of horizontal mixing and of decay. These will be discussed in § 6.3.2.

### 6.3 Simulation of *Oscillatoria agardhii* with the integrated model

To assess the suitability of the Markermeer for the growth of *Oscillatoria agardhii*, the model *ALGA* has been incorporated in the 2-dimensional models *STRESS-2d* and *CLEAR*. With the integrated model the Markermeer in its present state has been simulated to assess the differences between the model *ALGA* and the integrated model.

#### 6.3.1 Incorporation of *ALGA* in *STRESS-2d* and *CLEAR*

The integration of the model *ALGA* was conducted similarly to the integration of the model *CLEAR* within *STRESS-2d*. The net increase of biomass is estimated using the under water light field produced by the model *CLEAR*. The biomass concentration is computed every half time step in the implicit part of the advection diffusion equation of the *WAQUA* model, similar to the suspended solids concentration. Hence, the horizontal transport of algae is estimated as well. With the computed biomass and the suspended solids concentration the attenuation of light is computed prior to the estimation of the net biomass increase in the next half time step.

By the direct integration of *ALGA* within the *WAQUA-STRESS-2d-CLEAR* model, horizontal transport and an advanced numerical solution of the mass balance equation are included. The computation of light attenuation is easily incorporated too. Unfortunately, the direct integration has some major disadvantages as well. Firstly, the same time step and grid size are used for the model *ALGA* as used for the *WAQUA-STRESS-2d* model, whereas a much larger time step and grid size would have been appropriate for *ALGA*. Hence, the computation time is unnecessarily enlarged. Secondly, for each simulation of the algal growth model, the water movement and sediment resuspension and sedimentation model are simulated as well, while at least in the calibration phase this is often not needed because there is no feed back from *ALGA* to *STRESS-2d*.

#### 6.3.2 Optimization of the parameters of the integrated model

At first the integrated model has been used to simulate the principal calibration period used by Vermij (1992), June, July and August 1989, and the same parameter set (Table 6.5). The results for site Y111 and Y112 are presented in Appendix 15. The simulated *O. agardhii* numbers in the integrated model are very different from the observed values and the values simulated with the original *ALGA*. It seems that production is overestimated. This is true for both sites, though the phenomenon is much more pronounced for site Y112 than for site Y111. This may be magnified by the large difference in the modelling of horizontal mixing between the two models. The effect of horizontal mixing is probably highly overestimated by the model *ALGA*, which thus balanced the overestimation of growth in shallow parts of the lake.

Assuming that growth is in principal modelled well but that rates are overestimated, this may be compensated by increasing the decay or respiration rate, as was suggested by the simulations of the field experiments. With the integrated model simulations are done for the same period, using higher decay rates. The results are included in Appendix 15. From the simulation results, a decay rate of  $0.0032 \text{ h}^{-1}$  is selected. This leads to an overestimation at Y112 and an underestimation at Y111.

Another simulation has been performed for the entire year 1988, using two different initial concentrations;  $50 \cdot 10^6$  (A) and  $5 \cdot 10^9$  *O.agardhii*- $\text{m}^{-3}$  (B), results are presented in Appendix 15. Due to the high decay rate ( $0.0032 \text{ h}^{-1}$ ), the concentration in spring is very low and not compensated by growth in summer. Apart from an overestimation of the growth or an underestimation of the decay, new problems are now encountered. As the decay rate is constant over the entire year, a high decay rate necessary for the summer months implies an enormous decrease of algae during the winter months. Besides, the model is extremely sensitive to the used initial concentrations. Unfortunately, algae concentrations are never measured in winter.

In a set of simulations of the entire years 1988 and 1989, different combinations of initial concentrations and decay rates have been tested, the most important results are included in Appendix 15. In addition the effect of an increase in horizontal transport was studied. Decreasing the Manning-value or increasing the wind stress coefficient, may increase stream velocities and horizontal transport of *O.agardhii*, but the effect is minor. Different values of  $E_{\text{crit}}$  were used as well, but an increase of  $E_{\text{crit}}$  did only aggravate the problem. The best results were produced by a simulation with an initial value of  $5 \cdot 10^9$  *O.agardhii*- $\text{m}^{-3}$  and a decay rate of  $0.0026 \text{ h}^{-1}$  (D).

As the simulation results are highly sensitive to the value of the decay rate, the problem may be caused by the fact that the decay rate is constant over the year. This was based on the assumption that grazing and sedimentation of *O.agardhii* are negligible and decay is dominated by mortality. If grazing or sedimentation of *O.agardhii* are not insignificant, the decay rate should not be considered constant over the year as both sedimentation and grazing will be less in winter. Therefore a simulation is performed in which the sedimentation and resuspension of *O.agardhii* is modelled as well, by including *O.agardhii* in the resuspension/sedimentation part of STRESS-2d. For *O.agardhii* a fall velocity ( $w_s$ ) of  $1.16 \cdot 10^{-6} \text{ m} \cdot \text{s}^{-1}$  is used (Vermij, 1992) and a decay rate of  $0.0020 \text{ h}^{-1}$ . The resuspension parameters were considered equal to the suspended solids fraction with the lowest fall velocity  $SS_1$ . Hence, a critical maximum bottom wave orbital velocity ( $U_{b,cr}$ ) of  $0.40 \cdot 10^{-3} \text{ m} \cdot \text{s}^{-1}$  and a resuspension constant ( $K$ ) of  $0.72 \cdot 10^{-6} \text{ kg} \cdot \text{m}^{-3}$  were used. The initial concentration in the sediment layers at January 1, 1988 was assumed to be  $0 \text{ kg} \cdot \text{m}^{-3}$ . The results were not better than those with parameter set D.



### 6.3.3 Validation of the model ALGA

Results of the simulation of the growth of *Oscillatoria agardhii* in the Markermeer with the integrated model and the original parameter set of ALGA, are disappointing, as far as simulated *O.agardhii* numbers are concerned. Fine tuning of the integrated model on the measurement results of 1988 and 1989 did improve the results considerably. However, further calibration of the integrated model seems needed to obtain an accurate simulation of the growth of *O.agardhii* in the Markermeer.

The model ALGA in its present form is not capable to simulate the measured nett production in the experiments. In the integrated form simulation of the measured numbers of *O.agardhii* does not agree with measured numbers. Though the incorporation of fast adaptation of growth parameters to variations in light conditions within hours is an improvement compared to models with fixed growth parameters, the model structure evidently does not accurately describe all the relevant processes of growth of *O.agardhii*. This may be due to the artificial critical irradiance value ( $E_{crit}$ ), the rather simple description of the loss rate, the omittance of competition with other algae, the absence of slow adaptation of growth parameters to variations in light energy within days or the absence of refined formulations of nutrient limitation.

No refined mechanisms for nutrient limitation are included in the model, though it is recognized that temporal nutrient limitation of phytoplankton growth does occur from time to time (Vermij, 1992). Thus, the model ALGA is a worst case model for the growth of *O.agardhii* in the Markermeer area. If applied carefully, the model may be used to compare simulation results for different scenarios, but the simulated absolute numbers of *O.agardhii* have little value.

## 7 Application of the integrated model

The integrated model comprises the models *WAQUA*, *STRESS-2d*, *CLEAR* and *ALGA*, describing respectively the horizontal water movement; sediment transport, resuspension and sedimentation; the under water light field and the light limited growth of *Oscillatoria agardhii*. The objective of the development of the integrated model was to support the decision making processes of the authorities as far as water quality aspects of the Markermeer are concerned.

Today's management stresses the importance of the lake as an open water system with durable and valuable ecosystems. Strategies are directed to harmonize the different social and ecological functions of the lake. Detailed management measures are not formulated yet, though certain actions such as increased flushing of the lake, deepening of shipping channels have been mentioned (Ministries, 1990).

In this chapter, the results of simulation with input data of 1988 and 1989 for three different situations or scenarios are described, comprising:

- \* simulation of the present situation. First, this scenario is used as a final validation of model behaviour over longer periods. Secondly, the effect of annual variability in the weather is studied;
- \* simulation of the effects of impoldering of the Markerwaard. In this scenario the lake surface is reduced to approximately one third of its current size, which implies considerable changes to lake morphometry and morphology;
- \* simulation of the effects of increased flushing. In this scenario the supply of water into the lake and the release of water are increased considerably, effecting the water balance and residence time.

Though the direct enforcement of the last two strategies is remote, they illustrate the applicability of the models in very different situations.

Simulation of the effects of development and management measures always involves a kind of prediction. As long as the model is used within the range of conditions it has been calibrated and tested for, prediction is characterized by relatively small extrapolations at relatively small changes in system input. Examples of such applications are the simulation of annual variability in weather and the effect of flushing on hydrology, sediment transport and light field. Different kinds of applications are made if management measures will change the system considerably. As long as the system is well defined, and governing laws and rules are well known, reliable predictions beyond the calibrated range of variables can still be made (Van Straaten, 1986). This may apply to the simulation of the effect of impoldering of the Markerwaard on hydrology, sediment transport and light field. Focusing on the ecosystem management and modelling, the system itself and the governing laws and rules are less well defined. According to Van Straaten (1986) the basic problem in ecosystem management is that processes or system parts which are not important in the present situation, may actually become impor-

tant in a future, strongly perturbed situation. This leaves us with the dilemma of Beck:

- \* either we use a model incorporating well calibrated processes only, with the risk to predict the wrong future with great precision,
- \* or we incorporate processes, which can not be calibrated. This may lead then to a correctly predicted future but with such a large uncertainty that the results have no practical value.

In order to elude the second option, the algal growth model focuses on the processes relating growth to available light energy, with simple assumptions about decay and nutrient limitations. Unfortunately, regarding these assumptions, this may lead to the first postulate of Beck. As the algal growth component of the integrated model describes average trends only and the reliability of predictions is limited, a distinction is made between the physical models, *WAQUA*, *STRESS-2d* and *CLEAR*, and the biological model, *ALGA*, in the evaluation of the model simulations.

## **7.1 Simulation of the present conditions**

The 'present' conditions are the conditions as observed in 1988 and 1989. The characteristics of the Markermeer, including morphometry and morphology, are described extensively in Chapter 2. The depth schematization is shown in Figure 4.2. Water management procedures and water quality characteristics of these years are described in Chapter 3 and summarized in § 7.1.1.

### **7.1.1 Characterization of the simulation period**

Final model simulations are restricted to a data set of two years: 1988 and 1989. The weather conditions in both years were very different; 1988 was a year with a rainfall higher than average for the Netherlands, over 900 mm near Lelystad, 1989 was a rather dry year, with a total rainfall of approximately 630 mm. The average wind speed in both years is comparable but temperatures and global irradiance were considerably higher in 1989 than in 1988. Hence, evaporation figures of 1989 are higher than those of 1988. The water balance of both years is presented in Appendix 2 and examined in § 2.2.1.

In the present-day management of the Markermeer, the residence time of water in the lake area is influenced by the inlet and outlet of water by sluices and pumping stations on the borders of the lake (flushing). The inlet and outlet of water by discharges are about two to three times higher than the contributions of precipitation and evaporation, § 2.2.1. The residence time is estimated at 1.5 to 2.5 year. The target water level of the lake in winter is 0.40 m -NAP, in summer 0.20 m -NAP (§ 2.2.1). The water discharged into the lake contains nutrients, chloride, phytoplankton, etc. As the concentration of blue-green algae in the IJsselmeer is generally higher than the concentrations in the Markermeer, the dis-

charge of water from the IJsselmeer into the Markermeer may influence the concentrations and growth of blue-green algae in the Markermeer considerably. Some influence can further be expected from water originating from the Eemmeer and Gooimeer, but as the amount of water is much less and part of it is withdrawn by the Oranjesluices and the sluices near Zeeburg without effective mixing with the main water body, this effect is ignored. Water quality characteristics of the Markermeer in 1988 and 1989 are described in Chapter 3 and summarized in Appendix 4. In 1989, a temporary bloom of *Oscillatoria agardhii* was observed, while in 1988 chlorophyll-a concentrations were generally lower and no blooms of blue-green algae were observed.

In the hydraulic model *WAQUA*, options are provided to simulate discharges (both positive and negative). Facilities to incorporate precipitation and evaporation are not provided. If discharge stations are incorporated for the inlet and outlet sites listed in Appendix 2, but no evaporation or precipitation is included, simulated water levels will be unrealistic. In summer, discharges in the lake by sluices and pumping stations are large, to compensate the loss by evaporation. As evaporation is not incorporated, the estimated water level rise during summer months may well be over 0.5 m. In winter the opposite will be simulated, as precipitation is not included. A water level rise of 0.5 metre has a notable effect on the water depth and subsequently on processes as resuspension and sedimentation, the total underwater irradiance and the estimated concentrations of sediment and phytoplankton. Hence, the effect of flushing of the lake is not estimated adequately in this manner. Therefore an artificial water balance is composed:

- a the daily variations in inlet and outlet of water are considered as not important, inlet and outlet of water are balanced per month;
- b per month the nett inlet or outlet of water is used. For all pumping stations and river discharges nett and gross discharge are equal and positive all over the year. For most of the sluices, inflow or discharge may occur but do not change within a month with the exception of the Krabbersgat- and Houtribsluices. Using nett figures per month leads to small round off errors only (Appendix 2);
- c the amount of water leaving the lake system per month at different stations and the concentrations in this water are unchanged. This means that the number and residence time of the phytoplankton cells remain unchanged;
- d a water level rise by precipitation surplus is compensated by increasing the discharges of the discharging stations proportionally in the simulations;
- e a water level decrease by a precipitation deficit is compensated by decreasing the discharges of the discharging stations proportionally in the simulations;
- f If the water is discharged through the Krabbersgat- or Houtribsluices into the Markermeer, measured cell numbers of *Oscillatoria agardhii* in the IJsselmeer (Vermij and Janissen, 1991) are used as concentrations. As no phytoplankton data of the winter months are

available, *O.agardhii* numbers for November through March are obtained by linear interpolation;

- g if the inflow through the Krabbersgat- or Houtribsluices into the Markermeer is changed to compensate for precipitation or evaporation effects (d and e), *O.agardhii* concentrations are changed accordingly in order to keep the number of *O.agardhii* cells identical to the measured numbers (Figure 7.1).

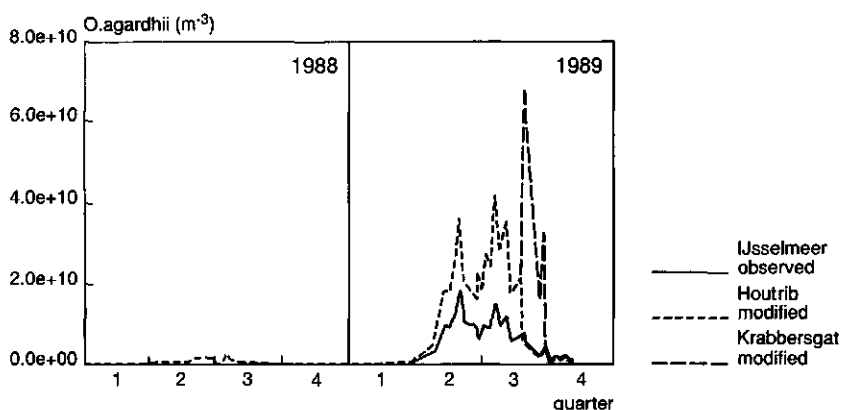


Figure 7.1 Observed and the modified *O.agardhii* concentrations in discharged water from the IJsselmeer

In Appendix 16 the modified water balance is presented. With these artifices, the computed water level in the lake coincides rather well with the observed levels, without changing the mass balances for phytoplankton. This is illustrated in Figure 7.2. However, the nett advective flow around the discharge stations, river mouths and sluices is affected, but compared to the effect of wind driven circulation these artifices will not display a notable effect on the circulation patterns in the lake.

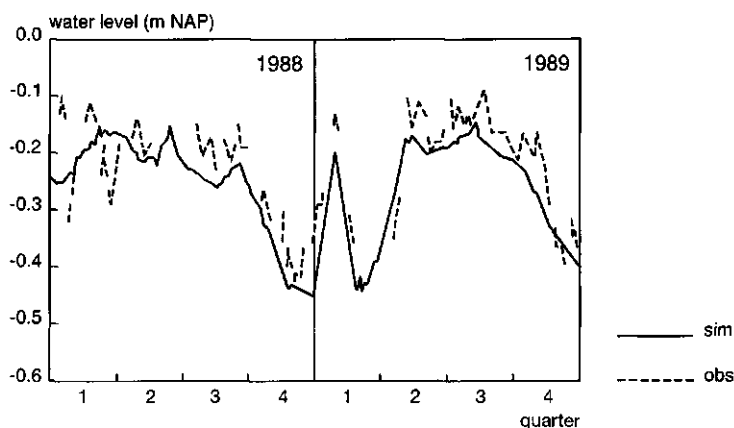
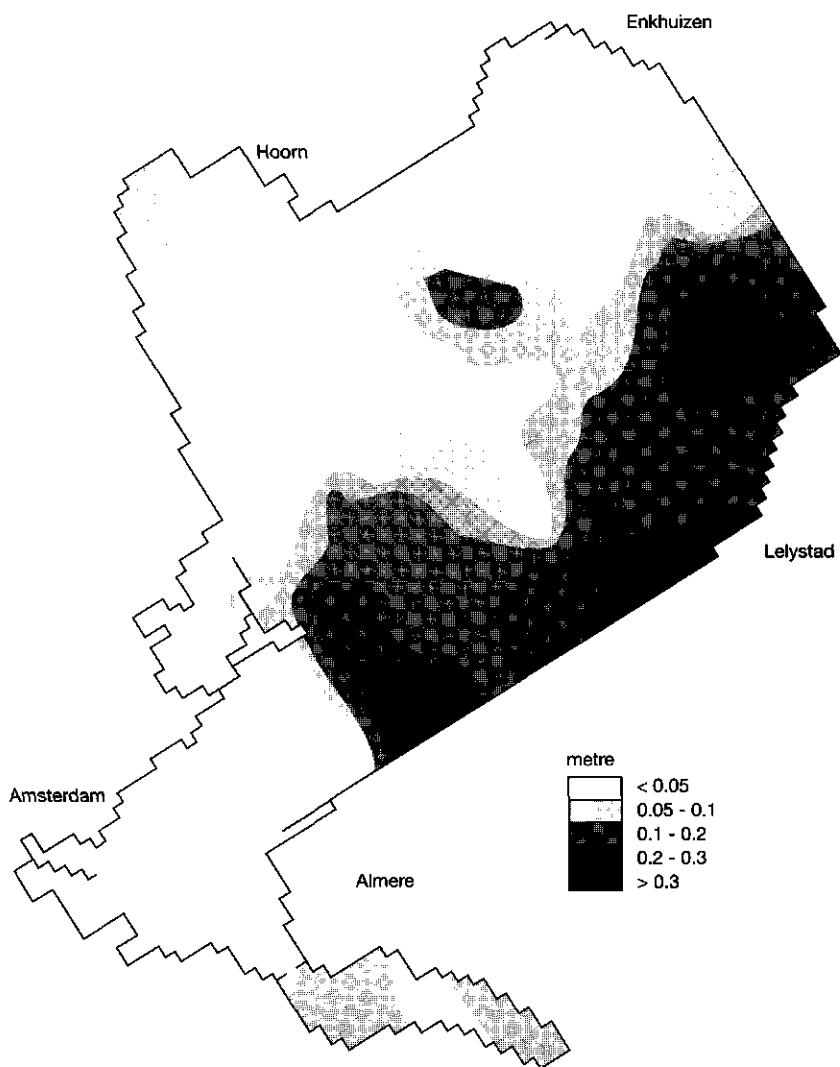


Figure 7.2 Simulated and observed water level at Y111 in 1988 and 1989

### 7.1.2 Sediment transport and the light field for the present conditions

Suspended solids concentrations and the under water light field often change dramatically within hours and differ considerably in each part of the lake. Short term calibration of *STRESS-2d* and *CLEAR*, focusing on hourly dynamics, were performed and are described in Chapters 4 and 5. Both models produced good results for short term simulation. Cumulative data over years are needed for long term validation of the models. Such data are only available of the thickness and location of the IJsselmeer deposit. The spatial distribution of the IJsselmeer deposit is the result of years of sediment transport and will not change dramatically within two years if the morphometry and morphology of the lake remains unchanged. The thickness of the bottom layer simulated with *STRESS-2d*, representing the thickness of the IJsselmeer deposit at the start of the simulation and after two simulated years, are presented in Figure 7.3. At the starting point of the simulation, two main areas are covered with a thick layer of IJsselmeer deposit; an area between the island of Marken and Almere and an area near Lelystad. Additionally, a small elliptical area in the middle of the lake is covered with a 10 centimetre layer. At the end of the simulation the two main areas still exist, but some relocation of material from the area near Lelystad to the area between Marken and Almere did occur. The elliptical area in the middle of the lake has disappeared. As no extensive relocation of sediment is expected to appear in two years, it may be concluded that the processes defined in *STRESS-2d* are sufficient for the simulation of sediment transport over periods of months to a few years, but for long term simulation model adaptations or recalibration is needed.



*Figure 7.3a Simulated thickness of the bottom layer at the start of the simulation (1 January 1988)*

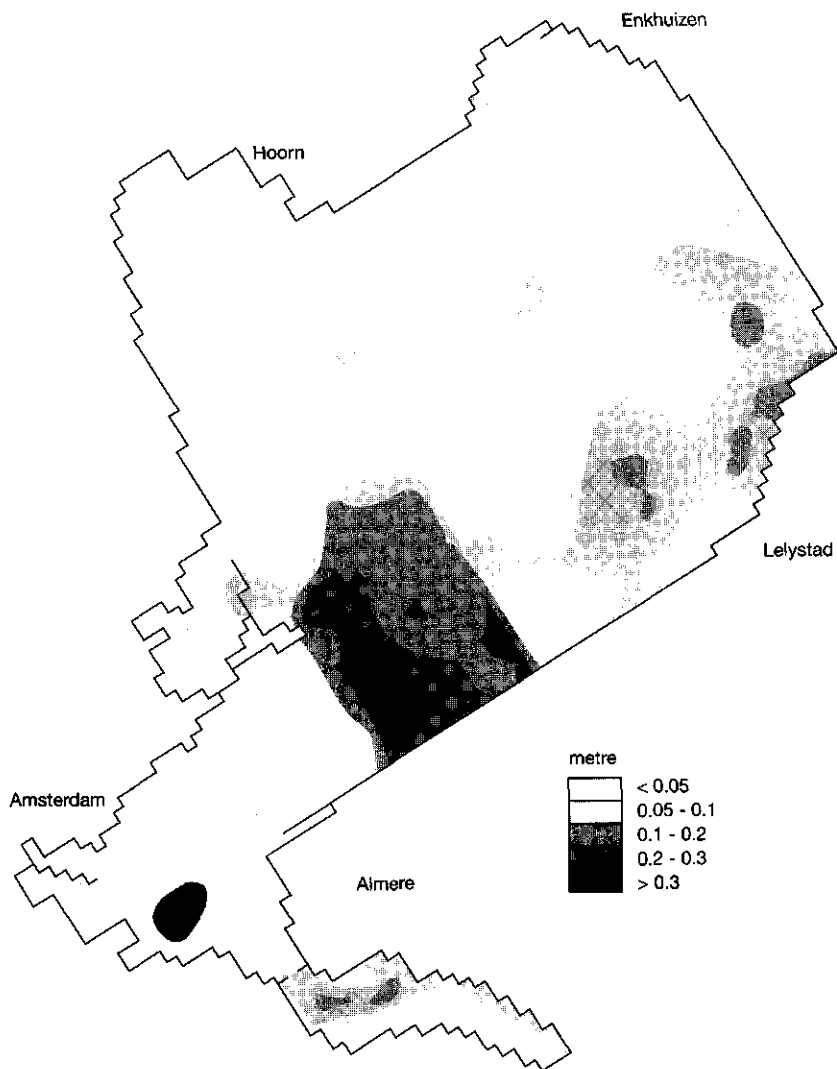


*Figure 7.3b Simulated thickness of the bottom layer at the end of the simulation (31 December 1989)*

To assess the spatial characteristics of sediment transport and light field in the lake through the years, the average sediment concentration and light attenuation in 1988 and 1989 are computed for 13 different sites in the lake. The location of the sites is presented in Figure 7.4.



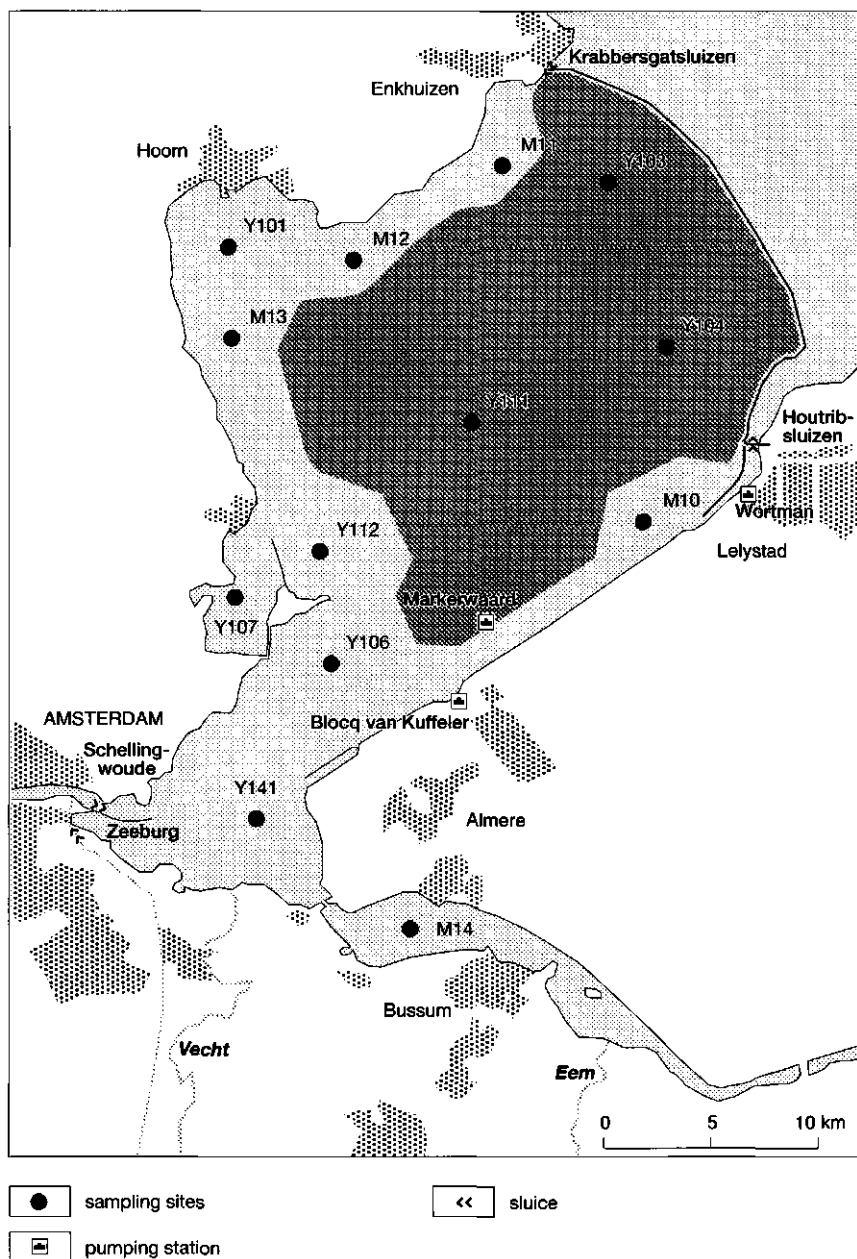


Figure 7.4 Location of the pilot sites

The biennial average values and the maximum daily averages are presented in Figure 7.5. As differences in wind speed and direction between 1988 and 1989 are small (§ 3.2.2), no distinction has been made between 1988 and 1989.

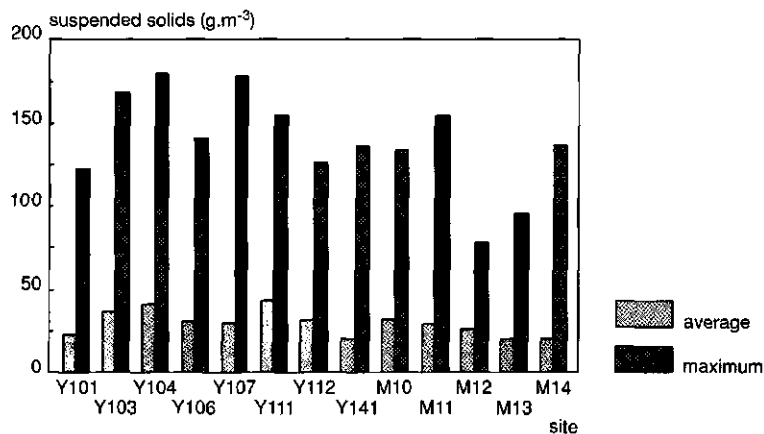


Figure 7.5 Biennial average and maximum daily average of simulated suspended solids concentration per site

The highest suspended solids concentrations are computed for the eastern part of the lake with the thick silt layer (Y104, Y111) and with the longest fetches during wind from the west (Y103). Occasionally, very high concentrations are found in the Gouwzee (Y107). In the Hoornse Hop (Y101, M12, M13) the average suspended solids concentrations are low because of the sheltered location during western winds and the sandy soil.

At most sites, the average concentrations of the fractions with the smallest fall velocity, SS<sub>1</sub> and SS<sub>2</sub>, are higher than those of fractions with the highest fall velocity (Figure 7.6). However, the maximum concentration of SS<sub>4</sub> is by far the highest. Hence, it may be concluded that the suspended solids concentration is mainly determined by the slowly settling fractions, but during stormy conditions the most important contribution is made by SS<sub>4</sub>. This is a direct effect of the composition of the sediment layers, in which SS<sub>1</sub>, SS<sub>2</sub> and SS<sub>3</sub> have low concentrations and thus are easily exhausted. If the maximum contribution to the suspended solids concentration of the various fractions is compared, the same tendency is observed. The contribution of SS<sub>4</sub> may reach up to 76 %. However the highest maximum contribution is found for SS<sub>1</sub>, up to 99 %, because the suspended solids may consist entirely of SS<sub>1</sub> during prolonged periods of low wind speeds.

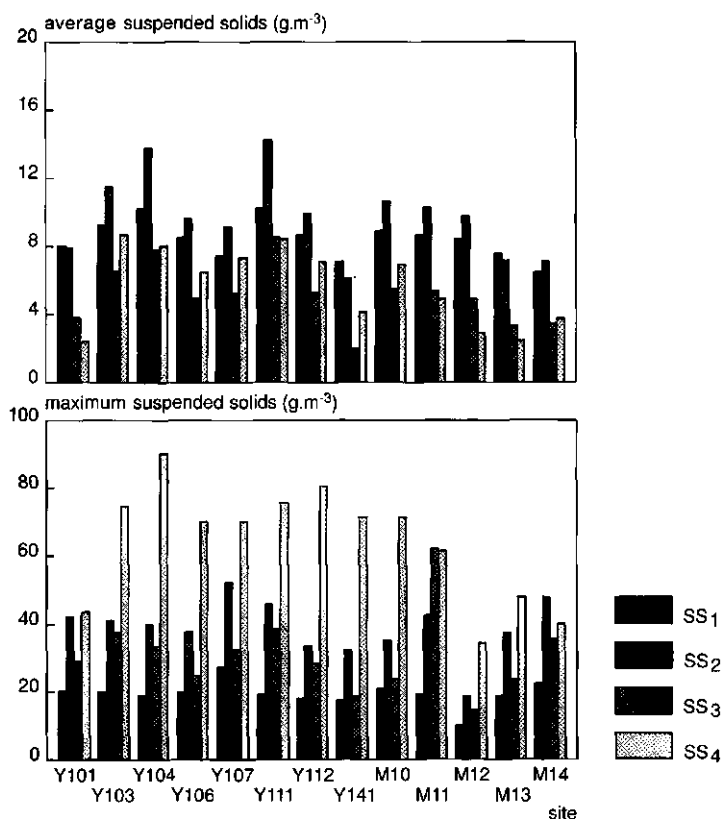


Figure 7.6 Biennial average and the maximum daily average of simulated suspended solids concentration of the various fractions per site

Two attenuation coefficients are computed,  $K_d\text{-SS}$  and  $K_d\text{-all}$ .  $K_d\text{-SS}$  is the attenuation coefficient derived from the attenuation by water, dissolved substances and sediment, but without the contribution of *O. agardhii* (Figure 7.7). In  $K_d\text{-all}$  all components included in the model *CLEAR* are combined.  $K_d\text{-all}$  is discussed along with the growth model (§ 7.1.3).

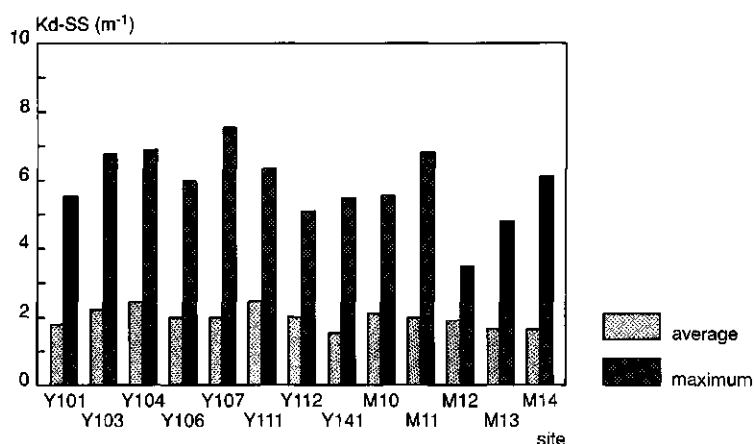


Figure 7.7 Biennial average and maximum daily average of simulated total attenuation per site

The variation in  $K_d\text{-SS}$  is entirely provoked by variations in the suspended solids composition. The spatial distribution of Figure 7.5 and 7.7 are very similar. However, the specific attenuation coefficients of the various fractions are rather different on a weight scale. Hence, the contribution of each fraction to the suspended solids concentration will differ from the contribution of each fraction to the attenuation coefficient. This is illustrated in Figure 7.8. The contribution of the fractions with the smallest fall velocity and resuspension constants,  $SS_1$  and  $SS_2$  constitute at least 70% of the total suspended solids concentrations on average. At the more sheltered sites with a sandy bottom in the IJmeer (Y141, Y106) and in the Hoornse Hop (Y101, M12, M13), this contribution reaches up to 80%. However, the contribution of the smaller fractions to the attenuation of light energy by suspended solids is at least 80% at all sites and reaches up to 90% of the attenuation by suspended solids. If the maximum contribution of the fractions to the suspended solids concentration and to the attenuation of light energy by suspended solids are compared, this tendency is even more noticeable: The maximum contribution of  $SS_4$  to the suspended solids concentration may reach up to 76%, but the contribution of  $SS_4$  to the attenuation of light by suspended solids is always less than 60%.

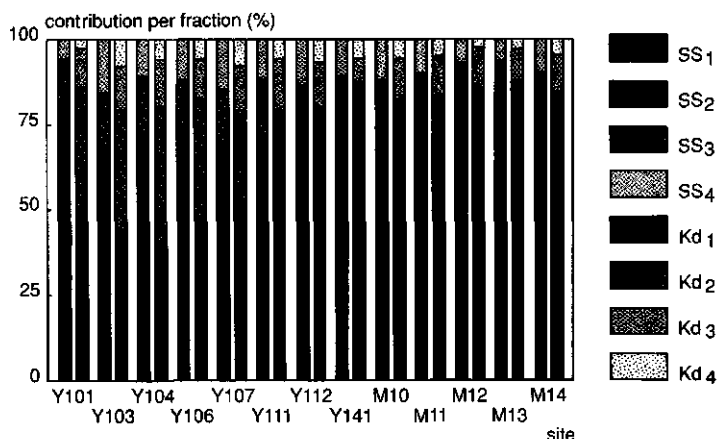


Figure 7.8 Contributions of the various fractions to the suspended solids concentration (SS) and to the total attenuation coefficient composed by water, dissolved substances and suspended solids ( $K_d$ -SS)

### 7.1.3 Simulation of the growth of *Oscillatoria agardhii* for the present conditions

The growth of *Oscillatoria agardhii* is simulated with the combined model *STRESS-2d*, *CLEAR* & *ALGA* for 1988 and 1989. The combined model is calibrated on the entire period as described in Chapter 6. Hence, validation on the same period is not significant. In the simulations described in this paragraph, the effect of flushing is incorporated. The discussion of results is restricted to some general observations on model efficiency and spatial effects.

In light limited phytoplankton populations, growth is expected to be higher in shallow parts for equal attenuation coefficients. However the attenuation coefficients in shallower areas are lower on average than in the deeper parts and thus growth of *O. agardhii* can be expected to be even higher in the coastal shallower areas. Mixing of course will smooth gradients. These processes are simulated by the integrated model, as is illustrated in Figure 7.9, which shows the spatial distribution of *O. agardhii* concentrations at noon in four successive weeks in the summer of 1989. During these weeks, the *O. agardhii* concentration increase gradually. At a certain time, concentrations decrease toward the middle part (deeper) of the lake and towards the lee-shore (higher attenuation). Mixing is a slow but important factor determining the concentrations.

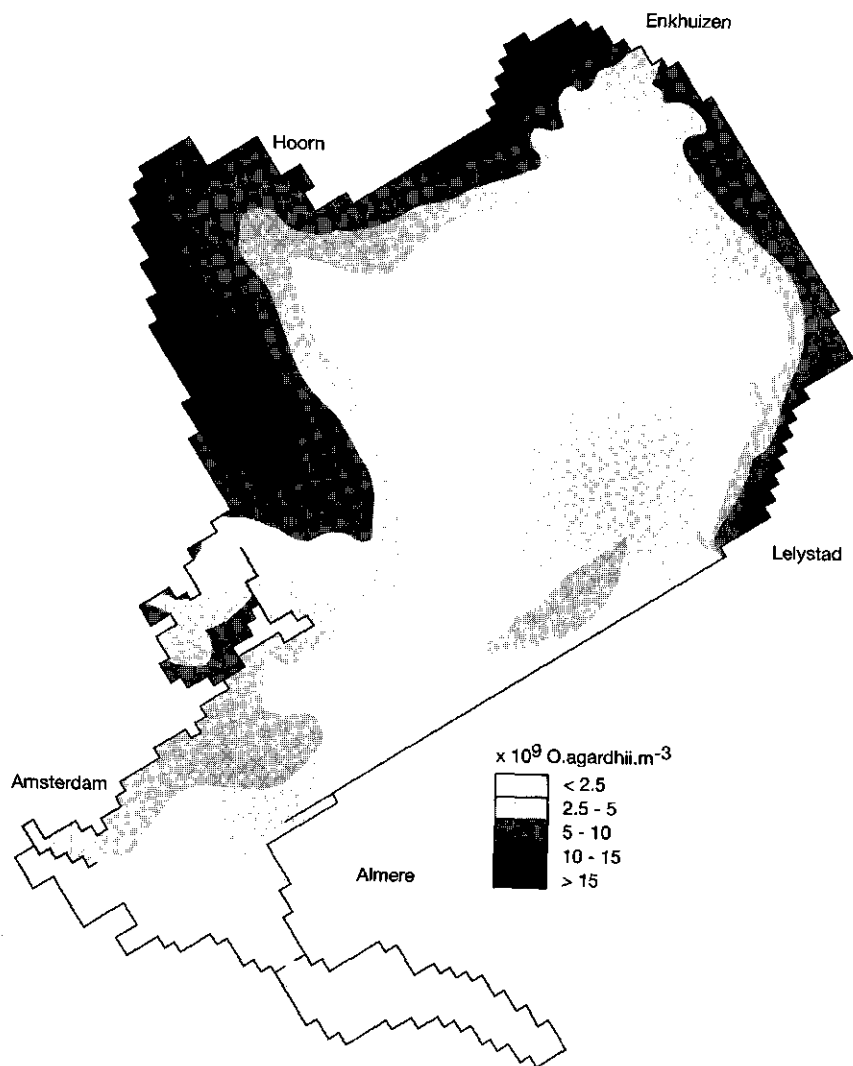
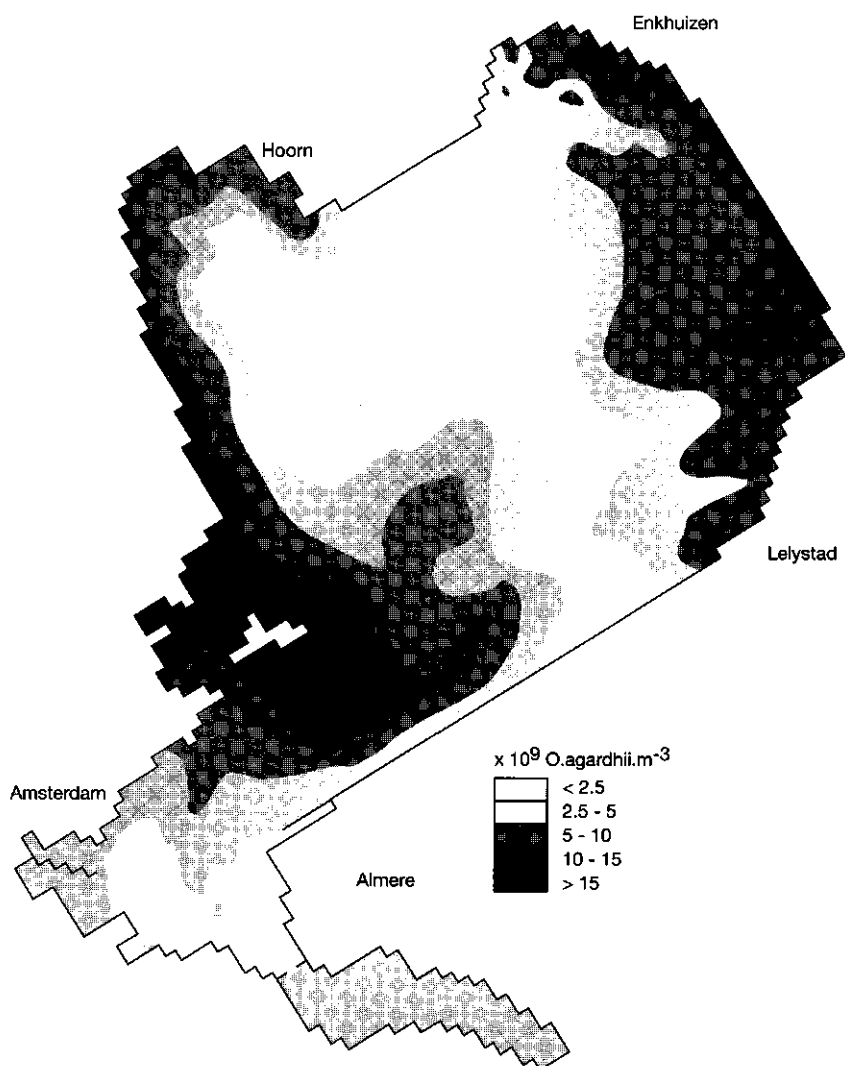


Figure 7.9a Simulated spatial distribution of *O. agardhii* around noon at 19 June 1989 in the Markermeer



*Figure 7.9b Simulated spatial distribution of O.agardhii around noon at 26 June 1989 in the Markermeer*

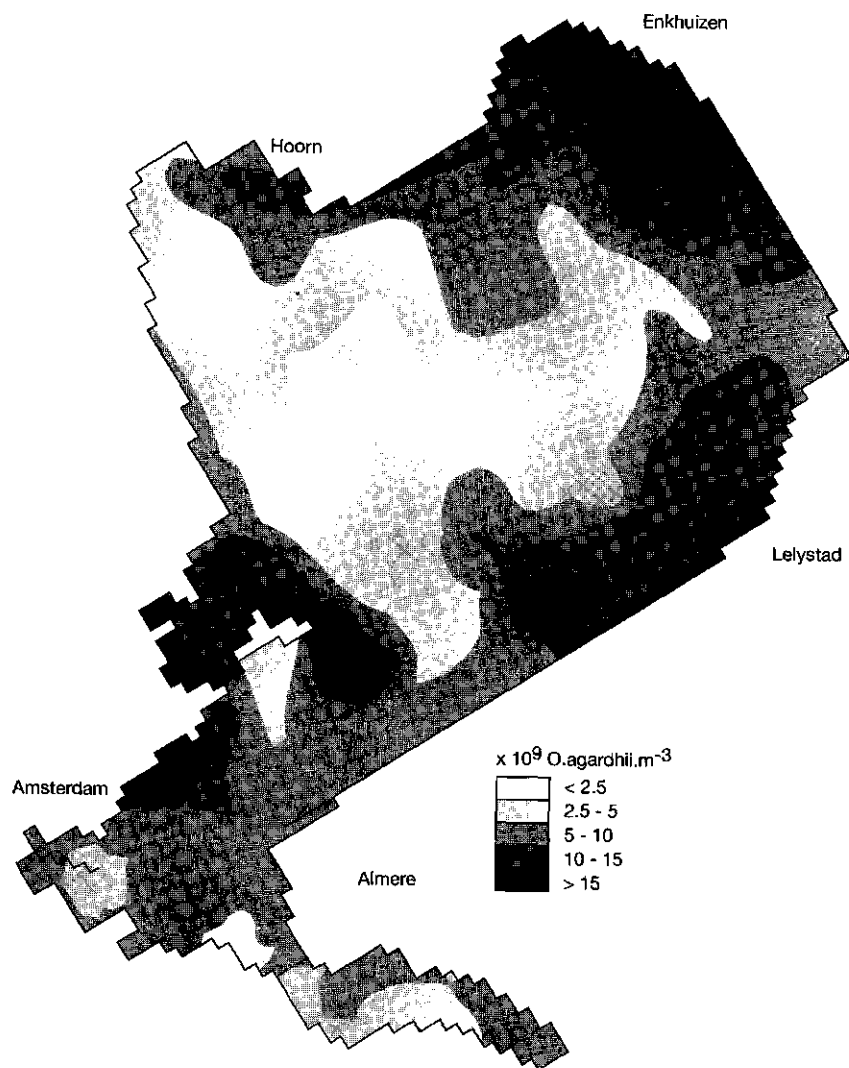


Figure 7.9c Simulated spatial distribution of *O. agardhii* around noon at 3 July 1989 in the Markermeer



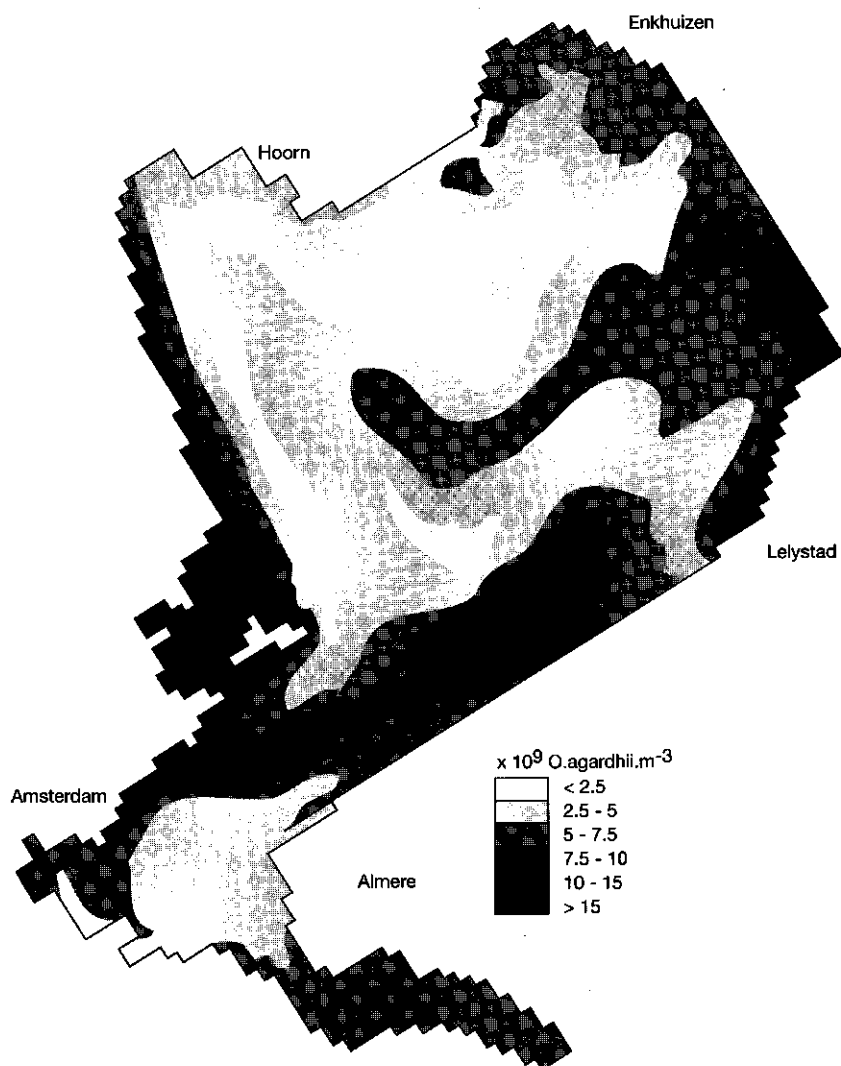


Figure 7.9d Simulated spatial distribution of *O. agardhii* around noon at 10 July 1988 in the Markermeer

The summer of 1988 is characterized by low temperatures and little sunshine and is in contrast with the summer of 1989 which is characterized by high temperatures and a lot of sunshine. The simulated concentration of *O.agardhii* is much higher in 1989 than in 1988. This is illustrated for site Y111 and Y112 in Figure 7.10 and for four additional sites in Figure 7.11.

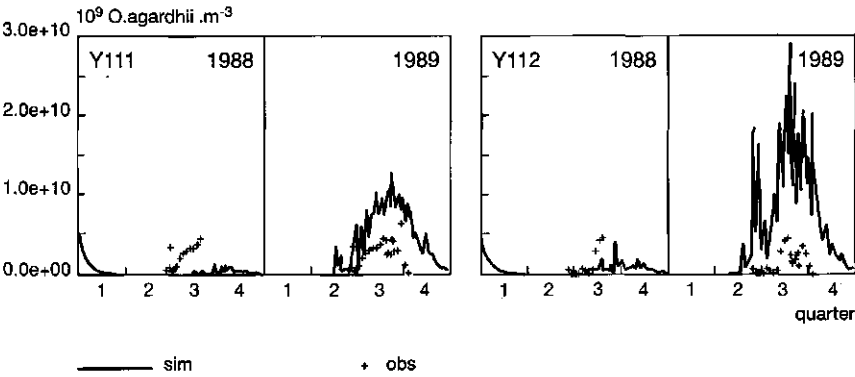


Figure 7.10 Time series of the simulated and measured concentration of *O.agardhii* for the present situation at site Y111 and Y112

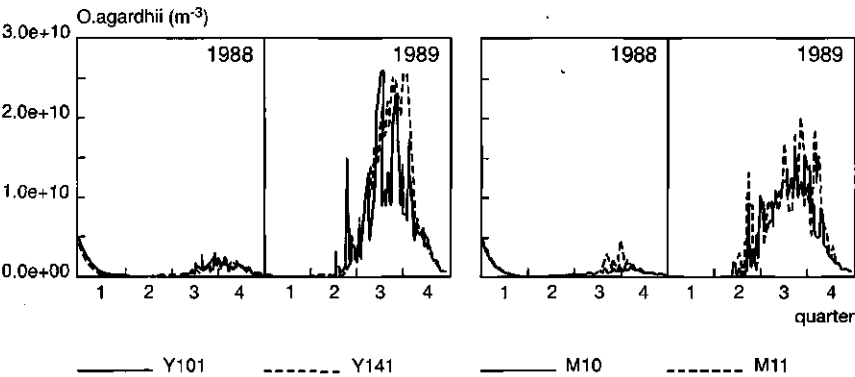


Figure 7.11 Time series of the simulated concentration of *O.agardhii* for the present situation at a site in the Hoornse Hop (Y101), a site in the IJmeer (Y141), a site near Lelystad-Haven (M10) an a site near Enkhuizen (M11)

By comparing simulated and observed values it is evident that the model efficiency is small. The model behaviour for the deeper part of the lake represented by Y111, is more accurate than that of the shallower parts (Y112). The effect of available light energy is clear: simulated values of 1988 are too small, values for 1989 are too high, especially at Y112. The lower measured concentration of *O.agardhii* in 1989 may be attributed to competition for phosphorus, which is not incorporated in the model. But difference between shallow and deep areas are not explained that easily. These differences are hard to explain, considering the knowledge of the occurrence of *O.agardhii* in the other lakes in the IJsselmeer area and the hypothesis of light limited growth of *O.agardhii* in the Markermeer. It may be concluded that though the model ALGA may produce acceptable results for the Wolderwijd and the IJsselmeer, its results for the Markermeer are still poor, which is not improved by incorporation in the integrated model. This may be attributed to a number of reasons; the simple description of the loss rate, the exclusion of competition effects, the unrefined description of nutrient limitation, the fact that slow adaptation of growth parameters is not included in the model, etcetera. All these reasons make that application of the biological model for the estimation of the effect of various management measures on the phytoplankton population in the Markermeer should be done with great care.

In Figure 7.12, the average *O.agardhii* concentrations are presented, simulated with the integrated model at 13 sites. Two sites are very different from the rest of the area: the Gouwzee (Y107) and the Gooimeer (M14). Differences between various sites in the main water body and in the IJmeer (Y141, Y106) occur, average concentrations in the IJmeer are slightly higher, but these differences are smoothed by mixing.

In the combined model, *O.agardhii* cells contribute to the attenuation coefficient and therefore self shadowing effects may occur. In Figure 7.13 the average and maximum total attenuation coefficient by water, dissolved substances, suspended solids and *O.agardhii* cells per site is presented. The average and maximum relative contribution of the simulated *O.agardhii* concentration is presented in Figure 7.14. Again, values simulated for the Gouwzee and Gooimeer (Y107, M14) are very different from the rest of the area. At those sites a high total attenuation coefficient with a high contribution of *O.agardhii* is simulated. In the rest of the lake, where the total attenuation coefficient is comparable, the average contribution of *O.agardhii* varies between 5 and 10%. In the IJmeer (Y141, Y106) and the Hoornse Hop (Y101, M12, M13) the average total attenuation coefficient is slightly lower and the contribution of *O.agardhii* slightly higher than in the deeper silty part of the lake. These results underline the importance of two-dimensional models for the simulation of *O.agardhii* growth, as far as variations in space and the exchange by mixing processes is concerned.

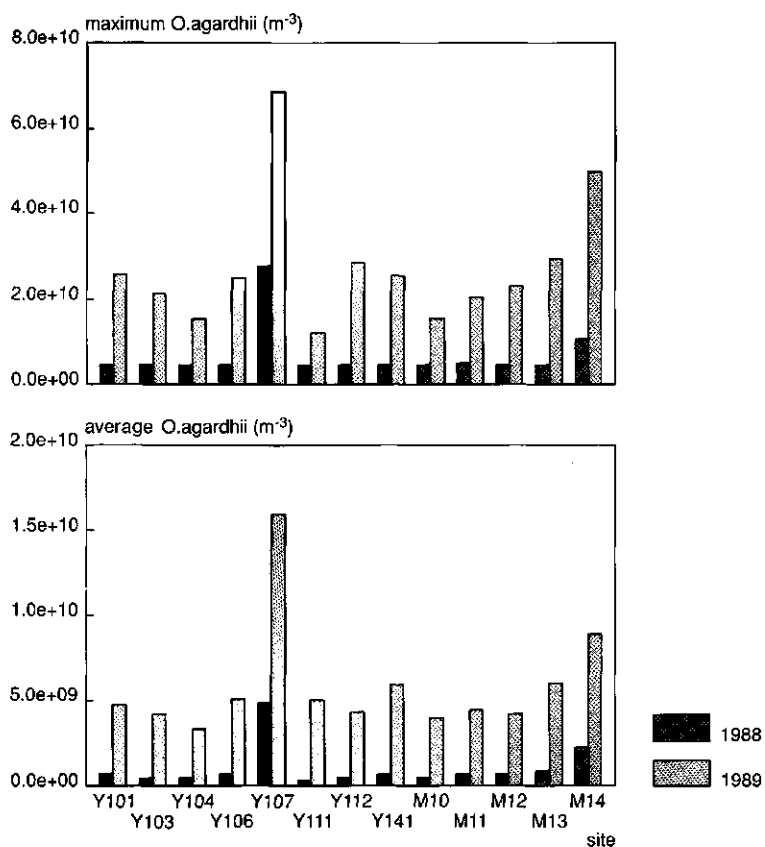


Figure 7.12 Annual average and maximum daily average of the simulated concentration of *O. agardhii* per site

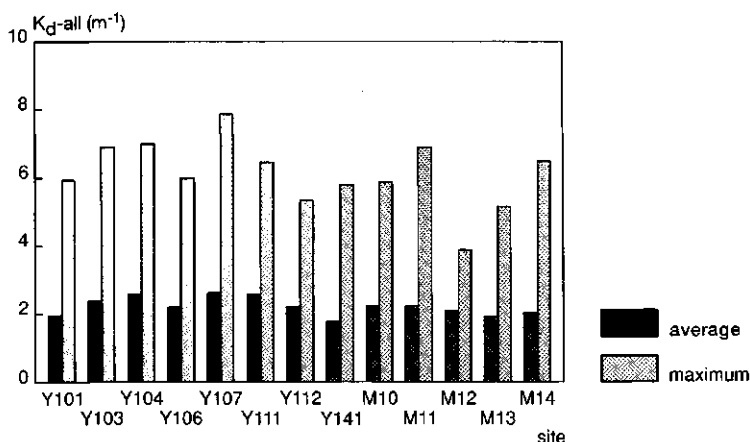


Figure 7.13 Biennial average and maximum daily average of the total attenuation coefficient ( $K_{d-all}$ ) per site

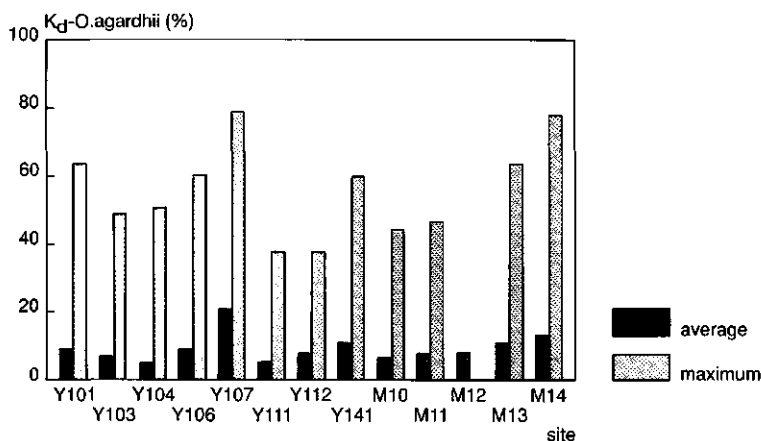


Figure 7.14 Biennial average and maximum daily average of the contribution of *O.agardhii* to the total attenuation coefficient ( $K_{d-O.agardhii}$ ) per site

In Figure 7.15, the average *O.agardhii* concentration is related to the average attenuation coefficient by water, dissolved substances and suspended solids, resulting in a linear relationship for the sites in the IJmeer and the main water body. The situation for the Gouwzee and Gooimeer is (again) entirely different. The simulation results of the growth of *O.agardhii* with the combined model, emphasize the importance of a two-dimensional approach as far as the spatial variability and the effects of mixing are concerned. As the simulation of observed

*O.agardhii* values is insufficient, the applicability of the model in scenario studies is limited.

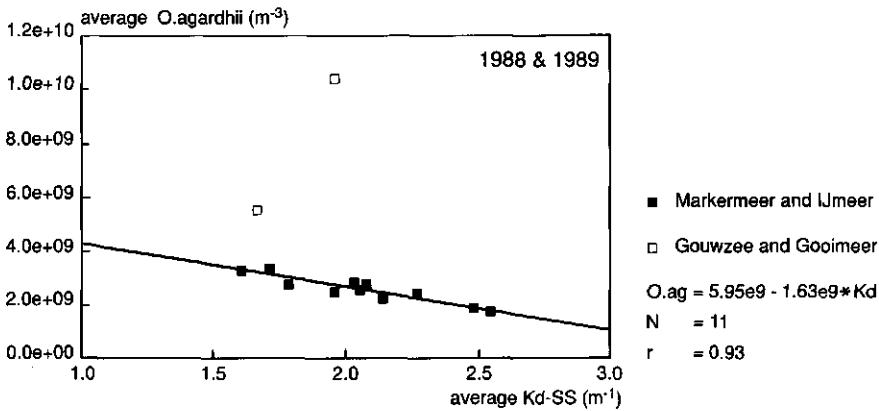


Figure 7.15 Biennial average of the simulated concentration of *O.agardhii* versus the biannual average of the simulated attenuation by suspended solids (average  $K_d$ -SS)

## 7.2 Simulation of the conditions after the inpoldering of the Markerwaard

In the history of the Zuiderzee project, the time tables and the design of the project changed as often as decision making and implementation were delayed. The construction of the Markerwaard has been postponed again in 1985, in 1990 the cabinet abandoned the project for the time being. During all the discussions many different plans for the Markerwaard were proposed. If in the near future the project shows up again, probably a new design will be proposed with it. However, to illustrate the usefulness of the model in the assessment of the inpoldering on sediment transport, the light field and the growth of *O.agardhii* the design known as the "Verkenningen Variant" (Rijkswaterstaat et al, 1985) is used. The boundaries are included in Figure 7.4.

### 7.2.1 Incorporation of the polder Markerwaard in the model schematization

The inpoldering of the Markerwaard will have an enormous effect on the morphometry of the lake, as only one third of the lake remains open water and instead of one large open water area, a string of lakes is created. The schematization of the lake remaining is presented in Figure 7.16.

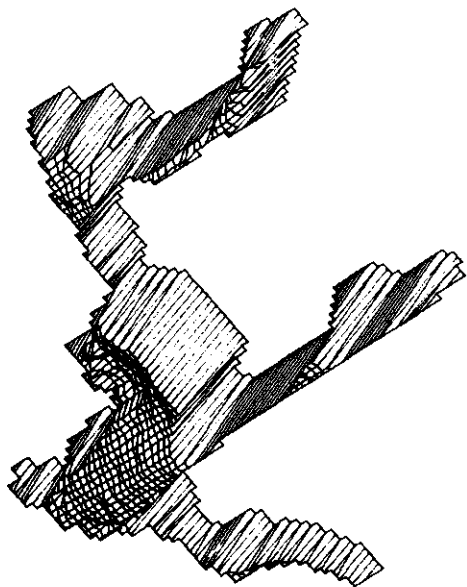


*Figure 7.16 Depth schematization of the lake remaining after reclamation*

The effect on the morphology of the lake is immense as well, as the thick layers of IJsselmeer deposit are entirely enclosed by the Markerwaard dike. Hence, in the remaining lake only the thin top layer of resuspendable material remains. However, probably during the construction of the Markerwaard-dike itself, stream patterns and internal sediment transport will change, therewith changing the morphology of the remaining water areas.

The effect of flushing after the construction of the Markerwaard will be more drastic than in the present situation. With the current flushing policies, combined with the additional discharges of the Markerwaard, the residence time of the water in the lakes, remaining after the construction of the Markerwaard, will be reduced to an average of 0.5 year. The discharge of the Markerwaard is estimated as the sum of seepage and nett precipitation. With a total seepage of  $0.7 \text{ mm} \cdot \text{day}^{-1}$ , the nett discharge is estimated at  $275 \cdot 10^6 \text{ m}^3 \cdot \text{year}^{-1}$  for 1988 and  $169 \cdot 10^6 \text{ m}^3 \cdot \text{year}^{-1}$  for 1989. For financial reasons, the construction of one single pumping station located at the Oostvaardersdiep is most feasible (Rijkswaterstaat et al, 1985). It is feasible that new flushing policies will be implemented, after the reclamation of the Markerwaard, but for these simulations no change in flushing policy is assumed. Two additions are made however: the discharge of the Markerwaard at the Oostvaardersdiep and the extra outlet of the same amount of water at Schellingwoude. In the simulations

of the combined model, the same procedure is used to modify the water balance as described in § 7.1.1.

If the same emissions are discharged after the construction of the Markerwaard on a much smaller lake area, the loads of pollutants like phosphate and chloride will increase. With the additional discharge of the Markerwaard itself, the loads on the lake per unit area will at least triple. On the other hand, mixing between the various small lake branches is limited and discharges are not evenly distributed along the lake. However, affect of changes in loads on the nutrient concentrations are not considered in the simulations, because only an elementary nutrient limitation is incorporated in the model.

### *7.2.2 Sediment transport and the light field for the Markerwaard conditions*

The effect of the construction of the Markerwaard on the sediment transport and the light field in the remaining water area is vast. The description of this change has been the main reason for the model development in the first place. To grasp the effect on the sediment transport, suspended solids concentrations at ten sites are compared for the current situation and after the construction of the Markerwaard in Figure 7.17. The location of the sites is included in Figure 7.4. The construction of the Markerwaard results in an overall decrease of the average suspended solids concentration of 1988 and 1989 in the remaining water areas. The effect is most pronounced at sites M10 and M11; sites in areas that are then located in secluded water areas. The effect is less pronounced in the IJmeer (Y106, Y141) and hardly noticeable in the Gooimeer (M14) and the Gouwzee (Y107). Tendencies found in the average suspended solids concentration are repeated in the maximum suspended solids concentration, except for site M12. Due to changes in stream patterns, the maximum suspended solids concentration at M12 is higher after the construction of the Markerwaard than before. The effect on the suspended solids concentration is mainly caused by decreases in fetch lengths and stream patterns. But during the construction of the Markerwaard dike portions of the IJsselmeer deposit may be relocated to areas where in the current situation little of these deposit is found. In that case, the suspended solids concentration after the construction of the Markerwaard may actually be higher than simulated under the current boundary conditions.



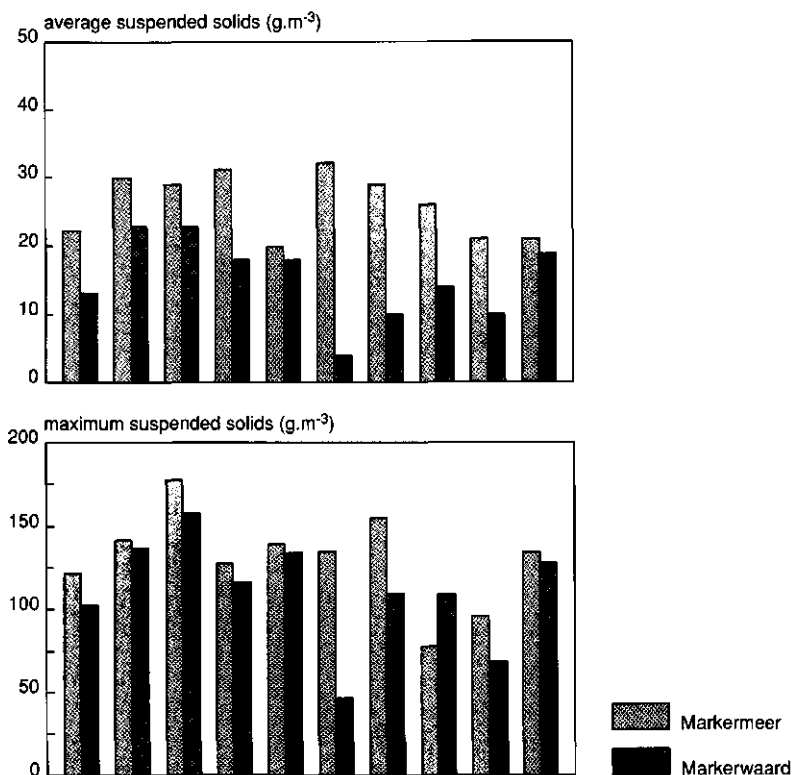


*Figure 7.17 Comparison of the biennial average and maximum daily average of the simulated total suspended solids concentration for the present situation (Markermeer) and after the construction of the Markerwaard*

Except for a direct effect on the total suspended solids concentration, the construction of the Markerwaard will also change the suspended solids composition and the fall velocity distribution. The contribution of the various fractions to the total suspended solids concentration in both situations is presented in Figure 7.18. A general decrease in fetches will tend to decrease the contribution of the larger fractions to the suspended solids concentrations. On the other hand, a decrease in exchange between the different lake areas will decrease the supply of suspended solids from other lake areas and increase the contribution of local resuspended material. A decrease in sediment transport thus may increase the contribution of the largest fraction. In Figure 7.18 both effects are observed. However, the effect on suspended solids composition seems much smaller than the effect on total suspended solids concentrations. Thus, the effect on the attenuation coefficient of the decrease in suspended solids concentration is much larger than the effect of the change in sediment composition. The differences in the simulated

attenuation coefficients for the present situation and after construction of the Markerwaard, will be very similar to the differences between the suspended solids concentrations of both situations.

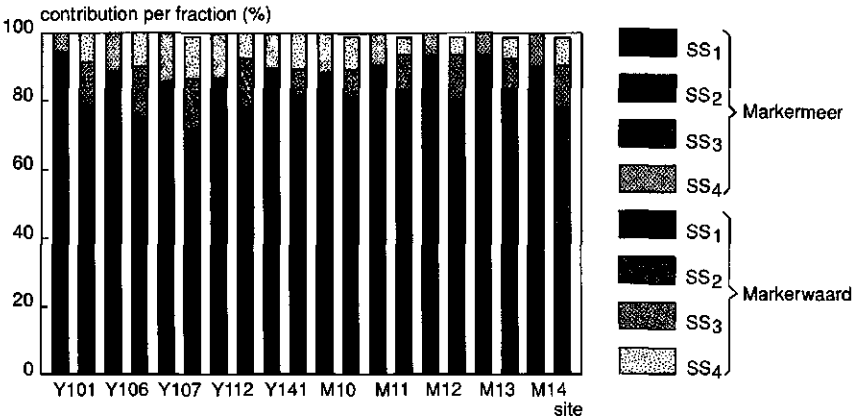


Figure 7.18 Contribution of the various fractions to the total suspended solids concentration for the present situation (Markermeer) and after the construction of the Markerwaard

### 7.2.3 Simulation of the growth of *Oscillatoria agardhii* for the Markerwaard conditions

The effect on the simulated concentration of *Oscillatoria agardhii* is summarized in Figure 7.19. The construction of the Markerwaard causes a general increase in the simulated concentration of *O. agardhii*. Though this increase is large, the differences between two different years are still greater than the differences between the two scenarios. The simulated *O. agardhii* concentrations for 1988 after construction of the Markerwaard approach the simulated numbers for the present situation of 1989. Hence, the effect of little sunshine may be compensated for by a lower attenuation by suspended solids and a decreased exchange between shallow and deeper parts. Simulated concentrations after the construction of the Markerwaard in the Gooimeer (M14) are scarcely affected, in the Gouwzee (Y107) the average concentrations actually decrease in 1988, probably due to the shorter residence time. The effect of the Markerwaard on the light limited growth of *O. agardhii* is a general increase in *O. agardhii* numbers. For a year with little sunshine like 1988, the relative effect is extensive, and the scales towards blooming of *O. agardhii* may actually be tipped. However, it should be realised that these results are preliminary as the quality of the prediction by the model ALGA is still limited. The effect of measures like changes in residence time, changes in shape or size of the Markerwaard, etc, on the concentration of *O. agardhii* can be simulated, in order to study effective measures against an increase in growth of *O. agardhii*.

In Figure 7.20 time series of simulated *O.agardhii* concentrations for the present situation and after construction of the Markerwaard are compared. In this figure the effect of the shorter residence time is clear. At Y101 and Y112 concentrations are higher after construction of the Markerwaard, but the peaks in concentrations are less pronounced. At M10, the residence time is too short to allow peak growth and concentrations are levelled of to the level of the IJsselmeer.

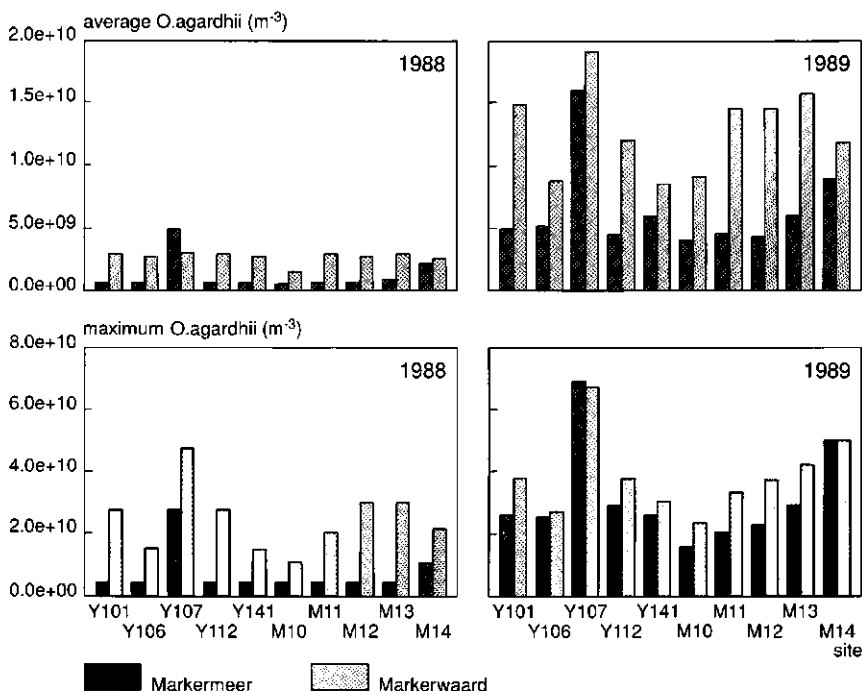


Figure 7.19 Comparison of the biennial average and maximum daily average of the simulated *O.agardhii* concentration for the present situation (Markermeer) and after the construction of the Markerwaard

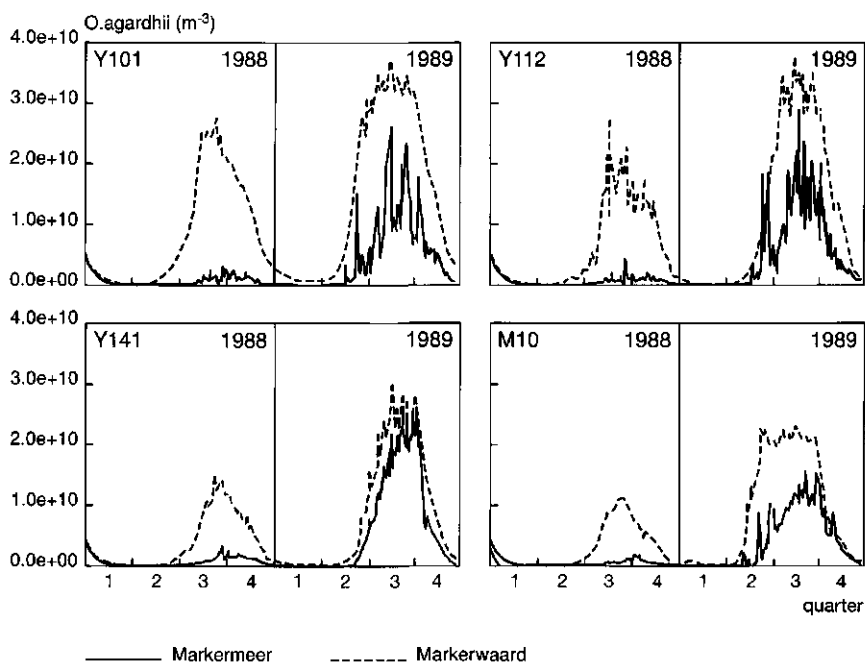


Figure 7.20 Comparison of time series of the simulated *O. agardhii* concentration for the present situation and after construction of the Markerwaard at four sites

### 7.3 Simulation of the conditions during increased flushing

To simulate the effect of increased flushing on the phytoplankton concentrations a second flushing strategy is formulated. The numbers are based on a proposed strategy to decrease the chloride concentration in summer, in order to improve the water quality of the water for agricultural purposes (Van Hoorn and Kolvoort, 1991). In this strategy, the outlet of water through the Oranjesluices (Schellingwoude) is increased up to  $40 \text{ m}^3 \cdot \text{s}^{-1}$  in winter and  $70 \text{ m}^3 \cdot \text{s}^{-1}$  in summer. In the present flushing strategy the average discharge through the Oranjesluices was  $11 \text{ m}^3 \cdot \text{s}^{-1}$  in 1988 and 1989, with an average monthly value of  $32 \text{ m}^3 \cdot \text{s}^{-1}$  in the summer of 1989. The effect on the water balance of the proposed strategy is far-reaching as the residence time of the water would decrease from two years to one.

#### 7.3.1 Incorporation of increased flushing in the model

To maintain observed water levels in the model simulation, increased flushing with discharges of  $40 \text{ m}^3 \cdot \text{s}^{-1}$  in winter and  $70 \text{ m}^3 \cdot \text{s}^{-1}$  in summer is implemented in the artificial water balance discussed in paragraph

§ 7.1.1. The same amount of water has to be discharged into the lake. This amount is distributed over the Houtrib- and the Krabbersgatsluices in a ratio of 4:1. This ratio is based on the capacity of the sluices, which are estimated at 800 and 200 m<sup>3</sup>·s<sup>-1</sup> respectively. The modified water balance is summarized in Appendix 16. As the discharges are adapted in order to maintain observed water levels, the concentration of cell numbers *O.agardhii* in the discharges of the Krabbersgat- and Houtribsluices are adapted as well, the resulting concentration is presented in Figure 7.21. However, the adaptations are much smaller than in the case discussed in § 7.1.1. As the discharge into the lake is much larger the necessary corrections are smaller.

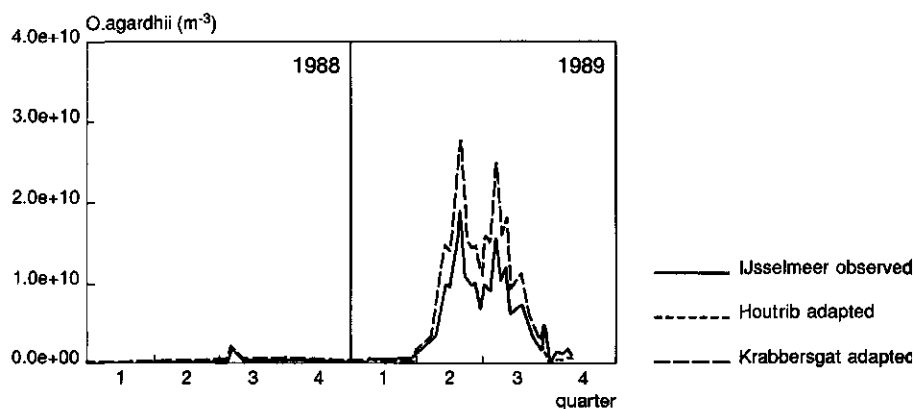


Figure 7.21 Observed and adapted *O.agardhii* concentrations in discharged water from the IJsselmeer for increased flushing

### 7.3.2 Sediment transport and the light field during increased flushing

The effect of flushing on sediment transport is small, the effect on resuspension and sedimentation is nil. A small amount of sediment is withdrawn from the system as the sediment concentration of the water leaving the area is the same as the concentration at the site of the outlet. However, the residence time of the sediment in the water is very short and the supply of sediment from the silty part of the lake is that high, that no detectable effects on the simulated sediment concentrations are observed.

A significant effect on the total underwater irradiance can be expected for the contribution by *O.agardhii* to the attenuation coefficient.

### 7.3.3 Simulation of the growth of *Oscillatoria agardhii* during increased flushing

The effect of flushing on the simulated numbers of *O.agardhii* is shown in Figure 7.22. Except for a tiny increase, the effect on the biennial average concentration is hardly noticeable on most sites. The increase of the *O.agardhii* concentration is caused by the high number of *O.agardhii* cells in the IJsselmeer water, discharged through the Houtrib- and Krabbersgatsluices (Figure 7.21). The expected effect should be most marked on the concentration at M10, due to its location very near the Houtribsluices, while 80 % of the extra discharged water is discharged through these sluices. However, even at this site the effect is hardly traceable.

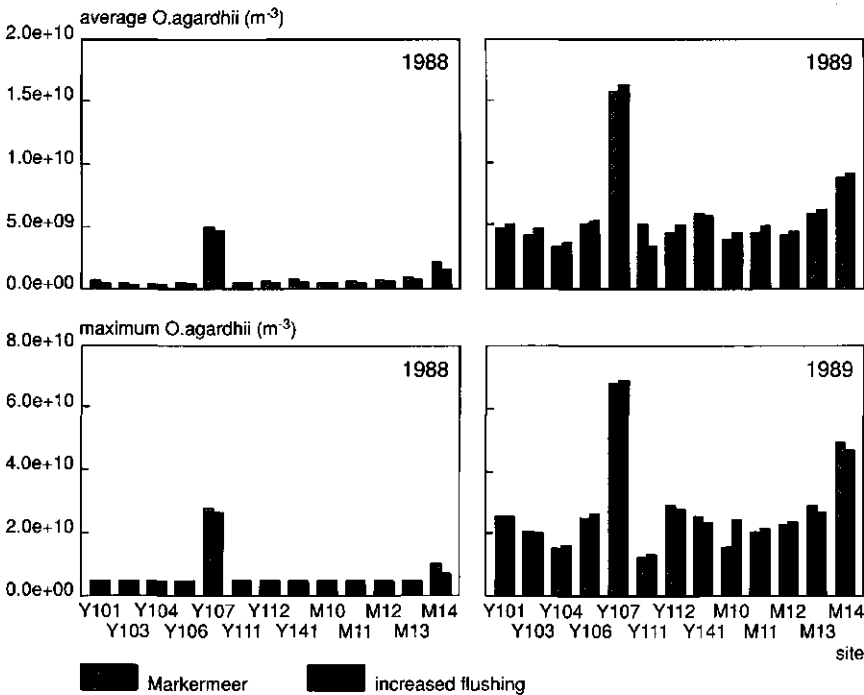


Figure 7.22 Comparison of the biennial average and maximum daily average of the simulated concentration of *O.agardhii* for the present situation (Markermeer) and with increased flushing

In Figure 7.23, the simulated *O.agardhii* concentration is presented at four sites Y101, Y111, Y141 and M10. The effect on the concentration in the IJmeer (Y141) and the main water body (Y111) is untraceable. The trend at site M10, near the Houtribsluices, shows a new peak in July 1989, caused by a high concentration of *O.agardhii* in the discharged

water from the IJsselmeer. In reality this effect will be less pronounced as the actual concentration is somewhat lower, but has been adapted for the simulations to equalize the water balance (Figure 7.21).

As the suspended solids concentration are not noticeably affected by increased flushing and the effect on the *O.agardhii* concentration is only minor, no important effect on the under water light field is observed.

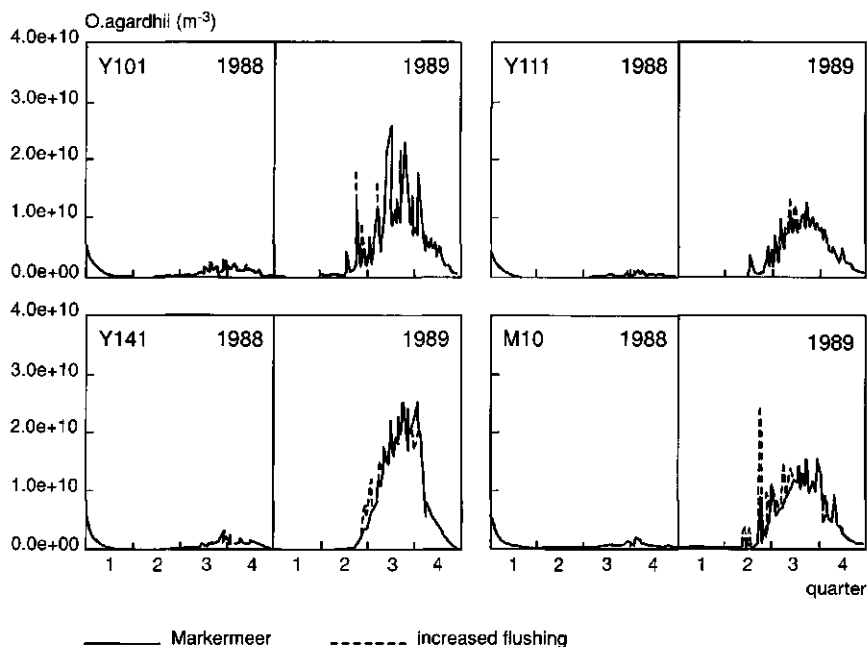


Figure 7.23 Comparison of time series of the simulated *O.agardhii* concentration for the present situation and with increased flushing at four sites

## 8 Conclusions

The main objectives of the Markermeer study, as described in this thesis, are:

- to increase the insight and the quantitative information on the relationships between the growth of *O. agardhii* and the controlling characteristic physical conditions of the lake, focusing on the effect of wind-wave induced resuspension of suspended solids on the light field;
- to develop a deterministic model that describes the relationship between suspended solids, the light field and the growth of *Oscillatoria agardhii* (Figure 1.2).

It can be concluded that, with the exception of the modelling of the growth of *Oscillatoria agardhii*, these objectives are met. This is discussed in some more detail in the following paragraphs.

### 8.1 Characterisation of the physical conditions

The results of the weekly measurements confirmed that both the suspended solids concentration and the attenuation coefficient of light energy are often high and very fluctuating.

#### 8.1.1 Suspended solids

From the data of the weekly measurements it can be concluded that the suspended solids content of the water varied both in time and in space between 7 and 180 g·m<sup>-3</sup>, with average values between 40 and 50 g·m<sup>-3</sup>. The composition of the suspended solids was variable too: the percentage of organic matter of the total suspended solids varied between 15 and 75%, with an average value around 38%. This ratio decreased when the content of the total suspended solids rose. Hence, resuspension of sediment does not only increase the content of total suspended solids but changes the composition of the suspended solids as well. Vertical gradients of suspended solids content were hardly ever observed.

The sedimentation flux increased when the concentration of suspended solids concentrations increased. The sedimentation flux at a certain site may vary between 1 and 200 g·m<sup>-2</sup>·h<sup>-1</sup>. The internal load of the lake is in the order of magnitude of one billion tons per year. From fall velocity experiments it can be deduced that the fall velocity distribution also varies when variations in the suspended solids concentration occur. The contribution of the fractions with a high fall velocity to the total suspended solids concentration increased when the concentrations of suspended solids grew. During stormy events, significant wave height rose up to 1 m and sediment was resuspended and distributed over the water column. If the wave characteristics grew, and therewith the driving force for resuspension, the amount of suspended sediment increased and the contribution of the solids with a higher fall velocity to the total sus-



pended solids concentration increased as well. Hence, a certain relationship is established between the resuspension characteristics and the sedimentation characteristics of the lake sediment. The mean fall velocity of the suspended solids ranges from  $10 \cdot 10^{-6}$  to  $100 \cdot 10^{-6}$  m·s<sup>-1</sup>.

### 8.1.2 *Light field*

From weekly measurements of the vertical downward attenuation coefficient in 1988 and 1989 at Y111 and Y112, it can be concluded that the attenuation coefficient in the Markermeer is often high and very variable indeed. The average measured value of the vertical downward attenuation coefficient was 3.8 m<sup>-1</sup> at Y112 and 3.4 m<sup>-1</sup> at Y111. The minimum and maximum measured values were respectively 0.4 and 11.4 m<sup>-1</sup>. The linear correlation between the measured attenuation coefficient and the total suspended solids concentration at a specific site was high for 1988, 0.91, but much lower for 1989, 0.78. The estimated regression curve is different for both years, probably due to the variable composition of the suspended solids in both years. Variations in suspended solids compositions were accounted for in measurements of the beam attenuation coefficient with samples from the fall velocity experiments (§ 8.1.1). From these measurements, the specific beam attenuation coefficient of the various fractions is estimated. This method is not very accurate but the results showed that suspended solids with different fall velocities have different attenuation characteristics as well. With linear regression results of the vertical downward attenuation coefficient and the beam attenuation coefficient, the specific vertical downward attenuation coefficient was computed for each fraction. These results show that the specific attenuation coefficient is higher for suspended solids with lower fall velocities than for suspended solids with higher fall velocities.

With the estimated specific attenuation coefficients, the estimated background attenuation by dissolved substances, the chlorophyll-a data and the average concentrations of the components, the contribution of the various components to the total attenuation of light energy was estimated. The contribution of chlorophyll-a, suspended solids and the background attenuation were respectively 25, 57 and 18%. The contribution of 57% by suspended solids originated for 30% from the fraction with the smallest fall velocity, SS<sub>1</sub>, for 18% from SS<sub>2</sub>, for 5% from SS<sub>3</sub> and for 4% from SS<sub>4</sub>.

Continuous measurements of irradiance at three depths at both sampling sites are used to estimate hourly variations in the attenuation coefficient. In these measurements a slight decrease of the attenuation coefficient with the depth was observed, but this effect was often obscured by the inaccuracy of the used sensors. In fact, it was experienced that the utmost care is needed in the method of sensor installation and calibration, and in the measurement itself. The slight decrease in attenuation coefficient was also observed in the weekly manual measurements as

long as the water in the Markermeer was relatively clear. In turbid water this effect could not be noticed.

## **8.2 Relationships between sediment transport and the light field and the growth of *Oscillatoria agardhii***

With the results of the on site experiments in the Markermeer, performed with *O.agardhii* suspensions obtained from the Nijkerkernauw, the insight and the quantitative information on the relationships between the growth of *O.agardhii* and the characteristic physical conditions of the Markermeer have increased.

### **8.2.1 Monitoring**

Weekly field measurements at Y111 and Y112 in the Markermeer, showed that the chlorophyll-a content of the water increases when the concentrations of suspended solid rises. Thus, the phytoplankton concentration is affected by resuspension and sedimentation. However, the ratio of the chlorophyll-a/organic matter increases when the concentrations of suspended solid decrease. Hence, a significant effect of growth on the phytoplankton biomass does also occur. These effects are average effects for the total phytoplankton population present in the lake between April and November. Specific effects on the *Oscillatoria agardhii* population may be different as no sedimentation of *O.agardhii* has been observed in the fall velocity distribution experiments. As no *O.agardhii* blooms occurred in the Markermeer during the observed period, no supplementary information on the specific behaviour of *O.agardhii* could be gained from the weekly monitoring.

### **8.2.2 Light and dark bottle experiments**

From the experiments, performed with glass bottles filled with *O.agardhii* obtained from the Nijkerkernauw, it could be concluded that growth of *O.agardhii* is possible in the summer around noon in the Markermeer, as far as the light field is concerned. The maximum gross production that was observed totalled  $14 \text{ gO}_2 \cdot \text{gChla}^{-1} \cdot \text{h}^{-1}$ . As the relationship between the production per unit chlorophyll-a and the available irradiance (= the efficiency) varied from day to day, adaptation of growth parameters to the light conditions probably occurred. Though some effect of vertical mixing on the growth of *O.agardhii* has been found, no systematic increase or decrease has been observed.

### **8.2.3 Cylinder experiments**

After some start up problems, the operation of the production experiments of *O.agardhii* in a perspex cylinder placed at Y112 was easy.

From the measurement results it can be concluded that prolonged growth of *O. agardhii* is possible for periods of weeks during the summer months in the Markermeer, as far as the light conditions are concerned. The same maximum gross production rate for *O. agardhii* as in the bottle experiments is obtained: a range of 12 – 14 gO<sub>2</sub>·gChla<sup>-1</sup>·h<sup>-1</sup> for temperatures of around 20°C. Maximum respiration rates of 2.5 gO<sub>2</sub>·gChla<sup>-1</sup>·h<sup>-1</sup> were found for the same temperatures. A mixing depth of 2.8 metres is not prohibitive for growth of *O. agardhii* with maximum mean underwater irradiance values > 100 μE·m<sup>-2</sup>·s<sup>-1</sup>.

The experimental data have shown clearly that maximum production and the light utilization efficiency are not constant, but that their values are frequently or maybe even continuously subject to adaptation. Two kinds of adaptation have been observed:

- |                        |   |
|------------------------|---|
| <i>slow adaptation</i> | adaptation of growth parameters to low irradiance levels (mean under water irradiance < 100 μE·m <sup>-2</sup> ·s <sup>-1</sup> ) occurs within a few days;   |
| <i>fast adaptation</i> | at sunrise, light utilization efficiency is high but this may change during the day. During days with high maximum mean under water irradiance values (> 200 μE·m <sup>-2</sup> ·s <sup>-1</sup> ), growth parameters of <i>O. agardhii</i> usually adapt to high light conditions within a few hours. During days with lower maximum values, growth parameters tend to keep their high efficiency. |

Though the experiments produced valuable information about the growth characteristics of *O. agardhii* under the light conditions of the Markermeer, the experiments were not conclusive whether or not light is the limiting factor for the growth of *O. agardhii* in the Markermeer in the long run.

### 8.3 Model development and reliability

The model that has been developed to simulate the effect of management measures on the water quality of the Markermeer, focusing on the growth of *O. agardhii*, combines a sediment transport model (*STRESS-2d*), a light attenuation routine (*CLEAR*) and a growth model for *O. agardhii* (*ALGA*, developed by Vermij, 1992).

#### 8.3.1 Sediment transport, resuspension and sedimentation

The suspended solids concentration in the water of the Markermeer can be simulated rather accurately with the two-dimensional model for sediment transport, resuspension and sedimentation in shallow lakes, *STRESS-2d*. The accuracy of the model applied to the Markermeer is very high during at least 85 % of the year. The suspended solids concentration during storm events is sometimes simulated less well. As

extreme wind events occur generally outside the growing season, peak events are less important within the scope of this project.

Sedimentation fluxes are well described by a linear relationship between the settling velocity and the suspended solids concentration, as long as four different fractions are distinguished with different fall velocities. Variations in the fall velocity are thus accounted for by a varying contribution of the fractions to the total suspended solids concentration.

In the model, resuspension is induced by wind waves. The simulation of wind waves with a stationary model leads to good agreement between measured and simulated wave characteristics. Resuspension by flow, boats and fish has been ignored. Apparently this is a good concept, considering the good results in the simulation of suspended solids concentration.

The description and calibration of the two layer bottom model is primitive. In the model the rate at which sediment becomes available for resuspension is constant and not affected by the wind induced bottom stress, as the transport between the two layers occurs at a constant rate. Inclusion of a wind dependent exchange rate between the two layers would be a more realistic representation of the processes and could also improve the simulation of suspended solids during stormy events. Because some allocation of sediment at certain locations is simulated with the model in its present form, which is not observed in the field, improvement of the bottom model is recommendable for the simulation of long term effects.

### 8.3.2 Light field

The model *CLEAR* is based on the measurement of specific attenuation coefficients of various fractions, distinguished by fall velocity. Although these measurements were not very accurate, results of this method are consistent. Combined with sediment transport models the simulated attenuation coefficients agree rather well with measured data and the approach is an improvement compared to multiple regression on chemical composition data.

At present, apart from *O.agardhii* no other algae are incorporated in the model *CLEAR*. Hence, its application is limited to *O.agardhii* dominated lakes and can be considered to provide a 'worst case' condition. Validation of the model on the Markermeer itself is not really possible. Extension of the model with other algae would be useful for a wider application.

The use of a depth averaged vertical downward attenuation coefficient is allowed, because the model is used for the estimation of the total and the mean under water irradiance. No significant differences have been observed between the total under water irradiance estimated with a

mean attenuation coefficient and the total under water irradiance estimated from measurements at many different depths.

### 8.3.3 *Phytoplankton growth*

The modelling of the growth of *Oscillatoria agardhii* in the Markermeer is based on non-equilibrium concepts. Hence, competition with other algae is excluded but time scales and environmental fluctuations are important. With two dynamic non-equilibrium models, the production of *O.agardhii* as measured in the experiments, has been simulated. With the relatively simple model *SIMPLE*, which simulates light limited production with fixed growth parameters, simulation of the measured production is poor. Differences between the parameter sets, calibrated to describe individual experiments, were considerable. Therefore it has been concluded that adaptation of the parameters to the light conditions occurs and that this adaptation should be incorporated in an *O.agardhii* growth model.

In the model *ALGA*, developed by Vermij (Vermij, 1992), adaptation of growth parameters to light conditions is incorporated. An upper and lower boundary are set for the maximum productivity and the light utilization efficiency. If the under water irradiance is higher than the threshold value, these parameters approach the lower boundaries (high light conditions). With underwater irradiance levels lower than the threshold value, these parameters approach the upper limits (low light conditions). This construction accounts for the fast adaptation of growth parameters observed in the experiments (§ 8.2.3). Application of the model to the data of the field experiments, leads to calibrated values of the threshold values that are that low, that the growth parameters are equal to the lower boundaries for most of the time. The slow adaptation of growth parameters to the light conditions, as observed in the experiments, is not incorporated in *ALGA*. Simulation of the growth of algae for periods of months in the deeper parts of the lake showed rather good results. Unfortunately, the fact that the growth of *O.agardhii* is less in the shallower parts of the lake than in the deeper parts, could not be simulated with the model. Although the modelling of adaptation of growth parameters in *ALGA* is an improvement compared to fixed parameter models, the model *ALGA* does not yet result in an accurate simulation of the production measured in the experiments.

Simulation of the growth of *O.agardhii* by combination of the model *ALGA* with the models *STRESS-2d* and *CLEAR* has led to rather poor results, which is mainly due to imperfections in the biological part of the model, e.g: the constant loss rate, the absence of slow adaptation, the exclusion of competition with other species, etcetera. A high loss rate, as calibrated by Vermij, led to a dramatic decrease of cell numbers in winter, which was not compensated by growth in summer. The use of a lower loss rate led to some improvement of the simulation results.

## 8.4 Applications

An operational tool that assesses the effects of development and management measures on the suspended solids concentrations and the light field in the Markermeer is available, with the combination of *STRESS-2d* and *CLEAR* and the described parameter sets for the Markermeer. With some care the effect on the concentration of *O.agardhii* can be simulated as well, by combination of *STRESS-2d* and *CLEAR* and the model *ALGA*. The applicability of the models to assess the effect of development and management measures is broad, as is illustrated by two very different scenario studies: the effect of the construction of the Markerwaard and the effect of increased flushing.

### 8.4.1 The Markerwaard

The effect of the construction of the Markerwaard on the simulated suspended solids content and the attenuation coefficient is vast. In general, lower suspended solid concentrations and attenuation coefficients are simulated in the areas remaining after the construction, due to reduction in fetch lengths and changes in flow patterns. The Gouwzee, IJmeer and Gooimeer are hardly affected.

Although some care should be taken with the interpretation of the simulation results of the biological model, it can be concluded that the growth of *Oscillatoria agardhii* in the water areas remaining after the construction of the Markerwaard will probably increase compared to the present situation. Hence, this seems to agree with the conclusions of the IJff committee, that the possibility of the temporary blooms of *Oscillatoria agardhii* is expected to increase.

### 8.4.2 Increased flushing

The effect of increased flushing with water from the IJsselmeer on the suspended solids concentration and the attenuation coefficient is minimal, even though the residence time of the water is halved in this scenario. Increased flushing causes a small increase in the numbers of *Oscillatoria agardhii*, as the concentration of *O.agardhii* is usually higher in the IJsselmeer than in the Markermeer. This effect is noticed especially near the discharging sluices, but diminishes at some distance of the sluices because it is absorbed in the larger water body.

## References

- Aalderink, R.H., L. Lijklema, J. Breukelman, W. van Raaphorst and B. Brinkman, 1984. Quantification of wind induced resuspension in a shallow lake. *Water Science and Technology*, 17: 903-914.
- Bakema, A.H., 1988. Empirische lichtmodellering voor een aantal Nederlandse meren. Waterloopkundig Laboratorium Delft, T387. The Netherlands (*In Dutch*).
- Baker, E.T. and J.W. Lavelle, 1984. The effect of particle size on the light attenuation coefficient of natural suspensions. *Journal of Geophysical Research*, 89:8197-8203.
- Banks, R.B., 1975. Some features of wind action on shallow lakes. *Journal of the Environmental Engineering Division*, EE5: 813-827.
- Berger, C., J.E.G. Bouman, P.J. Ente, J.de Jong, E.Schultz, E.J.B. Uunk, G.A.M. Menting, 1986. De kans op blauwalgenbloeien in de randmeren van de Markerwaard. RWS, directie Flevoland, FLevobericht 268. Lelystad, The Netherlands (*In Dutch*).
- Berger, C., 1987. Habitat en ecologie van *Oscillatoria agardhii* Gomont. RWS, dir. Flevoland, Van Zee tot Land, 54. Lelystad, The Netherlands (*In Dutch*).
- Berger, C. and H.E. Sweers, 1988. The IJsselmeer and its phytoplankton- with special attention to the suitability of the lake as a habitat for *Oscillatoria agardhii* Gom., *Journal of Phytoplankton Research*, 10:579-599.
- Berger, C., 1988. Habitatskenmerken *Oscillatoria agardhii* Gom. RWS, dir. Flevoland, Werkdocument 1988-48 cbw. Lelystad, The Netherlands (*In Dutch*).
- Blom, G., 1989. Beïnvloeding transport fosfaatrijk slib in het Veluwemeer. Landbouwniversiteit Wageningen, Vakgroep Natuurbeheer. The Netherlands (*In Dutch*).
- Blom, G., 1991. Slib, slibtransport en lichtklimaat in de randmeren. Landbouwniversiteit Wageningen, Vakgroep Natuurbeheer, nr. 91-15. The Netherlands (*In Dutch*).
- Blom, G., E.H.S. Van Duin, R.H. Aalderink, L. Lijklema and C. Toet, 1992. Modelling sediment transport in shallow lakes interactions between sediment transport and sediment composition. *Hydrobiologia* 235/236: 153-166. B.T. Hart & P.G. Sly (Eds.) *Sediment/Water Interactions*.
- Blom, G. and C. Toet, 1991. A sediment transport model for lake Ketel- a tool for water management. Submitted to *Journal of Water Science and Technology*. System analysis in water quality management II.
- Bouws, E., J.J. Ephraums, J.A. Ewing, P.E. Francis, H. Gunther, P.A.E.M. Janssen, G.J. Komen, W. Roosental and W.J.P. de Voogt, 1985. A shallow water intercomparison of three numerical wave prediction models (SWIM). *Quart. J. R. Met. Soc.*, 111:1087-1112.
- Bouws, R., 1986. Verwachting van zeegang door middel van groeicurves: bevindingen verkregen aan de hand van de Markermeerdataset. KNMI: 00-86-33, de Bilt, The Netherlands (*In Dutch*).
- Bretschneider, C.L., 1966. Wave generation by wind, deep and shallow water. In: Ippen (Ed.). *Estuary and coastline hydrodynamics*. Engineering Society Monographs, McGraw-Hill Inc.
- Bricaud, A., A. Morel and L. Prieur, 1981. Absorption by dissolved organic matter of the sea (yellow substance) in the UV and visible domain. *Limnol. Oceanogr.*, 26: 43-53.

- Brinkman, A.G. and W. Van Raaphorst, 1986. De fosfaathuishouding in het Veluwemeer. PhD-thesis, University of Twente, Enschede, The Netherlands (*In Dutch*).
- Bruinsma, Y., I.E.J. van Lieshout and E.H.S. van Duin, 1992. Meetopstellingen Markermeer; methoden en resultaten 1989. RWS, directie Flevoland 1992-?? Iio, Lelystad, The Netherlands (*In Dutch*).
- Buiteveld, H., C. Meulstee, E.H.S. van Duin and G.N.M. Stokman, 1990. Water quality applications of Landsat Imagery in the Lake IJssel area. In: Proceedings of the International Symposium on Remote Sensing and Water Resources, Enschede, The Netherlands. p:617-626.
- Buiteveld, H. and M. Donze, 1991. The optical properties of water. *In prep.*
- CERC, 1977. (Coastal Engineering Research Centre) Shore protection manual, volume I. Department of the Army. U.S. Government Printing Office Washington, D.C. (USA).
- CERC, 1984. (Coastal Engineering Research Centre) Shore protection manual, volume I. Department of the Army. U.S. Government Printing Office Washington, D.C. (USA)
- Commissie IJff, 1984. Advies van de commissie Algenbloei westelijke randmeren Markerwaard. Hilversum, The Netherlands (*In Dutch*).
- De Beaufort, L.F. (Ed.), 1954. Veranderingen in de flora en fauna van de Zuiderzee (thans IJsselmeer) na de afsluiting in 1932. Verslag van de onderzoeken ingesteld door de Zuiderzee-commissie der Nederlandse Dierkundige Vereniging. De Boer, Den Helder, The Netherlands (*In Dutch, summary in English*).
- De Groote, H.W., 1992. De groei van *O. agardhii* in het Markermeer. Landbouwniversiteit Wageningen, doctoraalverslag (*In Dutch*). *In prep.*
- De Rijk, M.G., 1990. Beheersverslag Rijkswateren IJsselmeergebied 1988. RWS, directoraat Flevoland, Lelystad (*In Dutch*).
- DiGiano, F.A., L. Lijklema and G. Van Straaten, 1978. Wind induced dispersion and algal growth in shallow lakes. *Ecological Modelling*, 4: 237-252.
- DiToro, D.M., 1978. Optics of turbid estuarine waters: approximations and applications. *Water Research*, 12: 1059-1068.
- Falkowski, P.G., 1984. Physiological responses of phytoplankton to natural light regimes. IRL Press Limited, Oxford, Great Britain.
- Foy, R.H. and R.V. Smith, 1980. The role of carbohydrate accumulation in the growth of planktonic *Oscillatoria* species. *British Physiological Journal*, 15:139-150.
- Fukuda, M.F. and W. Lick, 1980. The entrainment of cohesive sediments in freshwater. *Journal of Geophysical Research*, 85: 2813-2824.
- Gulati, R.D., E.H.R.R. Lammens, M.L. Meijer and E. Van Donk, 1989. Biomanipulation- Tool for Water Management. Proceedings of an International Conference, Amsterdam, The Netherlands, August 1989. Reprinted from *Hydrobiologia* 200/201, 1990.
- Gons, H.J., R. Veeningen and R. Van Keulen, 1986. Effects of wind on a shallow lake ecosystem: Resuspension of particles in the Loodrecht lakes. *Hydrological Bulletin* 20: 109-120.
- Gordon, T.W., 1977. Modelling temperature and light adaptation. Center for Ecological Modelling, Rensselaar Polytechnic Institute, New York. Report no. 2.
- Håkanson, L. and M. Jansson, 1983. Lake sedimentology. Springer Verlag, Berlin, BRD



- Harris, G.P., 1986. Phytoplankton ecology: Structure, function and fluctuation. Chapman and Hall, London, Great Britain.
- Hasselman, K., D.B. Ross, P. Müller and W. Sell, 1976. A parametric wave prediction model. *Journal of Physical Oceanography*, 6:200-229.
- Hebbink, A., 1991. Verbal information
- Hosper, S.H., J.R. Eulen, and S.J. Kloosterhuis, 1980. Ontwikkeling van grenswaarden voor doorzicht, chlorofyl, fosfaat en stikstof. CUWVO, 2<sup>e</sup> Eutrofiëring enquête. RWS, Rijksinstituut voor de Zuivering van Afvalwater (*In Dutch*).
- Hosper, S.H., M.L. Meijer and J.R. Eulen, 1986. Herstel van het Veluwemeer, recente ontwikkelingen. *H<sub>2</sub>O*, 19:416-420 (*In Dutch, summary in English*).
- Huber-Pestalozzi, G., 1966. Das Phytoplankton des Süßwassers. In: Die Binnengewässer von Prof. Dr. August Thiemann, Band XVI, Teil 1. Stuttgart, E. Schweizerbartsche Verlagsbuchhandlung.
- Hutchinson, G.E., 1957. A treatise on limnology, part I. John Wiley and Sons, New York, USA.
- Jagtman, E. and G. Van Urk, 1988. Algen in het Markermeer: groei of resuspensie? *H<sub>2</sub>O*, 21:606-610 (*In Dutch, summary in English*).
- Jassby, A.D. and T. Platt, 1976. Mathematical formulation of the relationship between photosynthesis and light for phytoplankton. *Limnology and Oceanography*, 21 (4): 540-547.
- Jerome, J.H., R.P. Bukuta and J.E. Bruton, 1990. Determination of available subsurface light for photochemical and photobiological activity. *J. Great Lakes Res.*, 16:436-443.
- Jewson, D.H., J.F. Talling, M.J. Dring, M.M. Tilzer S.I. Heaney and C. Cunningham, 1984. Measurement of photosynthetically available radiation in freshwater: comparative tests of some current instruments used in studies on primary production. *Journal of Phytoplankton Research*, 6, 259-273.
- Kuijpers, A.M.T. and E.H.S. Van Duin, 1988. Meer over zwevende stof en licht in water. RWS, directie Flevoland, werkdocument 1988 94-cbw, Lelystad, The Netherlands (*In Dutch*).
- Kirk, J.T.O., 1983. Light and photosynthesis in aquatic ecosystems. Cambridge University Press, Cambridge, USA.
- Kirk, J.T.O., 1977. Attenuation of light in natural waters. *Aust. J. Mar. Freshwater Res.*, 28:497-508.
- Lam, D.C.L. and J.M. Jaquet, 1976. Computations of physical transport and regeneration of phosphorus in Lake Erie, Fall 1970. *J. Fish. Res. Board Can.* 33: 550-563.
- Langerak, A., J. Dijkzeul and G.K. Verboom, 1983. IJking model. In: Gebruik en toepassing WAQUA, cursus materiaal. Rijkswaterstaat - Delft Hydraulics, The Netherlands (*In Dutch*).
- Lee, D.H. and K.W. Bedford, 1987. Resuspension and sorting effects on tributary sediment loads to lake Erie. In: Proceedings of AIRH-Congres, IAHR, Lausanne. p:56-61.
- Leendertse, J.J., 1967. Aspects of a computational model for long period water wave propagation. Memorandum RM-5294-PR, Rand Corporation, Santa Monica, USA.

- Leendertse, J.J., 1987. Design considerations of the SIMSYS2D/WAQUA system. In: Gebruik en toepassing van WAQUA. Cursus-syllabus, Rijkswaterstaat/Delft Hydraulics, The Hague, The Netherlands (*In Dutch*).
- Lick, W., 1982. Entrainment, deposition and transport of fine grained sediments in lakes. *Hydrobiologia*, 91: 31-40.
- Lick, W., 1986. Modelling the transport of fine-grained sediments in aquatic systems. *Sci. Total Environ.*, 55:219-228.
- Lijklema L., G. Blom, R.H. Aalderink and E.H.S. Van Duin, 1990. Sediment transport in shallow lakes; two case studies related to eutrophication. In: Transport and Transformation of Contaminants near the Sediment Water Interface, DePinto, J.V. (Ed.). Springer Verlag, Berlin.
- Loogman, J.G., 1982. Influence of photoperiodicity on algal growth kinetics. PhD-thesis, University of Amsterdam, The Netherlands.
- Luettich, R.A., 1987. Sediment resuspension in a shallow lake. PhD-thesis, Massachusetts Institute of Technology, Boston, Ms, USA.
- Luettich, R.A., D.R.F. Harleman and L. Somlyódy, 1990. Dynamic behaviour of suspended sediment concentrations in a shallow lake perturbed by episodic wind events. *Limnol. Oceanogr.*, 35: 1050-1067.
- Mehta, A.J. and E. Partheniades, 1975. An investigation of the depositional properties of flocculated fine sediments. *Journal of Hydraulic Research*, 4:361-381.
- Meijer, M.L., E. Jagtman, M.P. Grimm and S.H. Hosper, 1990. Toepassing van actief biologisch beheer op grote schaal. *H<sub>2</sub>O*, 24:652-656 (*In Dutch, summary in English*).
- Ministerie van Verkeer en Waterstaat, Ministerie van Landbouw, Natuurbeheer en Visserij and Ministerie van Volkshuisvesting, Ruimtelijke Ordening en Milieubeheer, 1990. Interim beheersplan Markermeer. Ministerie The Hague, The Netherlands (*In Dutch*).
- Mugie, A.L., 1989. De gegevensverwerking van de stappenbaken op Y111 and Y112 in 1989. RWS, directie Flevoland, werkdocument 1989 -37liw, Lelystad, The Netherlands (*In Dutch*).
- Mugie, A.L., A. Oldenkamp and E.H.S. Van Duin, 1989<sup>1</sup>. Meetopstellingen Markermeer; methoden en resultaten 1987. RWS, directie Flevoland 1989-5 liw, Lelystad, The Netherlands (*In Dutch*).
- Mugie, A.L., P. Derks and E.H.S. Van Duin, 1989<sup>2</sup>. Meetopstellingen Markermeer; methoden en resultaten 1988. RWS, directie Flevoland 1989-28 liw, Lelystad, The Netherlands (*In Dutch*).
- Mur, L.R., M.J. Van Hezewijk and P.M. Visser, 1990. Phytoplankton Markermeer. Eindconclusie. Laboratorium voor Microbiologie, University of Amsterdam, The Netherlands (*In Dutch*).
- Nor, A.V., 1991. Letter to colleagues, concerning the oxygen secretion in the dark. Unpublished.
- O'Melia, 1985. The influence of coagulation and sedimentation on the fate of particles, associated pollutants and nutrients in lakes. In: W. Stum (Ed.). Chemical processes in lakes. Wiley and Sons, New York (USA), p:207-224.
- Pamatmat, M.M., 1988. Catalase activity and the hydrogen peroxide cycle. *Arch. Hydrobiol. Verein. Ergebn. Limnol.*, 31:107-114.

- Partheniades, E., 1965. Erosion and deposition of cohesive soils. Journal of the Hydraulic Division, HY1:105-139.
- Partheniades, E., 1971. Erosion and deposition of cohesive materials. In: H.W. Shen (Ed.). River Mechanics, Vol. II, 25-1 ~ 25-89.
- Partheniades, E., 1972. Results of recent investigation on erosion and deposition of cohesive sediments. ???
- Pennak, R.W., 1978. Anomalous primary production conditions in some Colorado alpine lakes. Int. Verh., 20:434-437.
- Post, A.F., J.G. Loogman and L.R. Mur, 1984. Regulation of growth and photosynthesis of *Oscillatoria agardhii* grown with a light/dark cycle. FEMS Microbiology Ecology, 31: 97-102.
- Post, A.F., R. de Wit and L.R. Mur, 1985<sup>1</sup>. Interactions between temperature and light intensity on growth and photosynthesis of the cyanobacterium *Oscillatoria agardhii*. J. Plankton Research, 7:487-495.
- Post, A.F., J.G. Loogman and L.R. Mur, 1985<sup>2</sup>. Regulation of growth and photosynthesis by *Oscillatoria agardhii* grown with a light/dark cycle. FEMS Microbiology Ecology, 31:97-102.
- Post, A.F., 1986. Transient state characteristics of adaptation to changes in light conditions for the cyanobacterium *Oscillatoria agardhii*. Arch. Microbiology, 145:353-357.
- Post, A.F., J.G. Loogman and L.R. Mur, 1986. Photosynthesis, Carbon Flow and Growth of *Oscillatoria agardhii* Gomont in Environments with a periodic supply of light. Journal of General Microbiology, 132:2129-2136.
- Preisendorfer, R.W., 1961. Application of radiative transfer theory to light measurements in the sea. Union Geod. Geophys. Inst. Monogr., 10.
- Reynolds, C.S., 1984. The ecology of freshwater phytoplankton. Cambridge University Press, Cambridge, Great Britain.
- Reynolds C.S., R.L. Oliver and A.E. Walsby, 1987. Cyanobacterial dominance: the role of buoyancy regulation in dynamic lake environments. New Zealand Journal of Marine and Fresh Water Research, 21:379-390.
- Rijkswaterstaat- Directie Zuiderzeewerken and Rijksdienst voor de IJsselmeerpolders, 1985. De Waterstaatkundige hoofdstructuur van de Markerwaard. Lelystad, The Netherlands.
- Sanders, T.G., R.C. Ward, J.C. Loftis, T.D. Steele, D.D. Adrian and Vujica Yevjevich, 1983. Design of networks for monitoring water quality. Water Resources Publications, Littleton, USA.
- Saville, T., E.W. McClendon and A.L. Cochran, 1962. Freeboard allowances for waves in inland reservoirs. Journal of Waterways and Harbors Division, WW2: 93-124.
- Smith, R.C. and Baker, K.S., 1981. Optical properties of the clearest natural waters. Appl. Opt., 20:177-184.
- Sheng, Y.P and W. Lick, 1979. The transport and resuspension of sediments in a shallow lake. Journal of Geophysical Research, 84: 1809-1826.
- Stelling, G., 1984. On the construction of computational methods for shallow water flow problems, Rijkswaterstaat, Rijkswaterstaat communications, 35. The Hague (The Netherlands).

- Stutterheim, E. and J.G.C. Smits, 1985. Haalbaarheidsstudie naar de modellering van zware metalen met het model Charon, door toepassing op het systeem Ketelmeer-IJsselmeer. Delft Hydraulics, S578-S457. Delft, The Netherlands (*In Dutch*).
- Terwindt, J.H.J., 1977. Deposition, transportation and erosion of mud. In: Interactions between sediments and freshwater.
- Tilzer, M.M., 1983. The importance of fractional light absorption by photosynthetic pigments for phytoplankton productivity in Lake Constance. Limnology and Oceanography (*In press*).
- Tsai, C.H. and W. Lick, 1986. A portable device for measuring sediment resuspension. J. Great Lakes Res., 12: 314-321.
- Van Duin, R.H.A. and G. de Kaste, 1985. A pocket guide to the Zuyder Zee project. RWS, directie Flevoland, Lelystad, The Netherlands.
- Van Duin, E.H.S., A.M.T. Kuipers and A. Oldenkamp, 1988. Zwevende stof en licht in water. RWS, directie Flevoland, werkdocument 1988-1 cbw, Lelystad, The Netherlands (*In Dutch*).
- Van Duin, E.H.S. and L. Lijklema, 1989<sup>1</sup>. The development of an operational two-dimensional water quality model for Lake Marken, The Netherlands. Water Science and Technology, 21:1817-1820.
- Van Duin, E.H.S. and L. Lijklema, 1989<sup>2</sup>. Modelling photosynthesis and oxygen in a shallow, hypertrophic lake. Ecological Modelling, 45:243-260.
- Van Duin, E.H.S., G. Blom, L. Lijklema and M.J.M. Scholten, 1992. Aspects of modelling sediment transport and light attenuation in Lake Marken. Hydrobiologia, 235/236: 167-176. B.T. Hart & P.G. Sly (Eds.). Sediment/Water Interactions.
- Van Duin, E.H.S. and G. Blom, 1992. STRESS-2d: A two dimensional model for sediment transport, resuspension and sedimentation in shallow lakes (*In preparation*).
- Van Eerden, M.R. and M. Zijlstra, 1986. Natuurwaarden van het IJsselmeergebied. RWS, dir. Flevoland, Flevovericht 273. Lelystad, The Netherlands (*In Dutch*).
- Van Hoorn, D. and Kolvoort, J., 1991. Intern memo betreffende doorspoeling Markermeer. Rijkswaterstaat, directie Flevoland, Lelystad, The Netherlands (*In Dutch*).
- Van Leussen, W., 1986. Laboratory experiments on the settling velocity of mud flocs. In: S.Y. Wang, H.W. Shen and L.Z. Ding (Eds.), Proceedings of the third International Symposium on River Sedimentation, p:1803-1812. The University of Mississippi, USA.
- Van Liere, L., 1979. *Oscillatoria agardhii* Gomont. Experimental Ecology and Physiology of a Nuisance Blooming Cyanobacterium. Zeist, De Nieuwe Schouw, The Netherlands.
- Van Liere, L. and L.R. Mur, 1979. Growth kinetics of *Oscillatoria agardhii* Gomont in continuous cultures, limited in its growth by the light energy supply. Journal of General Microbiology, 115: 153-160.
- Van Liere, L. and L.R. Mur, 1980. Occurrence of *Oscillatoria agardhii* and some related species, a survey. In: J. Barica and L.R. Mur (Eds.), Developments in Hydrobiology, 2:67-77.
- Van Straaten, G., 1986. Identification, uncertainty assessment and prediction in lake eutrophication. PhD-thesis University of Twente, The Netherlands.
- Van Urk, G., T.H. Helmerhorst and H. Ruiter, 1990. A critical review of the Dutch standard method for the determination of chlorophyll-a. H<sub>2</sub>O, 23:554-559 (*In Dutch, summary in English*).

- Verduin, J., 1982. Components contributing to light extinction in natural waters. In: Method of Isolation. Arch. Hydrobiologia, 93(3): 303-312.
- Vermij S. and R. Janissen, 1991. Analyse van de habitat van *Oscillatoria agardhii*. Intern rapport 1991- 17 Iio. RWS, directie Flevoland, Lelystad (*In Dutch*).
- Vermij S., 1992. Modelleren van de groei van *Oscillatoria agardhii*. Intern rapport 1992-1 Iio. RWS, directie Flevoland, Lelystad (*In Dutch*).
- Visser, T.A.M., 1991. Onderzoek naar de primaire produktie van *Oscillatoria agardhii* en modelleren van de groei in het Markermeer. Intern Rapport 1991- 20 Iio. RWS. Directie Flevoland, Lelystad, The Netherlands (*In Dutch*).
- Vlag, D.P., 1990. Een model voor resuspensie en sedimentatie van slib. Toepassing op het Markermeer. Riza, nota nr. 91.005. Lelystad, The Netherlands (*In Dutch*).
- Vollenweider, R.A., 1974. A manual on methods for measuring primary production in aquatic environments. IBP Handbook no 12. Blackwell Scientific Publications, Oxford.
- Ward, R.C., J.C. Loftis and G.B. McBride, 1990. Design of water quality monitoring systems. Van Nostrand Reinhold, New York, USA.
- Werkgroep Normering, 1986. Interim rapport, onder water bodem overleg RWS-DGMH.
- Winkels, H.J., A.M.T. Kuijpers, E.H.S. Van Duin and R. Koopstra, 1989. De IJsselmeerafzetting in het Markmeergebied; onderzoeksresultaten 1988. RWS, directie Flevoland, werkdocument 1989-25 Iiw. Lelystad (The Netherlands) (*In Dutch*).
- Wibaut- Isebreë Moens, N.L., 1954. Plankton. In: Veranderingen in de flora en fauna van de Zuiderzee (thans IJsselmeer) na de afsluiting in 1932. L.F. De Beaufort (Ed.). De Boer, Den Helder, The Netherlands (*In Dutch, summary in English*).
- Wolters, H.A., 1992. Verbal information.
- Zevenboom, W., A. Bij de Vaate and L.R. Mur, 1982. Assessment of factors limiting growth rate of *Oscillatoria agardhii* in hypertrophic lake Woldrwijd, 1978, by use of physiological indicators. Limnology and Oceanography, 27:39-52.

## Appendix 1: Symbols and abbreviations

### Symbols

|                           |   |   |
|---------------------------|---|---|
| $a$                       | = absorption coefficient  | ( $m^{-1}$ )                                |
| $a_g(380)$                | = absorption coefficient at 380 nm  | ( $m^{-1}$ )                                |
| $A$                       | = coefficient related to particle concentration                               | ( $m^{2.1} \cdot m^{-3}$ )                  |
| AFDW                      | = ash free dry weight concentration   | ( $g \cdot m^{-3}$ )                        |
| Aph                       | = Aphanizomenon species ratio   | (%)   |
| $b$                       | = scattering coefficient  | ( $m^{-1}$ )                                |
| $B$                       | = experimentally determined coefficient                                       |   |
| Bac                       | = Bacillariophyceae species ratio   | (%)   |
| $C$                       | = wave celerity   | ( $m \cdot s^{-1}$ )                        |
| $C_1, C_2, C_3, C_4, C_5$ | = constants   |   |
| $C_d$                     | = decay constant  | ( $s^{-1}$ )                                |
| $C_i$                     | = concentration of component $i$  | ( $g \cdot m^{-3}$ )                        |
| $C_{nut}$                 | = nutrient concentration  | ( $g \cdot m^{-3}$ )                        |
| $C_{p,LH}$                | = adaption rate $P_{max}$ , from low to high irradiance                       | ( $s^{-1}$ )                                |
| $C_{p,HL}$                | = adaption rate $P_{max}$ , from high to low irradiance                       | ( $s^{-1}$ )                                |
| $C_{a,LH}$                | = adaption rate $\alpha$ , from low to high irradiance                        | ( $s^{-1}$ )                                |
| $C_{a,HL}$                | = adaption rate $\alpha$ , from high to low irradiance                        | ( $s^{-1}$ )                                |
| $Ch$                      | = Chézy coefficient   | ( $m^2 \cdot s^{-1}$ )                      |
| Chla                      | = chlorophyll-a concentration   | ( $mg \cdot m^{-3}$ )                       |
| Clor                      | = Chlorococcales species ratio  | (%)   |
| $Co_i$                    | = concentration of component $i$  | ( $g \cdot m^{-3}$ )                        |
| Cr                        | = Courant number  | (-)   |
| $d_s$                     | = diameter of a sphere having the same volume as an irregular shaped particle | (m)   |
| $D_h$                     | = horizontal eddy diffusivity   | ( $m^2 \cdot s^{-1}$ )                      |
| $D_v$                     | = vertical eddy diffusivity   | ( $m^2 \cdot s^{-1}$ )                      |
| dayn                      | = Julian daynumber  | (-)   |
| $dV$                      | = particle volume per unit fluid volume                                       | (-)   |
| DECAY                     | = decay   | ( $O. agardhii \cdot m^{-2} \cdot s^{-1}$ ) |
| DO                        | = Dissolved Oxygen concentration at depth $z$                                 | ( $g \cdot m^{-3}$ )                        |
| DO'                       | = dissolved oxygen concentration in the water column                          | ( $g \cdot m^{-3}$ )                        |
| DOC                       | = Dissolved Organic Carbon concentration                                      | ( $g \cdot m^{-3}$ )                        |
| $e$                       | = porosity  | (-)   |
| $E_{cr}$                  | = critical threshold value for growth parameters                              | ( $\mu E \cdot m^{-2} \cdot s^{-1}$ )       |
| $E_d$                     | = downward irradiance (photon flux density of PAR)                            | ( $\mu E \cdot m^{-2} \cdot s^{-1}$ )       |
| $E_{d,\lambda}$           | = downward irradiance at wavelength $\lambda$                                 | ( $\mu E \cdot m^{-2} \cdot s^{-1}$ )       |
| $E_{d,o}$                 | = downward irradiance near the water surface                                  | ( $\mu E \cdot m^{-2} \cdot s^{-1}$ )       |
| $E_{mean}$                | = mean under water irradiance   | ( $\mu E \cdot m^{-2} \cdot s^{-1}$ )       |
| $E_{opt}$                 | = optimal irradiance for production   | ( $\mu E \cdot m^{-2} \cdot s^{-1}$ )       |
| $E_s$                     | = scalar irradiance (photon flux density of PAR)                              | ( $\mu E \cdot m^{-2} \cdot s^{-1}$ )       |
| $E_T$                     | = total under water irradiance  | ( $\mu E \cdot m^{-2} \cdot s^{-1}$ )       |
| $E_u$                     | = upward irradiance (photon flux density of PAR)                              | ( $\mu E \cdot m^{-2} \cdot s^{-1}$ )       |
| $f$                       | = Coriolis parameter  | ( $s^{-1}$ )                                |
| $f_i$                     | = function of fetch parameter   |   |
| $f_z$                     | = function of depth parameter   |   |
| $F$                       | = effective fetch   | (m)   |
| $F_l$                     | = fetch length  | (m)   |
| $F_w$                     | = fetch width   | (m)   |
| FF                        | = effective fetch parameter   | (-)   |
| $g$                       | = acceleration due to gravity   | ( $m \cdot s^{-2}$ )                        |
| $h$                       | = distance from the reference plane to the bottom                             | (m)   |
| $H_c$                     | = minimum value of $H_s$ in the estimation of model behaviour                 | (m)   |
| $H_s$                     | = significant wave height   | (m)   |
| HH                        | = wave height parameter   | (-)   |

|                   |  |  |
|-------------------|--|--|
| $I_s$             | = total incident solar radiation (300-3000 nm)   | (W·m <sup>-2</sup> )                           |
| IOS               | = InOrganic Solids concentration   | (g·m <sup>-3</sup> )                           |
| Phaeo             | = phaeophytine concentration   | (mg·m <sup>-3</sup> )                          |
| $K_d$             | = specific vertical downward attenuation coefficient   | (m <sup>2</sup> ·g <sup>-1</sup> )             |
| $K_{d,i}$         | = specific partial downward attenuation coefficient of component i                           | (m <sup>2</sup> ·g <sup>-3</sup> )             |
| $K_i$             | = constants  |  |
| $K_d$             | = vertical downward attenuation coefficient of PAR   | (m <sup>-1</sup> )                             |
| $K_{d,i}$         | = partial vertical downward attenuation coefficient of component i                           | (m <sup>-1</sup> )                             |
| $K_{d,l}$         | = vertical downward attenuation coefficient of wave-length l                                 | (m <sup>-1</sup> )                             |
| M                 | = Manning coefficient  | (m <sup>1/2</sup> ·s <sup>-1</sup> )           |
| $M_c$             | = mass transport by consolidation  | (m·s <sup>-1</sup> )                           |
| $M_e$             | = mass transport by erosion  | (m·s <sup>-1</sup> )                           |
| $M_t$             | = mass transport by turbation  | (m·s <sup>-1</sup> )                           |
| MSS <sub>t</sub>  | = sediment mass in top layer   | (g·m <sup>-2</sup> )                           |
| MSS <sub>i</sub>  | = sediment mass in lower layer   | (g·m <sup>-2</sup> )                           |
| N                 | = number of grid cells   | (-)  |
| N-Kjel            | = Kjeldahl Nitrogen  | (g·m <sup>-3</sup> )                           |
| N-NO <sub>x</sub> | = Nitrogen oxides concentration  | (g·m <sup>-3</sup> )                           |
| N-NH <sub>4</sub> | = Ammonium nitrogen concentration  | (g·m <sup>-3</sup> )                           |
| N-Osc             | = cell number of Oscillatoria agardhii   | (m <sup>-3</sup> )                             |
| n( $d_p$ )        | = particle size distribution function of diameter  | (-)  |
| Mic               | = Microcystus aeruginosa ratio   | (%)  |
| O                 | = coefficient of form resistance   | (-)  |
| Osc               | = Oscillatoria species ratio   | (%)  |
| pH                | = acidity  | (-log[H <sup>+</sup> ])                        |
| P                 | = productivity   | (s <sup>-1</sup> )                             |
| $P_{max}$         | = maximum productivity   | (s <sup>-1</sup> )                             |
| $P_{max,H}$       | = Pmax at high irradiance values   | (s <sup>-1</sup> )                             |
| $P_{max,L}$       | = Pmax at low irradiance values  | (s <sup>-1</sup> )                             |
| $P_{nut}$         | = productivity based on available nutrients  | (s <sup>-1</sup> )                             |
| $P_{opt}$         | = optimal productivity without nutrient limitation   | (s <sup>-1</sup> )                             |
| P-ort             | = phosphor in ortho-phosphate  | (g·m <sup>-3</sup> )                           |
| P-tot             | = total phosphor concentration   | (g·m <sup>-3</sup> )                           |
| POC               | = Particular Organic Carbon concentration  | (g·m <sup>-3</sup> )                           |
| PP                | = primary production   | (O.agardhii·m <sup>-2</sup> ·s <sup>-1</sup> ) |
| $Q_{nut}$         | = minimal internal nutrient concentration  | (g·O.agardhii <sup>-1</sup> )                  |
| Rmax              | = maximum respiration rate at 20 °C  | (h <sup>-1</sup> )                             |
| RESP              | = respiration  | (O.agardhii·m <sup>-2</sup> ·s <sup>-1</sup> ) |
| S                 | = source (or sink) term  | (g·m <sup>-3</sup> ·s <sup>-1</sup> )          |
| Secchi            | = Secchi-disk depth  | (m)  |
| Sce               | = Scenedesmus species ratio  | (%)  |
| SS                | = Suspended solids concentration   | (g·m <sup>-3</sup> )                           |
| SS <sub>i</sub>   | = suspended solids concentration of fraction i   | (g·m <sup>-3</sup> )                           |
| SS <sub>b</sub>   | = background suspended solids concentration  | (g·m <sup>-3</sup> )                           |
| SSQ               | = weighted root of the sum of squares of the difference between estimated and observed value |  |
| t                 | = time   | (s)  |
| $t_d$             | = wind duration  | (s)  |
| $t_h$             | = time   | (h)  |
| $t_s$             | = characteristic time for settling   | (s)  |
| $t_t$             | = characteristic time for turbulent diffusion  | (s)  |
| tt                | = wind duration parameter  | (-)  |
| T                 | = temperature  | (°C)   |
| $T_s$             | = significant wave period(s)   |  |
| $T_w$             | = wave period  | (s)  |
| TOC               | = Total Organic Carbon concentration   | (g·m <sup>-3</sup> )                           |
| TT                | = wave period parameter(-)   |  |
| u                 | = vertically averaged fluid velocity in x-direction  | (m·s <sup>-1</sup> )                           |
| u                 | = fluid velocity in x direction  | (m·s <sup>-1</sup> )                           |

|                                |   |   |
|--------------------------------|---|---|
| $U_{10}$                       | = wind velocity measured at an elevation of 10 metres         | ( $m \cdot s^{-1}$ )                                      |
| $U_a$                          | = wind stress factor  | ( $m^{-1}$ )  |
| $U_b$                          | = maximum bottom wave orbital velocity                        | ( $m \cdot s^{-1}$ )                                      |
| $U_{b,cr}$                     | = critical maximum bottom wave orbital velocity               | ( $m \cdot s^{-1}$ )                                      |
| $U_{max}$                      | = maximum production rate at 20 °C                            | ( $h^{-1}$ )  |
| $v$                            | = vertically averaged fluid velocity in y-direction           | ( $m \cdot s^{-1}$ )                                      |
| $\nu$                          | = fluid velocity in y direction                               | ( $m \cdot s^{-1}$ )                                      |
| $V$                            | = kinematic viscosity   | ( $m^2 \cdot s^{-1}$ )                                    |
| $w$                            | = fluid velocity in z direction                               | ( $m \cdot s^{-1}$ )                                      |
| $w_s$                          | = settling velocity of suspended solids relative to the fluid | ( $m \cdot s^{-1}$ )                                      |
| $x$                            | = horizontal coordinate                                       | (m)   |
| $X_{an}$                       | = Xanthophyllae   | (%)   |
| $y$                            | = horizontal coordinate                                       | (m)   |
| $Y$                            | = yield coefficient   | ( $gO_2 \cdot gChla^{-1}$ )                               |
| $z$                            | = depth   | (m)   |
| $z_c$                          | = critical thickness of the sediment top layer                |   |
| $z_t$                          | = thickness of the sediment top layer                         | (m)   |
| $zz$                           | = depth parameter   | (-)   |
| $\alpha$                       | = light energy utilization efficiency                         | ( $s^{-1} \cdot (\mu E \cdot m^{-2} \cdot s^{-1})^{-1}$ ) |
| $\alpha_1, \alpha_2, \alpha_3$ | = angles  | (°)   |
| $\alpha_H$                     | = $\alpha$ at high irradiance values                          | ( $s^{-1} \cdot (\mu E \cdot m^{-2} \cdot s^{-1})^{-1}$ ) |
| $\alpha_L$                     | = $\alpha$ at low irradiance values                           | ( $s^{-1} \cdot (\mu E \cdot m^{-2} \cdot s^{-1})^{-1}$ ) |
| $\beta$                        | = coefficient of proportionality                              | ( $m \cdot s^{-1}$ )                                      |
| $\beta_d$                      | = limiting value of $\beta$                                   | ( $m \cdot s^{-1}$ )                                      |
| $\tau$                         | = velocity diffusion coefficient                              | ( $m^2 \cdot s^{-1}$ )                                    |
| $\epsilon$                     | = beam attenuation coefficient                                | ( $m^{-1}$ )  |
| $\lambda$                      | = wave length   | (m)   |
| $\xi$                          | = water level elevation relative to the reference plane       | (m)   |
| $\tau_c$                       | = maximum bottom stress due to currents                       |   |
| $\tau_u^x$                     | = component of the wind stress in x-direction                 | ( $m \cdot s^{-2}$ )                                      |
| $\tau_u^y$                     | = component of the wind stress in y-direction                 | ( $m \cdot s^{-2}$ )                                      |
| $\tau_w$                       | = maximum bottom stress due to waves                          | ( $m \cdot s^{-2}$ )                                      |
| $\tau_{w,cr}$                  | = critical maximum bottom stress due to waves                 | ( $m \cdot s^{-2}$ )                                      |
| $\sigma$                       | = density of water  | ( $g \cdot m^{-3}$ )                                      |
| $\sigma_s$                     | = sediment or particle density                                | ( $g \cdot m^{-3}$ )                                      |
| $\theta$                       | = zenith angle  | (°)   |
| $\theta_p$                     | = temperature coefficient for production                      | (-)   |
| $\theta_r$                     | = temperature coefficient for respiration                     | (-)   |
| $\Phi$                         | = resuspension flux   | ( $g \cdot m^{-2} \cdot s^{-1}$ )                         |
| $\Phi_s$                       | = gross sedimentation flux                                    | ( $g \cdot m^{-2} \cdot s^{-1}$ )                         |
| $\varphi$                      | = angle of solar elevation                                    | (°)   |
| $\phi$                         | = latitude  | (°)   |



## Abbreviations

|           |   |
|-----------|---|
| ADI       | = Alternating Direction Implicit  |
| dFL       | = directie Flevoland  |
| CLEAR     | = Combined Light Energy Attenuation Routine   |
| KNMI      | = Koninklijk Nederlands Meteorologisch Instituut<br>Royal Netherlands Meteorological Institute                      |
| LUW       | = Landbouwniversiteit Wageningen<br>Agricultural University of Wageningen   |
| MRE       | = Mean Relative Error   |
| NAP       | = Nieuw Amsterdams Peil (Amsterdams Reference Level)  |
| RWS       | = Rijkswaterstaat   |
| RIJP      | = Rijksdienst voor de IJsselmeerpolders,<br>IJsselmeerpolders Development Authority                                 |
| SSQ       | = Sum of Square Roots: mean of the sum of the square root of the<br>difference between measured and observed values |
| STRESS-2d | = two dimensional model for Sediment Transport REssuspension<br>and Sedimentation in Shallow lakes                  |
| SWE       | = Shallow Water Equations   |
| ZZW       | = dienst Zuiderzeewerken  |

# Appendix 2: Water balance of the Markermeer area

1988  
MAIN INPUT AND OUTPUT OF THE MARKERMEER AREA (10<sup>3</sup> m<sup>3</sup>·year<sup>-1</sup>)

| month | tot <sup>1</sup> | subtot <sup>2</sup> | Hout<br>in | K'rab.<br>in | Scheltw.<br>in | Zeeb.<br>in | Eem<br>in | Vech<br>in | BvK<br>in | Wort<br>in | Wkag<br>in | OostP<br>in | Drieb<br>in | Mon<br>out | Schid<br>in | Eclam<br>in | Precip<br>in | Sto <sup>3</sup> |
|-------|------------------|---------------------|------------|--------------|----------------|-------------|-----------|------------|-----------|------------|------------|-------------|-------------|------------|-------------|-------------|--------------|------------------|
| jan   | -14              | -121                | 1          | 1            | 0              | 14          | 32        | 6          | 82        | 4          | 6          | 2           | 3           | -1         | 4           | 1           | 113          | 26               |
| feb   | 40               | -17                 | 0          | 0            | 0              | -14         | 24        | 5          | 55        | 2          | 4          | 1           | 2           | -1         | 4           | 0           | 69           | 59               |
| mar   | -22              | -53                 | 0          | 0            | 0              | 1           | 18        | 8          | 53        | 2          | 4          | 1           | 2           | 0          | 9           | 0           | 52           | 0                |
| apr   | -14              | 35                  | 20         | 35           | 0              | 0           | 6         | 10         | 10        | 2          | 1          | 0           | 0           | 0          | 0           | 0           | 10           | -33              |
| may   | 91               | 151                 | 81         | 82           | 0              | 0           | 15        | 15         | 11        | 1          | 0          | 0           | 0           | 0          | 0           | 0           | 19           | 37               |
| jun   | 43               | 100                 | 15         | 83           | 0              | 1           | 23        | 20         | 1         | 2          | 0          | 0           | 0           | 0          | 0           | 0           | 7            | -41              |
| jul   | 1                | 2                   | 0          | 9            | 0              | 1           | 17        | 18         | 6         | 8          | 2          | 1           | 1           | 0          | 0           | 0           | 63           | -15              |
| aug   | 74               | 98                  | 81         | 66           | 0              | -23         | -11       | 10         | 19        | 4          | 1          | 0           | 1           | 0          | 0           | 0           | 47           | 33               |
| sep   | -24              | -31                 | 0          | 14           | 0              | -31         | -14       | 18         | 12        | 14         | 8          | 2           | 1           | 0          | 0           | 0           | 46           | -67              |
| oct   | -72              | -104                | 0          | 1            | 0              | -13         | -11       | 12         | 6         | 19         | 11         | 3           | 1           | -1         | 3           | 0           | 53           | -78              |
| nov   | 7                | -15                 | 0          | 1            | 1              | 0           | 24        | 0          | 11        | 1          | 1          | 1           | 1           | 0          | 0           | 0           | 33           | -11              |
| dec   | 123              | 49                  | 0          | 0            | 0              | -8          | 17        | 6          | 36        | 21         | 4          | 1           | 2           | -1         | 3           | 0           | 77           | 185              |
| total | 234              | 94                  | 178        | 303          | 1              | 23          | 217       | 125        | 304       | 67         | 27         | 9           | 14          | -5         | 23          | 2           | 590          | 96               |
|       |                  |                     | -562       | -134         | -121           | -162        |           |            |           |            |            |             |             |            | -210        | -6          | -450         |                  |

<sup>1</sup> including precipitation and evaporation

<sup>2</sup> excluding precipitation and evaporation

<sup>3</sup> storage computed from measured water level alterations

## Appendix 2: Continuation

1989  
MAIN INPUT AND OUTPUT OF THE MARKERMEER AREA ( $10^3 \text{ m}^3 \text{ year}^{-1}$ )

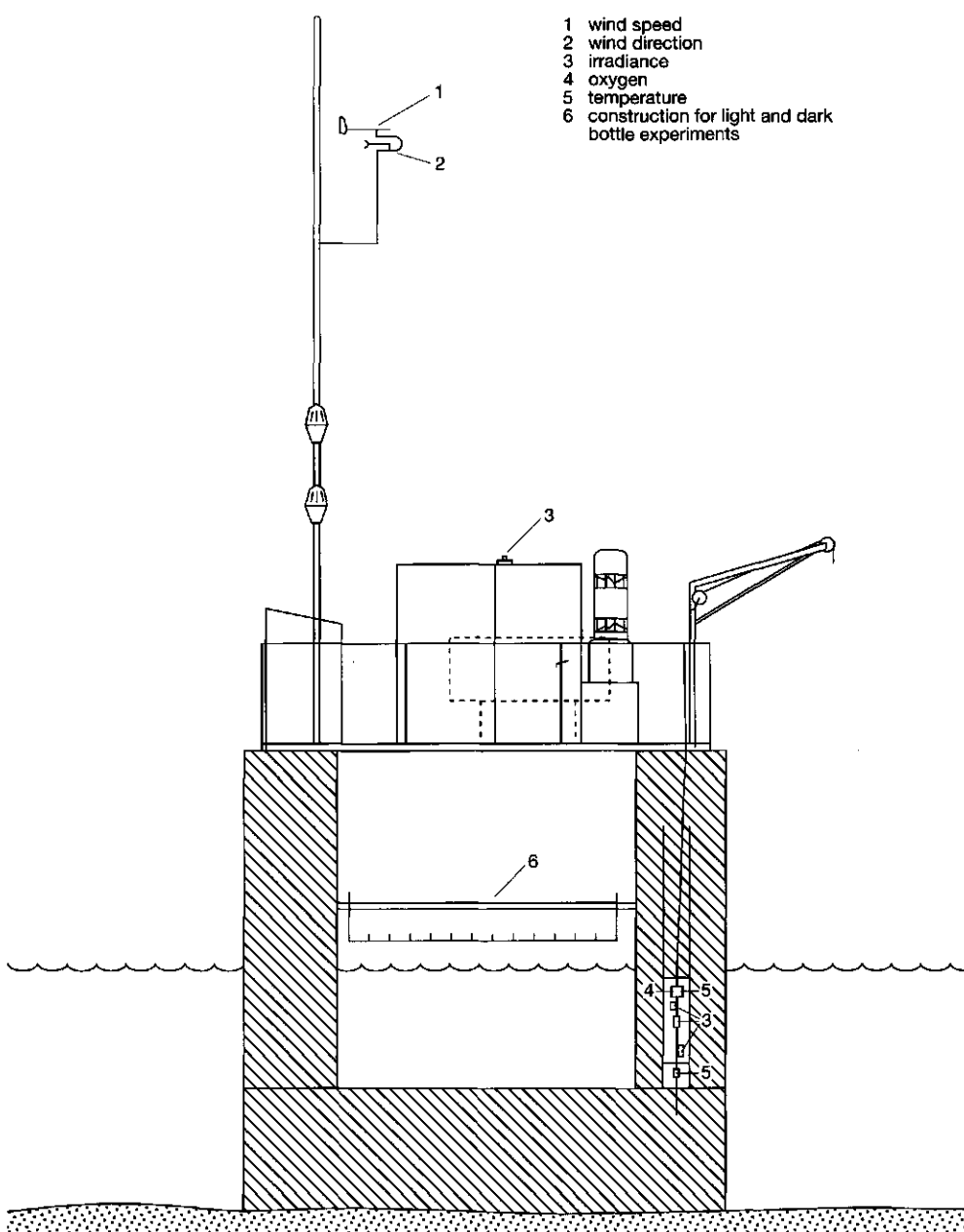
| month | tot <sup>1</sup> | subtot <sup>2</sup> | Hout<br>in | Krab.<br>in | Schielw<br>in | Zeeb.<br>in | Eem<br>in | Vech<br>in | BuK<br>in | Wort<br>in | WkGg<br>in | Oosip<br>in | Drieb<br>in | Mon<br>out | Schd<br>in | Edam<br>in | Precip<br>in | Sto <sup>3</sup> |
|-------|------------------|---------------------|------------|-------------|---------------|-------------|-----------|------------|-----------|------------|------------|-------------|-------------|------------|------------|------------|--------------|------------------|
| jan   | -231             | -237                | 14         | 0           | 0             | 0           | -13       | 35         | 2         | 10         | 5          | 1           | 0           | 0          | 0          | 0          | 13           | -215             |
| feb   | -2               | -23                 | 0          | 1           | 0             | 0           | -9        | 15         | 0         | 10         | 6          | 2           | 0           | 0          | 0          | 1          | 35           | 55               |
| mar   | 81               | 33                  | 45         | 33          | 0             | 3           | -9        | 23         | 3         | 36         | 9          | 4           | 1           | 0          | 3          | 1          | 80           | 143              |
| apr   | 14               | 20                  | 28         | 59          | 0             | 5           | -11       | 17         | 13        | 8          | 6          | 1           | 0           | 0          | 0          | 0          | 31           | -19              |
| may   | 64               | 155                 | 112        | 139         | 0             | 0           | -18       | 10         | 16        | 7          | 1          | 0           | 0           | 0          | 0          | 0          | 8            | 19               |
| jun   | 116              | 151                 | 95         | 119         | 0             | 0           | -17       | 16         | 20        | 6          | 7          | 0           | 0           | 0          | 0          | 0          | 58           | 22               |
| jul   | 68               | 117                 | 55         | 111         | 0             | 0           | -15       | 20         | 21        | 7          | 7          | 1           | 0           | 0          | 0          | 0          | 35           | -26              |
| aug   | 87               | 116                 | 34         | 105         | 0             | 0           | -13       | 28         | 19        | 6          | 4          | 0           | 0           | 0          | 0          | 0          | 38           | -15              |
| sep   | 4                | 22                  | 0          | 55          | 0             | 0           | -12       | 9          | 18        | 10         | 4          | 0           | 0           | 0          | 0          | 0          | 30           | -67              |
| oct   | -91              | -134                | 0          | 11          | 2             | 0           | -17       | 11         | 2         | 11         | 8          | 1           | 0           | 0          | 0          | 0          | 67           | -44              |
| nov   | -102             | -102                | 0          | 12          | 0             | 0           | -13       | 28         | 0         | 14         | 4          | 1           | 0           | 0          | 0          | 0          | 11           | -41              |
| dec   | 1                | -49                 | 0          | 10          | 3             | 4           | -7        | 21         | 2         | 26         | 17         | 3           | 1           | 0          | 1          | 0          | 54           | 115              |
| total | -9               | 68                  | 382        | 654         | 3             | 12          | -156      | 232        | 118       | 152        | 77         | 13          | 5           | 2          | 5          | 3          | 460          | -67              |
|       |                  |                     | -371       | -288        | -351          |             |           |            |           |            |            |             |             |            | -176       | -241       | -520         |                  |

<sup>1</sup> including precipitation and evaporation

<sup>2</sup> excluding precipitation and evaporation

<sup>3</sup> storage computed from measured water level alterations

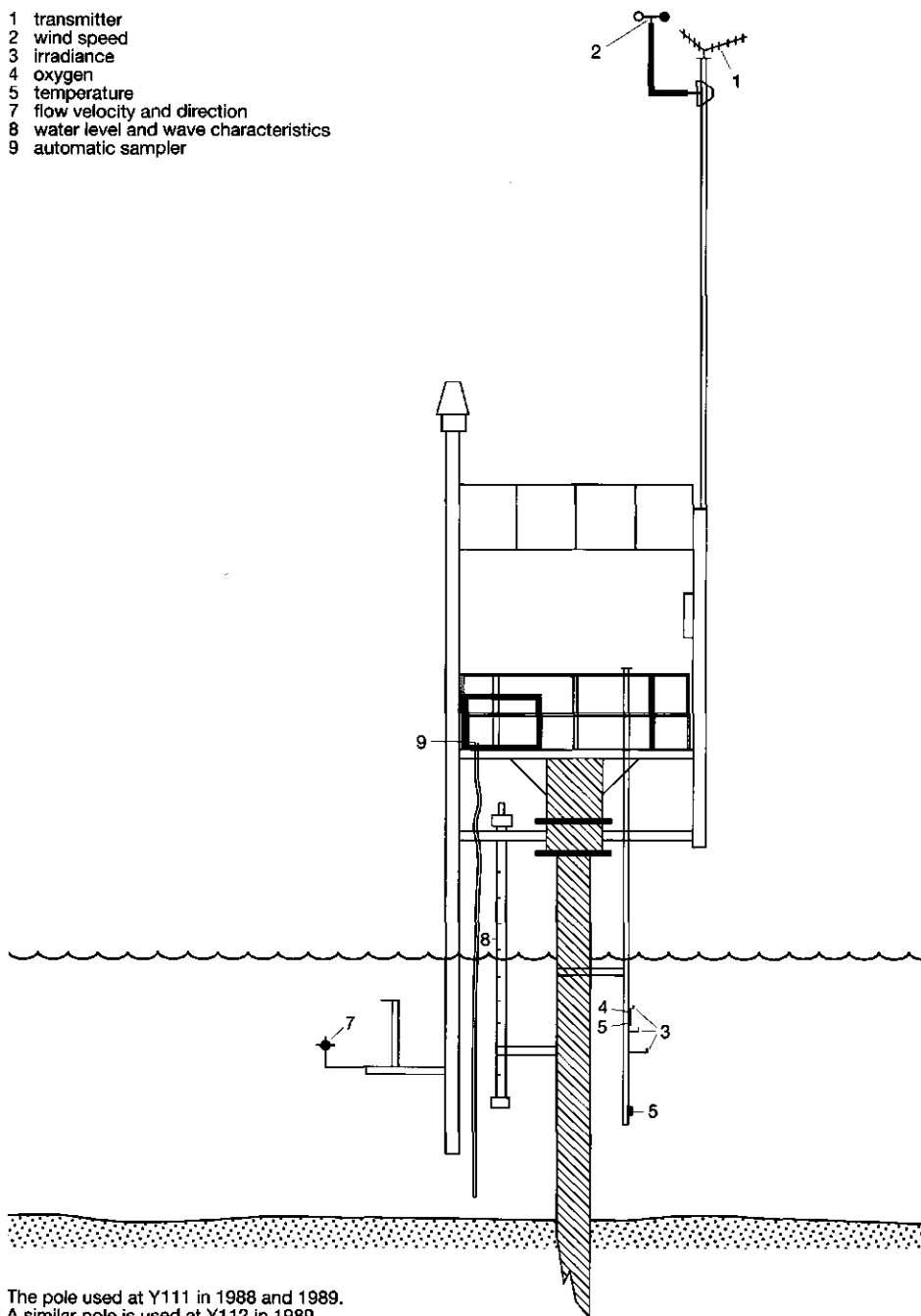
### Appendix 3: Equipment



The platform used at Y112 in 1987 and 1988

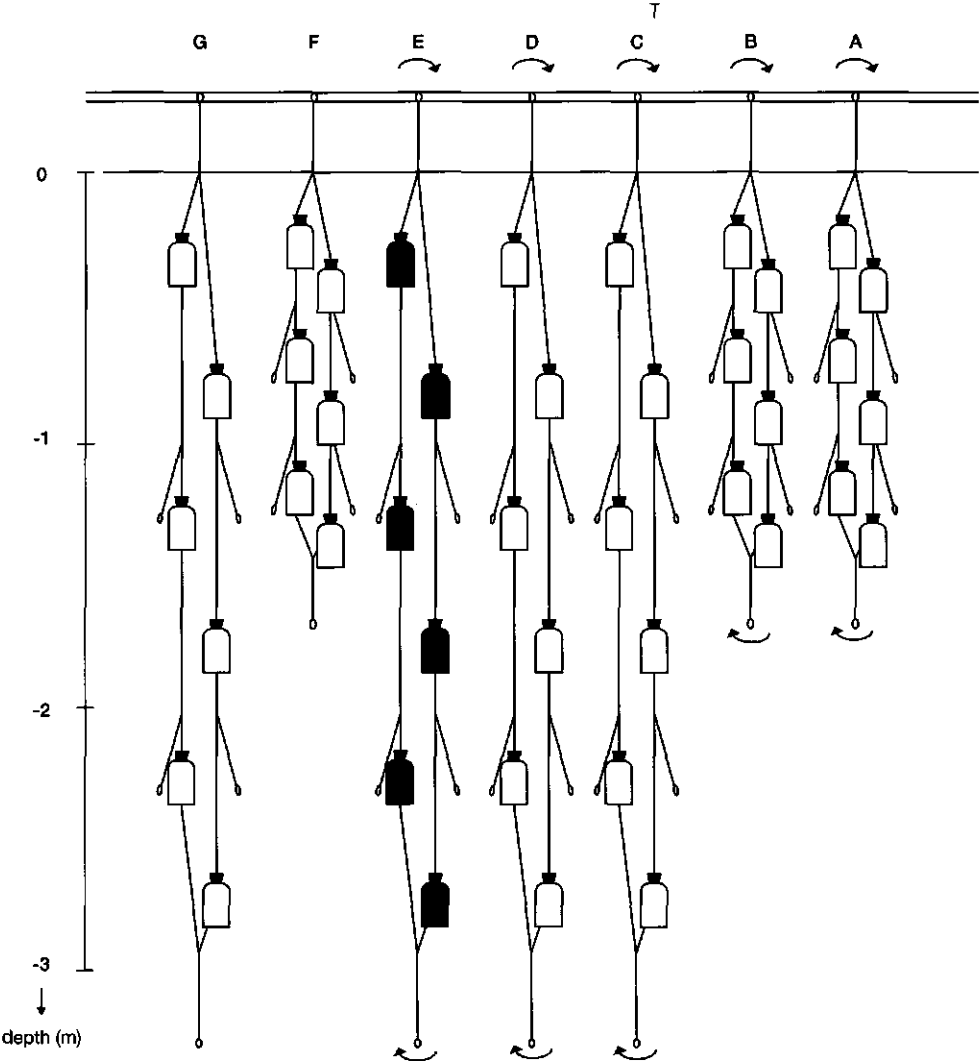
### Appendix 3: Continuation

- 1 transmitter
- 2 wind speed
- 3 irradiance
- 4 oxygen
- 5 temperature
- 7 flow velocity and direction
- 8 water level and wave characteristics
- 9 automatic sampler



The pole used at Y111 in 1988 and 1989.  
A similar pole is used at Y112 in 1989.

Appendix 3: Continuation

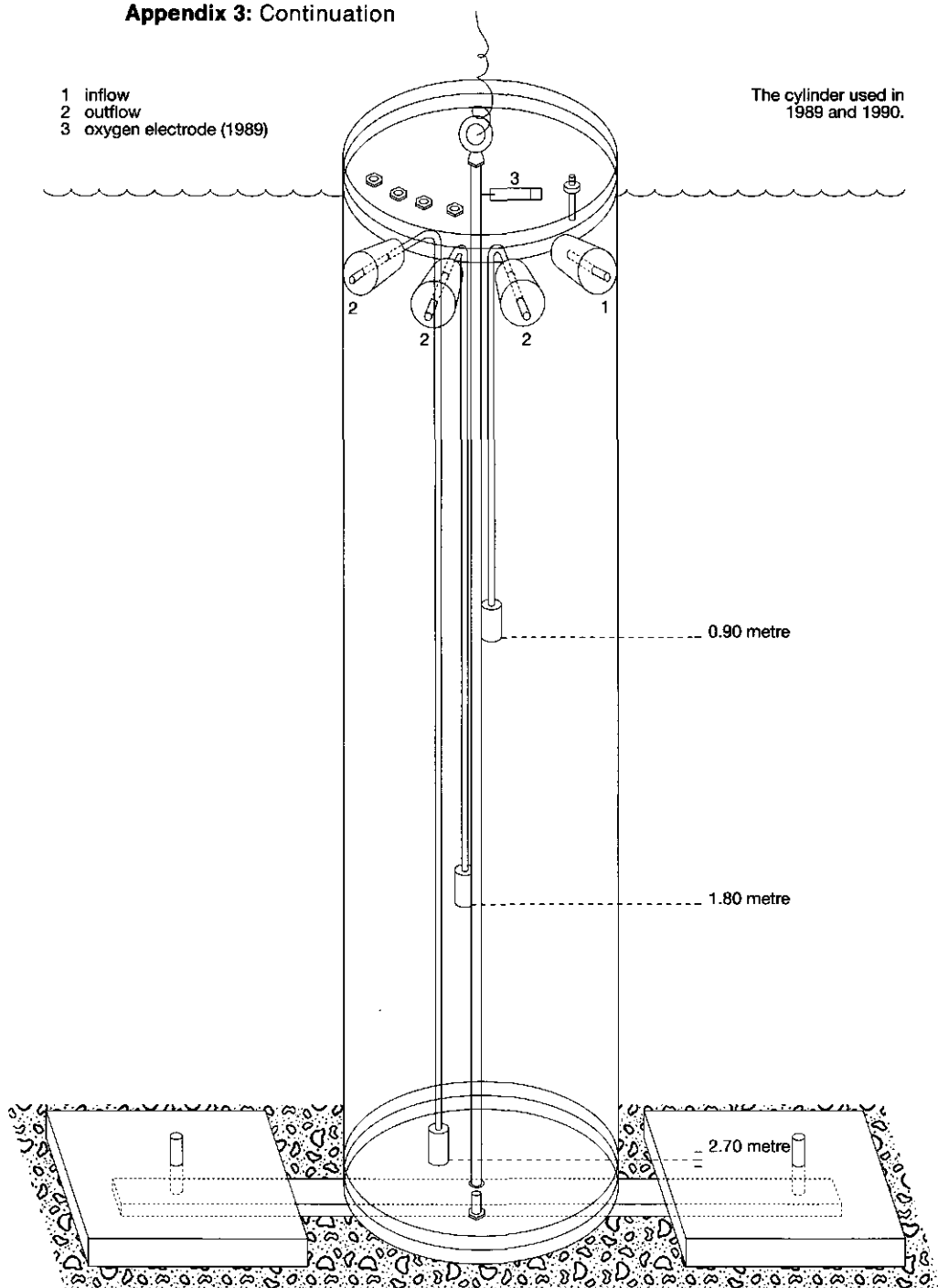


the light and dark bottle experiment as conducted in 1990

### Appendix 3: Continuation

- 1 inflow
- 2 outflow
- 3 oxygen electrode (1989)

The cylinder used in  
1989 and 1990.



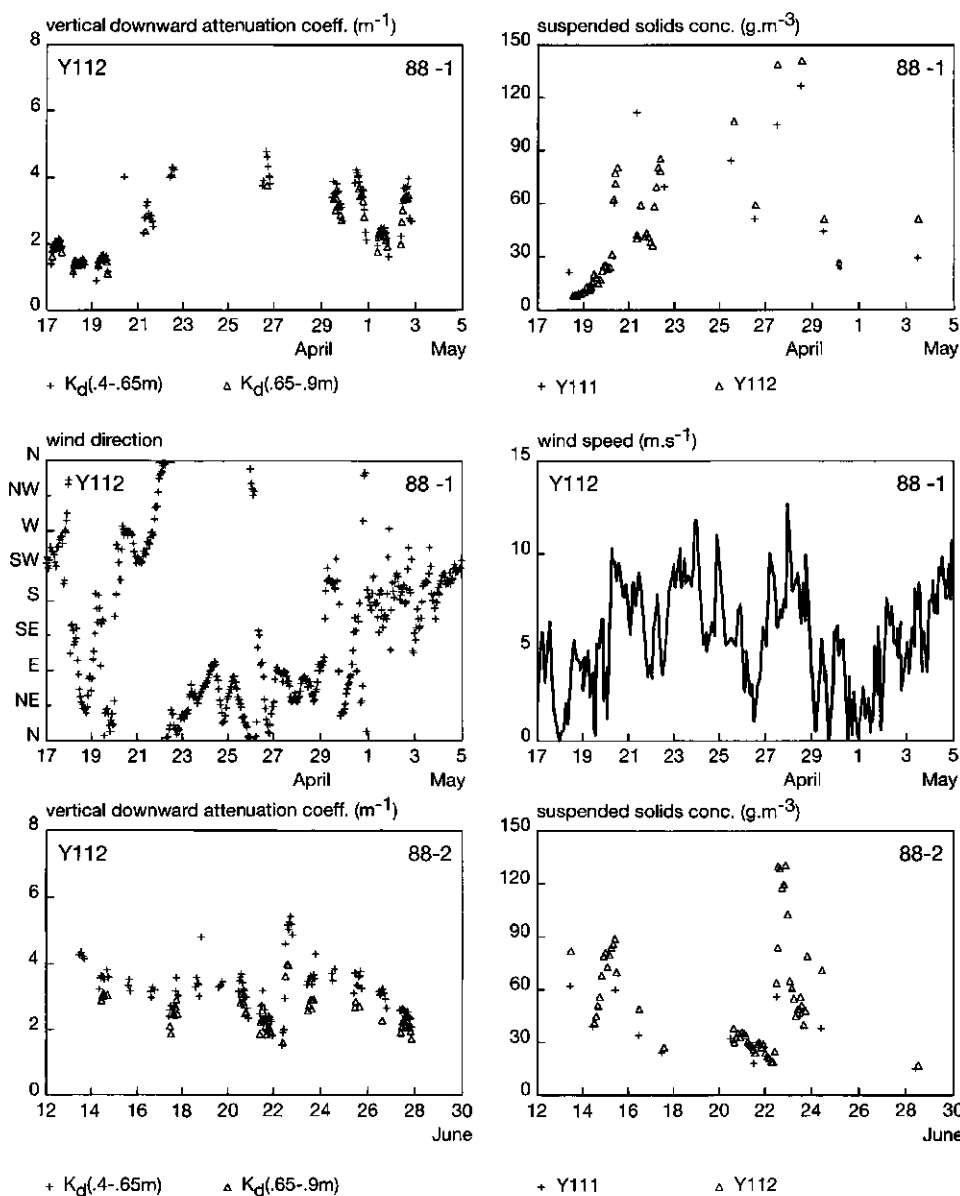
Appendix 4: Summary of weekly measurement data

| variabel          | average |      |      |      | minimum |      |      |      | maximum |      |      |      |
|-------------------|---------|------|------|------|---------|------|------|------|---------|------|------|------|
|                   | 1987    |      | 1988 |      | 1989    |      | 1987 |      | 1988    |      | 1987 |      |
|                   | Y111    | Y112 | Y111 | Y112 | Y111    | Y112 | Y111 | Y112 | Y111    | Y112 | Y111 | Y112 |
| Temperature-srf   | 14.3    | 14.6 | 13.3 | 13.6 | 16.8    | 17.3 | 6.0  | 8.5  | 5.2     | 5.0  | 8.5  | 21.5 |
| Temperature-1/2 z | 14.1    | 14.5 | 12.8 | 13.4 | 17.1    | 16.7 | 7.9  | 8.0  | 5.2     | 5.0  | 8.5  | 21.0 |
| Oxygen-srf        | 10.6    | 10.8 | 11.2 | 11.3 | 10.6    | 10.8 | 8.7  | 9.0  | 8.9     | 9.5  | 8.8  | 13.0 |
| Oxygen-1/2 z      | 10.5    | 10.6 | 10.9 | 11.2 | 10.6    | 10.8 | 8.5  | 8.9  | 9.0     | 9.1  | 8.5  | 12.6 |
| pH-srf            | 8.3     | 8.5  | 8.4  | 8.5  | 8.6     | 8.6  | 7.9  | 7.8  | 7.9     | 7.9  | 7.9  | 8.8  |
| pH-1/2 z          | 8.4     | 8.5  | 8.4  | 8.4  | 8.6     | 8.6  | 7.9  | 7.8  | 8.0     | 7.9  | 8.1  | 8.8  |
| Secchi-depth      | .48     | .46  | .45  | .37  | .50     | .49  | .15  | .10  | .15     | .15  | .10  | 1.2  |
| SS1-srf           | 43.0    | 43.0 | 52.4 | 59.8 | 29.7    | 36.2 | 7.0  | 7.0  | 13.0    | 12.1 | 9.7  | 10.2 |
| SS1-1/2 z         | 42.0    | 43.4 | 52.2 | 59.2 | 30.2    | 32.3 | 7.2  | 8.6  | 13.9    | 12.1 | 9.8  | 10.7 |
| AFDW-srf          | 14.0    | 14.0 | 16.2 | 16.4 | 11.6    | 12.2 | 2.4  | 2.4  | 5.4     | 5.5  | 5.5  | 5.2  |
| AFDW-1/2 z        | 14.5    | 14.0 | 16.2 | 16.1 | 11.9    | 12.2 | 1.9  | 2.4  | 6.1     | 4.8  | 5.0  | 5.3  |
| AFDW/SS-1/2 z     | 42      | 35   | 36   | 34   | 48      | 41   | 22   | 19   | 21      | 15   | 19   | 21   |
| Chla-srf          | 54      | 54   | 76   | 73   | 59      | 54   | 13   | 13   | 38      | 28   | 17   | 15   |
| Chla-1/2 z        | 63      | 55   | 75   | 73   | 60      | 55   | 17   | 14   | 31      | 28   | 24   | 15   |
| Phae-srf          | 26      | 26   | 26   | 26   | 13      | 12   | 4    | 4    | 0       | 0    | 0    | 0    |
| Phae-1/2 z        | 95      | 86   | 44   | 43   | 44      | 43   | 30   | 28   | 9       | 6    | 6    | 6    |
| Cell number       | 1.1     | 1.1  | 1.1  | 1.1  | 4.5     | 3.0  | 0    | 0    | 0       | 0    | 0    | 0    |
| O.agardhii        | 2       | 2    | 4    | 17   | 14      | 14   | 1    | 1    | 1       | 1    | 1    | 1    |
| O.agardhii        | 7.1     | 7.2  | 7.1  | 7.2  | 7.1     | 7.2  | 3.0  | 2.2  | 3.0     | 2.2  | 3.0  | 2.2  |
| POC <sup>5</sup>  | 6.7     | 7.0  | 6.7  | 7.0  | 6.7     | 7.0  | 6.2  | 6.4  | 6.2     | 6.4  | 6.2  | 6.4  |
| DOC <sup>5</sup>  | .10     | .09  | .12  | .12  | .10     | .11  | .02  | .01  | .04     | .01  | .03  | .03  |
| P-total           | .01     | .01  | .01  | .01  | .01     | .01  | .00  | .00  | .00     | .00  | .00  | .00  |
| P-PO <sub>4</sub> | 1.2     | 1.2  | 1.6  | 1.5  | 1.6     | 1.6  | .7   | .7   | 1.1     | 1.1  | 1.0  | .9   |
| N-Kjeldahl        | .12     | .11  | .22  | .23  | .05     | .10  | .0   | .0   | .0      | .0   | .0   | .0   |
| N-NO <sub>3</sub> | .04     | .02  | .06  | .06  | .06     | .07  | .0   | .0   | .01     | .0   | .0   | .01  |
| N-NH <sub>4</sub> |         |      |      |      |         |      |      |      |         |      |      |      |

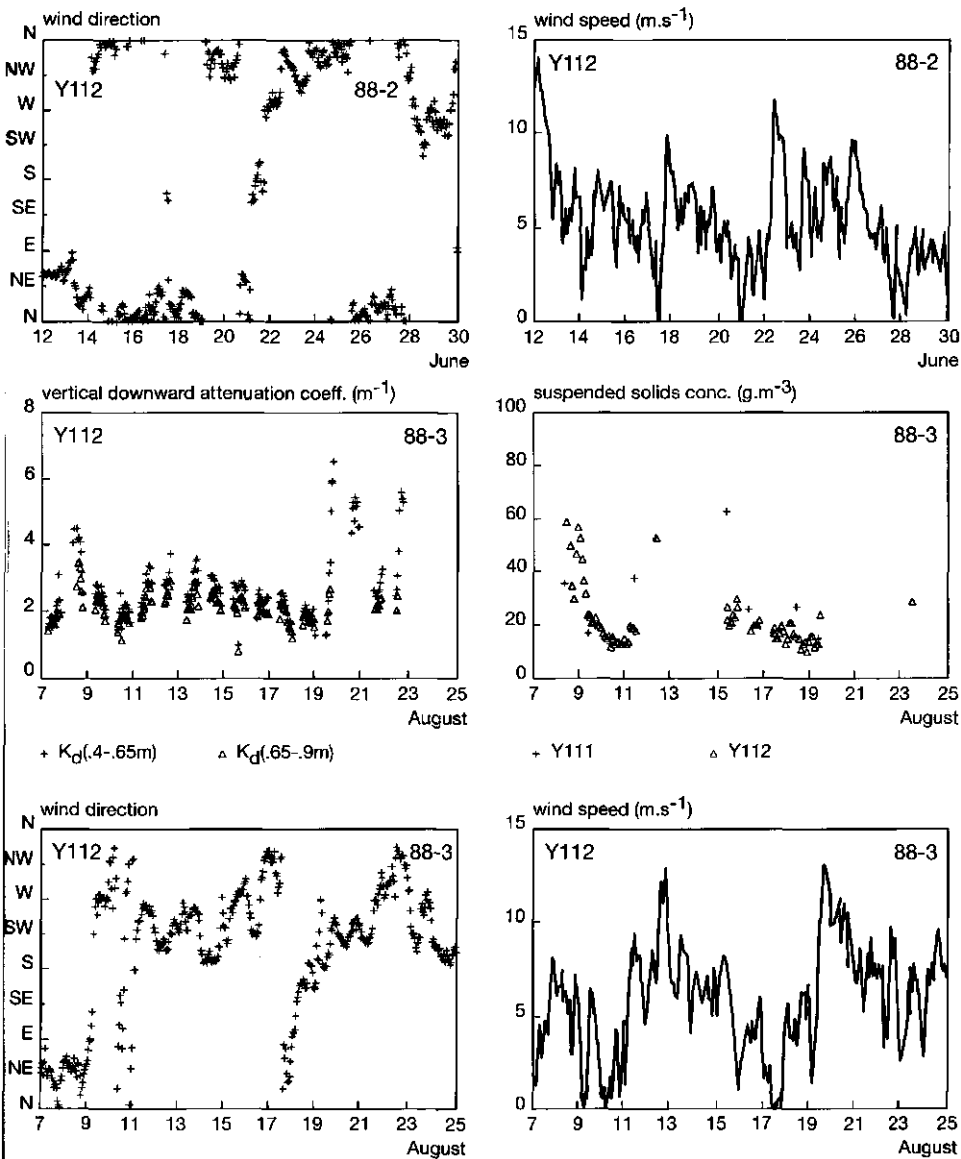
<sup>1</sup> SS = suspended solids      <sup>3</sup> Chla = Chlorophyll-a      <sup>5</sup> POC = Particulate Organic Carbon  
<sup>2</sup> AFDW = Ash Free Dry Weight      <sup>4</sup> Phae = Phaeophytine      <sup>6</sup> DOC = Dissolved Organic Carbon



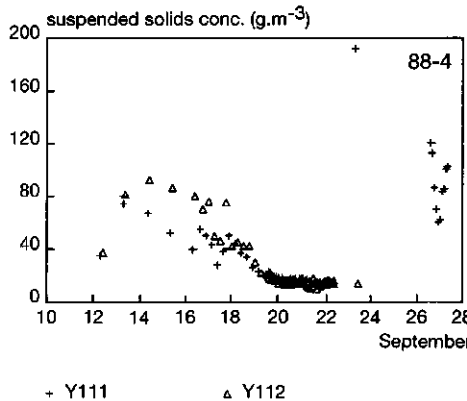
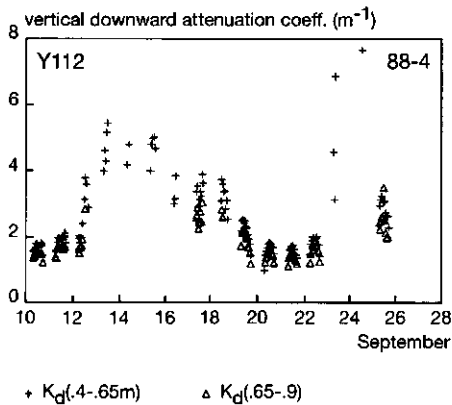
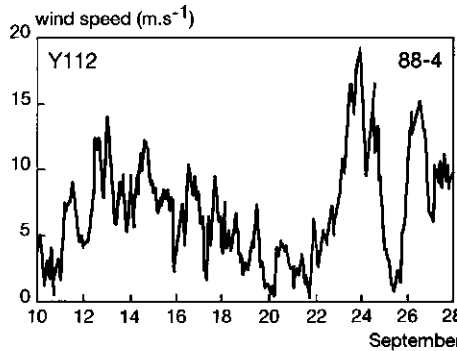
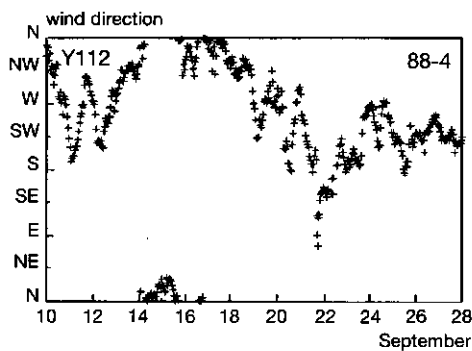
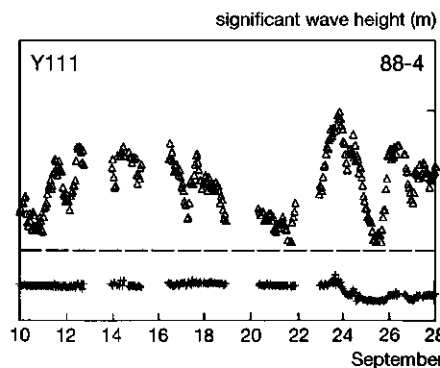
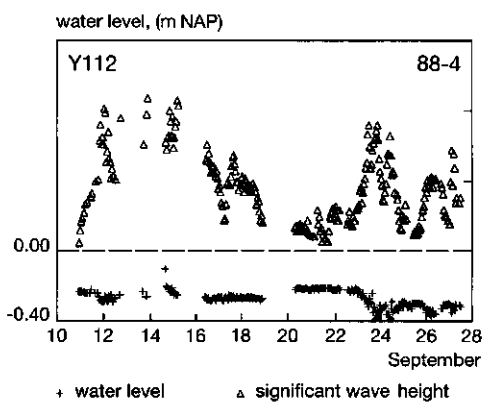
## Appendix 5: Data of the high frequency sampling periods



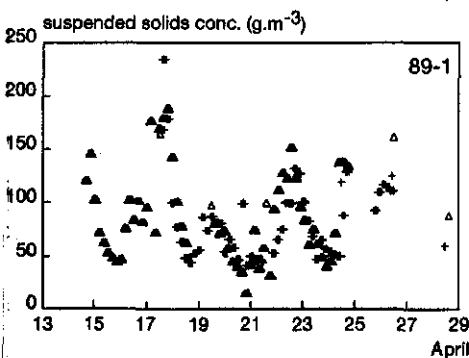
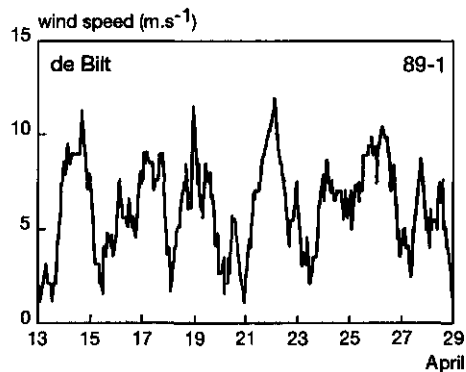
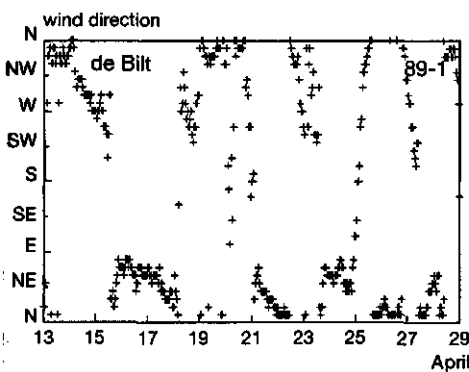
Appendix 5: Continuation



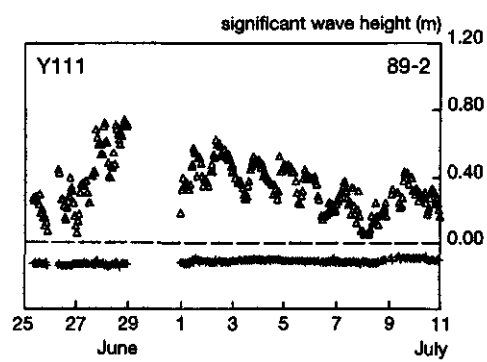
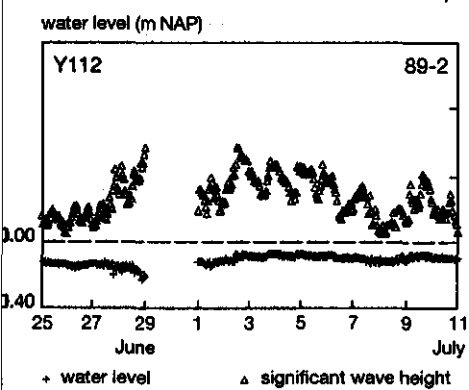
## Appendix 5: Continuation



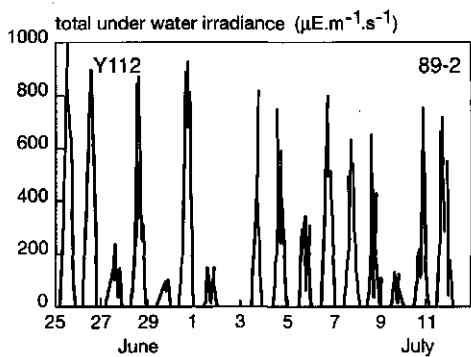
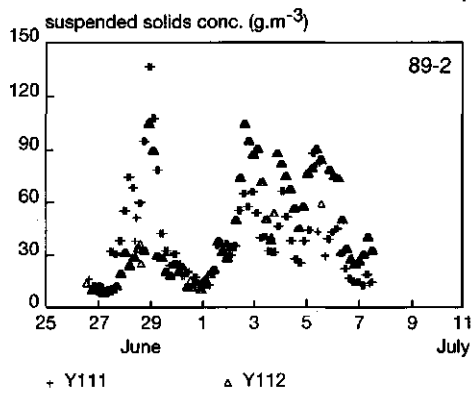
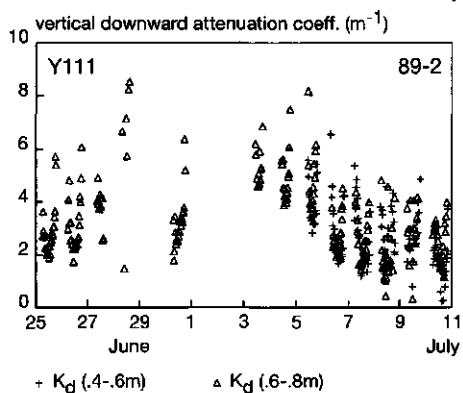
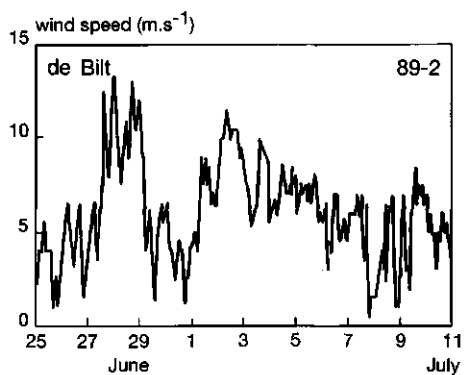
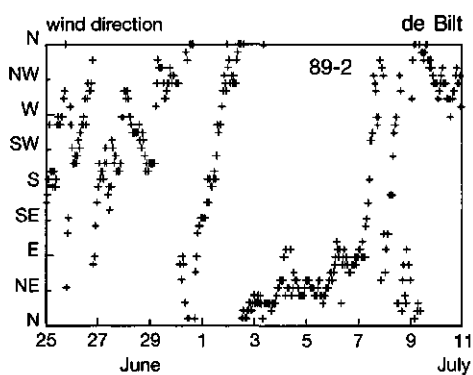
Appendix 5: Continuation



+ Y111  
Δ Y112

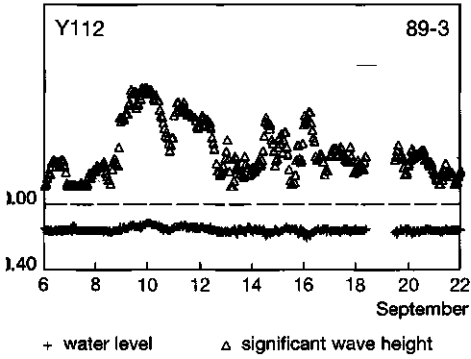


## Appendix 5: Continuation

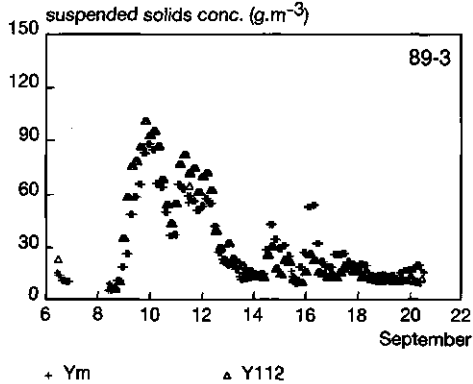
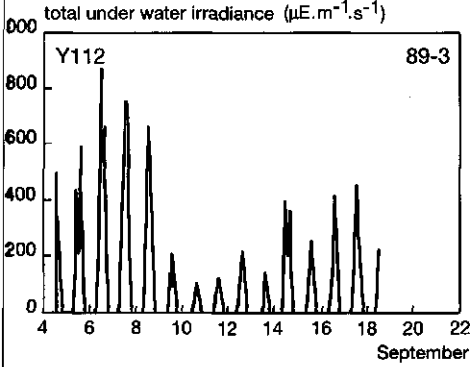
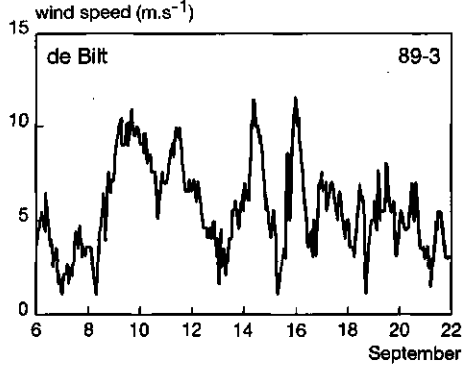
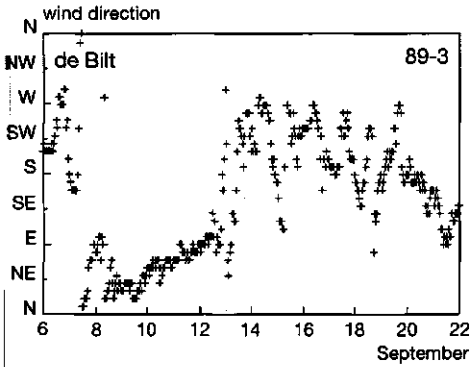
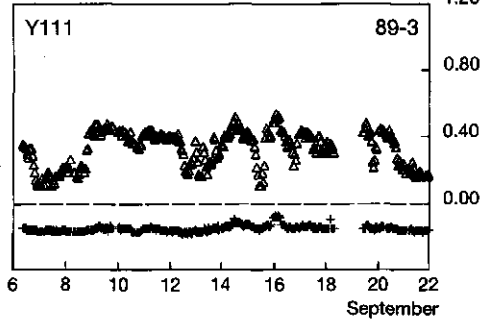


Appendix 5: Continuation

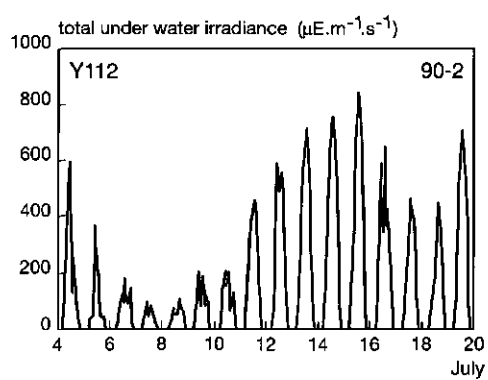
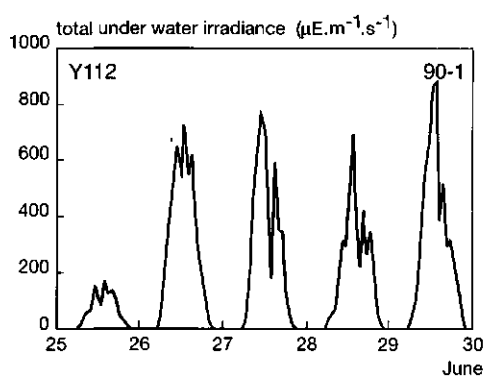
water level (m NAP)



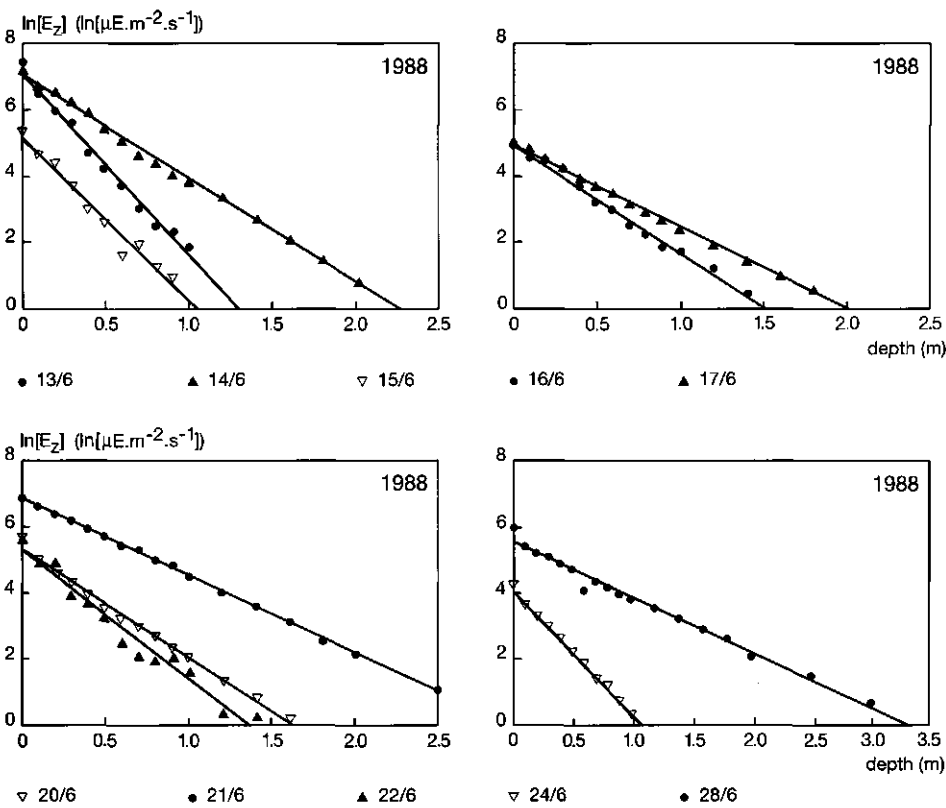
significant wave height (m)



## Appendix 5: Continuation



Appendix 6: Examples of incident irradiance measurements at Y112

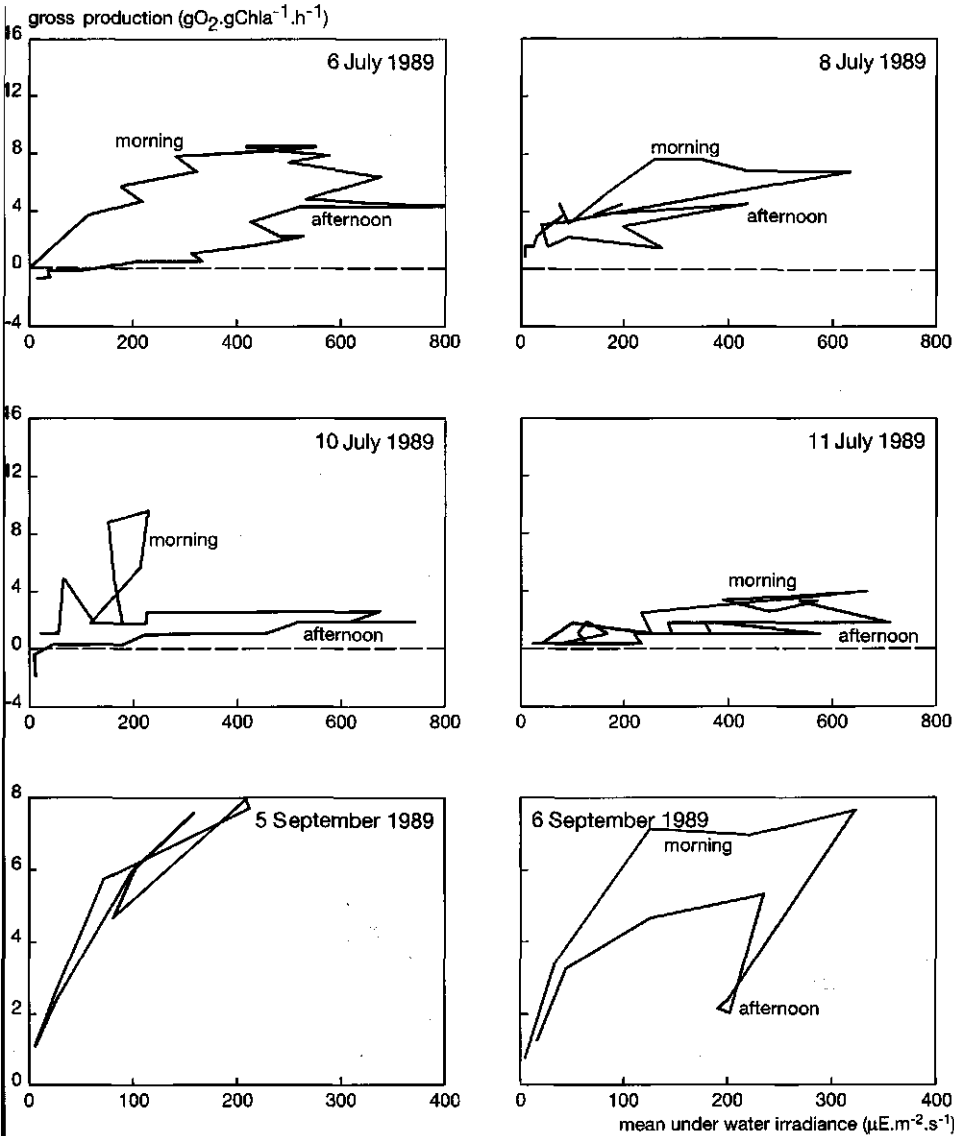




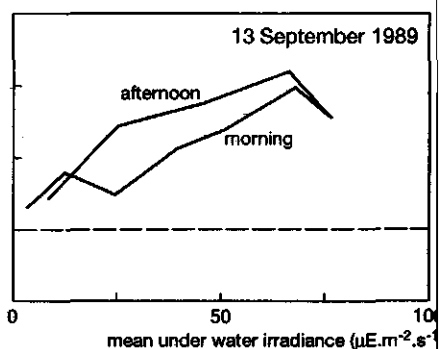
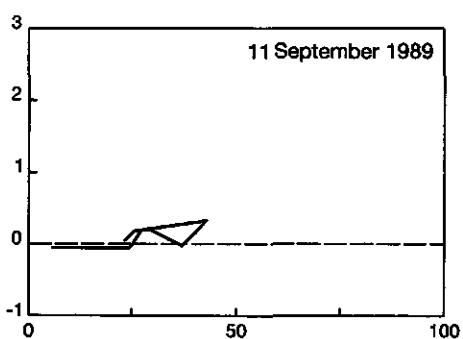
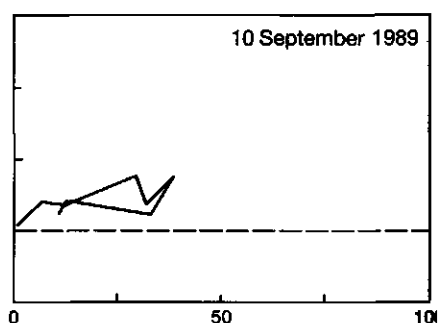
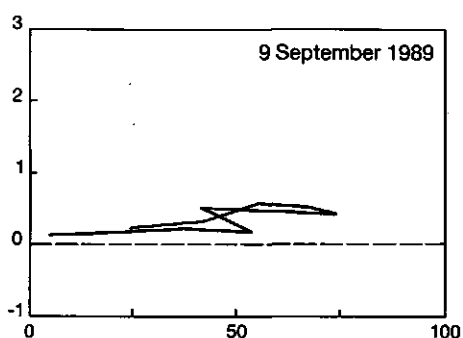
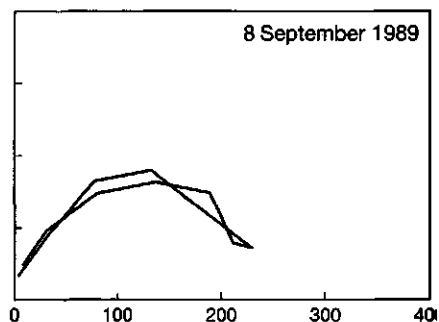
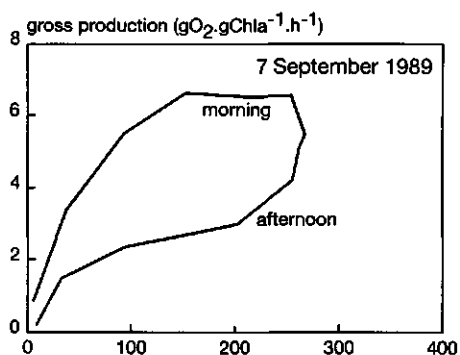
## Appendix 7: Composition of the nutrient solution

| Solution | dilution | components   | concentration (g·m <sup>-3</sup> ) |
|----------|----------|--|------------------------------------|
| 1        | 1:1000   | Na <sub>2</sub> -EDTA  | 4500                               |
|          |          | H <sub>3</sub> BO <sub>3</sub>   | 2860                               |
|          |          | Co(NO <sub>3</sub> ) <sub>2</sub> ·6H <sub>2</sub> O                               | 80                                 |
|          |          | CuSO <sub>4</sub> ·5H <sub>2</sub> O   | 80                                 |
|          |          | MnCl <sub>2</sub>  | 1810                               |
|          |          | (NH <sub>4</sub> ) <sub>6</sub> Mo <sub>7</sub> O <sub>24</sub> ·4H <sub>2</sub> O | 2                                  |
|          |          | NH <sub>4</sub> VO <sub>3</sub>  | 10                                 |
|          |          | ZnSO <sub>4</sub>  | 220                                |
| 2        | 1:100    | NaHCO <sub>3</sub>   | 10000                              |
| 3        | 1:1000   | K <sub>2</sub> HPO <sub>4</sub>  | 25000                              |
| 4        | 1:1000   | MgSO <sub>4</sub> ·7H <sub>2</sub> O   | 50000                              |
| 5        | 1:1000   | CaCl <sub>2</sub> ·2H <sub>2</sub> O   | 13000                              |
| 6        | 1:500    | MaNO <sub>3</sub>  | 250000                             |
| 7        | 1:1000   | Na <sub>2</sub> EDTA   | 4360                               |
|          |          | FECL <sub>3</sub> ·6H <sub>2</sub> O   | 3150                               |

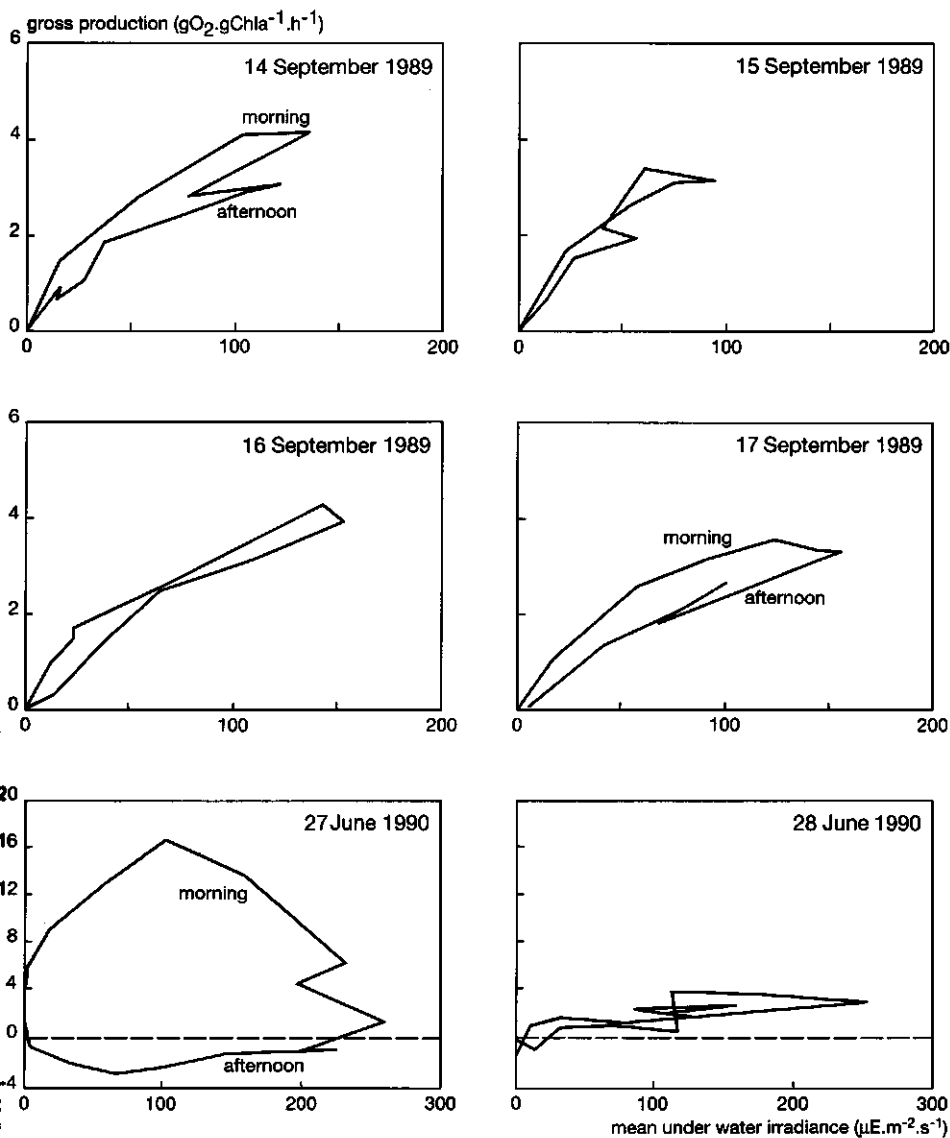
**Appendix 8:** Gross primary production rates related to the under water irradiance in the cylinder



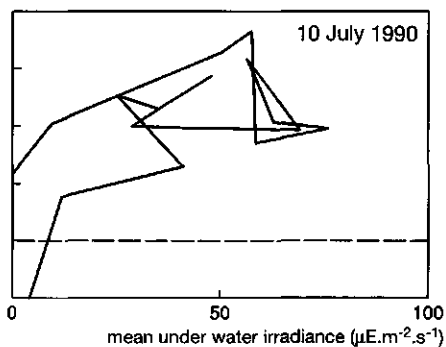
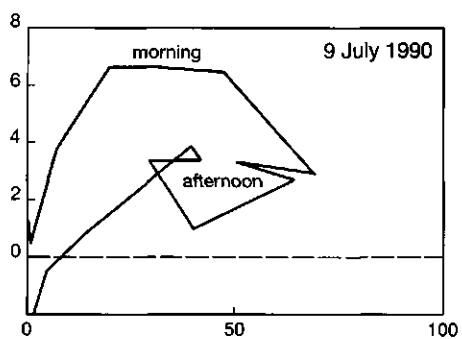
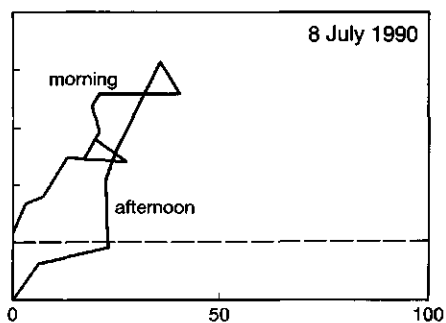
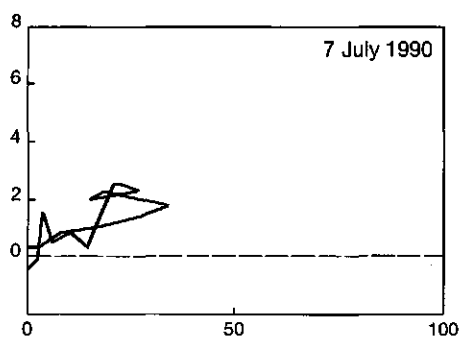
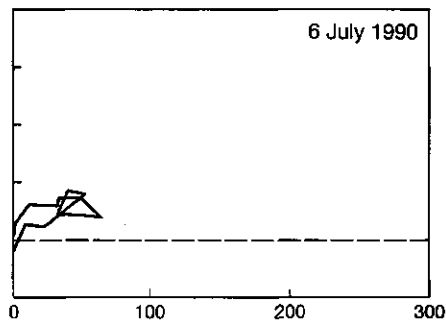
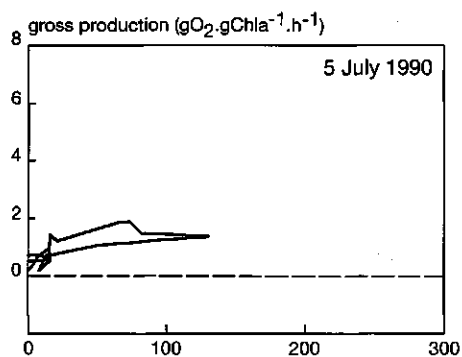
## Appendix 8: Continuation



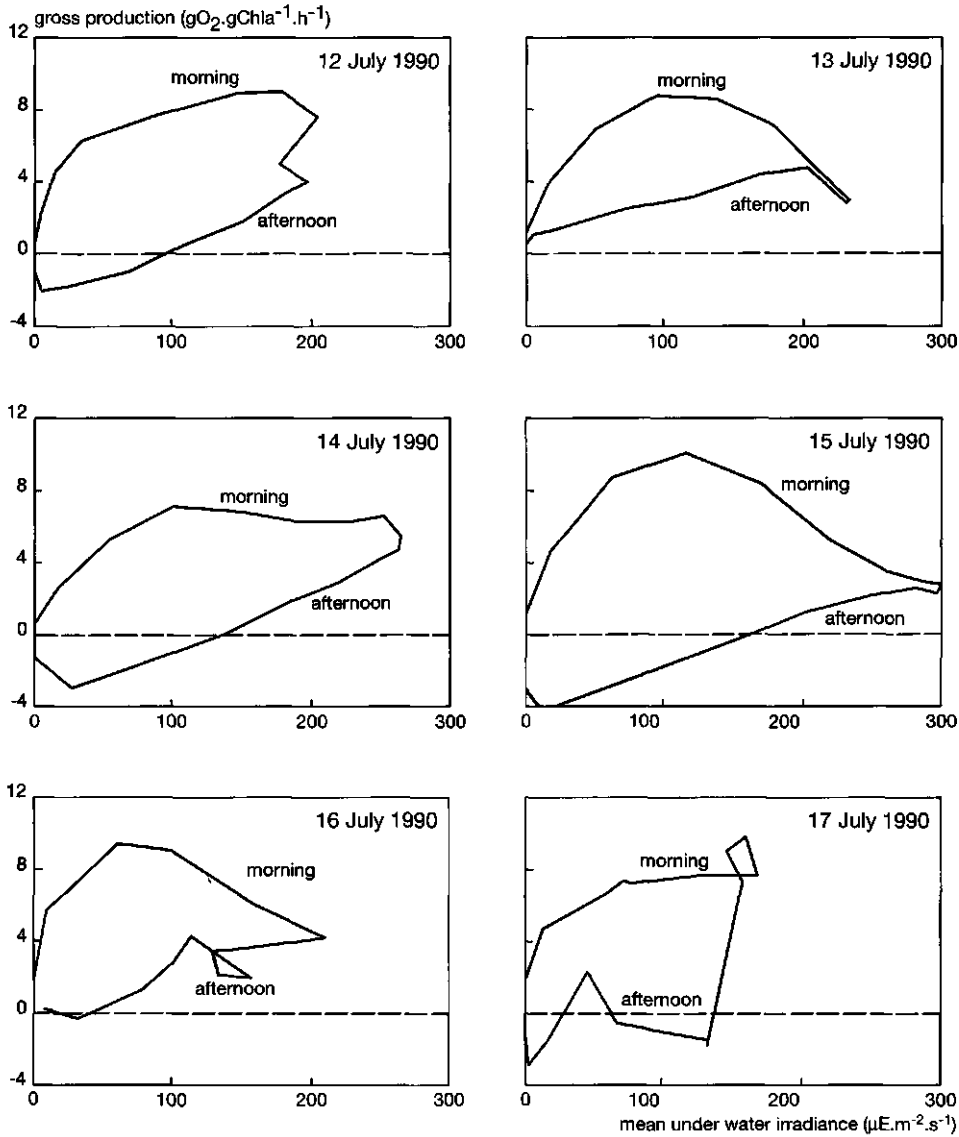
**Appendix 8: Continuation**



# Appendix 8: Continuation



Appendix 8: Continuation



## Appendix 9: Behaviour of the different wave models

| id | model  | period | site | Hc  | Hs   |       |     | TS   |       |     |
|----|--------|--------|------|-----|------|-------|-----|------|-------|-----|
|    |        |        |      |     | N    | SSQ   | MRE | N    | SSQ   | MRE |
| 1a | CERC1s | 1988   | Y111 | 0.1 | 1696 | 0.016 | 17  | 1775 | 0.036 | 10  |
| 1b |        | 1989   | Y111 |     | 2373 | 0.030 | 23  | 2367 | 0.036 | 10  |
| 1c |        | 1989   | Y112 |     | 2712 | 0.020 | 21  | 2712 | 0.045 | 11  |
| 2a | CERC2s | 1988   | Y111 | 0.1 | 1696 | 0.019 | 19  | 1775 | 0.043 | 10  |
| 2b |        | 1989   | Y111 |     | 2373 | 0.034 | 25  | 2367 | 0.040 | 10  |
| 2c |        | 1989   | Y112 |     | 2712 | 0.024 | 24  | 2712 | 0.049 | 12  |
| 3a | CERC2d | 1988   | Y111 | 0.1 | 1395 | 0.020 | 20  | 1775 | 0.259 | 24  |
| 3b |        | 1989   | Y111 |     | 1951 | 0.032 | 24  | 2367 | 0.224 | 22  |
| 3c |        | 1989   | Y112 |     | 2225 | 0.022 | 23  | 2712 | 0.196 | 23  |
| 4a | BOUWSs | 1988   | Y111 | 0.1 | 1696 | 0.032 | 28  | 1775 | 0.108 | 19  |
| 4b |        | 1989   | Y111 |     | 2373 | 0.036 | 29  | 2373 | 0.086 | 17  |
| 4c |        | 1989   | Y112 |     | 2712 | 0.028 | 29  | 2712 | 0.092 | 17  |
| 5a | BOUWSd | 1988   | Y111 | 0.1 | 1700 | 0.032 | 28  | 1782 | 0.111 | 19  |
| 5b |        | 1989   | Y111 |     | 2389 | 0.035 | 29  | 2383 | 0.085 | 17  |
| 5c |        | 1989   | Y112 |     | 2727 | 0.028 | 29  | 2727 | 0.092 | 17  |
| 6a | BOUWs  | 1988   | Y111 | 0.0 | 1783 | 0.032 | 28  | 1776 | 0.108 | 19  |
| 6b |        | 1989   | Y111 |     | 2668 | 0.036 | 29  | 2373 | 0.089 | 17  |
| 6c |        | 1989   | Y112 |     | 3124 | 0.028 | 29  | 2712 | 0.092 | 17  |
| 7a | BOUWSs | 1988   | Y111 | 0.2 | 1317 | 0.031 | 25  | 1776 | 0.108 | 19  |
| 7b |        | 1989   | Y111 |     | 1712 | 0.032 | 26  | 2373 | 0.086 | 17  |
| 7c |        | 1989   | Y112 |     | 1571 | 0.028 | 26  | 2712 | 0.092 | 17  |

id = run identification number

Hc = minimum value of measured wave height used for validation

N = number of measured values used for validation

SSQ = Root of the Sum of Square Roots of the differences between measured and computed values, divided by the number of values

MRE = Mean Relative Error

# **Appendix 10: Optimization of the parameters of the sedimentation/resuspension model**

| id              | site | 1989<br>SSQ | 89-2<br>F% | 89-3<br>F% | trap<br>F% | U <sub>b</sub>     | C   | z <sub>c</sub> | K <sub>1</sub>       | K <sub>2</sub>        | K <sub>3</sub>       | K <sub>4</sub>        |
|-----------------|------|-------------|------------|------------|------------|--------------------|-----|----------------|----------------------|-----------------------|----------------------|-----------------------|
| 1a              | Y111 | 1.278       | 32         | 22         | 16         | U <sub>b</sub> -G  | C-G | .006           | 1.05·10 <sup>5</sup> | 9.54·10 <sup>6</sup>  | 1.56·10 <sup>4</sup> | 2.23·10 <sup>4</sup>  |
|                 | Y112 | 1.038       | 36         | 22         | 11         |                    |     |                |                      |                       |                      |                       |
| 1b              | Y111 | 1.280       | 27         | 23         | 28         |                    |     |                | 6.50·10 <sup>7</sup> | 1.14·10 <sup>6</sup>  | 6.36·10 <sup>5</sup> | 1.60·10 <sup>4</sup>  |
|                 | Y112 | 1.031       | 26         | 22         | 23         | U <sub>b</sub> -G  | C-G | .006           | 7.54·10 <sup>7</sup> | 1.07·10 <sup>5</sup>  | 1.08·10 <sup>4</sup> | 1.89·10 <sup>4</sup>  |
| 2a              | Y111 | 1.278       | 33         |            | 18         | U <sub>b</sub> -G  | C-G | .008           |                      |                       |                      |                       |
|                 | Y112 | 1.038       | 34         | 30         | 12         |                    |     |                |                      |                       |                      |                       |
| 2b              | Y111 | 1.279       | 30         |            | 23         |                    |     |                | 6.42·10 <sup>7</sup> | 1.08·10 <sup>5</sup>  | 5.85·10 <sup>5</sup> | 1.87·10 <sup>4</sup>  |
|                 | Y112 | 1.033       | 29         | 24         | 22         | U <sub>b</sub> -G  | C-G | .008           | 8.76·10 <sup>7</sup> | 8.81·10 <sup>6</sup>  | 7.36·10 <sup>5</sup> | 1.12·10 <sup>4</sup>  |
| 3a              | Y111 | 1.278       | 31         | 19         | 8          | U <sub>b</sub> -M  | C-G | .006           |                      |                       |                      |                       |
|                 | Y112 | 1.033       | 33         | 28         | 11         |                    |     |                | 6.13·10 <sup>7</sup> | 8.04·10 <sup>6</sup>  | 4.17·10 <sup>5</sup> | 1.04·10 <sup>4</sup>  |
| 3b <sup>1</sup> | Y111 | 1.280       | 26         | 24         | 14         |                    |     |                | 8.69·10 <sup>7</sup> | 1.04·10 <sup>5</sup>  | 2.13·10 <sup>5</sup> | 1.04·10 <sup>4</sup>  |
|                 | Y112 | 1.033       | 26         | 22         | 16         | U <sub>b</sub> -M  | C-G | .006           | 7.15·10 <sup>7</sup> | 9.37·10 <sup>6</sup>  | 1.03·10 <sup>5</sup> | 1.04·10 <sup>4</sup>  |
| 4a              | Y111 | 1.278       | 33         | 21         | 17         | U <sub>b</sub> -M  | C-G | .008           |                      |                       |                      |                       |
|                 | Y112 | 1.035       | 31         | 26         | 17         |                    |     |                | 1.11·10 <sup>6</sup> | 8.36·10 <sup>6</sup>  | 1.59·10 <sup>5</sup> | 8.93·10 <sup>5</sup>  |
| 4b              | Y111 | 1.280       | 28         | 24         | 22         |                    |     |                | 6.08·10 <sup>7</sup> | 6.84·10 <sup>6</sup>  | 2.97·10 <sup>5</sup> | 8.91·10 <sup>5</sup>  |
|                 | Y112 | 1.032       | 25         | 22         | 22         | U <sub>b</sub> -M  | C-G | .008           | 7.61·10 <sup>7</sup> | 1.11·10 <sup>5</sup>  | 1.22·10 <sup>5</sup> | 29.03·10 <sup>5</sup> |
| 5a              | Y111 | 1.279       | 32         | 22         | 9          | U <sub>b</sub> -K  | C-G | .006           |                      |                       |                      |                       |
|                 | Y112 | 1.280       | 26         | 23         | 6          |                    |     |                |                      |                       |                      |                       |
| 5b              | Y111 | 1.030       | 25         | 22         | 10         | U <sub>b</sub> -K  | C-G | .006           |                      |                       |                      |                       |
|                 | Y112 | 1.030       | 25         | 22         | 10         |                    |     |                |                      |                       |                      |                       |
| 6a              | Y111 | 1.279       | 35         | 20         | 7          | U <sub>b</sub> -K  | C-G | .008           |                      |                       |                      |                       |
|                 | Y112 | 1.030       | 27         | 24         | 12         |                    |     |                |                      |                       |                      |                       |
| 6b              | Y111 | 1.281       | 25         | 24         | 5          |                    |     |                | 7.78·10 <sup>7</sup> | 24.00·10 <sup>6</sup> | 3.87·10 <sup>5</sup> | 8.58·10 <sup>5</sup>  |
|                 | Y112 | 1.029       | 25         | 24         | 10         | U <sub>b</sub> -K  | C-G | .008           | 6.64·10 <sup>7</sup> | 1.21·10 <sup>5</sup>  | 1.22·10 <sup>5</sup> | 29.00·10 <sup>5</sup> |
| 7a              | Y111 | 1.280       | 29         | 21         | 7          | U <sub>b</sub> -K' | C-G | .008           |                      |                       |                      |                       |
|                 | Y112 | 1.030       | 27         | 23         | 14         |                    |     |                |                      |                       |                      |                       |
| 7b              | Y111 | 1.280       | 29         | 21         | 7          |                    |     |                | 6.03·10 <sup>7</sup> | 1.06·10 <sup>5</sup>  | 1.15·10 <sup>5</sup> | 9.50·10 <sup>5</sup>  |
|                 | Y112 | 1.030       | 24         | 21         | 12         | U <sub>b</sub> -K' | C-G | .008           |                      |                       |                      |                       |

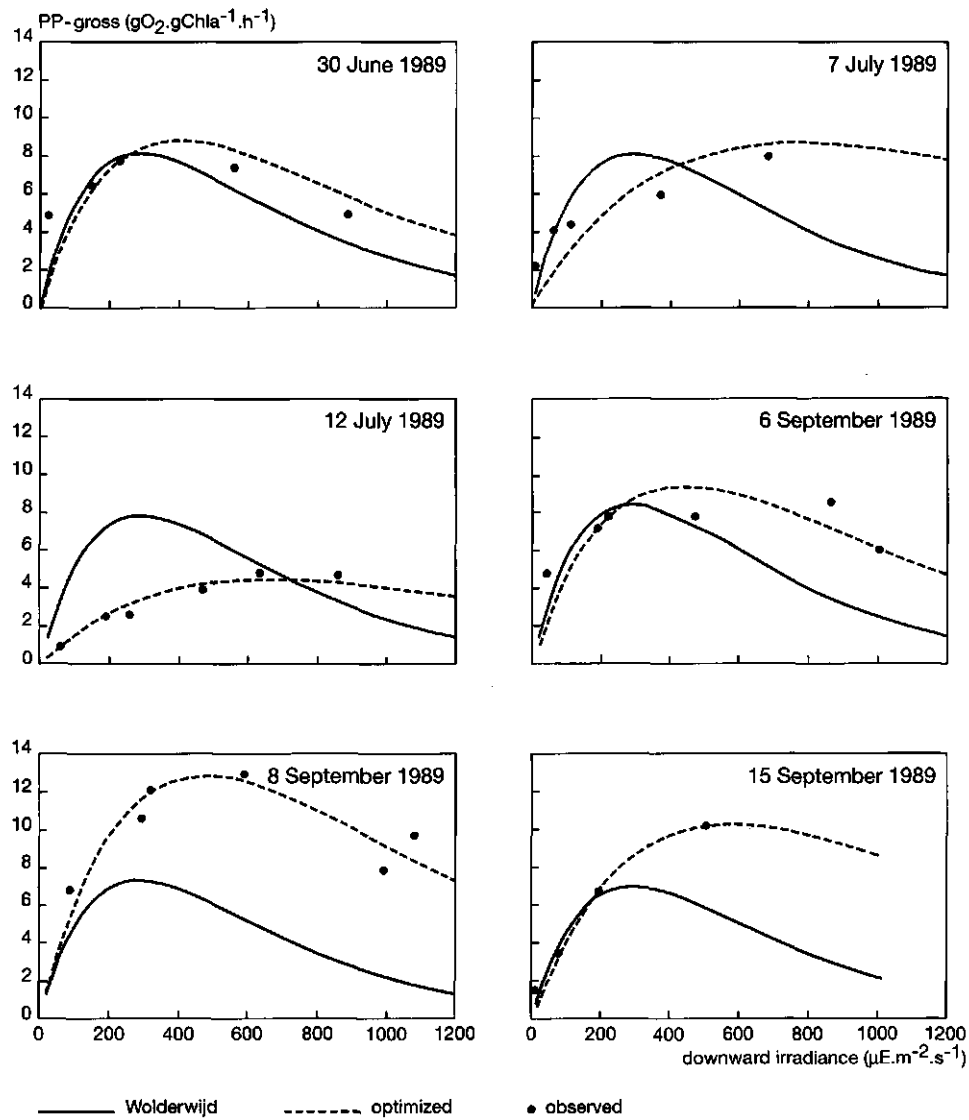


# Appendix 10: Continuation

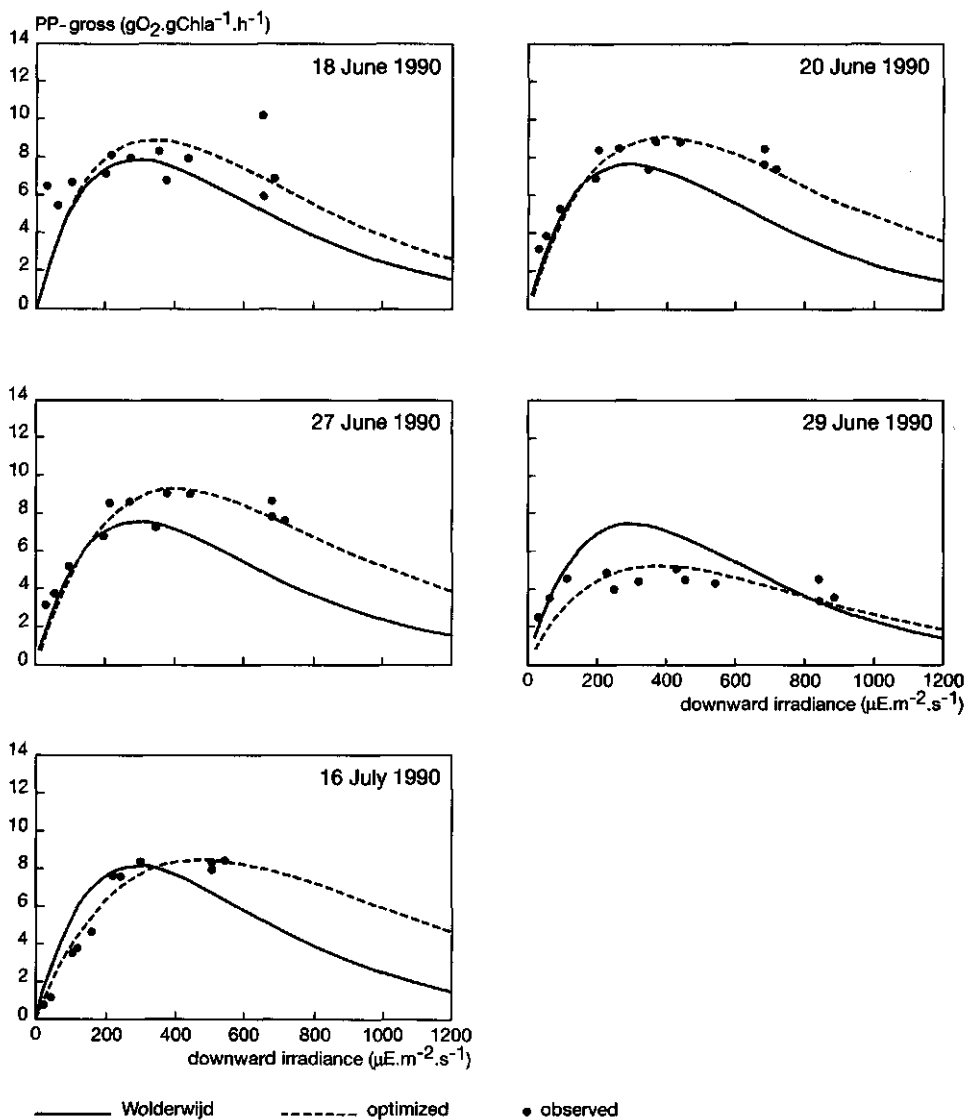
| id               | site               | 1989<br>SSQ        | 89-2<br>F%         | 89-3<br>F%         | trap<br>F%         | U <sub>b</sub>    | C   | z <sub>c</sub> | K <sub>1</sub>        | K <sub>2</sub>        | K <sub>3</sub>        | K <sub>4</sub>       |
|------------------|--------------------|--------------------|--------------------|--------------------|--------------------|-------------------|-----|----------------|-----------------------|-----------------------|-----------------------|----------------------|
| 8a               | Y111               | 1.279              | 31                 | 19                 | 7                  | U <sub>b</sub> -M | C-K | .006           | 9.58·10 <sup>7</sup>  | 9.33·10 <sup>6</sup>  | 6.95·10 <sup>5</sup>  | 1.17·10 <sup>4</sup> |
|                  | Y112               | 1.032              | 33                 | 23                 | 8                  |                   |     |                |                       |                       |                       |                      |
| 8b <sup>1</sup>  | Y111               | 1.278              | 26                 | 22                 | 14                 |                   |     |                |                       |                       |                       |                      |
|                  | Y112               | 1.030              | 25                 | 21                 | 14                 | U <sub>b</sub> -M | C-K | .006           | 7.15·10 <sup>7</sup>  | 9.17·10 <sup>6</sup>  | 3.57·10 <sup>5</sup>  | 1.10·10 <sup>4</sup> |
| 9a <sup>1</sup>  | Y111               | 1.278              | 32                 | 19                 | 9                  | U <sub>b</sub> -M | C-K | .008           | 7.56·10 <sup>7</sup>  | 8.49·10 <sup>6</sup>  | 8.34·10 <sup>5</sup>  | 1.04·10 <sup>4</sup> |
|                  | Y112               | 1.033              | 33                 | 28                 | 10                 |                   |     |                |                       |                       |                       |                      |
| 9b               | Y111               | 1.279              | 31                 | 21                 | 3                  |                   |     |                |                       |                       |                       |                      |
|                  | Y112               | 1.032              | 31                 | 25                 | 2                  | U <sub>b</sub> -M | C-K | .008           | 7.10·10 <sup>7</sup>  | 1.01·10 <sup>6</sup>  | 3.29·10 <sup>5</sup>  | 1.11·10 <sup>4</sup> |
| 10a              | Y111               | 1.279              | 31                 | 27                 | 12                 | U <sub>b</sub> -M | C-K | .004           | 22.00·10 <sup>6</sup> | 26.43·10 <sup>6</sup> | 7.68·10 <sup>5</sup>  | 1.17·10 <sup>4</sup> |
| 10b              | Y111               | 1.281              | 28                 | 21                 | 15                 |                   |     |                |                       |                       |                       |                      |
|                  | Y112               | 1.033              | 29                 | 20                 | 14                 | U <sub>b</sub> -M | C-K | .004           | 1.13·10 <sup>8</sup>  | 1.01·10 <sup>6</sup>  | 2.84·10 <sup>5</sup>  | 1.27·10 <sup>4</sup> |
| 11a              | Y111               | 1.279              | 31                 | 20                 | 4                  | U <sub>b</sub> -K | C-K | .006           | 8.89·10 <sup>7</sup>  | 9.09·10 <sup>6</sup>  | 4.61·10 <sup>5</sup>  | 8.75·10 <sup>5</sup> |
|                  | Y112               | 1.031              | 31                 | 26                 | 9                  |                   |     |                |                       |                       |                       |                      |
| 11b <sup>1</sup> | Y111               | 1.280              | 27                 | 21                 | 6                  |                   |     |                |                       |                       |                       |                      |
|                  | Y112               | 1.030              | 25                 | 21                 | 10                 | U <sub>b</sub> -K | C-K | .006           | 6.34·10 <sup>7</sup>  | 9.37·10 <sup>6</sup>  | 2.67·10 <sup>5</sup>  | 8.89·10 <sup>5</sup> |
| 12a              | Y111               | 1.279              | 33                 | 20                 | 10                 | U <sub>b</sub> -K | C-K | .008           | 8.57·10 <sup>5</sup>  | 1.15·10 <sup>5</sup>  | 1.20·10 <sup>5</sup>  | 8.53·10 <sup>5</sup> |
|                  | Y112               | 1.032              | 29                 | 26                 | 15                 |                   |     |                |                       |                       |                       |                      |
| 12b <sup>1</sup> | Y111               | 1.279              | 28                 | 21                 | 12                 |                   |     |                |                       |                       |                       |                      |
|                  | Y112               | 1.030              | 24                 | 21                 | 15                 | U <sub>b</sub> -K | C-K | .008           | 5.77·10 <sup>7</sup>  | 1.16·10 <sup>5</sup>  | 21.00·10 <sup>5</sup> | 8.59·10 <sup>5</sup> |
| 13a              | Y111               | 1.280              | 31                 | 26                 | 9                  | U <sub>b</sub> -K | C-K | .004           | 22.00·10 <sup>6</sup> | 6.66·10 <sup>6</sup>  | 2.09·10 <sup>5</sup>  | 9.62·10 <sup>5</sup> |
| 13b              | Y112               | 1.030              | 27                 | 20                 | 9                  | U <sub>b</sub> -K | C-K | .004           | 1.09·10 <sup>5</sup>  | 7.88·10 <sup>6</sup>  | 2.32·10 <sup>5</sup>  | 1.03·10 <sup>4</sup> |
|                  |                    | U <sub>ben,1</sub> | U <sub>ben,2</sub> | U <sub>ben,3</sub> | U <sub>ben,4</sub> |                   |     |                | C <sub>c</sub>        | C <sub>a</sub>        | C <sub>t</sub>        |                      |
|                  | U <sub>G</sub>     | 0.0008             | 0.0060             | 0.0260             | 0.1000             |                   |     |                | 1.0·10 <sup>8</sup>   | 1.0·10 <sup>8</sup>   | 1.6·10 <sup>8</sup>   |                      |
|                  | U <sub>G</sub> (M) | 0.0004             | 0.0030             | 0.0130             | 0.0500             |                   |     |                | 0.5·10 <sup>8</sup>   | 0.5·10 <sup>8</sup>   | 1.6·10 <sup>8</sup>   |                      |
|                  | U <sub>G</sub> -K  | 0.0002             | 0.0015             | 0.0065             | 0.0100             |                   |     |                |                       |                       |                       |                      |
|                  | U <sub>G</sub> -K' | 0.0000             | 0.0015             | 0.0065             | 0.0100             |                   |     |                |                       |                       |                       |                      |

<sup>1</sup> These parameter sets are validated with the STRESS-2d model.  
<sup>2</sup> These parameters got assigned their predetermined boundary value (minimum or maximum).

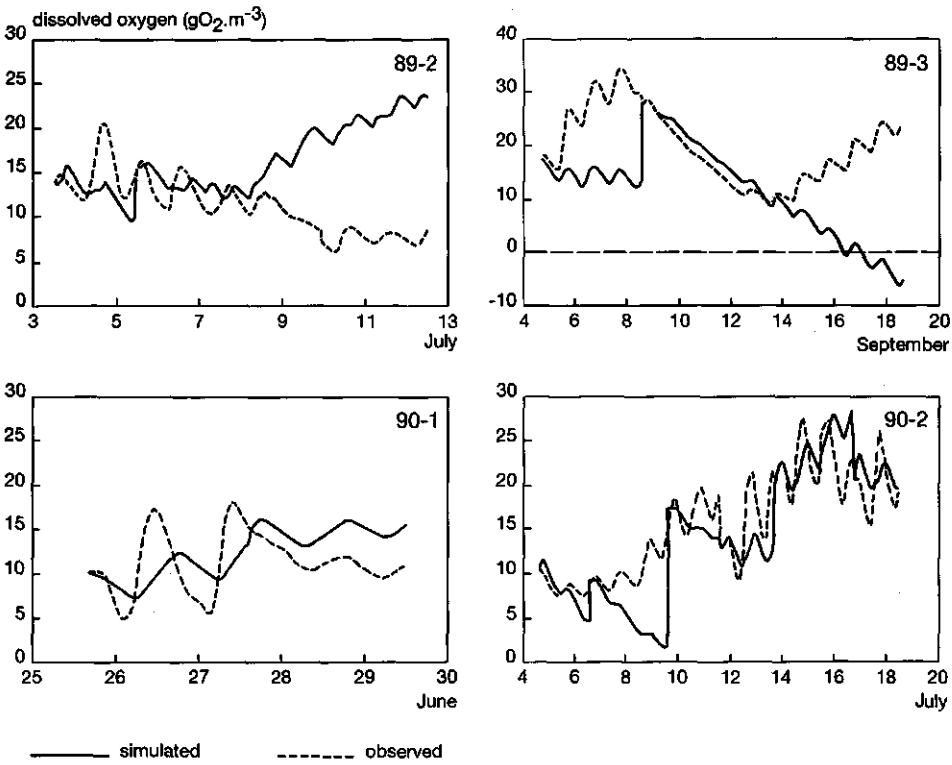
**Appendix 11: Simulation of the bottle experiments with the model  
*SIMPLE***



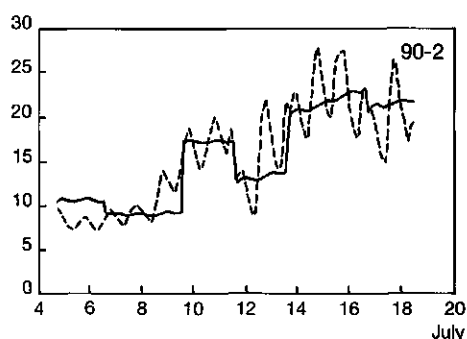
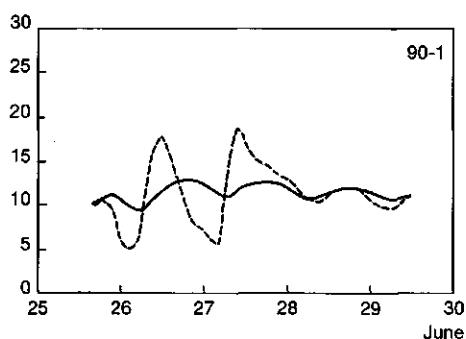
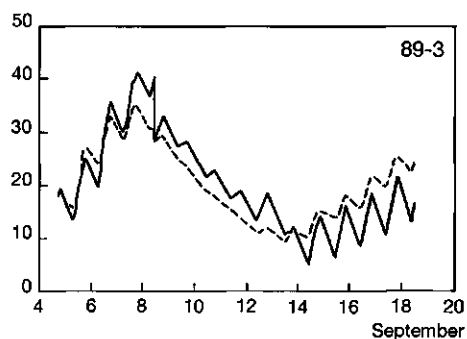
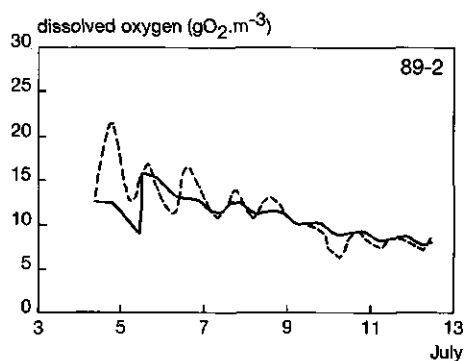
## Appendix 11: Continuation



**Appendix 12: Simulation of the cylinder experiments with the model  
SIMPLE**

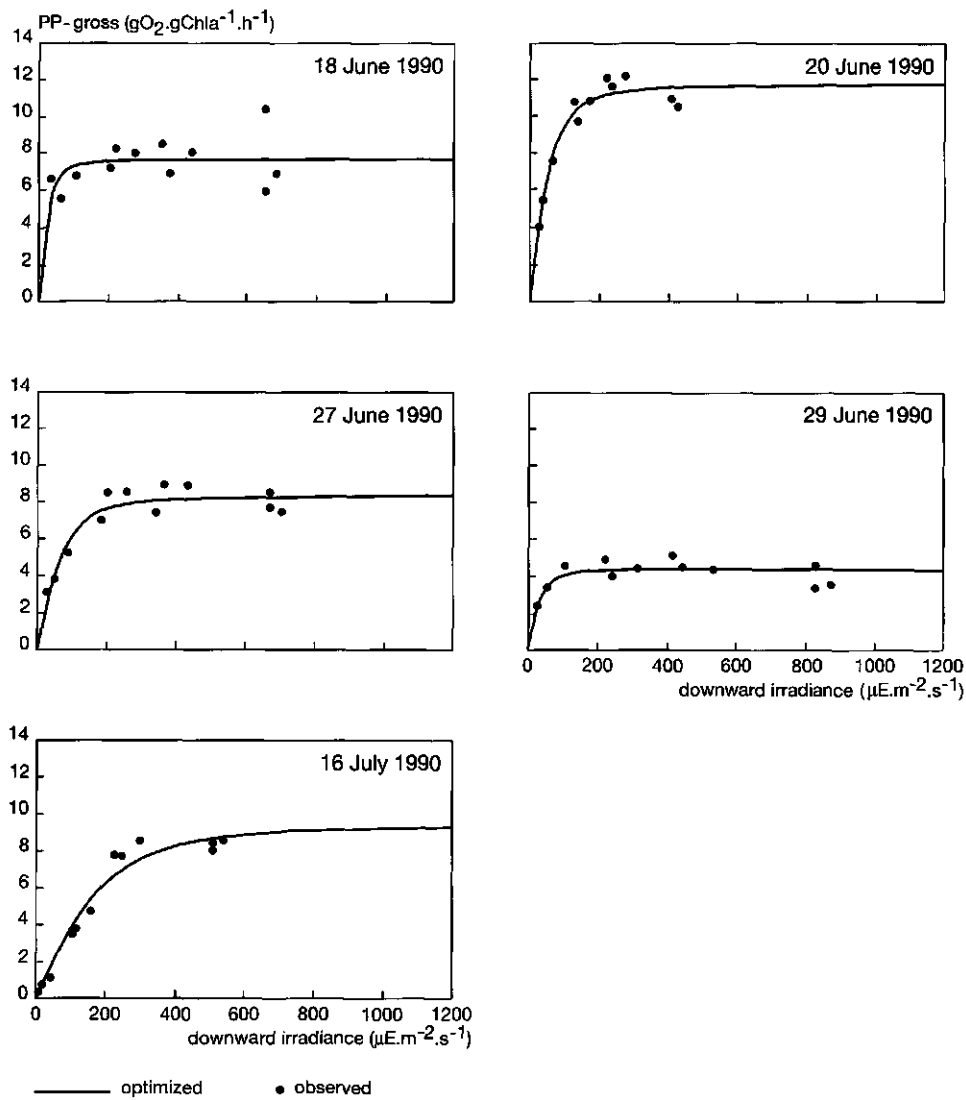


## Appendix 12: Continuation

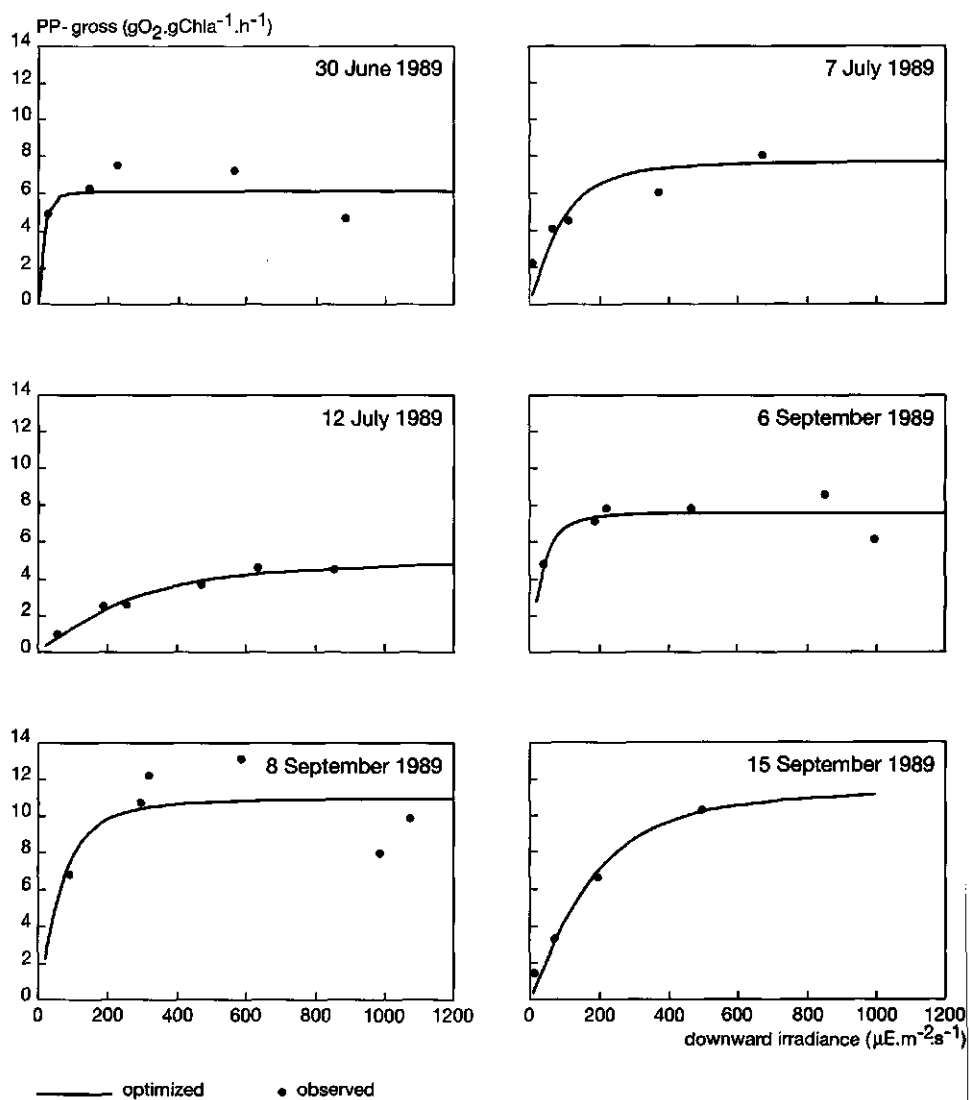


—— calibrated      - - - - - observed

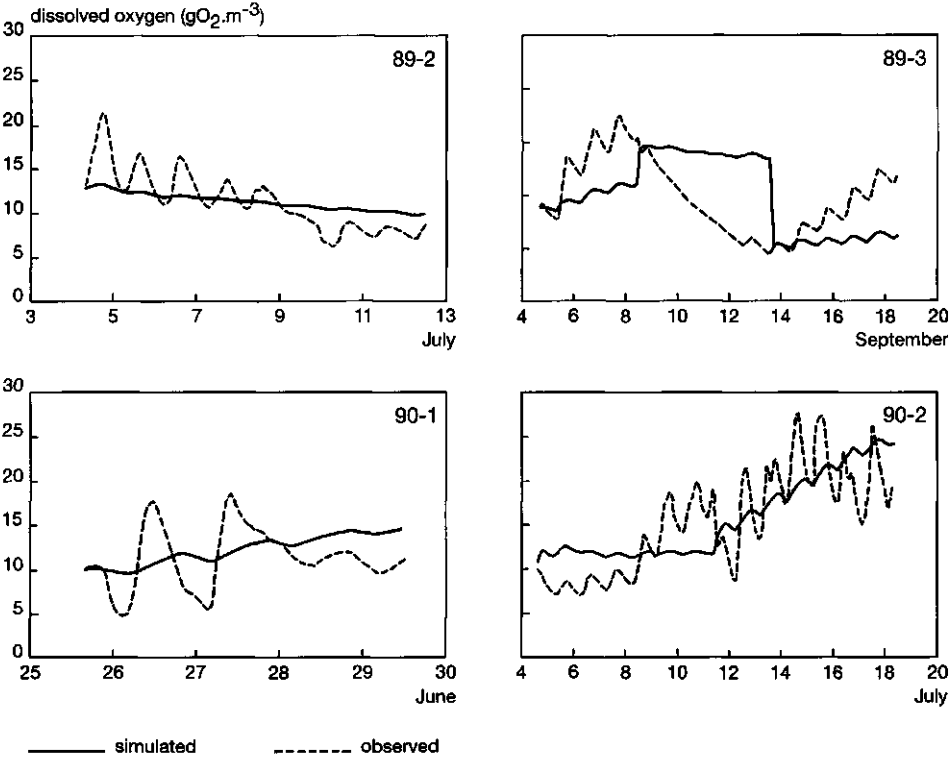
**Appendix 13:** Simulation of the bottle experiments with the model ALGA



# Appendix 13: Continuation



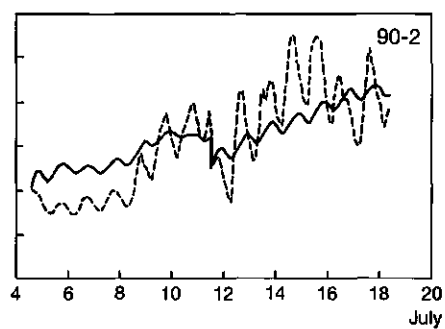
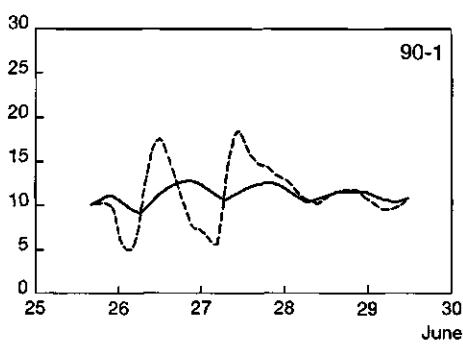
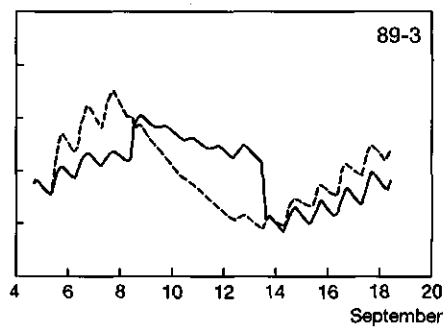
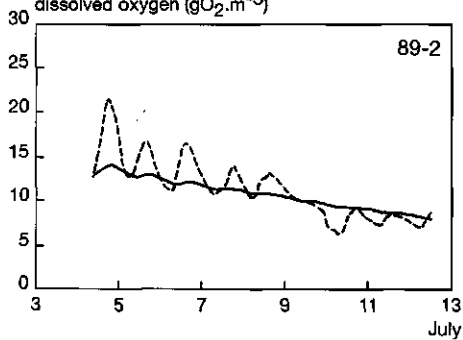
**Appendix 14:** Simulation of the cylinder experiments with the model  
**ALGA**





## Appendix 14: Continuation

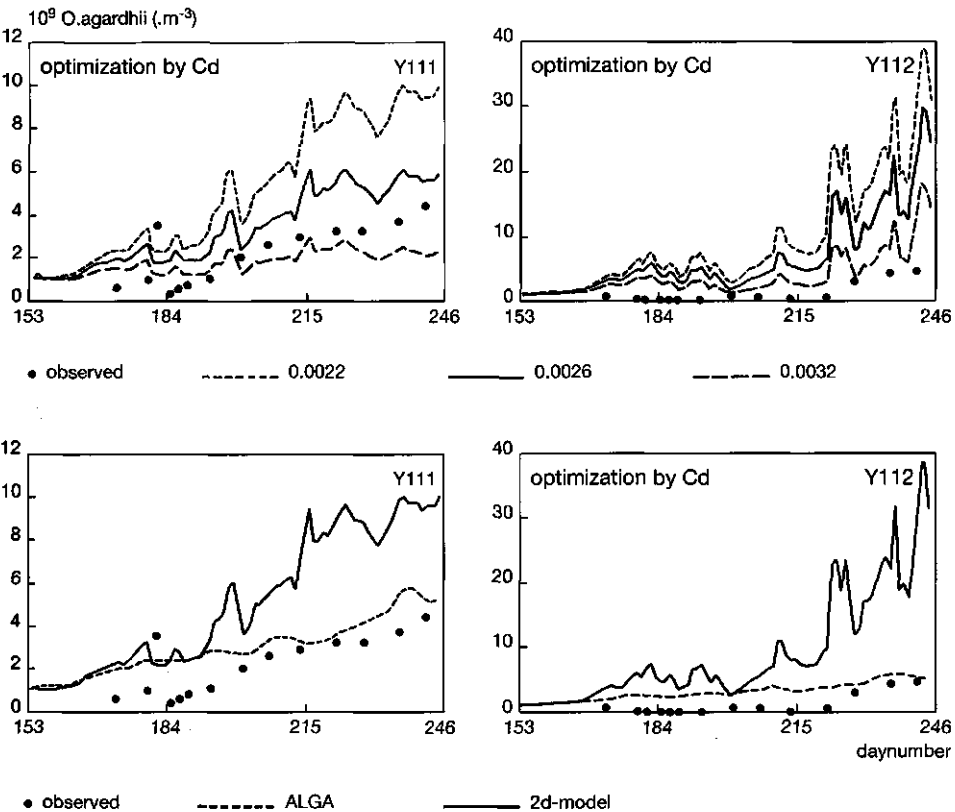
dissolved oxygen ( $\text{gO}_2\cdot\text{m}^{-3}$ )



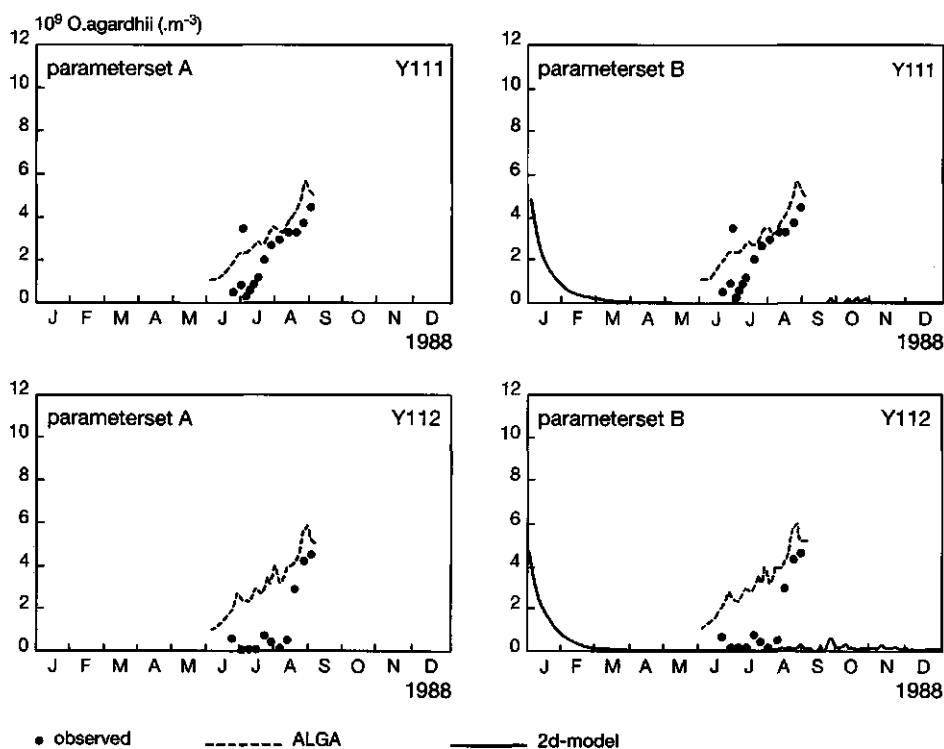
—— calibrated

----- observed

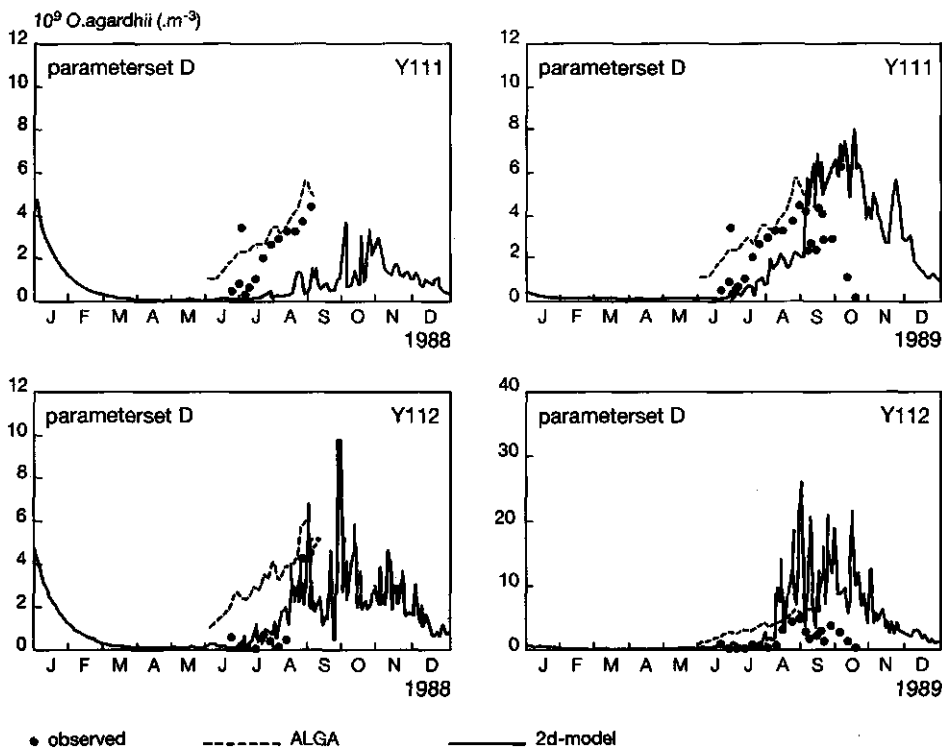
Appendix 15: Optimization of the integrated model



# Appendix 15: Continuation



Appendix 15: Continuation



# Appendix 16: Modified water balance

| 1988 | Houtr | Krab. | Schew | Zeeb. | Eem | Vecht | Bvku | Wort | Wkoge | Oostp | Drieb | Mond | Schard | Edam | nett |
|------|-------|-------|-------|-------|-----|-------|------|------|-------|-------|-------|------|--------|------|------|
| jan  | -222  | -36   | 0     | 0     | 67  | 12    | 170  | 7    | 12    | 4     | 6     | -1   | 5      | 2    | 26   |
| feb  | -86   | -17   | 0     | -12   | 44  | 9     | 98   | 3    | 7     | 2     | 3     | -1   | 8      | 1    | 59   |
| mar  | -121  | -23   | 0     | -4    | 27  | 13    | 82   | 3    | 6     | 2     | 4     | 0    | 11     | 1    | 0    |
| apr  | 4     | 7     | 0     | -24   | 1   | 2     | 0    | 0    | 0     | 0     | 0     | 0    | -25    | 0    | -33  |
| may  | 36    | 37    | 0     | -20   | 7   | 7     | 5    | 0    | 0     | 0     | 0     | 0    | -35    | 0    | 37   |
| jun  | 1     | 8     | 0     | -16   | 2   | 2     | 0    | 0    | 0     | 0     | 0     | 0    | -37    | -1   | -41  |
| jul  | 0     | 5     | -23   | -10   | 12  | 13    | 4    | 5    | 1     | 1     | 1     | 0    | -22    | -1   | -15  |
| aug  | 38    | 41    | -31   | -14   | 6   | 12    | 2    | 5    | 0     | 0     | 0     | 0    | -26    | -1   | 33   |
| sep  | -53   | 2     | -13   | -10   | 8   | 5     | 6    | 3    | 1     | 0     | 0     | -1   | -14    | -1   | -67  |
| oct  | -78   | -25   | -34   | -4    | 18  | 9     | 29   | 16   | 4     | 1     | 2     | -1   | -15    | 0    | -78  |
| nov  | 0     | -5    | -7    | -14   | 27  | 0     | 13   | 1    | 1     | 1     | 1     | 0    | -27    | 0    | -11  |
| dec  | -2    | -13   | -11   | -11   | 44  | 15    | 92   | 53   | 10    | 3     | 5     | -1   | 0      | 0    | 185  |
|      | -482  | -20   | -121  | -139  | 262 | 98    | 504  | 98   | 43    | 14    | 23    | -5   | -178   | -2   | 96   |

| 1989 | Houtr | Krab. | Schew | Zeeb. | Eem  | Vecht | Bvku | Wort | Wkoge | Oostp | Drieb | Mond  | Schard | Edam | nett |
|------|-------|-------|-------|-------|------|-------|------|------|-------|-------|-------|-------|--------|------|------|
| jan  | -172  | -82   | -8.8  | -13.4 | 50.3 | 2.4   | 13.6 | 7.1  | 1.7   | .5    | .7    | -10.1 | -5.6   | .1   | -215 |
| feb  | 0     | -15   | -9.7  | -8.7  | 48.1 | .0    | 33.9 | 18.7 | 5.4   | 1.4   | .1    | -14.7 | -8.6   | 3.3  | 56   |
| mar  | -27   | 33    | -25.5 | -8.2  | 49.9 | 6.8   | 78.9 | 20.6 | 8.7   | 2.7   | .6    | -1.0  | 5.9    | 2.8  | 148  |
| apr  | 20    | 41    | -82.4 | -13.0 | 12.0 | 8.4   | 5.7  | 4.0  | 1.0   | .3    | .3    | -7.1  | -9.5   | .0   | -19  |
| may  | 58    | 71    | -53.0 | -16.8 | 5.0  | 8.5   | 3.4  | .5   | -5    | .1    | .0    | -24.0 | -32.8  | -3   | 19   |
| jun  | 48    | 60    | -34.7 | -14.8 | 6.1  | 10.3  | 3.2  | 3.5  | -1    | .1    | .0    | -23.0 | -37.8  | -1.1 | 22   |
| jul  | 20    | 40    | -33.1 | -13.2 | 7.2  | 7.3   | 2.6  | 2.4  | .2    | .2    | .1    | -22.2 | -34.5  | -1.6 | -26  |
| aug  | 11    | 35    | -11.9 | -11.6 | 9.3  | 6.3   | 1.9  | 1.3  | .1    | .1    | .0    | -22.9 | -31.4  | -1.2 | -15  |
| sep  | 0     | 5     | -14.3 | -17.1 | .9   | 1.7   | 1.0  | .4   | .0    | .0    | .0    | -18.0 | -24.8  | -1.5 | -67  |
| oct  | -55   | -45   | -12.4 | -13.3 | 40.0 | 7.2   | 41.8 | 29.2 | 3.1   | 1.3   | .3    | -13.4 | -27.4  | -6   | -44  |
| nov  | -22   | -66   | -30.7 | -7.1  | 63.9 | 1.1   | 32.6 | 8.2  | 1.9   | .5    | .2    | -10.9 | -12.0  | -9   | -41  |
| dec  | -36   | -23   | -31.5 | -6.9  | 69.6 | 6.8   | 88.4 | 56.5 | 9.1   | 2.3   | 1.3   | -8.6  | -14.3  | .3   | 115  |
| tot  | -155  | 53    | -348  | -144  | 365  | 66    | 307  | 152  | 31    | 9     | 4     | -176  | -233   | -1   | -67  |